DECEMBER, 1951

Journal of METALS

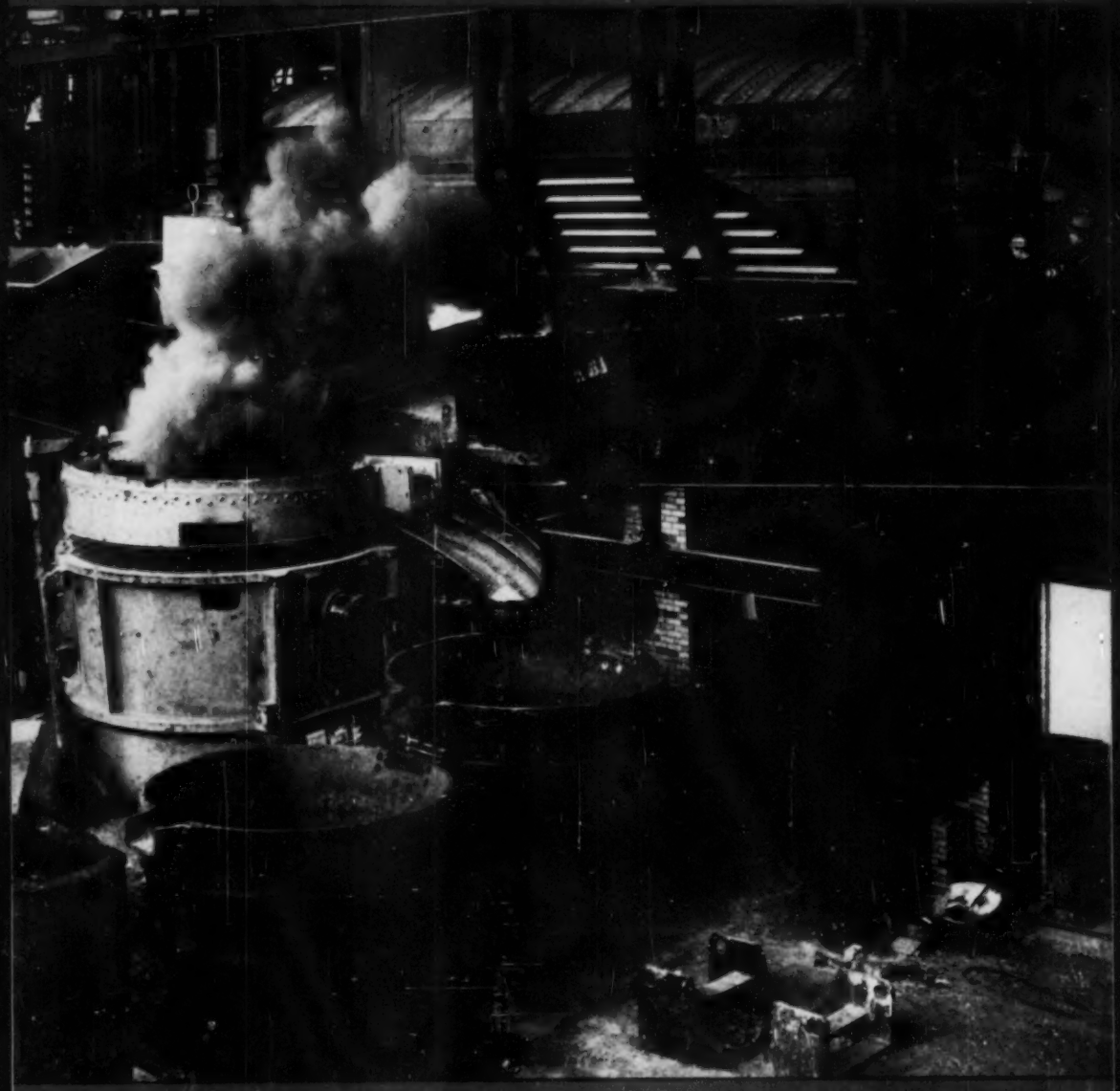

December JOURNAL OF METALS Highlight:

Electric Furnace Steel Conference Program Issue

this is Lan-cer-amp

actual size and color LAN-CER AMP #1

—the ingenious combination of rare earth metals which is now conserving vital alloys and improving the physical properties of cast and wrought steel. Every day greater tonnage of Lan-cer-amp treated steel is being produced. Write or call. Let us discuss our latest developments with you.

American Metallurgical Products company

3600 Forbes Street · Pittsburgh 13, Pa.

Journal of **METALS**

VOL. 3, NO. 12 — DECEMBER, 1951

Published to provide a continuing, authoritative, and up-to-date record of technological, engineering, and economic progress in all branches of the metals industry by the Metals Branch American Institute of Mining and Metallurgical Engineers, Inc. 29 West 39th Street, New York 18

THOMAS E. LLOYD
Manager of Publications
Editor, Journal of Metals

A. S. COHAN — Associate Editor
D. G. GARRETT, MARGARET BAGG — Assistant Editors
GRACE PUGSLEY — Production Manager
W. J. SEWING — Asst. Prod. Mgr.

METALS BRANCH COUNCIL
C. C. Long — Chairman
E. O. Kirkendall — Secretary
R. M. Brick — IMD Chairman
T. L. Joseph — ISD Chairman
O. C. Ralston — EMD Chairman
M. Gensamer, D. S. Eppelsheimer, H. K. Work, Evan Just

TECHNICAL PUBLICATIONS COMMITTEE
J. T. Laudermilk — Chairman
E. J. Kennedy, Jr. — Secretary

AUXILIARY PUBLICATIONS COMMITTEE CHAIRMEN
M. Gensamer — Institute of Metals Div.
A. G. Forrest — Iron & Steel Div.
J. Glasser — Extract. Metal Div.

JAMES A. STANGARONE
Advertising Manager
B. C. SNELL
Regional Manager, Pittsburgh
1110 McDonald Place, Sewickley, Pa.

The AIME Publishes:
Journal of Metals
Mining Engineering
Journal of Petroleum Technology

COVER

Tapping the first open hearth furnace at the Jones & Laughlin Steel Corp.'s new open hearth shop at its Pittsburgh Works. When completed, the shop will have a capacity of 2 million tons of steel a year. This photo shows the furnace just as the jet topper was exploded, before the steel flowed into the runner.

NEWS

Journal of Metals Reporter	1115	New Products	1107
Open Hearth Section News	1216	AIME News	1213
Employment Service	1111	Coming Events	1105
Meet the Authors	1101	Personals	1219
Electric Furnace Steel Committee	1119		
Electric Furnace Steel Program	1120		

TECHNICAL FEATURES

Experiences With Chromite Hearths in Electric Furnaces	A. L. Feild	1123
J & L Dedicates 2 Million Ton Open Hearth Shop		1126
Grinding Methods Evolved for Titanium		1128
Modern Trends in Electric Furnace and Transformer Design	R. J. McCurdy	1130

TRANSACTIONS

Recovery of Vanadium from Titaniferous Magnetite	S. S. Cole, J. S. Breitenstein	1133
Low Grade Bauxites and Clays as Potential Aluminum Resources	K. K. Kershner, C. W. Funk, W. A. Calhoun	1138
Mechanism of Grain Refinement in Aluminum Alloys	F. A. Crossley, L. F. Mondolfo	1143
Constitution of Ti-Al Alloys	H. R. Ogden, D. J. Maykuth, W. L. Finlay, R. I. Jaffee	1150
Model for Dendrite Growth Form in Metals and Alloys	R. B. Pond, S. W. Kessler	1156
A Survey of the Sulphur Problem Through the Various Operations in the Steel Plant	T. E. Brower, E. M. Larsen	1163
Solubility of Gaseous Nitrogen in Gamma Iron and the Effect of Alloying Constituents—Aluminum Nitride Precipitation	L. S. Darken, R. P. Smith, E. W. Filer	1174
Effect of Varying the Rate of Reduction on the Magnetic Properties, Ultimate Tensile Strength, and Resistivity of 18-8 Stainless Steel Wire	S. Starchheim	1181
Correlation Between Electrical Conductivity and Temperature Coefficient of Resistance of Solid-Solution Alloys	M. Hansen, W. R. Johnson, J. M. Parks	1184
Metallurgical Mechanism for Mercury Stress Cracking of Copper Alloys	W. D. Robertson	1190
Rate of Evaporation of Zinc at Low Pressures	H. W. St. Clair, M. J. Spendlove	1192
Vapor Pressures of Zinc Over AgZn Alloys	E. E. Underwood, B. L. Averbach	1198
Analytical Representation of Certain Phase Boundaries	W. Rostoker	1203
Surface Tension of Solid Silver	E. P. Funk, H. Udin, J. Wulff	1206
Surface Tension of Solid Gold	H. H. Buttner, H. Udin, J. Wulff	1209

TECHNICAL NOTES

Crystallographic Angles for Tin	J. F. Nicholas	1142
Surface Effect in the Cleavage of Zinc Monocrystals	J. J. Gilman	1148
Useful Etchants for Electron Metallography	W. L. Grube	1171
Change in Yield Strength During Aging in Iron	C. A. Wert	1179
Eutectoid Decomposition of the Delta Phase of the Cu-Sn System	C. C. Wang, M. Hansen	1212

Published the first day of each month by the American Institute of Mining and Metallurgical Engineers, Inc., 29 West 39th Street, New York 18, N. Y. Telephone: PEnnsylvania 6-9220. Subscription $8 per year for non-AIME members in United States and North, South and Central America; $9, foreign; $6 for AIME members, or $4 additional in combination with a subscription to "Mining Engineering" or "Journal of Petroleum Technology". Single copies, 75 cents; special issues, $1.50 . . . The AIME is not responsible for any statement made or opinion expressed in its publications. . . . Copyright 1951 by the American Institute of Mining and Metallurgical Engineers, Inc. . . . Registered cable address, AIME New York . . . Indexed in Engineering Index, Industrial Arts Index and Chemical Abstracts . . . Reentered as second-class matter Sept. 21, 1949, at the post office at New York, N. Y., under the Act of March 3, 1879. Additional entry established at Manchester, N. H.

Advertisement

ELECTROMET Data Sheet

Published by Electro Metallurgical Company, A Division of Union Carbide and Carbon Corporation, 30 East 42nd Street, New York 17, N. Y. In Canada: Electro Metallurgical Company of Canada, Limited, Welland, Ontario.

ALLOYS FOR THE STEEL, IRON, AND NON-FERROUS INDUSTRIES

BORON ALLOYS

PRODUCT*	NOMINAL COMPOSITION	USES
Ferroboron Min. 10.00% Boron Grade	Silicon.....max. 1.50% Aluminum.....max. 0.50% Carbon.....max. 1.50%	Increases hardenability of steel; also, for additions to malleable iron and aluminum alloys.
Min. 17.50% Boron Grade	Silicon.....max. 1.50% Aluminum.....max. 0.50% Carbon.....max. 0.50%	
Manganese-Boron	Boron.....min. 17.50% Manganese...approx. 75% Silicon.....max. 1.50% Carbon.....max. 3% Iron.....max. 5%	Used to cleanse and deoxidize non-ferrous alloys.
Nickel-Boron	Boron.....15 to 18% Silicon.....max. 1.50% Aluminum.....max. 1.00% Carbon.....max. 0.50% Iron.....max. 3.00% Nickel.....Balance	Special boron alloy used principally for deoxidizing nickel and its alloys.
Boron Carbide	Boron.....45 to 50% Carbon.....45 to 50%	Deoxidizer for non-ferrous alloys.
Calcium Boride	Boron.....38 to 42% Calcium.....27 to 32% Carbon.....15 to 20%	Welding rod coating.
SILCAX Alloy	Boron.....0.55 to 0.75% Silicon.....35 to 40% Calcium.....9 to 11% Aluminum.....6 to 8% Titanium.....9 to 11% Zirconium.....3 to 5%	A complex boron addition agent for increasing the hardenability of steel.

CALCIUM ALLOYS

PRODUCT*	NOMINAL COMPOSITION	USES
Calcium-Silicon	Calcium.....30 to 33% Silicon.....60 to 65% Iron.....1.50 to 3%	Deoxidizer for quality ingot steel. Also used in high-tensile gray irons.
Calcium-Manganese-Silicon	Calcium.....16 to 20% Manganese.....14 to 18% Silicon.....53 to 59%	A complex deoxidizer used widely in production of steel castings.
Calcium Metal		
Regular Grade	Calcium.....98% (Cylinders, Slabs, Cut Pieces, or Turnings)	Reducing agent in metallurgical applications, deoxidizer and degasifier for non-ferrous metals, particularly magnesium.
Distilled Grade	Calcium...approx. 99.90% (Irregular pieces from pea size to 14 in. lumps)	For special applications requiring calcium of very high purity.

CHROMIUM ALLOYS

PRODUCT*	NOMINAL COMPOSITION	USES
Low-Carbon Ferrochrome	Chromium.....67 to 71% Silicon.....0.30 to 1.00% Carbon (10 Grades) max. 0.03 to max. 2.00%	Production of stainless steels and high-temperature alloys requiring low carbon content.
High-Carbon Ferrochrome		
Max. 4.50, 5.00, or 6.00% Carbon Grade	Chromium.....67 to 70% Silicon..... 1 to 2%	For production of engineering alloy steels and other alloy steels of moderate chromium content.
Max. 7.00% Carbon Grade	Chromium.....66 to 69% Silicon..... 1 to 3%	
Min. 7.00% Carbon Grade	Chromium.....65 to 68% Silicon..... 1 to 3%	
Nitrogen-Bearing Low-Carbon Ferrochrome	Chromium.....67 to 71% Silicon.....0.30 to 1.00% Carbon.....max. 0.10% Nitrogen....approx. 0.75%	For additions of nitrogen to improve properties of high-chromium steels.
"SM" Ferrochrome	Chromium.....60 to 65% Silicon ..... 4 to 6% Carbon.... .... 4 to 6% Manganese .... 4 to 6%	A high-solubility chromium additior for steel or iron in either furnace or ladle.

CHROMIUM ALLOYS cont.

PRODUCT*	NOMINAL COMPOSITION	USES
Foundry Ferrochrome High-Carbon Grade	Chromium.....62 to 66% Silicon..... 7 to 10% Carbon..... 5 to 7%	Developed especially for high-solubility ladle additions of chromium to improve composition and properties of cast iron.
Low-Carbon Grade	Chromium.....50 to 54% Silicon.....28 to 32% Carbon.....max. 1.25%	
Chromium Metal Low-Carbon Grades	Chromium.....min. 97% Carbon .....max. 0.10% and 0.50% Iron.....max. 1%	Production of wide variety of non-ferrous chromium-bearing alloys, including electrical resistance alloys and high-temperature alloys.
High-Carbon Grade	Chromium.....87 to 90% Carbon..... 9 to 11% Iron.....max. 1.25%	
"EM" Ferrochrome-Silicon No. 1 Grade	Chromium.....39 to 41% Silicon.....42 to 46% Carbon.....max. 0.05%	In production of stainless steels, these alloys are used to reduce metal oxides from the slag back into bath.
No. 2 Grade	Chromium.....36 to 39% Silicon.....36 to 39% Carbon.....max. 0.05% Aluminum..... 7 to 9%	
"EM" Ferrosilicon-Chrome	Chromium.....50 to 54% Silicon.....28 to 32% Carbon.....max. 1.25%	For adding chromium and silicon to steels containing up to 1 or 2 per cent chromium.
"EM" Chromium Briquets (Hexagonal Shape)	Chromium.....2 lb. Total Weight.....3½ lb.	For adding chromium to cast iron in the cupola.

COLUMBIUM ALLOYS

PRODUCT*	NOMINAL COMPOSITION	USES
Ferrocolumbium	Columbium.....50 to 60% Silicon.....max. 8% Carbon.....max. 0.40%	Stabilizer in austenitic chromium-nickel stainless steels. Also constituent of high-temperature alloys.
Ferrotantalum-Columbium	Columbium...approx. 40% Tantalum.....approx. 20% Cb+Ta .....min. 60% Silicon.....4 to 6% Carbon.....max. 0.30%	Another stabilizer, used to supplement ferrocolumbium, in austenitic chromium-nickel stainless steels. Also used in high-temperature alloys.

MANGANESE ALLOYS

PRODUCT*	NOMINAL COMPOSITION	USES
Standard Ferromanganese Regular Grade	Manganese.....78 to 82% Carbon.....approx. 7% Silicon.....max. 1%	Most common means of adding manganese to steel for both alloying and deoxidizing purposes. Also for counteracting sulphur in steel and cast iron.
Low-Phosphorus Grade	Manganese.....78 to 82% Carbon.....max. 7% Silicon.....max. 2% Phosphorus...max. 0.10%	
Low-Carbon Ferromanganese Low-Phosphorus Grade	Manganese.....min. 90% Carbon.....max. 0.07% Phosphorus...max. 0.06%	Additions of manganese to steels of low-carbon specification, particularly stainless steels of 18 per cent chromium, 8 per cent nickel type.
Regular Grades	Manganese.....85 to 90% Carbon ....max. 0.07, 0.11 to 0.15, 0.30, or 0.50%	
Regular Grade (High-Silicon)	Manganese.....80 to 85% Carbon.....max. 0.75% Silicon..... 5 to 7%	
Medium-Carbon Ferromanganese	Manganese.....80 to 85% Carbon.....max. 1.25 to 1.50%	For making low- and medium-carbon manganese steel and Hadfield steel.
Silicomanganese		
Max. 1.5 % Carbon Grade	Manganese.....65 to 68% Silicon.....18 to 20%	A versatile alloy useful as furnace block, deoxidizer, and also for making manganese additions to steel in the ladle or in the furnace.
Max. 2.00% Carbon Grade	Manganese.....65 to 68% Silicon.....15 to 17.50%	
Max. 3.00% Carbon Grade	Manganese.....65 to 68% Silicon.....12 to 14.50%	

*All of the alloys and metals listed are produced in the usual lump, crushed, or ground sizes, except where other special forms are indicated.

PRODUCT*	NOMINAL COMPOSITION	USES
MANGANESE ALLOYS cont.		
Low-Iron Ferromanganese	Manganese.....85 to 90% Carbon.....approx. 7.00% Silicon.....max. 3% Iron.....max. 2%	For high manganese additions to certain non-ferrous alloys, particularly aluminum.
Manganese Metal	Manganese.....min. 96% Carbon.....max. 0.20% Silicon.....max. 1.00% Iron.....max. 2.50%	Used both as deoxidizer and alloy in production of numerous non-ferrous metals and alloys.
"EM" Silico-manganese Briquets (Square Shape)	Manganese.....2 lb. Silicon.....½ lb. Total Weight.....3½ lb.	For adding manganese (with silicon) to cast iron in the cupola.
"EM" Ferro-manganese Briquets (Oblong Shape)	Manganese.....2 lb. Total Weight.....3 lb.	For adding manganese (without silicon) to cast iron in the cupola.
SILICON ALLOYS		
50% Ferrosilicon		
Regular Grade	Silicon.....47 to 51%	Deoxidizer for most grades of killed or semi-killed steel. Blocking grade specially sized for maximum efficiency.
Blocking Grade	Silicon.....47 to 51%	
Low-Aluminum Grade	Silicon.....47 to 51% Aluminum.....max. 0.40%	
65% Ferrosilicon		
Low-Aluminum Grade	Silicon....61.50 to 66.50% Aluminum.....max. 0.50%	Mainly for production of electrical sheet steel.
75% Ferrosilicon		
Regular Grade	Silicon.....73 to 78%	Deoxidizer and alloy for production of high-silicon spring and electrical sheet steel. Graphitizing inoculant for cast iron.
Low-Aluminum Grade	Silicon.....73 to 78% Aluminum.....max. 0.50%	
85% Ferrosilicon		
Regular Grade	Silicon.....83 to 88%	Enables melter to add higher percentages of silicon without chilling metal in ladle. Graphitizing inoculant for cast iron.
Low-Aluminum Grade	Silicon.....83 to 88% Aluminum.....max. 0.50%	
90% Ferrosilicon		
Regular Grade	Silicon.....92 to 95%	Permits large additions of silicon without harmful chilling effect.
Low-Aluminum Grade	Silicon.....92 to 95% Aluminum.....max. 0.50%	
Silicon Metal		
Regular Grade	Silicon.....min. 97 or 98% Iron.....max. 1 or 2%	Additions of silicon to non-ferrous metals, particularly aluminum and copper, to improve physical properties.
Purified Grade	Silicon....99.70 to 99.90% Iron.....005 to .015%	For applications in non-ferrous industry requiring silicon of high purity.
Low-Calcium Grade	Silicon.....min. 97% Iron.....max. 1% Calcium.....max. 0.10%	For the production of high-silicon aluminum alloys where calcium is detrimental.
Low-Aluminum Grade	Silicon.....min. 98% Iron.....max. 1% Aluminum.....max. 0.10%	For the production of silicon-copper alloys where aluminum is detrimental.
"SMZ" Alloy	Silicon.....60 to 65% Manganese..... 5 to 7% Zirconium..... 5 to 7%	Particularly strong graphitizing inoculant used in making ladle additions to cast iron.
Special Graphitizer	Ferrosilicon Compound	Acts as both deoxidizer and graphitizer in cast iron. Useful in controlling chilling tendencies.
Magnesium-Ferrosilicon	Silicon.....approx. 46% Magnesium..approx. 8.5%	For ladle addition to cast iron to obtain special properties.
Barium-Silicon	Barium.....40 to 50% Silicon.....45 to 55%	For deoxidation of non-ferrous alloys.
"EM" Silicon Briquets (Cylindrical Shape)		
Large Size	Silicon.....2 lb. Total Weight.....5 lb.	For adding silicon to cast iron in the cupola.
Small Size	Silicon.....1 lb. Total Weight.....2½ lb.	

"Electromet," "EM," "Silcaz," "SM," and "SMZ," are trade-marks of Union Carbide and Carbon Corporation.

PRODUCT*	NOMINAL COMPOSITION	USES
TITANIUM ALLOYS		
Ferrotitanium	Titanium.....27 to 32% Carbon.....max 0.10%	For adding titanium to stabilized austenitic chromium-nickel stainless steels and to high-temperature metals.
Silicon-Titanium	Titanium.....40 to 50% Silicon.....45 to 50% Iron.....max. 3%	For additions of titanium to steels or non-ferrous alloys.
Manganese-Nickel-Titanium	Titanium.....43 to 48% Nickel.....approx. 25% Manganese.....max. 8% Aluminum.....max. 18% Iron.....max. 5%	Deoxidization of nickel alloys.
TUNGSTEN ALLOYS		
Ferrotungsten	Conforming to A.S.T.M. Spec. A 144-39	For production of tool and die steels; also high-temperature alloys.
Tungsten Metal Powder		Production of tungsten steels and cast tungsten carbide.
Melting Grade	Tungsten.....min. 98.80% Total Carbon..max. 0.25%	
Calcium Tungstate Nuggets	Tungstic Oxide..68 to 72%	For production of tool steels and high-temperature alloys by direct reduction.
VANADIUM ALLOYS		
Ferrovanadium	Vanadium.....50 to 55% Carbon....max. 0.20, 0.50, or 3.00% Silicon....max. 1.50, 2.00, or 8%	Production of tool and engineering steels, high-strength structural steels, non-aging rimming steels, and wear-resistant irons.
Vanadium Oxide		
Fused	V_2O_5.....86 to 89% Na_2O.....approx. 10% CaO.....approx. 2%	For addition of vanadium to steel and for manufacturing catalysts.
Sodium Polyvanadate (Red Cake)	V_2O_5.....approx. 85% Na_2O.....approx. 9% CaO.....approx. 2% H_2O.....approx. 2.5%	For manufacture of vanadium compounds, including vanadium catalysts.
High-Purity Ammonium Metavanadate	V_2O_5.....approx. 99.50% NH_4VO_3.....min. 99%	
ZIRCONIUM ALLOYS		
12 to 15% Zirconium Alloy	Zirconium.....12 to 15% Silicon.....39 to 43% Carbon.....max. 0.20%	This zirconium alloy is a powerful deoxidizer. It also increases depth of hardening.
35 to 40% Zirconium Alloy	Zirconium.....35 to 40% Silicon.....47 to 52% Carbon.....max. 0.50%	Deoxidizer for fine grades of alloy steels. Used for adding larger amounts of zirconium.
Nickel-Zirconium	Zirconium.....25 to 30% Nickel.....40 to 50% Aluminum....approx. 15% Silicon.....max. 10% Iron.....max. 5%	Effective for deoxidizing and degasifying nickel and its alloys.

IF YOU HAVE A METALS PROBLEM

More than 50 different alloys and metals are produced by ELECTROMET in hundreds of varying compositions and sizes. If you need help in selecting the proper alloys, or have some specific metallurgical problem, be sure to consult one of ELECTROMET'S specially trained metallurgists and engineers. Address your inquiries to one of the offices listed below.

Birmingham 3, Ala.....Brown-Marx Building
Chicago 1, Ill.....230 N. Michigan Avenue
Cleveland 14, Ohio.....Union Commerce Building
Detroit 2, Mich.....6-240 General Motors Building
Los Angeles 58, Calif.....2724 Leonis Boulevard
New York 17, N. Y.....30 East 42nd Street
Pittsburgh 22, Pa.....2207 Oliver Building
San Francisco 6, Calif.....22 Battery Street
In Canada: Electro Metallurgical Company of Canada Limited, Welland, Ontario

for

dependable hardenability with maximum properties in low alloy boron steels

USE *Grainal* ALLOYS

For boron-treated steels, whether made in the electric furnace or in the open hearth, Grainal alloys are used successfully to increase hardenability.

A larger quantity of Grainal is usually required in electric furnace practice because of the higher nitrogen content characteristic of steels produced by this method. The conversion of the nitrogen content of the steel to an ineffective compound, as is done by some of the components of Grainal, permits a minimum amount of boron to produce the desired effects.

Grainal alloys are metallurgically balanced so that the larger additions required by electric furnace steels can be made safely without exceeding the boron limit for hot shortness.

VANADIUM CORPORATION OF AMERICA

420 LEXINGTON AVENUE • NEW YORK 17, N.Y. • DETROIT • CHICAGO • CLEVELAND • PITTSBURGH

MAKERS OF ALLOYS

VANCORAM

CHEMICALS AND METALS

delivers uniform steel at lower cost

by reducing surging and transformer heating . . . thus improving power factor and lowering power cost

The Whiting Hydro-Arc Furnace employs hydraulic power transmission for positioning electrodes, thus eliminating the time-lag between demand and electrode response. It provides definitely controlled production on a more efficient basis and delivers uniform steel worked under ideal conditions that until recently were considered obtainable only in the laboratory.

WHITING hydro-arc electric furnace

electrode arms and clamps designed for greater safety, convenience, and economy

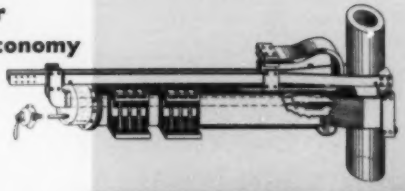

The electrode arms and clamps are an important feature of Hydro-Arc construction. Melters need not climb over the furnace into oppressive heat and fumes to slip electrodes — they can be slipped from the floor by merely pressing a lever. Electrodes can be adjusted in less than 30 seconds.

top-charging for further economy and increased output

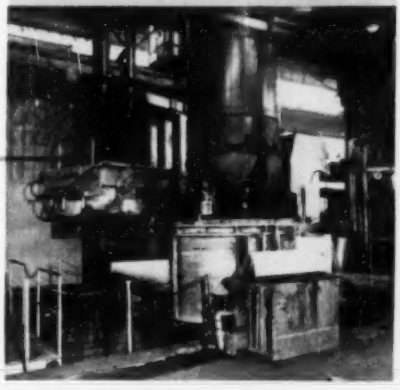

Top-Charging Hydro-Arc Furnaces provide additional savings. The roof, suspended at four points, swings aside while the charging bucket lowers into the furnace and discharges without jarring or damaging refractories. The furnace can be completely charged in 5 to 7 minutes after tapping, making "down time" negligible, reducing costs, and increasing the number of melts per day.

WHITING CORPORATION

15601 LATHROP AVENUE, HARVEY, ILL.

Offices in Chicago, Cincinnati, Detroit, Houston, Los Angeles, New York, Philadelphia, Pittsburgh, and St. Louis. Representatives in other principal cities. Canadian subsidiary: Whiting Corporation (Canada) Ltd., Toronto, Ontario. Export Department: 30 Church Street, New York 7, New York.

Yes! AJAX Induction Melting Furnaces are Versatile!

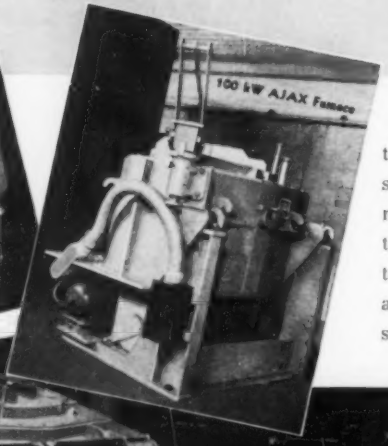

For many years AJAX has been the pioneer in the development of standard frequency induction furnaces for melting metals. Today this type of equipment has been adapted to the full range of non-ferrous metals and alloys and to a great variety of sizes ranging from 20 to 1000 kW.

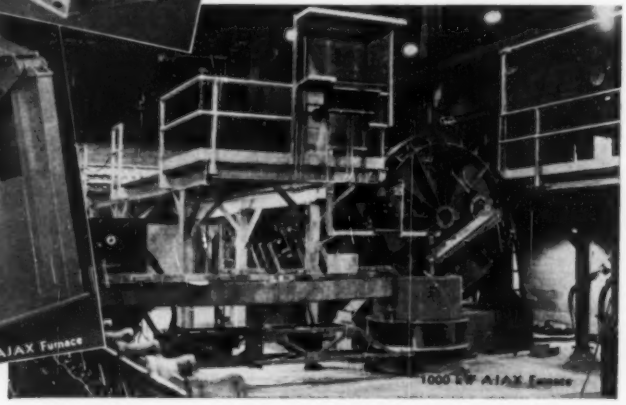

AJAX Induction Melting Furnaces are now adapted for the following applications: Die Castings, Permanent Mold Castings, Sand Castings, Billets for Rolling and Extrusion, Recovery of Scrap, Galvanizing and Aluminizing of Steel and many others.

For special applications an Automatic Electromagnetic Pump allows continuous feeding of molten metal into the molds as they move past. Hand ladling is eliminated. Temperature, of course, is also automatically regulated and there is no chance of overheating the bath at any time during the melting cycle.

AJAX ENGINEERING CORP., TRENTON 7, N. J.

AJAX TAMA-WYATT **INDUCTION MELTING FURNACE**

AJAX ELECTRO METALLURGICAL CORP., and Associated Companies
AJAX ELECTROTHERMIC CORP., Ajax Northrup High Frequency Induction Furnaces
AJAX ELECTRIC CO., INC., The Ajax Metycen Electric Salt Bath Furnace
AJAX ELECTRIC FURNACE CORP., Ajax Wyatt Induction Furnaces for Melting

World's Largest Graphite Electrodes

for More Power, More Capacity, Greater Economy

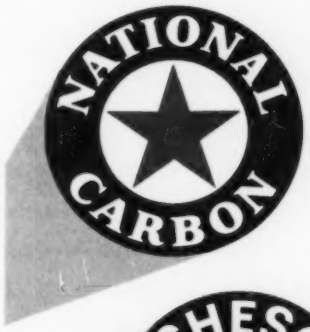

Giant Graphite Electrodes from National Carbon Company's new Columbia, Tenn. plant open new horizons in electric furnace development and promise greater power input and increased tonnage output.

For the first time, large scale production of 110"-long graphite electrodes in 20, 24, 30 and 40 inch diameters not only makes possible new, advanced furnace design but their extra length means greater economy because fewer joint assemblies are needed. Get all the facts about National Carbon Company's new "King-Size" graphite electrodes. Write our nearest District Office now.

The terms "National" and "Acheson" and the "National" and "Acheson" Seals distinguish products of Union Carbide and Carbon Corporation

NATIONAL CARBON COMPANY
A Division of
Union Carbide and Carbon Corporation
30 East 42nd Street, New York 17, N. Y.
District Sales Offices: Atlanta, Chicago, Dallas, Kansas City, New York, Pittsburgh, San Francisco
Foreign Department: New York, U.S.A.

IN CANADA: National Carbon Limited
Montreal, Toronto, Winnipeg

The Heat's On !

• • • • And from heats such as this will come high alloy, high quality steel to implement our ever increasing defense needs . . . our constantly growing demand for specialized steels to make possible the production of most everything we use in our daily lives.

Helping America's electric arc furnaces meet modern metallurgical requirements . . . to operate efficiently and economically under tough conditions . . . calls for the ultimate in refractories. General Refractories is an important factor in meeting this challenge.

In electric furnaces such as this you'll find sidewalls, bottoms and tapping

GENERAL REFRACTORIES

GENERAL REFRACTORIES COMPANY
PHILADELPHIA

spouts of General's basic materials . . . roofs of General's silica, fireclay or high alumina. General Refractories products are specifically designed to meet all operating conditions.

Whenever the steel industry faces a new refractories problem, General offers the world's most modern research facilities to find the solution. And General offers the productive capacity of 43 mines and 29 plants, here and abroad . . . 18 sales offices . . . 200 distributing agencies. Put your problem, concerning application or supply, up to General Refractories—the company that offers a complete refractories service.

A Complete Refractories Service

Stronger, Better Castings can be made with BORON

Do you know how much your iron and steel castings can be improved in physical properties, notwithstanding present restrictions, by proper use of Boron? A wealth of information, based on research and practical experience, is at your service. MCA, a pioneer in developing the metallurgical uses of Boron, gladly offers its advice on this very timely subject, to aid any user of Molybdenum, Tungsten, or Boron.

AMERICAN Production, American Distribution, American Control, Completely Integrated

Offices: Pittsburgh, New York, Chicago, Cleveland, Detroit, Los Angeles, San Francisco

Sales Representatives: American Steel and Supply Co., Chicago; Edgar L. Fink, Detroit; Brumley-Donaldson Co., Los Angeles, San Francisco

Subsidiaries: Cleveland-Tungsten, Inc., Cleveland, O.; General Tungsten Manufacturing Co., Inc., Union City, N.J.

Works: Washington, Pa.; York, Pa.

MOLYBDENUM CORPORATION OF AMERICA
Grant Building Pittsburgh, Pa.

MCA

Metal WON'T Penetrate ...

TAYLOR ZIRCON hearths and side walls in aluminum remelting furnaces

Damage caused by penetration of hearth and side wall refractories by aluminum metal is the principal cause of furnace failure. As *Taylor Zircon* refractories are inherently *resistant* to "wetting" by pure aluminum and most of the aluminum wrought alloys, they are ideally suited for the construction of hearths and side walls in aluminum remelting furnaces.

But Taylor Zircon's properties don't stop there. Here are further advantages that pay off in cleaner metal—higher yield—longer furnace life:

- Contaminated or penetrated hearths are a source of inclusions and dirty metal. Taylor Zircon brick, bonded with thin, tight joints of Taylor Zircon Cement, are *not* penetrated by the metal. The metal remains clean, free from contamination by refractory inclusions.
- As Taylor Zircon contains a negligible amount of free silica, silicon pick-up is eliminated.
- Open hearth furnaces lined with Taylor Zircon can be cleaned or scraped, either h-o-t or cold, in *one-half* to *one-third* the time required to clean fire clay, super-duty or high alumina brick lined furnaces.
- Metal composition can be changed without allowing for the loss of three or four wash heats. No metal will be trapped within or below the working face of the Zircon hearth, in a properly designed furnace.

Cleaning the interior of a 10-Ton Dempsey re-melt furnace, constructed with Taylor Zircon hearth and side walls, after having produced 13,800,000 lbs. of alloy No. 142 in approximately 10 months. Note the ease with which dross can be removed from the Taylor Zircon brick.

There are certain aluminum die cast alloys containing copper, silicon, magnesium and titanium for which zircon is not recommended. Your Taylor representative will be glad to discuss Taylor Zircon possibilities for your plant. Write for your free copy of Bulletin No. 202.

Exclusive Agents in Canada:
REFRACTORIES ENGINEERING AND SUPPLIES, LTD.
Hamilton and Montreal

The **CHAS. TAYLOR SONS Co.**
A SUBSIDIARY OF NATIONAL LEAD COMPANY
REFRACTORIES SINCE 1864 • CINCINNATI • OHIO • U.S.A.

STOKES MICROVAC PUMPS...are basic to Vacuum Processing

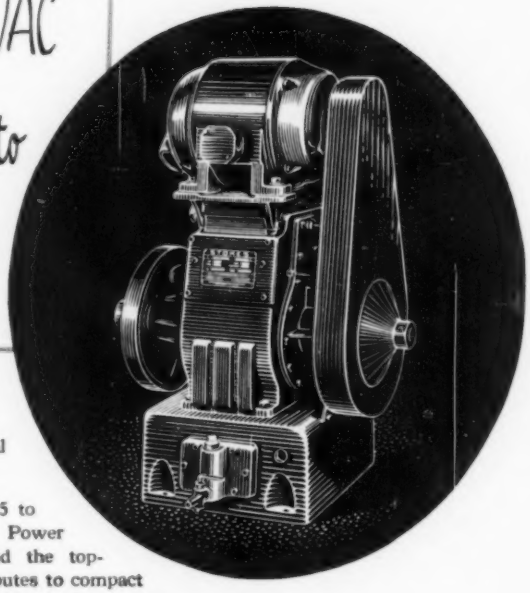

High volumetric and mechanical efficiency make these famous pumps economical and reliable units in any vacuum system.

Capacities of Stokes Microvac Pumps run from 15 to 500 cfm . . . pressures to 10 microns absolute. Power consumption is low and the top-mounted motor contributes to compact design requiring minimum floor space.

Send for FREE Stokes Vacuum Calculator. This slide rule determines needed pump capacity for any job...shows Centigrade to Fahrenheit conversion. Other useful conversion tables and scales on reverse of rule.

Lubrication of the four moving parts (including the exhaust valve of corrosion-resistant Teflon) is fully automatic. There are no stuffing-boxes or grease fittings, and no packing.

Parts are precision-finished, standard and interchangeable. Freedom from wear assures years of trouble-proof service.

Stokes is the only manufacturer of equipment for complete vacuum systems, including Microvac mechanical pumps, oil diffusion pumps, McLeod Gages and Vacuum Valves.

Consult with Stokes on the application of vacuum to vacuum sintering, melting, de-gassing, heat treating, inert gas purging, vacuum metallizing, and to other applications in which vacuum deserves exploration.

STOKES

STOKES MAKES
Plastics Molding Presses,
Industrial Tabletting
and Powder Metal Presses,
Pharmaceutical Equipment,
Vacuum Processing Equipment,
High Vacuum Pumps and Gages,
Special Machinery

F. J. STOKES MACHINE COMPANY, 5916 TABOR ROAD, PHILADELPHIA 20, PA.

HIGHEST RESOLUTION for Every Magnification

Plus- WIDEST SELECTION of Resolving Powers

Photographic Mag	OBJECTIVES						EYEPIECES			Approx Bellows Draw, In
	Achromatic		Fluorite		Apochromatic		Huyg	Hyper	Amp	
	Mag	N.A.	Mag	N.A.	Mag	N.A.				
25×	6.5×	0.10					5.0×			7.7
50×	6.5×	0.10					5.0×			15.4
75×	6.5×	0.10					6.4×			18.0
	8.0×	0.20					6.4×			14.6
	13.0×	0.25					5.0×			11.5
100×	8.0×	0.20					6.4×			19.5
	13.0×	0.25					5.0×			15.4
150×	13.0×	0.25					6.4×			18.0
200×	20.0×	0.40						10×		10.0
250×	20.0×	0.40						10×		12.5
500×	37.0×	0.65							10×	10.8
750×			55×	0.85	60×	0.95			10×	11.0
1000×			53×	1.00	60×	0.95			10×	9.8
1500×			85×	1.25	77×	1.40			10×	16.2
2000×					77×	1.40			10×	14.0
									10×	15.0
									10×	16.8
									10×	23.3

ASTM STANDARD MAGNIFICATIONS AND RECOMMENDED OPTICAL COMBINATIONS FOR PHOTOMICROGRAPHY

COMPARE the *Exclusive* Flexibility of Bausch & Lomb METALLOGRAPHS!

The variety of numerical apertures offered with Bausch & Lomb Metallographs gives you two important advantages . . . highest resolution for every magnification . . . plus a wide selection of resolving powers where specifically required. Resolution is controlled at will and not fixed for the average. Clearer, sharper, better defined visual and photomicrographic images are the result. These exclusive features make B&L Metallographs the world's finest for research and quality control—by *performance* proof.

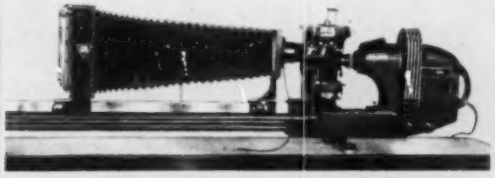

B&L RESEARCH METALLOGRAPH Catalog E-240

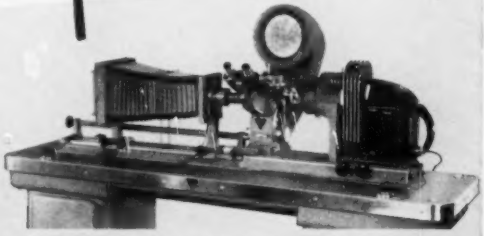

B&L BALPHOT METALLOGRAPH Catalog E-232

B&L PHOTOMICROGRAPHIC EQUIPMENT MODEL L Catalog E-210

B&L CM METALLURGICAL MICROSCOPE Catalog E-223

B&L STEREOSCOPIC WIDE FIELD MICROSCOPES Catalog D-15

COMPARE, **too, the *EXCLUSIVE* Adaptability of the *COMPLETE* Bausch & Lomb Line . . .**

In addition to B&L Metallographs there's a complete line of B&L precision instruments to help you save materials and manpower in all phases of metallurgical research and production.

WRITE for complete information to Bausch & Lomb Optical Co., 787-12 St. Paul St. Rochester 2, N. Y.

Bausch & Lomb *Metallurgical* Equipment

SWINDELL

P. O. BOX 1888
PITTSBURGH 30, PA.

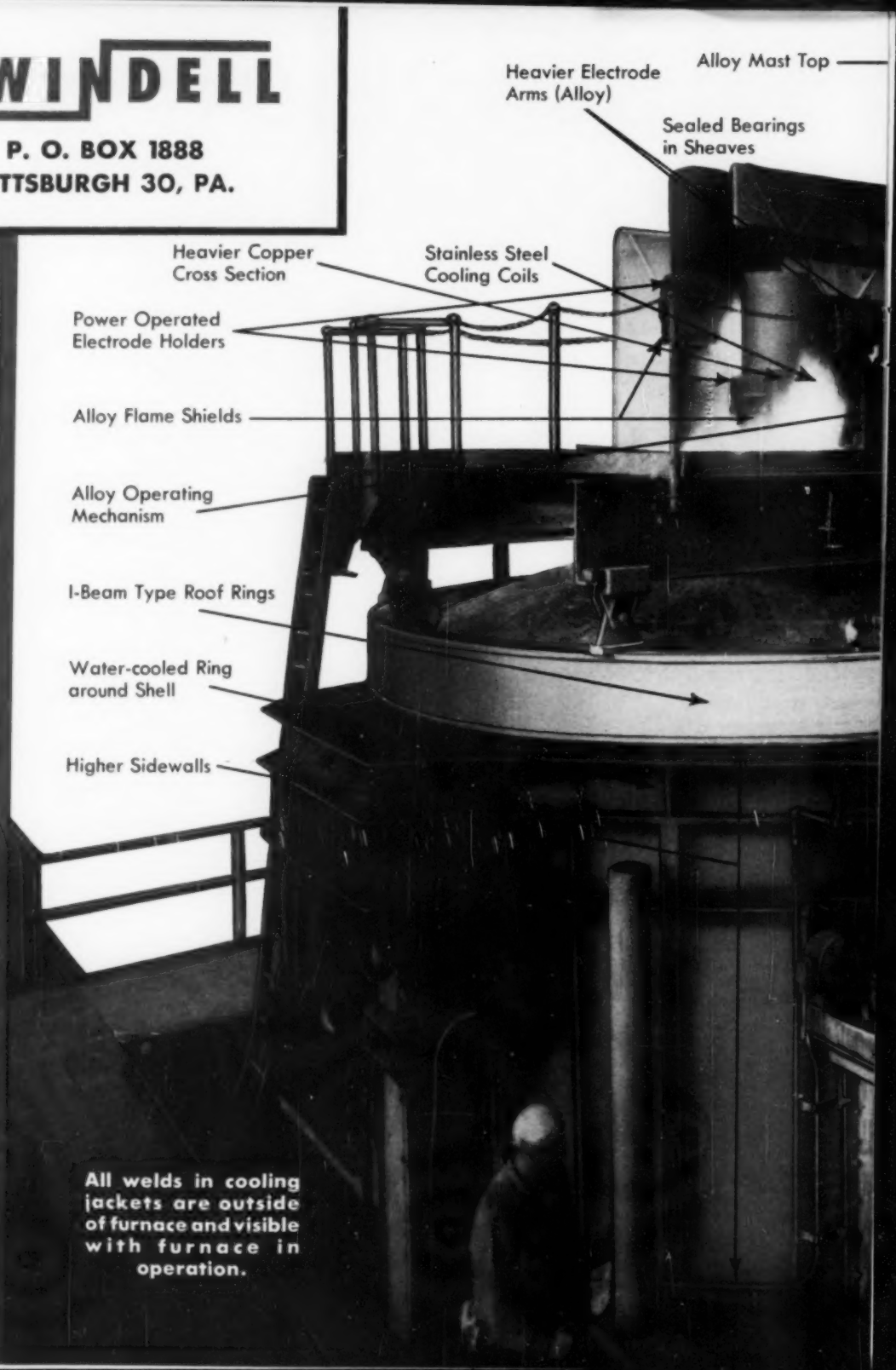

All welds in cooling jackets are outside of furnace and visible with furnace in operation.

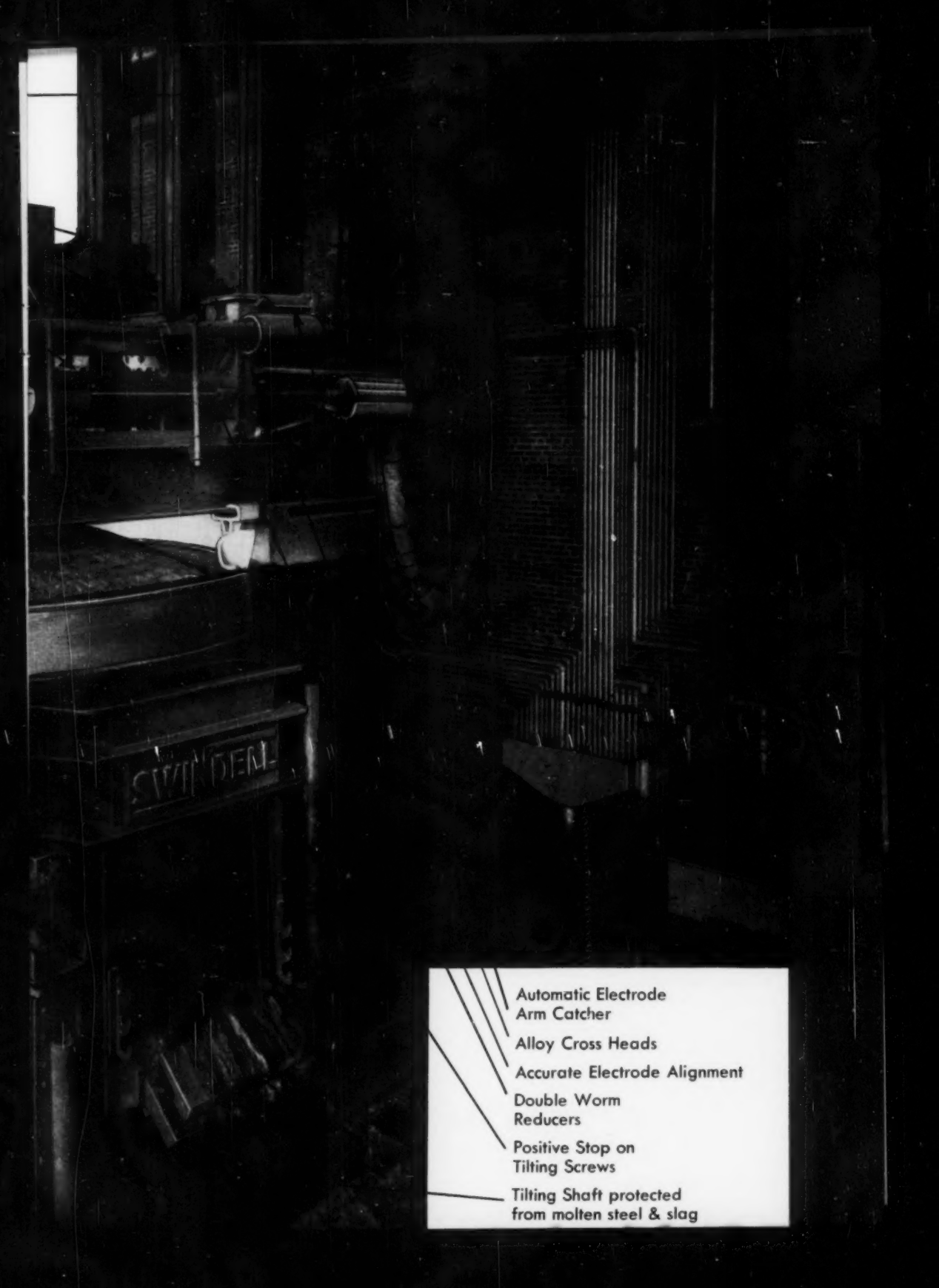
Automatic Electrode Arm Catcher
Alloy Cross Heads
Accurate Electrode Alignment
Double Worm Reducers
Positive Stop on Tilting Screws
Tilting Shaft protected from molten steel & slag

They're headed for

new frontiers

At the Laboratories' school for communications development training, the curriculum includes electronics, oscillations and waves, switching and transmission. Each subject is directly keyed to the latest fields of telephone research.

EACH year the Bell System selects hundreds of engineering graduates from technical schools, to find the answers to communications problems through the application of science and technology. A specifically qualified group joins Bell Laboratories to develop *tomorrow's* telephone system — also, in the present emergency, more powerful electronic devices for the armed services.

They come — thanks to the competence of our nation's educators—with an excellent grounding in fundamentals. To equip them still further, the Laboratories operate a school at graduate level for advanced communications.

The new men receive an intensive course in the latest theory and techniques. At the same time they take their places as members of the Technical Staff doing responsible work which, with their classroom instruction, reveals where they can make the most of their aptitudes.

More than ever America's future must depend on men and women who are trained to think far ahead in technology whether for tomorrow's telephones or national defense. By helping them, Bell Telephone Laboratories help make America's telephone system the world's best, help the armed forces keep our country strong.

BELL TELEPHONE LABORATORIES

Exploring and inventing, devising and perfecting, for continued improvements and economies in telephone service.

BULLETIN S-750

Electro STOPPER HEADS

FOR OPEN HEARTH
STEEL FOUNDRY
ELECTRIC FURNACE
MELTING

Teeming ingots from the ladle in open hearth shop

Electro Refractories & Abrasives Corporation

344 DELAWARE AVE. — West Coast Warehouse LOS ANGELES — BUFFALO 2, N. Y.

TOP QUALITY TELLS . . .

Electro SS STOPPER HEADS

RENDER UNUSUAL SERVICE IN ALL STEEL LADLES

Patent Applied for

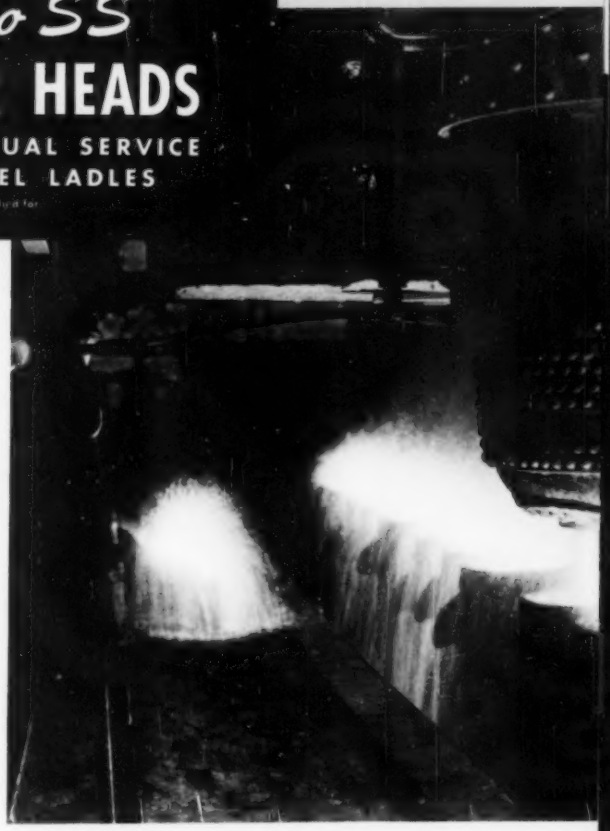

Steel plant metallurgists have been seeking Stopper Heads with properties that give greatest assurance from troublesome internal leakage-source cracks. We of Electro have developed a new composition that gives that assurance. It has been proved in the only practical way such proof is worthy of attention . . . IN ACTUAL USE. Here are some of the advantages of the Electro SS Stopper Heads for Open Hearth, Electric Furnace and Steel Foundry practice:

1. ECONOMY: Cleaner shutoffs.	**5. HIGH COLD STRENGTH . . .**
With resultant desirable savings in ingot cleaning.	Prevents premature failure during assembly.
2. NO SPALLING!	**6. GREAT HOT LOAD-BEARING CAPACITY . . .**
No Electro SS Head has ever shown any spalling cracks in laboratory tests. No Electro Head examined after actual everyday service has ever shown spalling cracks.	Resists ferrostatic head and mechanical stresses of the shutoff. Here again strict laboratory control of quality is evident by top performance.
3. EXCELLENT ABRASION RESISTANCE.	**7. PROPORTIONED THERMAL CONDUCTIVITY . .**
A good hard Head well able to withstand the erosive effect of molten steel. Please note Figure 3.	This prevents failure of the bolt due to excessive heat. Another important evidence of high quality.
4. HIGH SOFTENING POINT . . .	**8. UNIFORMITY—DEPENDABILITY.**
Eliminates sticking to the nozzle at steel pouring temperatures. Open Hearth personnel agree that a high softening point is essential for proper operation of a stopper.	Years of experience have resulted in control of materials and methods to provide maximum uniformity of product. Superior compositions for any steel in any size ladle.

Electro Field Engineers are available for personal consultation concerning recommendations on pouring practice and the use of Electro STOPPER HEADS.

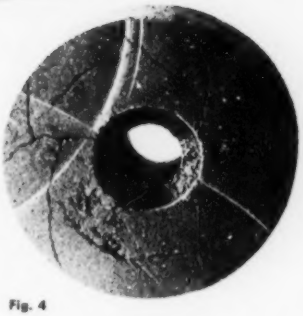

Fig. 4

Fig. 4

Standard clay graphite Stopper Head, cut thru center of body by Electro abrasive cutting-off wheel . . . after being subjected to thermal shock shows clearly the internal thermal shock characteristics with troublesome LEAKAGE-SOURCE CRACKS. This is an unretouched photograph.

Fig. 5

Fig. 5

Newest Electro composition Stopper Head, after the same thermal shock cut thru center of body by Electro abrasive cutting-off wheel . . . shows clearly by comparison, COMPLETE ABSENCE of potential leakage-source cracks. This is an unretouched photograph.

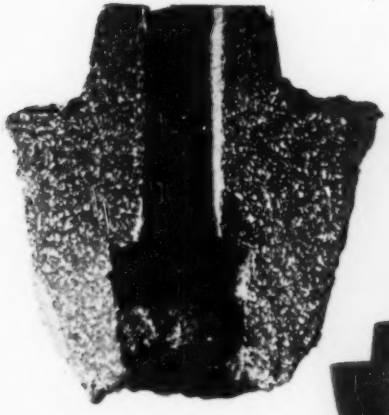

Fig. 3

Fig. 3

Newest Electro composition Stopper Head used in service and then cut thru center by Electro abrasive cutting-off wheel . . . to show clearly the complete absence of troublesome leakage-source cracks and only slight change in contour due to erosion by the steel. This is an unretouched photograph.

Electro-Carb GRAIN No. 90C

(SILICON CARBIDE MADE IN OUR OWN CANADIAN PLANT)

FOR STEEL DEOXIDATION

ELECTRO-CARB 90C for the deoxidation of steel offers numerous advantages:

1. **ECONOMY:** When used as an equivalent replacement for other common deoxidizers Electro-Carb shows marked economies. Electro-Carb may be used in combination with aluminum and as a partial replacement for aluminum.

2. **BETTER QUALITY:** Complete deoxidation, freedom from inclusions and random dispersion of impurities results in improved physical properties.

3. **CLEANLINESS:** The deoxidation reaction of Electro-Carb is exothermic and generates a gas which helps to cleanse the steel. No deleterious products are left in the steel.

ELECTRO-CARB 90C is also effective for recovery of some of the costly alloying elements, and deoxidation of some electric furnace steels.

We would appreciate the opportunity of offering further technical information which will result in economies in your operations.

ROLL GRINDING WHEELS. Among "Electro" specialties are wheels for Roll Grinding . . . probably the most exacting, difficult and ticklish operation of all types of cylindrical grinding. "Electro" has thus far been predominately active in the manufacture of wheels for rough grinding of hot mill rolls, but the valuable experience gained in this work has done much to aid in the production of finishing rolls of a very high quality.

Electro resin-bonded HIGH-SPEED GRINDING WHEELS are available for the grinding of Hardened Steel, Cast Iron, Chilled Iron, Rolls. Electro Field Engineers are glad to be of service in any problem concerning the foregoing mentioned rolls.

Electro
SINCE 1910

HIGH-SPEED GRINDING WHEELS
•
CRUCIBLES
•
STOPPERS
•
High Temperature CEMENTS
•
REFRACTORIES for Chemical and Ceramic Industries
•
ELECTROCARB (Silicon Carbide) ABRASIVE GRAIN

SNAGGING WHEELS, **resin-bonded.** Each snagging operation requires the engineering of a specific wheel . . . to achieve the lowest cost per ton of metal removed. It is not always the wheel that gives the longest life in hours which accomplishes the lowest cost. Neither does the wheel which removes the largest amount of metal per hour always achieve the lowest cost. This is where the services of Electro Field Engineers are highly desirable. Electro snagging wheels are used on Swing Frame, Floor Stand and Portable Machines for grinding a wide variety of ferrous and non-ferrous metals.

●

Grinding Manual 645, containing further information on the foregoing grinding gladly sent on request.

PLANTS AT: Buffalo, N. Y. and
Cap-de-la-Madeleine, P. Q., Canada

Electro Refractories & Abrasives Corporation

344 Delaware Ave. • Buffalo 2, N. Y.

MEET THE AUTHORS

F. A. CROSSLEY

T. E. BROWER

B. M. LARSEN

W. L. GRUBE

R. P. SMITH

F. A. Crossley (p. 1143) studied at Illinois Institute of Technology for his B.S., M.S., and Ph.D. degrees. Now professor and head of dept. of foundry engineering, Tennessee Agricultural & Industrial College, Nashville, he was formerly associated with Stripfounders Inc., and was instructor at Illinois Institute of Technology. Painting, swimming, and tennis are the pastimes of this member of AIME, ASM, AFS and Sigma Xi.

T. E. Brower (p. 1163) associate physical chemist at the research laboratory of U.S. Steel Corp., Kearney, N.J., has been with U.S. Steel for 21 years, nine of which were spent at Donora Works, American Steel & Wire Co. An AIME member, he received the Robert W. Hunt Award in 1948, and spends his spare time studying and collecting antiques and gardening.

B. M. Larsen (p. 1163) studied at the Universities of Wisconsin and Washington for his B.S. and M.S. degrees. Formerly with the U. S. Bureau of Mines, he has been with U. S. Steel Co. Research Laboratory since 1929, where he is now physical chemist and supervisor of process metallurgy research. About 16 papers have been presented before AIME by this member whose hobbies are music and sailing.

W. L. Grube (p. 1171), senior research physicist of the research laboratories div., General Motors Corp., Detroit, received B.Sc. and M.Sc. degrees from Ohio State University and University of Cincinnati. His hobbies are gardening and woodcraft.

R. P. Smith (p. 1174) received his B.S. and Ph.D. degrees from University of New Hampshire and Yale University, where he was an instructor. He is physical chemist at the Research Laboratory, U. S. Steel Co., belongs to ACS, and enjoys photography.

S. Storchheim (p. 1181), senior metallurgical engineer at Sylvania Electric Products Corp., Bayside, L. I., was formerly with Wilbur B. Driver Co. He holds B.S. and M.S. degrees from Brooklyn Polytechnic Institute, and is studying for his Ph.D. at New York University. This member of AIME, ASM, Tau Beta Pi, and Sigma Xi enjoys Boyscouting, music, and plays.

W. R. Johnson (p. 1184), a graduate of Massachusetts Institute of Technology, is research metallurgist for Armour Research Foundation, Illinois Institute of Technology. He has previously been associated with Halcomb Steel Div., Metlab Co., and Standard Steel Works.

M. J. Spendlove (p. 1192), metallurgist for U. S. Bureau of Mines, College Park, Md., served with the Bureau at Salt Lake City, Utah, and Dearborn, Mich. He received his B.S.E.E. degree from University of Utah, and is a member of AIME and AIEE. Home movies, sound recording, and good books occupy his spare time.

H. W. St. Clair (p. 1192), chief of light metals branch, minerals div., U. S. Bureau of Mines, Washington, D. C., has been metallurgist with the Bureau since 1935, and did pioneer research on sonic flocculation. Reading, music, and gardening are the hobbies of this member of AIME, ACS, and Sigma Xi, who graduated from University of Utah with B.S. and M.S. degrees.

E. R. Funk (p. 1206) received his B.S. degree from Worcester Polytechnic Institute, and M.S. and Sc.D. degrees from Massachusetts Institute of Technology, where he is assistant professor of metallurgy. He holds membership in AIME, ASM, AWS, Tau Beta Pi, and Sigma Xi.

F. H. Buttner (p. 1209), a graduate of Michigan State College, received his Sc.D. degree from Massachusetts Institute of Technology where he is research associate in metallurgy. This member of AIME, ASM, and Sigma Xi enjoys photography.

C. C. Wang (p. 1212) was born in Wusih, China, received his B.S. degree at Tang Shan Engineering College, and his M.S. degree from Illinois Institute of Technology. He is presently research assistant at Massachusetts Institute of Technology and studying for his Sc.D. degree. His hobbies are photography, traveling, and music.

C. W. Funk (p. 1138) attended University of Arizona, and graduated from Montana School of Mines and Missouri School of Mines, with B.Sc. and M.Sc. degrees. Before becoming physical metallurgist for Bureau of Mines, this AIME and ASM member was associated with Tin Processing Corp., and was research fellow for Ludlow-Saylor Co.

K. K. Kershner (p. 1138) received his B.S. and M.S. degrees from Missouri School of Mines where he be-

(Continued on page 1103)

S. STORCHHEIM

W. R. JOHNSON

M. J. SPENDLOVE

H. W. ST. CLAIR

Prove your need for

★ Electron * Microscopy— on the new GIANT SCREEN microscope at Norelco® laboratories

● For any investigations requiring high resolution, variable contrast microscopy coupled with electron diffraction—the NORELCO Application Laboratory is prepared to demonstrate the flexibility of this new instrument which has numerous exclusive features resulting in unmatched operating characteristics.

The giant screen provides a larger field coverage at any given magnification than most conventional microscopes, and immediately reveals electron diffraction patterns of specific crystallites.

Among added refinements—such as operating potentials to 100 KV, automatic focusing, relative insensitivity to vibration, and completely enclosed high voltage system—is a unique camera which permits from one to forty exposures on thin-emulsion, high-resolution film and can be operated without disturbing the vacuum.

* * *

And don't forget—our next biannual school on current applications of X-ray Diffraction, fluorescence and absorption analysis, spectrometry and *electron microscopy* will be held in the spring. Enroll now or write for data.

NORTH AMERICAN PHILIPS COMPANY, INC. Norelco

Foremost in X-ray progress since 1896

NORTH AMERICAN PHILIPS COMPANY, INC.

RESEARCH and CONTROL INSTRUMENTS DIVISION ★ DEPT. 1G-12, 750 S. FULTON AVENUE, MT. VERNON, N. Y.

IN CANADA: Philips Industries Ltd., 1203 Philips Square, Montreal ★ EXPORT REPRESENTATIVE: Philips Export Corporation, 750 South Fulton Avenue, Mt. Vernon, N. Y.

Meet the Authors

B. L. AVERBACH

came professor of chemistry. He is now chemist in the minerals technology div., metallurgy branch, U.S. Bureau of Mines. A member of AIME and ACS, his hobbies are baseball and fishing.

B. L. Averbach (p. 1198) studied at Rensselaer Polytechnic Institute for his B.S. and M.S. degrees, and received his Sc.D. degree from Massachusetts Institute of Technology where he is presently assistant professor of physical metallurgy. He has also been associated with U. S. Radiator Corp. and General Electric Co., and has authored many papers. A member of AIME and numerous professional societies here and abroad, he enjoys golf, squash racquets, photography, and cabinet making.

W. ROSTOKER

W. Rostoker (p. 1203) was born in Toronto, Canada, and graduated from University of Toronto and Lehigh University with B.A.Sc., M.A.Sc., and Ph.D. degrees. He is now research metallurgist for Armour Research Foundation, and assistant professor at Illinois Institute of Technology.

E. W. Filer (p. 1174), a graduate of Grove City College, served at the Irvin Works, U. S. Steel Co., and is now physical chemist at the Research Laboratory, Kearny, N. J. Golf and photography occupy his leisure hours.

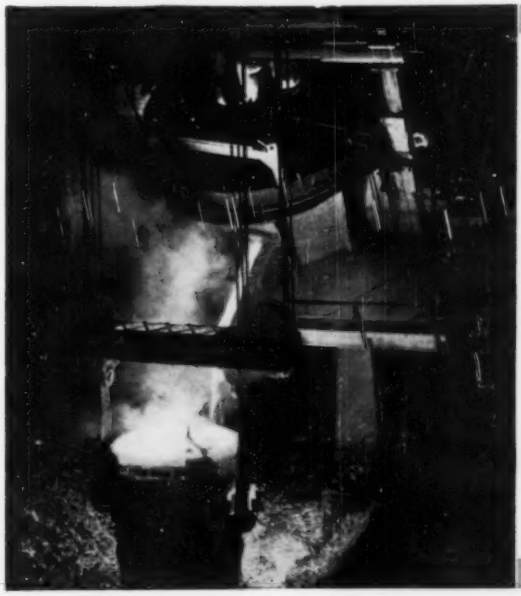

Heroult

ELECTRIC MELTING FURNACE

. . . as ever, the dependable furnace for the production of high-grade stainless, alloy and rimming steels.

Removable roof of new design now available for the larger furnaces.

AMERICAN BRIDGE COMPANY
General Offices: Frick Building, Pittsburgh, Pa.

Contracting Offices in New York, Philadelphia, Chicago, San Francisco and other principal cities
United States Steel Export Company, New York

USS **AMERICAN BRIDGE**
UNITED STATES STEEL

Buehler...

METALLURGICAL LABORATORY EQUIPMENT

. . . provides the metallurgist with the most complete line of modern designed precision machines for specimen mounting and preparation available anywhere in the world. This finely made equipment has been developed through a thorough understanding of the requirements of the metallurgist and a rigid insistance on perfection in the mechanical design and construction of each item.

Everything needed for metallurgical testing from cut-off machines, moulding presses, and grinders to the mechanical or electrolytic polishers is included in the Buehler line.

In setting up complete laboratories or adding items to present equipment the metallurgists will find in the Buehler line of coordinated equipment everything needed for producing the best work, with speed and accuracy.

Write for bulletin of new equipment or information on any specific item. We invite correspondence relative to setting up complete laboratories suitable for any particular requirement.

Exclusive U. S. agents for Amsler and Chevenard Testing Machines.

Operator using the new Model No. 1506 low speed polisher. Section of laboratory equipped with No. 1251 Duo Belt Sander—No. 1700 Electro Polisher—No. 1315 Press.

THE BUEHLER LINE OF SPECIMEN PREPARATION EQUIPMENT INCLUDES . . . CUT-OFF MACHINES • SPECIMEN MOUNT PRESSES • POWER GRINDERS • EMERY PAPER GRINDERS • HAND GRINDERS • BELT SURFACERS • MECHANICAL AND ELECTRO POLISHERS • POLISHING CLOTHS • POLISHING ABRASIVES

Buehler Ltd.
A PARTNERSHIP

METALLURGICAL APPARATUS
165 WEST WACKER DRIVE, CHICAGO 1, ILL.

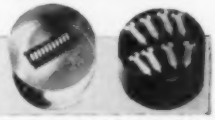

— Coming Events —

Dec. 2-5, American Institute of Chemical Engineers, annual meeting, Chalfonte-Haddon Hall, Atlantic City.

Dec. 5, AIME, Chicago Section, Chicago Bar Assn., Chicago.

Dec. 6, AIME, Philadelphia Section, Engineering Bldg., University of Pennsylvania, Philadelphia.

Dec. 6-8, AIME, Electric Furnace Conference, William Penn Hotel, Pittsburgh.

Dec. 7, AIME, Lehigh Valley Section, annual dinner meeting, Hotel Bethlehem, Bethlehem, Pa.

Dec. 26-31, American Assn. for Advancement of Science, annual meeting, Philadelphia.

Dec. 27-28, American Chemical Society, Div. of Industrial and Engineering Chemistry, symposium on nucleation, Northwestern University, Evanston, Chicago.

Jan. 9, 1932, AIME, Chicago Section, Chicago Bar Assn., Chicago.

Jan. 9, AIME, Connecticut Section, Hammond Metallurgical Laboratory, Yale University, New Haven, Conn.

Jan. 16, AIME, Bessemer Steel Committee, off-the-record meeting, Duquesne Club, Pittsburgh.

Jan. 16, AIME, Western Section, National Open Hearth Steel Committee, Rodger Young Auditorium, Los Angeles.

Jan. 16-18, Society of Plastic Engineers, Inc., annual national technical conference, Edgewater Beach Hotel, Chicago.

Feb. 8, AIME, Southwestern Section, National Open Hearth Steel Committee, Park Plaza Hotel, St. Louis.

Feb. 14, AIME, Philadelphia, Engineering Bldg., University of Pennsylvania, Philadelphia.

Feb. 18-21, AIME, annual meeting, Hotel Statler, New York.

Mar. 3-7, ASTM, spring meeting and committee week, Hotel Statler, Cleveland.

Mar. 12, AIME, Chicago Section, National Open Hearth Steel Committee, Del Prado Hotel, Chicago.

Mar. 16-19, American Institute of Chemical Engineers, Atlanta Biltmore Hotel, Atlanta.

Mar. 19, AIME, Western Section, National Open Hearth Steel Committee, Rodger Young Auditorium, Los Angeles.

Mar. 29, AIME, Philadelphia, Engineering Bldg., University of Pennsylvania, Philadelphia.

Mar. 31-Apr. 2, AIME, annual conference, Blast Furnace, Coke Oven, Raw Materials Committee and Open Hearth Steel Committee, William Penn Hotel, Pittsburgh.

Apr. 12, AIME, Philadelphia, Engineering Bldg., University of Pennsylvania, Philadelphia.

Apr. 21, AIME, Chicago Section, National Open Hearth Steel Committee, Phil Smidt & Sons, Whiting, Ind.

Apr. 25-26, AIME, New England Regional Conference, Kenmore Hotel, Boston.

May 6-9, Scientific Apparatus Makers' Assn., annual meeting, Edgewater Beach Hotel, Chicago.

May 11-14, American Institute of Chemical Engineers, French Lick Springs Hotel, French Lick, Ind.

May 22-24, American Society for Quality Control, annual convention, Onondaga County War Memorial, Syracuse, N. Y.

June 23-27, ASTM, 50th anniversary meeting, Hotel Statler, New York.

July 1-Sept. 30, Centennial of Engineering, Chicago.

Oct. 3, AIME, Southern Ohio Section, National Open Hearth Steel Committee, Deshler-Wallick Hotel, Columbus, Ohio.

Oct. 10, AIME, Eastern Section, National Open Hearth Steel Committee, Warwick Hotel, Philadelphia.

Oct. 10, AIME, Southwestern Section, National Open Hearth Steel Committee, Peoria, Ill.

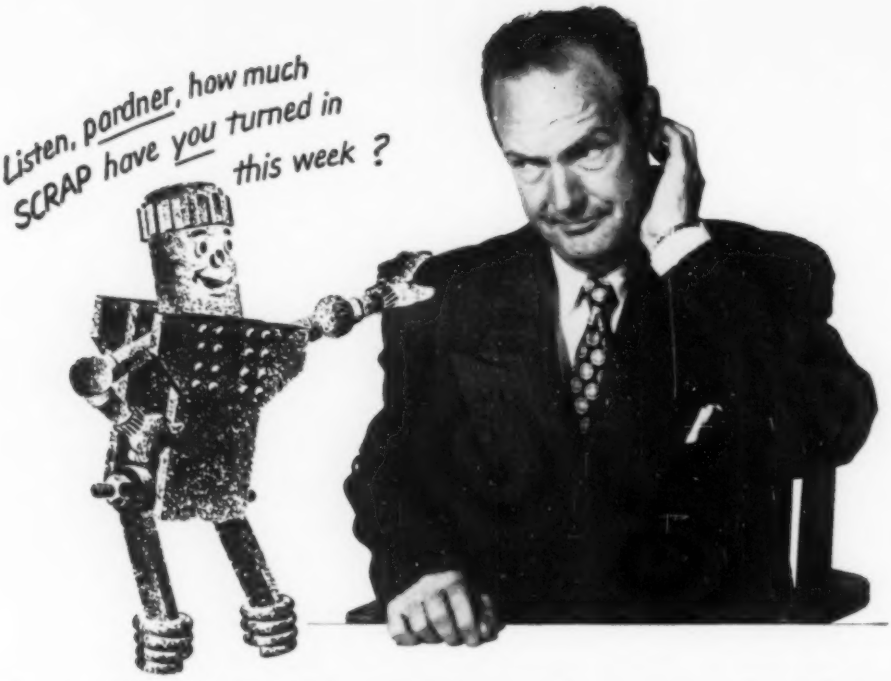

Today, the steel business is your business

—*it needs all your SCRAP, Now!*

SUPPOSE that every steel user were suddenly told that he had to turn in a half-ton of scrap before he could get a ton of steel. It would start the most gosh-almighty treasure hunt for scrap that ever happened.

In effect, this "no-scrap, no-steel" situation virtually exists. For without *all* the scrap that industry can search out and start on its way to the mills, steel production will surely drop. It's as serious as that.

More scrap is urgently needed. Today the mills are turning out more steel than ever before. But they're scraping the bottom of the barrel as far as scrap is concerned. Defense and domestic demands for steel simply cannot be met unless at least 100,000 tons of "purchased" scrap roll into the furnaces—*every day.*

The bulk of this scrap must come from industry. That's why we're asking for your all-out help. That's why it's so important that you make the drive for scrap part of your daily operations. Make it your business to encourage every employee to report any obsolete, broken or worn-out machinery, tool or equipment that has seen its day. From this dormant "junk" must come the heavy melting scrap that the mills need most. Don't let your scrap lie idle; send it on its way. How about it, pardner?

You'll find your local scrap dealers listed in the yellow pages of the phone directory.

USS

1-1326A

This page would ordinarily be used to tell you about

PRODUCTS OF UNITED STATES STEEL

but, because without SCRAP we cannot produce steel, we are asking instead for your all-out help in getting more SCRAP to the mills.

UNITED STATES STEEL SUBSIDIARIES

UNITED STATES STEEL

New Products

New Products | New Literature | New Services

For Further Information or Literature on any Product, Fill in the Coupon and Send to JOURNAL OF METALS
Students are Requested to Apply Directly to Manufacturers for Bulletins and Information

1—PRESSES: Designed to blank, draw, form, and pierce sheet metal parts, *Thunder Bay Mfg.* presses offer a complete range in capacities from 125 tons to 400 tons. A new feature, illuminated press beds, gives the operator full vision at all times for his task. Additional features include bed drilled for die cushion installation, ram length equal to bed length, no gib interference, and large gaps in columns for feeding of coil stock from the sides.

2—HIGH INTENSITY ILLUMINATOR: An iris-diaphragmed, high intensity viewer that allows study of the widest range of X-ray film, has been announced by *General Electric Co.* The wide range is possible because the opening can be steplessly dilated or contracted from a ¼ in. triangle to a 5 in. diam circle and a 100,000 candlepower lamp is used with an average life of 1000 hr at the rated voltage, 115 v. Film densities of from 0.5 to 4.5 can be penetrated by the new illuminator.

3—CONTINUOUS BALL MILL: Development of a new heavy duty continuous ball or tube mill has been announced by the *Patterson Foundry & Machine Co.* Adaptable to fine or coarse grinding, wet or dry grinding, open or closed circuit grinding, the mill may be used for pulverized chemical raw materials, ceramic raw materials, minerals, and numerous finished products. The sizes range from 2 ft diam x 2 ft long, to 10 ft x 24 ft long.

4—TUMBLING MACHINE: A new model tumbling machine has been added to the *Gravi-i-Flo Corp.* line of equipment. Two 18x40-in. ID compartments offer increased capacity per area of floor space permitting grinding, deburring, and finishing of metal parts in larger quantities in faster time cycles. The compartments are furnished with ½ in. plate unlined or ¼ in. plate rubber lined and the 220-440 v, 5 hp motor has a magnetic brake.

5—CUTTING COMPOUND: Cutting compound offered by *Felt Products Mfg. Co.* is said to prevent galling and pitting of metal surfaces, permit higher cutting speeds and assure greater accuracy through maintenance of uniform cutting temperatures. It is recommended for boring, turning, tapping, threading, broaching, and other metal working operations.

6—HYPRO PLANER: One feature incorporated in this new planer introduced by *Giddings & Lewis Machine Co.* is bonded metallic ways to prevent scoring. A new method enables the manufacturer to permanently bond nonmetallic ways to the table, eliminating dowels, pins, screws and bolts, and assuring no scoring. The motor is mounted directly to the bed averting any possible chance of misalignment.

7—VAPOR WRAPPER: Unfinished ferrous metal parts are protected from rust during production stoppages when they are placed in a bin lined with vapor wrapper. This rust-inhibiting paper is a product of the *Nox-Rust Chemical Corp.* Whenever there is moisture in the air a chemical with which vapor wrapper is impregnated, volatilizes, inhibits this moisture, and renders it noncorrosive.

Free Literature

20—AIRCRAFT STEELS: Booklet including revised military specifications has been printed by *Joseph T. Ryerson & Son, Inc.* It also lists the sizes and analyses of aircraft steels carried in stock.

21—CALIBRATION SERVICE: A new catalog giving full details on a calibration service offered to industry is available from *Fischer & Porter Co.* In determining the exact characteristics of innumerable types of fluids under widely varying operating conditions, facilities have been developed which are unique among process equipment suppliers. These various facilities are fully discussed.

22—SILVER BRAZING: Answers to general questions on low temperature brazing, brazing alloys, joint design, heating, methods, and cleaning and inspection are contained in manual issued by *American Platinum Works.* All aspects of silver brazing applications and procedures are covered and drawings and charts are included.

23—PYROMETER SUPPLIES: Catalog gives useful technical data on application and use of thermocouple pyrometric supplies supplied by *Minneapolis-Honeywell Regulator Co.*, Brown Instruments Div. Catalog 100-4 shows views of all assemblies plus special molten metal, pencil type and midget thermocouples.

24—COPPER BASE CASTING ALLOYS: A new 40-page handbook has been issued by *Barth Smelting Corp.* containing Federal, Navy, ASTM, SAE, and AMS specifications for ingots, and castings used or produced by the nonferrous foundry industry. A data section has constitutional diagrams and other reference material.

25—CARBON AND GRAPHITE BRICK: Brochure issued by *National Carbon Co.* gives useful data on this corrosion resistant brick. Important features include thermal shock resistant, light weight, strength, and firm adhesion to bonding materials.

Journal of Metals
29 West 39th St.
New York 18, N. Y.

December

Please send me
- More Information ☐
- Free Literature ☐
- Price Data ☐

on items indicated

1	2	3	4	5	6	7	8	9	10
11	12	13	14	15	16	17	18	19	20
21	22	23	24	25	26	27	28	29	30
31	32	33	34	35	36	37	38	39	40

Name ..... Title .....
Company .....
Street .....
City and Zone ..... State .....

National Research

ONE

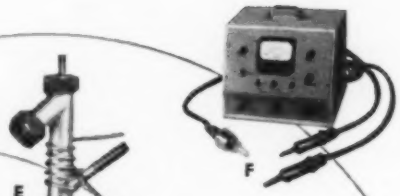

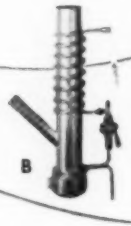

(A) B-4 Booster Pump. Takes over at forepressures as high as 1 m.m., handling large amounts of gas in range of 1 — 30 microns. Suitable for evaporators, furnaces, and other vacuum systems requiring high capacity in this range.

(B) H-2-P Purifying Diffusion Pump. Over 50 liters per second from 10^{-3} to 10^{-6} mm. range. Operates against forepressures as high as 0.300 mm. Blank-off 2×10^{-7} mm.

(C) Gas Free High Purity Metals. Copper, nickel, cobalt and iron. Special melts on request. Ingot weights up to 600 pounds.

(D) Alphatron® Vacuum Gauge. Accurate gauging from 10 mm. to 1 micron. A rugged metal ionization type instrument which can be adapted for recording, controlling, gas filling, and leak detection.

(E) B-1 Booster Pump. A small pump designed for rotary exhaust equipment used in miniature and subminiature tube production. Useful where a small pump is required to quickly obtain pressures in the region of one micron.

(F) Type 710 Thermocouple-Ionization Gauge Control. One instrument for scientific and industrial vacuum gauging. Incorporates two thermocouple gauges (1 — 1000 microns) and one ionization gauge (10^{-3} mm. to 10^{-8} mm. Hg. range) in one control. Automatic input regulation and protective circuit.

(G) Standard Vacuum Furnace. A versatile packaged unit to melt, pour, heat treat, degas, sinter, and anneal under high vacuum or controlled atmospheres. Temperatures up to 2000° C.

(H) Vacuum Seals. For introducing motion, power, or connecting gauges.

(I) High Vacuum Valves. Available in sizes ⅛" to 16". Low rate of leak.

(J) Vacuum Fusion Gas Analyzer. Analyzes metals and alloys, including titanium, for combined or dissolved oxygen, nitrogen, and hydrogen.

(K) Type 701 Thermocouple Gauge Control. A light, portable instrument for vacuum testing in range 1 — 1000 microns. Compact and rugged.

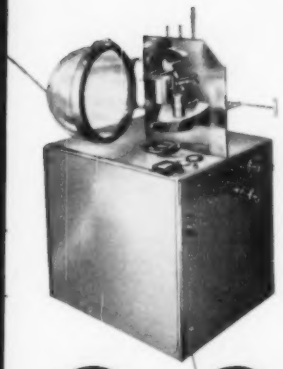

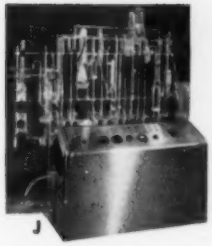

SOURCE!

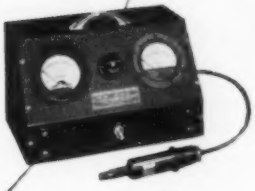

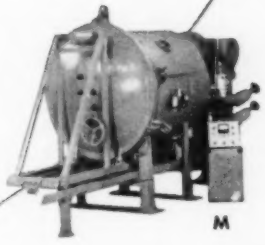

with a COMPLETE LINE *of* HIGH VACUUM EQUIPMENT

You may be using one or two of our products without realizing that at this one source you have available such a full line of high vacuum equipment.

You will find a unique quality in most of these products. They were created to "ideal" specifications drawn up by *manufacturers* who, in many cases, never dreamed we could fulfill their exacting requirements. The products are meeting these requirements day after day on production lines.

Let us supply all your high vacuum equipment needs. You will gain the benefits of a single source of supply plus the high standards of performance designed into National Research products. Write us for further details. National Research Corporation, Memorial Drive, Cambridge, Mass.

(L) H-16-P Purifying Diffusion Pump. Over 10,000 CFM in 10^{-5} range. Suitable for cyclotrons, commercial coating units, and other equipment demanding high pumping speed.

(M) Evaporators. Standard models from laboratory unit to high capacity tank type units.

*Reg. U. S. Pat. Off.

INDUSTRIAL RESEARCH
PROCESS DEVELOPMENT
HIGH VACUUM ENGINEERING
AND EQUIPMENT

METALLURGY
DEHYDRATION
DISTILLATION COATING
APPLIED PHYSICS

National Research Corporation

Seventy Memorial Drive, Cambridge, Massachusetts

...longer life
...like INTERNATIONAL GRAPHITE ELECTRODES

INTERNATIONAL *Graphite & Electrode* **CORP.**

A SPEER CARBON COMPANY SUBSIDIARY

ST. MARYS, PENNSYLVANIA

— Personnel Service —

THE following employment items are made available to AIME members on a non-profit basis by the Engineering Societies Personnel Service, Inc., operating in cooperation with the Four Founder Societies. Local offices of the Personnel Service are at 8 W. 40th St., **New York 18;** 100 Farnsworth Ave., **Detroit;** 57 Post St., **San Francisco;** 84 E. Randolph St., **Chicago 1.** Applicants should address all mail to the proper key numbers in care of the New York office and include 6c in stamps for forwarding and returning application. The applicant agrees, if placed in a position by means of the Service, to pay the placement fee listed by the Service. AIME members may secure a weekly bulletin of positions available for $3.50 a quarter, $12 a year.

POSITIONS OPEN

Sales Engineer, 25 to 35, mining or metallurgical training and experience, to sell ore dressing equipment. Reasonable traveling. Salary, $4000 to $5000 a year. Territory, eastern seaboard. Headquarters, New York. Y6254.

Design Engineer experienced in metal fabrication, tool design, dies, jigs, fixtures. Probably some board work. Salary, to $7500 a year. Location, New Jersey. Y6252.

Metallurgist, graduate, 30 to 45, with practical experience in martempering and austempering. State salary expected. Location, Pennsylvania. Y6251.

Engineers. (a) Process development and equipment engineer to take charge and develop new machinery in the metal manufacturing division. Salary to $7000 a year. (c) Junior Engineers, mechanical, electrical and industrial, with one to three years' experience for design, product control, specification writing and laboratory development in metal manufacturing organization. Salary open. Location, Philadelphia. Y6247.

Staff Aluminum Engineer, 35 to 45, with extrusion and forging experience. Should have a metallurgical or mechanical degree and considerable experience in aluminum production. Location, Michigan. Y6227D.

(Continued on page 1113)

WANTED—MELTING DEPARTMENT SUPERINTENDENT

Immediate opening for person having experience in electric arc furnace melting of tool, high speed, stainless, and specialty steels in long-established mill in Pittsburgh district. Should have considerable practical experience, technical background, and ability for handling men. Reply giving complete record of experience, qualifications, age, and references.

Box K-17
JOURNAL OF METALS

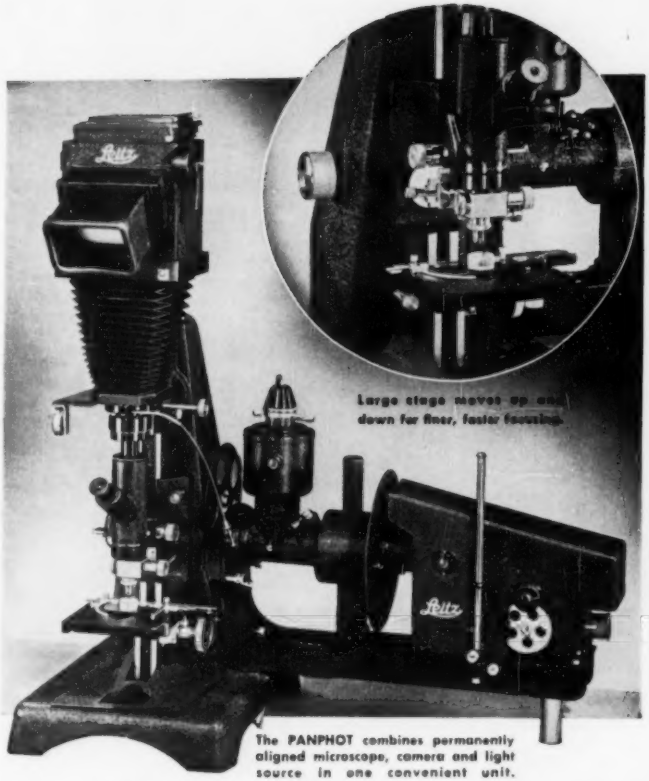

Large stage moves up and down for finer, faster focusing

The PANPHOT combines permanently aligned microscope, camera and light source in one convenient unit.

The Leitz Panphot

Universal Camera Microscope

Only the Leitz PANPHOT enables you to switch from microscopic observation to photo-micrography *without moving from your chair,* for it's the only universal camera microscope with operating parts for both functions right at hand. Changeover from one to the other is fast, simple, dependable. Now available to industrial and technical laboratories, the PANPHOT is a perfect combination of research microscope and reflex camera.

The PANPHOT permits the use of transmitted light, reflected light, darkfield illumination and polarized light. The permanently aligned light source provides a filament lamp for observation and an arc light for photo-micrography.

Easy observation of the image to be photographed is provided by a large ground glass in the reflex mirror camera. The camera accommodates 3¼" x 4¼" plates or cut film for black and white or color work.

A full range of accessories is available to equip the PANPHOT for every phase of photo-micrography, photo-macrography and for drawing and projecting micro-images.

Write today for information to Dept. JM

E. LEITZ, Inc., 304 Hudson Street, New York 13, N. Y.

LEITZ MICROSCOPES • SCIENTIFIC INSTRUMENTS
LEICA CAMERAS AND ACCESSORIES

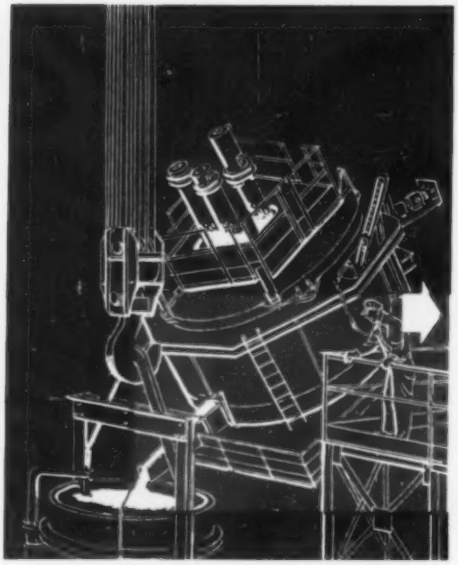

for maximum tonnage of high quality steel . . .

HARBISON-WALKER specialized electric furnace REFRACTORIES

To maintain peak production and dependable operation of electric furnaces, proper selection of refractories is essential. Conditions that affect refractory life vary in different types of furnaces. To meet your specific needs, Harbison-Walker provides a complete line of refractories from which you can select those having the particular characteristics required for various types of service. Among the well-known Harbison-Walker brands for electric furnace service are the following: VEGA and STAR silica refractories, METALKASE, MAGNEX, CHROMEX B, H-W MAGNAMIX and H-W D. B. GRAIN MAGNESITE.

Harbison-Walker Technical Service will gladly assist in selecting the refractories best suited to your individual operating conditions.

TRADE MARK REG. U.S. PAT. OFF.

Harbison-Walker Refractories Company

AND SUBSIDIARIES

WORLD'S LARGEST PRODUCER OF REFRACTORIES

General Offices . . . . . Pittsburgh 22, Pennsylvania

MATERIALS ENGINEERS

A Future
is offered
in AIRCRAFT
GAS TURBINES
at
GENERAL
ELECTRIC
at
Lockland, Ohio

Immediate openings for
Materials Engineers —

Metallurgical engineers, not interested in direct laboratory work, and mechanical engineers to work in an engineering group, responsible for all materials and manufacturing processes used in aircraft gas turbines. Excellent opportunity to become thoroughly acquainted with the gas turbine, and to broaden yourself for future advancement.

At least a B.S. degree in engineering is required. Applicants must be citizens of the United States.

Please Send Resume To:

Technical & Supervisory
Personnel
Aircraft Gas Turbine Dept.
General Electric Company
Lockland, Ohio

Personnel Service

(Continued from page 1111)

Engineers. (a) Executive, 30 to 50, with experience and record of accomplishment in administration of large mining and metallurgical operations. Salary, $15,000 a year. (b) Executive with minimum of 10 years' experience in operation of heavy chemical plants. Salary, $15,000 a year. Location, New Mexico. Y6226.

Chemical or Metallurgical Research Engineer, 30 to 50, engineering or science degree, experience in industrial research desired, and experience in product development design and testing. Work will be on product development, including studies of products, analysis of patents, etc. Salary open. Location, New York. Y6206.

General Manager to take charge of a new division. Must have background in production in forming and pressing of metal. Management experience also required. Salary, $15,000 a year. Location, Chicago, Ill. Y6161.

Assistant Metallurgist, graduate, with at least four years' ferrous and nonferrous experience, for analysis, testing and application with aircraft products company. Salary open. Location, New Jersey. Y5924.

Metallurgical Product Engineer, recent graduate, B.S. in metallurgy, for product engineering work on rod and wire. Excellent living conditions; housing available. Reply giving training, experience, age, salary desired, etc. Location, northern Pennsylvania. Y5832.

Melting Department Superintendent, experienced in electric arc furnace melting of tool, high speed, stainless and specialty steels in long established mill. Should have considerable practical experience, technical background and ability for handling men. Location, Pittsburgh Area. Y5910.

FOR SALE—Bausch & Lomb Research Metallograph. This equipment has been used, but is in good condition and is complete with objective lenses, eyepieces, etc. This equipment can be obtained at a substantial saving. Detailed information will be furnished upon request.
Box L-18 JOURNAL OF METALS

MEN AVAILABLE

Graduate Metallurgical Engineer, 49. Broad experience in melting, forging, rolling and heat treating steel, and manufacture of finished steel products. Has held following positions: General Manager, Works Manager, Consultant and Metallurgical Engineer. Recently completed South American contract. Desires responsible management or consulting position. Free to travel. Location immaterial. M-652.

Harper

DOUBLE DOOR *Electric* FURNACE
for BILLET and BAR HEATING

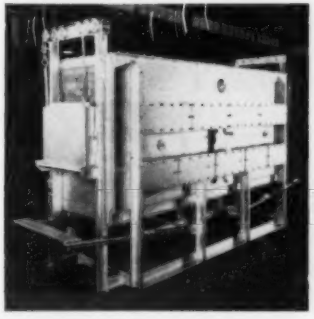

For speed in your general forging operations, specify Harper Electric Furnaces. Shown above is a versatile Harper Furnace designed for billet and bar heating of metals that require special atmospheres. This sturdy unit has a chamber size of 12" x 12" x 8' long with doors at each end.

Ninety kilowatts of power is supplied to the "Globar non-metallic heating elements to give rapid heating of heavy charges resulting in maximum production.

Accuracy of temperature control giving improved workability of billets and bars for rolling and drawing is provided through correct application of temperature control instruments.

Scale usually formed in heating is eliminated through accurate control of special atmospheres.

Double door forging furnaces of this general type are available in several sizes and we are equipped to build continuous furnaces with atmosphere controls for special operations. Write telling of your needs, stating type, size, weight of product and production required, firing cycle, available electric services and special characteristics, and Harper Engineers will be glad to recommend and quote on suitable equipment for you.

* Reg. T.M. Carborundum Company

HARPER ELECTRIC FURNACE CORPORATION
DEPT. No. 10, 39 RIVER STREET BUFFALO 2, N. Y.

Efficiency of

MINSTER PRESSES

Improved by use of

NICKEL ALLOYED IRONS, STEELS and BRONZES

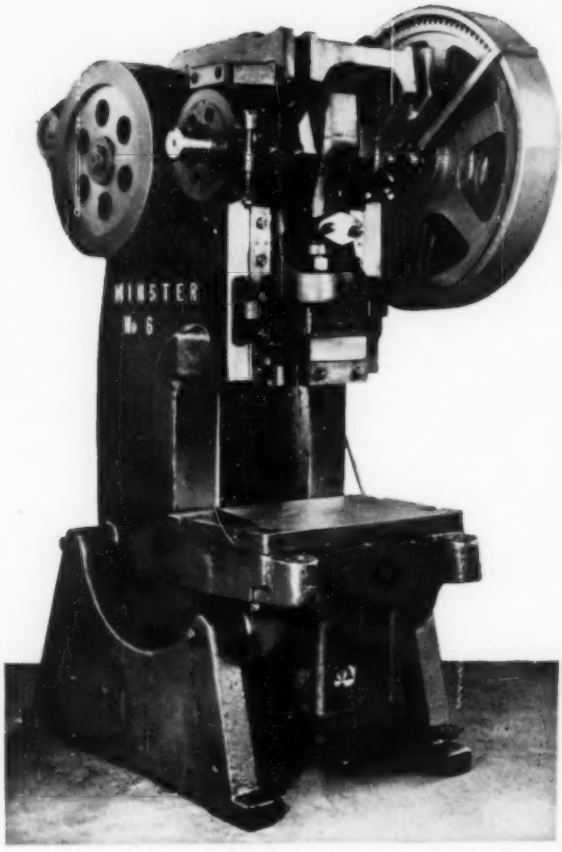

Nickel alloyed castings and forgings are used for vital components in the Minster line of mechanical power presses . . . which range from 12 tons to 1500 tons capacity.

THIS OPEN BACK inclinable press cuts handling costs. Not only can it deliver 60-ton pressure at the bottom of the stroke, but it permits a wide range of feed direction, parts ejection and scrap handling.

Moreover . . . to improve its performance and service life . . . the builder, The Minster Machine Company of Minster, Ohio, utilizes high strength nickel cast iron frames, nickel bronze bearings and forged nickel steel clutch parts.

Main frame and all component castings are produced in Minster's own foundry, from high tensile nickel alloy iron containing 0.90 to 1.75% nickel, depending upon use.

Ellwood City Forge Company of Ellwood City, Pa., forged all clutch throwout and striking parts from heat treated Type 2350 (3½% nickel) steel. This high carbon nickel steel provides stamina to withstand the high stress which occurs when the crankshaft accelerates from "idle" to "full speed" within a fraction of a second.

All bushing for crankshaft bearings, and for lower connection bearings are of 1½% nickel bronze . . . cast by Ryder Brass Foundry of Bucyrus, Ohio.

At the present time, the bulk of the nickel produced is being diverted to defense. Through application to the appropriate authorities, nickel is obtainable for the production of engineering alloys for many end uses in defense and defense supporting industries.

EMBLEM OF INCO SERVICE

THE INTERNATIONAL NICKEL COMPANY, INC. 67 WALL STREET NEW YORK 5, N. Y

Development and functional application of transistors is the responsibility of a Group on Transistors established by the Committee on Electronics of the Research and Development Board. RCA, GE, Bell Telephone, Sylvania, Raytheon, and MIT will have representatives on the Group.

Tungsten carbides are now in experimental use as bearing materials, and they are also being applied by welding techniques as a hard facing material.

General Electric's Carboloy Div. announced production of chromium carbides, half as heavy as tungsten carbide but about equal to it in strength. It is, in addition, highly resistant to corrosion.

Considerable progress has been made in grinding methods for titanium and titanium alloys, one of the real headaches in the fabrication of this metal. An interim progress report by Norton Co., indicates the answer to this problem is largely in lower grinding speeds.

Thermistors, powder metal buttons of minute size, are peculiarly sensitive to temperature changes as low as 0.001°C. The reaction is quite rapid. It is finding wide application in high speed power measuring devices, in biological research, in controlling and regulating temperatures in industrial processes, and is used in controlling electrical circuits. Carboloy Div. of General Electric is one of the major producers of Thermistors.

High top pressurizing of blast furnaces seems to have come into its own, with the announcement that Republic has converted seven of its 21 furnaces to pressure blowing and the fact that its new furnace will incorporate the system. Also, Armco Steel Corp. and Great Lakes Steel Corp. are putting up high pressure furnaces, and U. S. Steel is considering using high pressure in its new Fairless Works furnaces. One furnace at U. S. Steel's Edgar Thomson Works is a high pressure unit.

Interlake Iron Corp.'s expansion plans call for a new blast furnace at its Perry plant using a carbon hearth and carbon lining for about 40 ft up the stack. This will be the first time that an American furnace is carbon lined to this height.

Anaconda Copper Co., whenever the Government approves the project, is ready to finance the construction of a $40 million plant capable of producing 5400 tons of aluminum per year at Kalispell, Mont. Harvey Machine Co., which recently unsuccessfully sought an RFC loan to finance the Kalispell operation, will have a "small minority interest" in the undertaking.

Aerobrite, an additive to pickling baths in steel processing, is claimed to result in brighter finishes and the removal of surface iron salts. Also, it extends the life of pickling baths by eliminating sludging. American Cyanamid Co. introduced the new product. In nickel plating steel sheets prior to porcelain enameling, it can be used as a relatively nontoxic and cheap replacement for sodium cyanide.

Air Reduction Co. has developed a technique for using calcium carbide as a desulphurizing agent for iron.

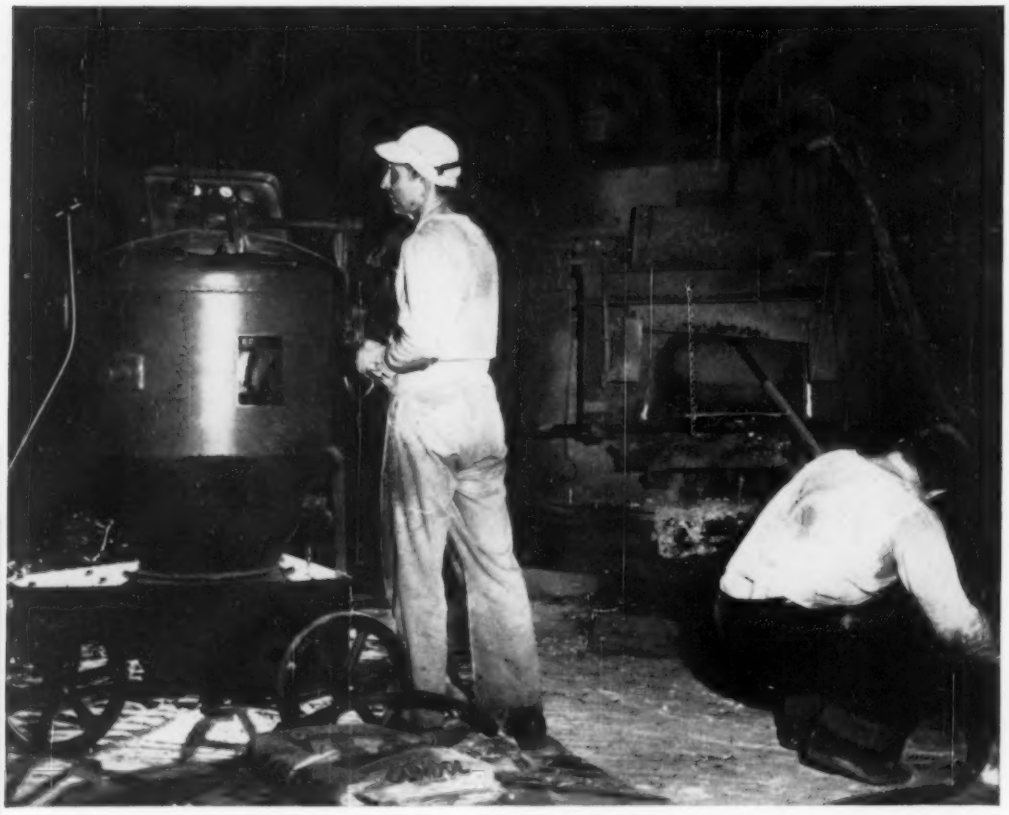

How a prominent tool steel producer cut relining cost $2.10 per heat

THE company that operates this 5-ton electric furnace specializes in fine quality tool steels.

Some months ago the company bought a BRI Gun in order to maintain the sidewalls with Gundol. Formerly the furnace had to be relined about every six weeks. With the BRI Gun, linings have been kept in such good repair that average life has been extended to seven weeks. The twenty-one additional heats per lining have reduced lining cost $2.10 per heat.

At this rate the direct dollar saving will pay for the gun in less than nine months—with the added steel production resulting from less frequent shutdowns providing a dividend on the investment.

Gundol or Gunmix and the BRI Gun—long since found essential for large furnace maintenance—now demonstrate their practical value for smaller furnaces too.

If you operate electric furnaces, regardless of size, the record proves that you can use the BRI Gun and one or more of our gun refractories to advantage.

Basic Refractories Incorporated 843 HANNA BUILDING, CLEVELAND 15, OHIO

Exclusive Agents in Canada: REFRACTORIES ENGINEERING AND SUPPLIES, LTD., Hamilton and Montreal

Ninth Annual Conference . . . Electric Furnace Steel Committee

William Penn Hotel, Pittsburgh, December 6 to 8, 1951

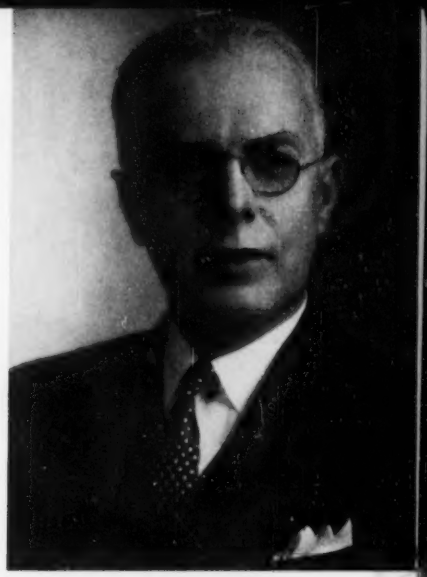

T. J. McLoughlin, Chairman

ELECTRIC FURNACE

IRON AND STEEL DIVISION • AMERICAN INSTITUTE OF MINING AND METALLURGICAL ENGINEERS

STEEL COMMITTEE

Members and Friends of the
Electric Furnace Steel Conference:

The Ninth Annual Conference on Electric Furnace Steel, sponsored by the Electric Furnace Steel Committee of AIME will be held at the William Penn Hotel, Pittsburgh, on Dec. 6, 7, and 8, 1951.

The Directors and the Electric Furnace Steel Executive Committee of the AIME extend a cordial invitation to you to attend these sessions.

The Conference Committee has arranged a program covering every phase of both acid and basic electric steelmaking processes. At present, when steel is so vital to the completion of our National plan for an impregnable defense, such subjects as the Availability and Conservation of Raw Materials; the Use of Special Charging Materials; the Replacement of Strategic Alloys with other Elements; Desulphurization and Sulphur Control; the Production of Low Carbon Stainless Steels and their Stabilization with Rare Earth Elements; Foundry Practice; Bottom Materials and Maintenance; all are of vital importance. The Educational Session on Dec. 8 is designed to be especially helpful to Furnace operators, metallurgists, and students.

The Annual Fellowship Dinner, at 7:00 pm on Thursday, Dec. 6 will be preceded by an informal reception and cocktail party at 6:30 pm. C. L. Austin, executive vice-president of Jones & Laughlin Steel Corp., will be the guest speaker at the Dinner, and C. W. King, executive vice-president of Allegheny-Ludlum Steel Corp., will be the Toastmaster.

The Conference Committee has spared no effort in planning a program which will maintain the standard of excellence established by previous Conferences and provide items of interest to electric furnace steel producers. May I at this time extend my thanks and sincere appreciation to the Chairmen and their Committees.

Sincerely yours,

T. J. McLoughlin

Chairman-Executive Committee

NINTH ANNUAL ELECTRIC FURNACE STEEL CONFERENCE
December 6, 7, 8, 1951, Pittsburgh, Pa.

100% Alloy recovery

WITH AJAX-NORTHRUP INDUCTION HEAT

Ajax-Northrup furnaces are famous for their ability to give back what you put into them. They melt *any* metal with minimum losses, at high speeds, and with extremely accurate control of analysis and pouring temperatures.

For example, a foundry using these furnaces to melt stainless steel for corrosion and heat resistant castings reports the following figures on recovery of elements going into the make-up of 18-8 type alloys:

Ni: 100% Cr: 99% Mn: 90%
Si: 94% Mo: 95% Cb: 92%

Another Ajax user saves $60,000 a year just by reducing chromium losses alone. Still another controls pouring temperatures within 20 deg. F., turns out castings so perfect that repair welding has been eliminated.

Ajax-Northrup can save metals and money for you, too. Write us today for details.

SEND FOR NEW INDUCTION HEATING AND MELTING BULLETIN

134

FOR HEATING AND MELTING

AJAX NORTHRUP

AJAX ELECTROTHERMIC CORPORATION

AJAX PARK
TRENTON 5, NEW JERSEY

Associate Companies
AJAX ELECTRO METALLURGICAL CORP.
AJAX ELECTRIC FURNACE CORPORATION
AJAX ELECTRIC COMPANY, INC.
AJAX ENGINEERING CORPORATION

Electric Furnace Steel Committee

R. H. FRANK

W. M. FARNSWORTH

R. K. KULP

Executive Committee

T. J. McLoughlin, Chairman
U. S. Steel Co., Pittsburgh
H. H. Blosjo
Minneapolis Electric Steel Casting Co.
J. A. Bowers
American Cast Iron Pipe Co.
C. W. Briggs
Steel Founders' Society
J. P. Gill
Vanadium Alloys Steel Co.
M. E. Goetz
Republic Steel Corp.
Ernest Kirkendall, Secretary
AIME, New York
Charles Locke
Armour Research Foundation
M. J. Meinen
Crucible Steel Co. of America
C. E. Sims
Battelle Memorial Institute
C. F. Staley
Armco Steel Corp.
H. F. Walther
Timken Roller Bearing Co.

Conference Committee

R. H. Frank, Chairman
Bonney-Floyd Co., Columbus, Ohio
Samuel Arnold, III
Consulting Engineer
J. H. Baldrey
Allegheny Steel Corp.
J. A. Berger
Molybdenum Corp. of America
Gerhard Derge
Carnegie Institute of Technology
A. C. Ogan
U. S. Steel Co.
R. H. Jacoby
Key Co.
John Juppenlatz
Lebanon Steel Foundry Co.
W. M. Farnsworth, Vice-Chairman
Republic Steel Corp., Massilon, Ohio
Floyd Lemmon
Ohio Steel Foundry Co.
J. S. Marsh
Bethlehem Steel Co.
C. G. Mickelson
American Steel Foundries Co.
C. B. Post
Carpenter Steel Co.
Gilbert Soler
U. S. Steel Co.
G. T. Stowe
E. J. Lavino & Co.
Clyde Wyman
Burnside Steel Foundry Co.

Finance Committee

R. K. Kulp, Chairman
Electro Met. Div., UCC
W. M. Charman, Jr.
Ferro Engineering Co.
V. J. Nolan
National Carbon Div., UCC
H. E. Orr
Vanadium Corp. of America
R. E. Rielly
Charles Taylor & Sons Co.

Committee on Arrangements

A. E. Bickell, Chairman
General Refractories Co.
R. W. Crozier
Electro Met. Div., UCC
Robert Watson
National Refractories Co.
J. G. Seanor
R. C. Remmey Son Co.
T. M. Walton, Jr.
Hiram Swank's Sons

Toastmaster:

C. W. KING, Executive Vice-President, Allegheny-Ludlum Steel Corp.

Speaker:

C. L. AUSTIN, Executive Vice-President, Jones & Laughlin Steel Corp.

Technical Program

Electric Furnace Steel Conference

WEDNESDAY, DECEMBER 5

6:30 p.m.—Rooms 566-68-70

Electric Furnace Steel Executive and Conference Committee Annual Dinner and Business Meeting.

GENERAL SESSION

THURSDAY, DECEMBER 6

9:30 a.m. to 9:45 a.m.—Ballroom

Welcoming Remarks:
By R. H. Frank, Chairman, Committee for the Ninth Annual Conference

Response:
By T. J. McLoughlin, Chairman, Electric Furnace Steel Executive Committee

JOINT TECHNICAL SESSION

THURSDAY, DECEMBER 6

9:45 a.m. to 12:15 p.m.—Ballroom

AVAILABILITY AND CONSERVATION OF RAW MATERIALS

Chairmen:

T. J. McLoughlin, Asst. to Vice President in Charge Operations, U. S. Steel Co., Pittsburgh, Pa.

W. M. Farnsworth, Asst. District Manager, Central Alloy & Chicago Dist., Republic Steel Corp., Massillon, Ohio

1. **Alloy Availability and Regulation:**

   Paper by Fred F. Franklin, National Production Authority, Washington, D. C.

2. **The Outlook for Electric Furnace Scrap:**

   A. Quantity, quality, and composition

   Paper by E. C. Barringer, Executive Vice President, Institute of Scrap Iron & Steel, Inc., Washington, D. C.

3. **Effective Use of Available Electric Steelmaking Materials and Facilities:**

   Paper by Gilbert Soler, Research & Development Dept., U. S. Steel Co., Pittsburgh, Pa.

2:00 to 5:00 p.m.—Ballroom

SPECIAL FEATURES IN ELECTRIC FURNACE PRACTICE

Chairmen:

R. H. Jacoby, Chief Metallurgist, Key Co., E. St. Louis, Ill.

G. Derge, Jones and Laughlin Professor of Metallurgy, Carnegie Institute of Technology, Pittsburgh, Pa.

1. **Sponge Iron and Charge Material:**

   A. A general review of developments in this country with consideration of prospects for commercial availability

   Paper by C. A. Scharschu, Director of Research, Allegheny-Ludlum Steel Corp., Brackenridge, Pa.

   B. Observations on Swedish practice

   Preprinted paper by D. J. Girardi, Metallurgist, Timken Roller Bearing Co., Canton, Ohio

2. **Boron in Electric Furnace Melting:**

   A. General review of use and practice

   Paper by Murray C. Udy, Research Metallurgist, Battelle Memorial Institute, Columbus, Ohio

   B. Special considerations in acid practice

   Paper by E. H. Berry, Chief Metallurgist, Dodge Steel Co., Philadelphia, Pa.

3. **Desulphurization and Sulphur Control:**

   A. Review of "Sulphur Symposium" of AIME from standpoint of applications to electric furnace operations

   Paper by G. Derge, Jones and Laughlin Professor of Metallurgy, Carnegie Institute of Technology, Pittsburgh, Pa.

   B. Use of CaC_2 additions in both acid and basic furnaces

   Preprinted paper by Sam F. Carter, Asst. Melting Superintendent, American Cast Iron Pipe Co., Birmingham, Ala.

   C. Paper by Etienne Spire, Research and Control Dept., L'Air Liquide, Montreal, Que., Canada

INGOT TECHNICAL SESSION

FRIDAY, DECEMBER 7

9:30 a.m. to 12:30 p.m.—Urban Room

STAINLESS STEEL

Chairmen:

W. M. Patterson, Electric Melting Consultant, Allegheny-Ludlum Steel Corp., Brackenridge, Pa.

H. M. Parker, Open Hearth Superintendent, Armco Steel Corp., Butler, Pa.

1. **Experience with Chromite Hearth:**

   Preprinted paper by A. L. Feild, Assoc. Director, Research Labs., Armco Steel Corp., Baltimore, Md.

   Paper by J. E. Herrod, Superintendent, #2 Electric Furnace Shop, U. S. Steel Co., Chicago, Ill.

   Paper by J. J. Green, Asst. Melt Shop Superintendent, Universal Cyclops Steel Corp., Bridgeville, Pa.

2. **Problems Encountered in the Production of 0.03 Pct Carbon Stainless Steels:**

   Paper by Walter Krafts, Chief Metallurgist, Union Carbide & Carbon Corp., Research Labs., Niagara Falls, N. Y., and H. P. Rassbach, Metallurgical Engineer — Development, Electro Metallurgical Co., Div. of Union Carbide & Carbon Corp., Chicago, Ill.

   Paper by R. Shaw, Allegheny-Ludlum Steel Corp., Brackenridge, Pa.

   Paper by J. E. Herrod, Superintendent #2 Electric Furnace Shop, U. S. Steel Co., Chicago, Ill.

   Paper by J. H. Kennedy, Superintendent #1 Melt Shop, Republic Steel Corp., Canton, Ohio

3. **Use of Rare Earth Elements:**

   Preprinted paper by C. B. Post, Metallurgist, D. G. Schoffstall, Melt Shop Metallurgist, and H. O. Beaver, Jr., Metallurgist, Carpenter Steel Co., Reading, Pa.

   Paper by C. W. Powell, Metallurgical Research Dept., Republic Steel Corp., Massillon, Ohio

   Paper by D. J. Girardi, Metallurgist, Timken Roller Bearing Co., Canton, Ohio

   Paper by J. H. Baldrey, Superintendent of Melting, Allegheny-Ludlum Steel Corp., Watervliet, N. Y.

4. **Titanium Alloys for Stabilizing Stainless Steel:**

Paper by Frank St. Vincent, Service Engineer, and R. W. Rebholz, Metallurgical Engineer, Vanadium Corp. of America, Pittsburgh, Pa.

Paper by S. F. Urban, Director of Research, Titanium Alloy Mfg. Div., National Lead Co., Niagara Falls, N. Y.

Paper by G. W. Hinkle, Metallurgical Dept., Republic Steel Corp., Massillon, Ohio

2:00 to 5:00 p.m.—Urban Room

BOTTOM MAINTENANCE AND FURNACE DESIGN

Chairmen:

H. C. Bigge, Superintendent Tool Steel Depts. & Open Hearth Dept. # 1, Bethlehem Steel Co., Bethlehem, Pa.

A. C. Ogan, Superintendent Electric Furnaces, U. S. Steel Co., Duquesne, Pa.

1. **Properties of Some Bottom Ramming Materials:**

Paper by M. P. Fedock, Ceramic Engineer, Republic Steel Corp., Canton, Ohio

2. **Use of High Magnesia Bottom Making Materials:**

Paper by L. W. Austin, Director of Research, Refractory Div., Kaiser Aluminum & Chemical Corp., San Jose, Calif., and J. A. Voss, Jr., Sales, Kaiser Aluminum & Chemical Corp., Akron, Ohio

Paper by H. M. Kraner, Ceramic Engineer, Bethlehem Steel Co., Bethlehem, Pa.

3. **Recent Trends in Mechanical Design of Electric Arc Furnaces and Transformers:**

Paper by R. J. McCurdy, #2 Melt Shop Superintendent, Republic Steel Corp., Chicago, Ill.

Formal Discussion:

Paper by Samuel Arnold, 3rd, Consulting Engineer, American Bridge Co., Pittsburgh, Pa.

Paper by J. R. Lee, Electrical Engineer, Pittsburgh Lectromelt Furnace Corp., Pittsburgh, Pa.

Paper by F. W. Brooke, Sr., Vice President, Swindell-Dressler Corp., Pittsburgh, Pa.

Paper by S. J. Myford, Melting Superintendent, Copperweld Steel Co., Warren, Ohio

Paper by C. F. Staley, Superintendent Open Hearths, Armco Steel Corp., Middletown, Ohio

CASTINGS TECHNICAL SESSION

FRIDAY, DECEMBER 7

9:30 a.m. to 12:30 p.m.—Monongahela Room

ACID VS. BASIC PRACTICE FOR CASTINGS

Chairmen:

C. E. Sims, Asst. Director, Battelle Memorial Institute, Columbus, Ohio

Clyde Wyman, Metallurgist, Burnside Steel Foundry Co., Chicago, Ill.

1. Preprinted paper "Basic Electric Arc Furnace Metal for Casting Production" by James T. Gow, Chief Metallurgist, and Vincent E. Belusko, Metallurgist, Electric Steel Foundry Co., Portland, Ore.
2. Preprinted paper "The Basic Electric Melting Process for the Production of Cast Steel" by Alexander Finlayson, Technical Director, Pacific Car & Foundry Co., Renton, Wash.
3. Preprinted paper "Acid Vs. Basic Practice for Steel Castings" by I. W. Sharp, Chief Metallurgist, American Steel Foundries, Verona, Pa.
4. Preprinted paper "Acid Vs. Basic Steel for Castings" by Donald Helman, Chief Metallurgist, and F. O. Lemmon, Melting Superintendent, Ohio Steel Foundry Co., Springfield, Ohio
5. Paper "Basic Practice at Crane Co." by H. A. Young, Asst. Chief Metallurgist, Crane Co., Chicago, Ill.
6. Paper "Boston Naval Shipyard Arc Furnace Practice" by William J. Richmond, Foundry Metallurgist, Boston Naval Shipyard, Boston, Mass.

2:00 to 5:00 p.m.—Monongahela Room

REFRACTORIES AND RESIDUAL ELEMENTS

Chairmen:

H. H. Blosjo, Metallurgist, Minneapolis Electric Steel Castings Co., Minneapolis, Minn.

H. H. Johnson, Chief Metallurgist, National Malleable & Steel Castings Co., Sharon, Pa.

1. **Refractories for Acid Electric Melting Furnaces:**

Paper by M. W. Demler and J. A. Pierce, Sales Engineers, Harbison-Walker Refractories Co., Pittsburgh, Pa.

Paper by G. S. Kennelley and T. M. Mordaunt, General Refractories Co., Chicago, Ill.

2. **Analysis of Residual Elements for Control Purposes:**

Preprinted paper "Methods for Preliminary Chemical Analysis of Carbon, Chromium and Molybdenum" by R. H. Jacoby, Chief Metallurgist, Key Co., E. St. Louis, Ill.

Preprinted paper "Preliminary Analysis for Carbon, Phosphorus and Sulphur in Steel" by L. H. Arner, Chief Chemist and H. H. Johnson, Metallurgist, National Malleable & Steel Castings Co., Sharon, Pa.

Preprinted paper "Analytical and Wage Standardization in the Chemical Laboratory" by C. M. Nettles, Metallurgist, Texas Electric Steel Casting Co., Houston, Texas

EDUCATIONAL SESSION

SATURDAY, DECEMBER 8

9:30 a.m. to 12:30 p.m.—Urban Room

PROCEDURE IN MAKING A HEAT OF STEEL

Moderator:

C. W. Briggs, Technical & Research Director, Steel Founders' Society of America, Cleveland, Ohio

1. **Preparation of Charge:**
2. **Charging:**
3. **Electrode Manipulations:**
4. **Melt-down:**
5. **Oxidation Practice:**
6. **Slag Practice; Shaping, Slag Removal:**
7. **Refining:**
   - A. Oreing, Oxygen
   - B. Temperature control
   - C. Preliminary tests
8. **Alloying:**
9. **Deoxidation:**
10. **Tapping Practice:**
11. **Ladle Practice:**
12. **Furnace Maintenance:**

Panel Members: (Each to talk on above topics prior to floor discussion and questions.)

Leland Peterson, Asst. Superintendent Melting, Timken Roller Bearing Co., Canton, Ohio

Harold Green, Asst. Superintendent Electric Furnaces, U. S. Steel Co., Duquesne, Pa.

E. C. Eiffler, Electric Furnace Superintendent, American Steel Foundries, Verona, Pa.

S. F. Carter, Asst. Melting Superintendent, American Cast Iron Pipe Co., Birmingham, Ala.

C. A. Faist, Research Metallurgist, Burnside Steel Foundry Co., Chicago, Ill.

John Wyandt, Asst. Superintendent #2 Melt Shop, Republic Steel Corp., Canton, Ohio

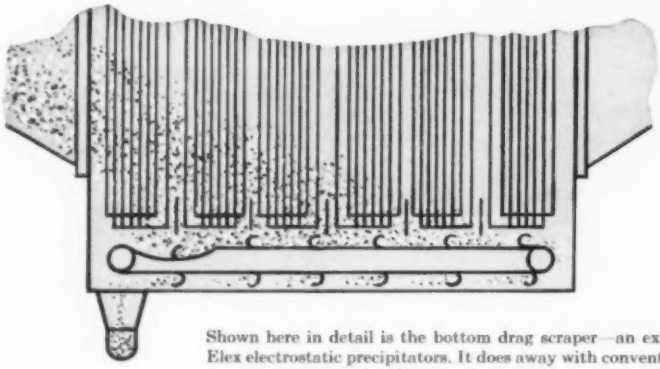

Let's be practical about precipitators

Shown here in detail is the bottom drag scraper—an exclusive feature of Koppers-Elex electrostatic precipitators. It does away with conventional hoppers and simplifies operation by removing dust continuously.

Continuous dust removal

is just one of the many advantages you get with

Koppers-Elex Electrostatic Precipitators

IN ADDITION to high recovery rates, Koppers-Elex electrostatic precipitators offer you *continuous dust removal*. The Koppers exclusive drag scraper operating on a flat bottom replaces the conventional type hopper—with its trouble of dust build-up and clogging. Dust is fed from the precipitator at a uniform rate which simplifies disposal or storage.

Other features of Koppers-Elex precipitators include separately energized multiple series fields—which provide maximum collection of very fine particles. This same feature protects your investment in still another way since the outage of one field does not halt the gas-cleaning action of the precipitator.

To get maximum recovery and effective nuisance abatement, specify Koppers-Elex electrostatic precipitators. For the metallurgical field Koppers has two distinct designs: the dry dust precipitator for hearth, flash, fluidized roasters, etc. . . . and the acid mist precipitator for secondary cleaning.

IF YOU HAVE A GAS-CLEANING PROBLEM, write and outline the details for us to review. There is no obligation. Just address your letter to: KOPPERS COMPANY, INC., *Precipitator Dept.*, 362 Scott St., Baltimore 3, Maryland.

PERFORMANCE GUARANTEED!

Koppers engineers protect your investment in an electrostatic precipitator by guaranteeing both the recovery or gas-cleaning *efficiency* and the *residual content* left in the gas after cleaning. Koppers-Elex electrostatic precipitators are designed, engineered, fabricated, erected, and guaranteed *under one contract* by Koppers Company, Inc.

KOPPERS

Koppers-Elex ELECTROSTATIC PRECIPITATORS

Experiences With Chromite Hearths In Electric Furnaces

by Alexander L. Feild

ONE of the earliest references to the use of chromite as a refractory was made in 1912 by F. T. Havard[1] who stated: "Within the last 20 years chromite has been used as a refractory material and the linings of many furnaces have withstood long sieges owing to the *assistance* which chromite brick lent. (The italics are the writer's). This is effective when used along the slag line, as a buffer layer between the magnesite bottom and the fire-brick foundation, or between the magnesite lower and fire-brick upper furnace walls. This chromite prevented the possible agglomeration or fritting of these two materials together."

Prior to Havard, J. H. Pratt and J. V. Lewis[2] referred to the use of chromite brick for use in basic open-hearth furnaces. Earlier references to such brick have not been found. The notable fact is that between the early references of Pratt and Lewis (1905), Havard (1912), and certain patent disclosures made in 1925 and 1926 which will be discussed later, it seems to have become a routine matter for authors of books on ferrous metallurgy to dismiss chromite brick from any particular consideration except as a *neutral* refractory layer between magnesite and silica in the open-hearth to prevent any fluxing action between the two latter refractories. An even more notable fact is the statement that occurs in the chapter on Furnace Refractories, p. 757 of the recently published "Basic Open-Hearth Steelmaking": "The principal weakness of chrome ore as a refractory is its sensitivity to iron oxide."

In a patent filed in 1925[3] reference was made to the use of a chromite bottom in the manufacture of *stainless iron* where such a chromite bottom was not described as having any superior refractory properties but was alleged to have a certain rather unusual advantage over magnesite. This chromite bottom of Shackelford *et al* was stated to exert a decarburizing action on a high-carbon stainless steel bath from the bottom while a basic slag high in chromium oxide but not high in iron oxide (no percentages of either chrome or iron oxide nor quantities by weight were disclosed) exerted a decarburizing action from the top, after which the heat was tapped. No reduction period was contemplated or disclosed. The idea was to produce stainless iron from high-carbon ferrochrome, an idea incidentally that was not new at that time.

A new 2-ton Heroult furnace, located in the electric furnace melting dept. of Central Alloy Steel Corp., Canton, Ohio, was allocated to melting research, and W. M. Farnsworth, superintendent, and the author, research engineer in charge of steel melting research were determined to make stainless iron from high-carbon ferrochrome. This was accomplished on a furnace bottom of chromite brick. The operating technique involved two new and novel procedures. First extremely large proportions of iron oxide at a hitherto unused high temperature was used to eliminate carbon from the high-carbon source; second, a slag reduction period was introduced in which the quantities of burnt lime and 75 pct ferrosilicon employed resembled a smelting rather than a melting operation.

ALEXANDER L. FEILD is Associate Director, Research Div., Armco Steel Corp. This paper will be presented at the Electric Furnace Steel Conference, Pittsburgh, Dec. 6 to 8, 1951.

Table I. Values of Metal and Slag for a Selected Heat

Metal Bath		Slag	
C, Pct	Cr, Pct	Cr_2O_3, Pct	Fe_2O_3, Pct
0.05	6.95	22.73	21.92
0.055	5.44	21.00	35.52
0.08	7.43	43.68	18.88
0.10	8.64		
0.11	8.90		
0.125	10.7		
0.13	11.9	30.95	10.56
0.14	13.47		
0.15	15.30		
0.18	17.09		

A United States patent application[4] was filed on Dec. 18, 1926. In this application there was described a procedure whereby ordinary base scrap was charged, melted down with the customary small amount of iron oxide to reduce the carbon content to a low value, and the slag removed. Thereafter an extremely heavy addition of low silica iron ore or clean roll scale in an amount equivalent to 625 to 780 lb per net ton of stainless steel ingots was added, melted, and the bath brought to a temperature then estimated to be in the neighborhood of 3250°F. Onto this highly heated slag high-carbon ferrochrome of the 4 to 6 pct carbon grade was charged in several successive lots. A boiling action ensued after each lot was charged with the result that the carbon content of the bath fell to the desired low percentage. Of course, toward the end of carbon oxidation at these extremely high temperatures the rate of carbon removal was gradually slowed down until the carbon content appeared to have reached some sort of stationary point. At the same time towards the end of this oxidation period the original highly fluid iron oxide slag thickened in consistency until an actual crust was formed over a large area of the slag bath. This patent application stated that "*the bottom is an ordinary chrome brick which would seem to be an excellent refractory for the purpose.*" Observation showed that the chrome bottom withstood the action of the highly fluid superheated iron oxide to a remarkable degree.

Samples of metal and slag were taken simultaneously from a number of heats during the progress of the oxidation period and illustrative values given in the patent application for a selected heat are shown in Table I.

At the conclusion of the oxidizing period, and without any slag-off, extremely large additions of burnt lime and ferrosilicon were made to reduce chromium and iron from the deep slag and to return these values efficiently to the metal bath. Chromium loss was stated to be 10 pct or less. Actually, during this experimental campaign at Canton, the loss of chromium was at times less than 5 pct.

Table II. Relation Between Carbon and Chromium During Oxidizing Period

Carbon, Pct	Chromium, Pct
0.30	15.0 to 17.0
0.20	14.0 to 15.0
0.14	11.0 to 13.0
0.12	9.0 to 11.5
0.10	8.5 to 10.5
0.08	7.5 to 10.0
0.06	7.0 to 9.5

William Farnsworth, during these experimental operations at Canton, invented a method for the direct remelting of stainless steel scrap for which an application[5] was filed on June 29, 1927, in the disclosure of which reference was made to the remarkable manner in which the chromite bottom withstood the fluid and highly-heated iron oxide slag during the oxidizing period. However, in the scrap remelting process a rammed magnesite bottom was preferred because it was thought that this bottom withstood the action of the reducing slag formed by the heavy additions of burnt lime and ferrosilicon better than the chromite bottom.

Both viewpoints undoubtedly were correct so far as these views extended. Opportunity did not present itself at that time to pursue the experiments further.

A few years later at Lockport, N. Y., new experimental work was initiated with a 6-ton Heroult furnace lined with chromite brick. These experiments progressed as far as a sizable commercial operation in the period 1929 to 1931. First the Canton experiments with high-carbon ferrochrome and base scrap were repeated on the larger scale in the production of stainless iron with essentially similar results. To minimize the progress of slag-line attack during the reducing period, chrome ore was used as a patching material. Also, it was discovered that a mixture of stainless scrap and high-carbon ferrochrome could be used in the initial charge to supply the entire needed chromium content of a final product having the same analysis as the stainless scrap which was utilized. Stainless steel production at Lockport during 1929 to 1931 was intermittent, the average melting campaign usually comprising one or two consecutive heats, followed by a shut-down. Six or seven consecutive heats was reached once or twice. The chromite-lined furnace could not be used for any other grades, either on account of a small chromium pickup from the slag-line area or because two other 6-ton furnaces, magnesite-lined, were available. Nevertheless, operations did get to the point where about 25 heats could be made on a chromite bottom in spite of those drawbacks to long life which could not be avoided.

The stainless scrap high-carbon ferrochrome process employing a chromite bottom was transferred to Baltimore in the latter half of 1931 by virtue of an initial contract with the Lockport concern, which gave it only shop rights to the invention. The company, at that time was known as the Rustless Iron Corp. of America, later as the Rustless Iron & Steel Corp., with which Armco Steel Corp., then The American Rolling Mill Co., established relations a few years later as a source of stainless steel ingots. Armco acquired Rustless by merger in 1946. The process originally developed at Lockport was improved almost from the start by Rustless. Credit is due to William B. Arness, formerly melting supt., and to Donald L. Loveless who succeeded him in 1938 after serving as chief melter from the start for these improvements and for perfecting what has come to be known informally as the "Rustless Process."

There was filed a patent application[6] on Sept. 4, 1931 relating to the use of a chromite bottom in conjunction with stainless scrap and high-carbon ferrochrome as sources of chromium. In this patent the data in Table II was given to exhibit in a general

way the relation between carbon and chromium during the oxidizing period.

The practice described was followed with 70 pct stainless scrap (ingot weight basis) for about a year, from which time onward it was further developed as stated above. These developments consisted among other things in the use of chrome ore as a source of chromium, with or without high-carbon ferrochrome, and in conjunction with stainless scrap. In 1945, at the Electric Furnace Steel Conference during the Basic Session on Steel, the Rustless process was discussed.

In Rustless practice, the bottom is lined with 9 in. straight chrome brick of the 3 in. series laid in 5 or 6 Rowlock courses to a thickness of 22½ to 27 in. The chromite side walls range from a thickness of about 34 in. to about 18 in. at the slag-metal interface and thence upward to about 15 in. The average consumption of chrome brick during the year 1950 amounted to less than 12 lb per net ton of stainless steel ingots. A typical analysis of the chrome brick in use would be about as follows: Cr_2O_3, 34.4 pct; FeO, 13.8 pct; Al_2O_3, 30.2 pct; MgO, 16.4 pct; and SiO_2, 2.0 pct.

Such brick is produced from the refractory grade of chrome ore, which is not to be confused with the ferroalloy grade where the base Cr_2O_3 percentage is 48 pct and the ratio of Cr to Fe is specified as 3 to 1 min. For the chrome ore used in the Rustless process the ratio of Cr to Fe is not important within certain limits. In other words, a lower ratio is not a handicap. Chromite bottom life for 12 and 16-ton Heroult furnaces is 800 heats and upwards, while for 25-ton Heroult furnace the bottom life is somewhat longer, 1000 heats and upwards. The average life of a conventional magnesite bottom producing stainless steel or, for that matter, any kind of electric furnace steel, is not as long.

As previously stated, it was disclosed in the original patent application, based on the Canton experiments, that the chromite bottom was exposed to unusually high bath temperatures of about 3250°F in carrying out the single slag oxidation-reduction process. This estimated temperature was based on the metal bath temperature at the end of the reduction period and was arrived at by the crude method of finding out how much cold stainless steel scrap could be quickly remelted by the metal bath with just enough cooling effect to bring the bath to the normally accepted tapping temperature.

In general, recent experience has confirmed the fact that the metal bath temperature at the end of the reduction period is somewhere in this neighborhood. These recent estimates are more reliable because they were obtained by optical pyrometer measurements on slag at tap. Platinum thermocouple readings by the immersion method at this same time have shown a temperature somewhat above the melting point of platinum which melts at 3191°F. In these measurements the platinum wire of the thermocouple melted, but the autographic temperature chart showed an approach to temperature equilibrium. Experimental measurements with a tungsten-molybdenum thermocouple at the end of the oxidizing period in the more highly-heated areas of the metal bath beneath the raised electrodes have given strong indications that at least locally metal temperatures of 3750°F are reached.

Experience has shown that at these highly elevated temperatures a magnesite bottom simply cannot exhibit in a Heroult electric steel furnace its usual superior properties as a refractory. Over a period of years a number of trials have been made with a magnesite bottom with the same result, namely, that at the end of a campaign of from one to three heats the magnesite bottom was more or less completely destroyed.

In the case of the process under discussion, chrome ore cannot serve as a slag or as a slag component to effect any significant decarburizing action on a stainless steel bath. From this it is obvious that the chromite bottom, which is substantially solid and less reactive than a high chromium-oxide slag, likewise exerts no decarburizing action. To effect decarburization by a slag at the elevated temperatures mentioned it is necessary to employ large quantities of some form of iron oxide such as magnetite concentrates or roll scale. Obviously, certain other metallic oxides readily reduced by iron, such as nickel oxide, would form iron oxide on coming in contact with the metal bath.

In the case of Rustless process, tapping temperatures are selected in accord with the same principles that apply to ordinary stainless melting practice. During the finishing stage of a heat the power input is relatively small, which permits the metal bath to fall to the desired tapping temperature. It is during this period that the preliminary chemical analyses are made. Metal temperature measurements by means of the platinum immersion thermocouple are made on all heats prior to tapping, and when necessary this metal bath is adjusted to the proper tapping temperature for each particular grade. The thermocouple technique employed is essentially that which was described in 1944 by L. F. Weitzenkorn during the session on Refining, Deoxidizing and Pouring at the Electric Furnace Steel Conference.[7]

For the sake of completeness, reference should be made to the session on refractories where E. J. Chelius[8] referred to the use of one 2½ in. flat course of chrome brick laid on top of magnesite brick, making a total bottom thickness of 14½ in., which had at that time been used in 35 and 70-ton furnaces largely devoted to stainless steel melting, presumably by a process involving the oxygen lance which was developed by him.

Finally, those who are sufficiently interested in the general subject will probably find it of interest to read what C. A. Zapffe[9] had to say about the use of the chromite bottom in connection with the Rustless process. Dr. Zapffe, as most of you know, had been a member of the research staff of Rustless in Baltimore.

References

[1] *Refractories and Furnaces*, First edition (1912), p. 9.

[2] Columbium and the Peridotites of Western North Carolina. *North Carolina Geological Survey*, vol. 1, (1905). pp. 387 to 389.

[3] E. J. Shackelford, W. B. D. Penniman, and J. R. Cain: *U. S. Patent* 1,622,977.

[4] A. L. Feild: *U. S. Application* 155,767, issued as *Patent* 1,812,941 with major revisions in disclosure on July 7, 1931.

[5] W. M. Farnsworth: *U. S. Patent* 1,744,374 issued Jan. 30, 1930.

[6] A. L. Feild: *U. S. Patent* 1,925,182, issued Sept. 5, 1933.

[7] L. W. Weitzenkorn: *Electric Furnace Steel Proc., AIME*, vol. 2 (1944), pp. 143 to 151.

[8] E. J. Chelius: *Electric Furnace Steel Proc., AIME*, vol. 2 (1944), p. 81.

[9] *Stainless Steels* (1949), ASM, pp. 244 to 247.

J & L Dedicates 2 Million Ton Open Hearth Shop

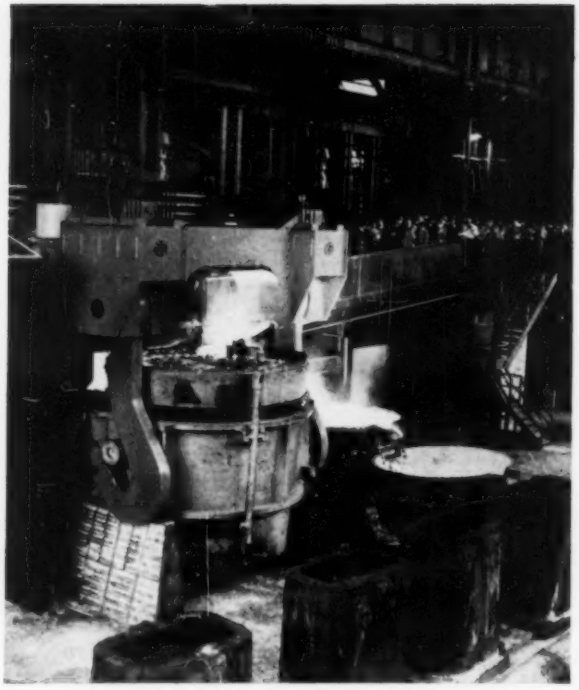

Tapping the first of J&L's new 11 open hearth furnaces at its Pittsburgh works.

A BAZOOKA boomed, there was a brilliant flash of light, and the steel poured from the taphole of the No. 4 furnace at Jones & Laughlin Steel Corp.'s new open hearth shop at its Pittsburgh Works on Oct. 30, 1951. The 250 tons of steel rushing into the huge ladle climaxed a 2 hr plant tour and dedication ceremony; and marked the completion of the first of 11 such furnaces in the new open hearth shop. While it will be some months before the remaining 10 furnaces are in regular production and the auxiliary equipment is operative, the 2 million ton a year shop has been only 17 months in the building. The cost is estimated at $70 million.

These 11 furnaces will incorporate every known successful design feature. They are of the suspended basic end and suspended basic port roof design. Each furnace rests on two concrete piers. The inside face of each pier extends to form a base for the front flush buggy in which the cinder pot is carried. The slag chute leads down through the charging floor to the cinder pot. Furnace body and uptakes are streamlined, and critical areas such as knuckles, uptakes, fantails, and flues are arranged for proper flowing of incoming and outgoing gases. Slag pockets are fitted with 4½ ft high false walls, which are dug out during repairs to facilitate removal of the slag pocket deposit.

One feature of the basic end-type furnace is the friability of the slag pocket deposit. Also basic ends withstand higher operating temperatures and permit longer furnace campaigns before replacement. The suspension arrangement permits patching without disturbing walls above or below the patched area.

The large bath area, 1050 sq ft and a depth of 31½ in., makes for a fast working furnace. These furnaces are equipped to burn gas, oil, or tar, or combinations of these fuels. Controls are arranged to handle oxygen for combustion and they will regulate the total amount of oxygen introduced into the furnace, ranging from straight air through any combination of air and oxygen.

Efficiency and economy were the keystones in the design of the material and scrap stockyard and scrap preparation. The system is highly mechanized, with magnet and bucket-type cranes, charging boxes, and charging cars. The three 10-ton magnet cranes are fast acting units and will be used to unload scrap from railroad cars into charging buggies and boxes on the same level as the railroad track. A scrap bin, running the full length of the loading track, will

C. E. Wilson, Director of Defense Mobilization, detonated the jet tapper that started the steel flowing from the first open hearth in the new shop.

permit uninterrupted operation while railroad shifts are made. The bin will be large enough to permit scrap separation.

Loaded cars will be weighed automatically as they pass over a track scale platform at a predetermined speed. If speed is too great, a light system becomes operative and the scale ceases to function. Scrap will be moved then to a lean-to building by an 80-ton diesel electric locomotive.

Fluxes and other additions will be supplied also from the stockyard, and will be handled by a 15-ton crane until the furnaces are completed. Then, all materials except scrap will be handled by overhead gravity feed bins located alongside the row of furnace stacks. Charge and feed ore, limestone, dolomite, rolls scale and other materials will be delivered from these bins to buggies spotted by a mine-type locomotive, which will deliver the material either to the lean-to building or to the furnaces. The lean-to building will run the full length of the furnace building, 1430 ft. It has three tracks, one for storing loaded buggies, one for unloading ferroalloys, etc., into floor bins, and the third is a running track.

The two hot metal mixers—800 ton capacity units—are electrically driven and end charged. End charging is performed by inserting a runner spout into the end of the mixer by means of a movable car. End charging avoids scouring the lining when loading mixers. Mixers are equipped with individual heating burners and combustion air supply. A safety provision in the event of electric power failure when pouring out is an emergency air-driven engine to return the mixer to horizontal position. A two section 150-ton scale at each mixer records and prints the weights. Maintenance is handled by a 60-ton crane.

The pouring pit runs the full length of the furnace building and is served by three ladle cranes of 350 tons capacity and almost 70-ft span. Three pouring platforms are respectively 277 ft, 497 ft, and 277 ft long and 13 ft wide. All are equipped with bins and scales for storage and weighing mold additions such as aluminum and ferrosilicon. Traveling jib cranes of 1-ton capacity serve these platforms, particularly for capping rimmed ingots.

Two 400-ton stripping machines are the latest built and most modern design. They are of the low type with telescoping screws, and use no counterweights.

The company held an official ceremony celebrating the tapping of the first of these 11 furnaces, with Defense Mobilizer Charles E. Wilson addressing a group of 300 guests. Mr. Wilson commented on the successful completion of the first of these 11 furnaces within 17 months from the time ground was broken, and stated the J&L unit represents the first major "bringing in of open hearth ingot production facilities in the steel industry since the beginning of the current emergency." In 1953, he said, the nation's steel ingot capacity will be 118 million tons a year.

J&L began an expansion and modernization program in 1946 that was estimated would cost $400 million. The open hearth shop at Pittsburgh is the largest single project of the program and will cost $70 million. By the time the whole program is completed, J&L's capacity will be increased 32 pct. The program includes work at practically all plants and at many of J&L mining operations: At Pittsburgh Works new facilities include this open hearth shop, a blooming mill, several soaking pits, a 10-in. bar mill, and scarfing yard facilities. At Aliquippa Works, tin plate facilities will be expanded by 50 pct, and new facilities include an electro-cleaning line, a tandem temper mill, an electrolytic tinning line, and a rod mill. Otis Works is getting a new blast furnace with 200,000 tons per year increase capacity, 2 open hearth furnaces, new soaking pits, and a new ore bridge. Improvements of cold mill facilities and ore dock are also underway.

An underground ore mine is being developed in Michigan, and new facilities at Minnesota and at Benson Mines in New York are being added. A new coal preparation plant at California, Pa. is in operation, and 2 diesel towboats and barges, added to river fleet, were put in service recently.

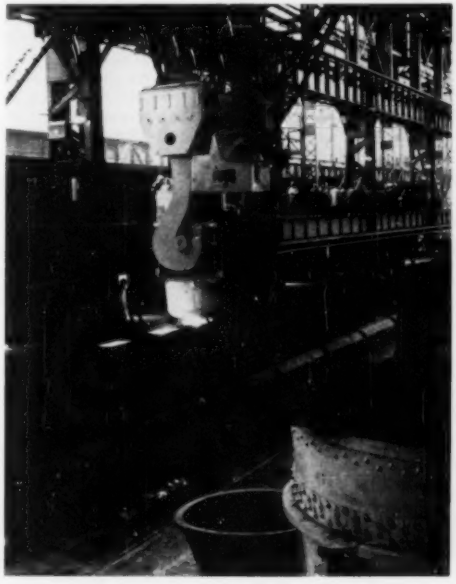

Teeming the first heat from a 250-ton ladle.

Grinding Methods Evolved for Titanium

Grinding a 12x15 in. titanium ingot on a swing-frame grinder.

The following information on grinding titanium is an interim and tentative report. The subject is so new that time has not permitted thorough investigation and development either in the laboratories or in the field.

These results, showing the unexpected, beneficial effects of low wheel speed, were obtained solely with vitrified bonded wheels on a small surface grinder. It is possible that similar results will be obtained with vitrified bonded wheels in other precision operations such as cylindrical or internal grinding, but experiments have not been run yet to determine whether this assumption is justified.

No information is available as yet that would indicate whether organic bonded wheels can be used to advantage at extremely low wheel speeds.

TITANIUM, whether commercially pure and soft, like Ti-75A, or moderately alloyed so as to strengthen and harden it considerably, like RC-130B or Ti-150A, is an unusual and difficult metal to grind because it wears the grinding wheel at an extremely high rate. Available evidence indicates that titanium wears an abrasive grain by some sort of surface reaction with it, probably for the same reason that molten titanium reacts with all known refractories.

Current surface grinding research at Norton Co. laboratories since March 1951 indicates that the high rate of wheel wear can be overcome by using *slow wheel speeds*.

The present stage of the research work concerns the study of the variables in a precision grinding operation. Each of the variables was studied for its effect on the *Grinding Ratio*, which is defined as the ratio of cubic inches of material removed to the cubic inches of wheel wear. This ratio is called the G value in this report. The higher the value of G, the lower is the wheel wear and hence the easier it is to maintain dimensional tolerances.

The advantage of knowing the value of G is that it permits calculating approximately the wheel wear on the diameter for a given size wheel and a given work surface area. Experience will indicate the tolerances that can be maintained for a certain amount of wheel wear. The G values for titanium and its alloys are roughly between 2 and 3 and this is just the range found for high carbon-high chromium die steels ground with a 32A46-H8VBE wheel. Therefore, the tolerances obtainable in grinding titanium alloys should be about the same as can be obtained in grinding similar size surfaces of parts made of this type of die steel.

Typical grinding results obtained on commercially pure titanium and three titanium alloys are presented in Table I. The conditions that were used are listed in Table II. The relative values of G in Table I are those obtained under this particular set

Table I. Results of Grinding Titanium and Its Alloys

Material	Hardness	G Value, In.	Profilometer Readings in Microinches Rough-ing	Finish-ing
Ti-75A	R_B 82	3.0	85	25
Ti-150A	R_C 37	2.3	40	15
RC-130B	R_C 37	2.0	40	15
RC-130B	R_C 42	2.0	40	15
Ferrochrome Ti (Experimental)	R_C 29	1.7	50	20

of grinding conditions, which are not necessarily the best for each of the materials investigated. Under another set of conditions, better values of G might be obtained for some of the materials and poorer for others.

Transcribing the data in Table I into radial measurements may be helpful. For example, a 3x3 in. bar of titanium RC 130B ground under the conditions in Table II, resulted in 0.015 in. depth of material removed at the conclusion of 0.020 in. downfeed. In finish grinding one of the titanium alloys, it was found that increasing the unit crossfeed from 0.010 to 0.025 in. approximately doubled the profilometer readings.

Although rolled titanium may vary considerably in its mechanical properties parallel and perpendicular to the rolling direction, no difference could be found in the grinding characteristics for these two directions.

The tests showed the following conditions:

a. *Abrasive*—32 *Alundum* abrasive is superior to all others. 38 *Alundum* is next best, but it wears about 20 pct more (20 pct lower value of G.).

b. *Grit Size*—60 grit is best for surface grinding. Finer grit sizes result in higher wear.

c. *Grade of Grinding Wheel*—K or L.

d. *Structure Number*—8 is better than 12P or 5.

e. *Bond*—Vitrified is probably best. Resinoid bonds have not been studied yet adequately.

f. *Treatment in Wheel*—Sulphur in the wheel as a treatment does not improve the grinding action.

g. *Grinding Fluids*—Various soluble oil compounds acted about the same in the preliminary experiments. More work needs to be done under improved grinding conditions.

h. *Wheel Speed*—2000 sfpm appears to give the lowest wheel wear; 3000 sfpm is almost as good. (Change the pulley or motor to obtain the desirable speed.)

i. *Table Speed*—Wheel wear is least between 400 to 500 ipm and increases at both lower and higher table speeds.

j. *Unit Downfeed*—0.001 in. maximum. Heavier downfeeds may cause burn and increase the wheel wear.

k. *Unit Crossfeed*—Maximum of 0.050 in. for 0.001 in. downfeed or 0.100 in. for 0.0005 in. downfeed; otherwise wheel wear increases.

l. *Width of Wheel*—Use widest wheel possible, even a recessed wheel to permit mounting.

m. *Diameter of Wheel*—Should be as large as possible to minimize radial wheel wear. Use full size wheel at low rpm. Most of the benefit of low wheel speed is lost if the low wheel speed is obtained by the use of a smaller diameter wheel.

Table II. Grinding Conditions Used to Obtain Data in Table I

Wheel	8 x ½ x 1¼ in. 32A60-L8VBE ALUNDUM Vitrified
Machine	NORTON 6 x 18 in. Surface Grinder
Wheel Speed	2200 sfpm
Table Speed	450 ipm
Unit Downfeed	0.001 in. for roughing, 0.00025 in. for finishing
Unit Crossfeed	0.050 in. for roughing, 0.010 in. for finishing
Total Downfeed	0.020 in.
Soluble Oil	1 to 40
Area Ground	7½ to 9 sq in. (average 8 sq in.)

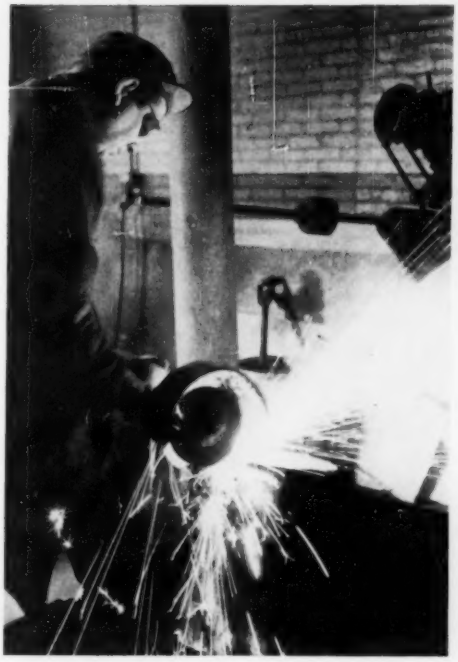

Offhand grinding a cast titanium ingot. The brilliantly white spark stream is characteristic of titanium.

Current surface grinding research on titanium and titanium alloys offers several conclusions:

1—Use aluminum oxide abrasive wheel 32A60-L8VBE or 32A60-K8VBE.

2—Use low wheel speeds of 2000 to 3000 sfpm. This is the key to the success of precision grinding titanium parts.

3—Table speeds should be fast, 400 to 500 ipm.

4—Downfeeds should not exceed 0.001 in. per pass if dimensional accuracy is important.

5—Grinding should be done wet whenever possible to minimize the fire hazard. Titanium in finely divided form is highly explosive in nature and in this respect is like magnesium. Avoid fluids which may contribute to the fire hazard.

6—Although the current experiments concerned surface grinding, the use of low wheel speeds appears to be applicable to vitrified wheels used in other precision operations like cylindrical or internal grinding. Experiments in this direction in the field should be encouraged.

Modern Trends In Electric Furnace And Transformer Design

by R. J. McCurdy

IMPROVEMENTS in design and practices can be visualized with present large electric furnaces that will eventually make it the most economical process for the production of steel. The electric furnace will be able to make steel more economically because of its comparative ability to conserve energy and materials. In going to larger shell diameters and increased power input, certain problems are encountered and there are many improvements yet to be desired.

The trend in design of the electric furnace in the past decade has been toward top charge and larger furnaces, with increased transformer capacity for fast melting. In many of the older installations, transformer size is being increased to provide faster melting rates and higher temperatures for steels requiring special treatment. The maximum size of the electric furnace has not been reached, and the possibilities of the really large furnace remain to be proven. However, there is little doubt in most operators' minds that the large electric furnace is practical.

Top charge really should not be discussed as a recent development. Swing aside roofs have been used since 1927. However, swing roofs on large furnaces (20 ft and up) have been in use only a few years. The good furnace must have a well designed roof and a workable means of roof removal.

The thoroughly modern furnace must be built to fit its particular job, and some variations may be required for the same capacity furnace. For example, the large integrated shop where there is an abundance of hot metal will call for a design capable of easy handling of that hot metal. This includes the capability of accepting pouring spouts. On the other hand, to operate with light, poorly prepared scrap, a greater height from sill plate to roof is desirable in order to increase volumetric capacity and thereby reduce the number of back charges.

Consider for a moment the problem of getting volumetric capacity up as high as possible. If a 20-ft diam furnace that has a hearth capacity of 100 tons measures 8 ft from sill level to the top of shell, the volumetric capacity of the furnace is 3080 cu ft. If the available scrap is of 25 lb per cu ft density, the furnace will hold 38 tons in one charge. Hence, to get a 100-ton heat, two back charges must be made.

Roof ring construction is very important and some improvements have been made. Heavier and larger diameter rings, some built considerably larger in diameter than the furnace shell, are being used. The use of these oversized roof rings results in getting the bottom flange or skewback cooler away from the heat to a point where there is no direct impingement of heat on the bottom flange or skewback cooler. This is true even when the side walls are cut back to a thickness of 2½ in. at the top of the shell.

R. J. McCURDY is No. 2 Melt Shop Superintendent, Republic Steel Corp., Chicago. This paper will be presented at the Electric Furnace Steel Conference, Pittsburgh, Dec. 6 to 8, 1951.

Another advantage of the oversized roof ring is that the weight of the roof, and in some designs part of the superstructure, is not carried on the side wall but rests on the steel construction of the furnace shell. This affords the side walls an opportunity to breathe.

Water Cooling

Water cooling has been the subject of considerable work. This is one phase of furnace design that can be overdone, and when carried too far results in excessive thermal losses. It has been found advantageous to cool the roof ring either with water-cooled skewbacks or by having oversized rings rest on water coolers at the seal. Such parts as doors and door jambs, electrode holders, arms and roof glands have been water-cooled for years. Hairpin coolers have been used at certain points on the side walls of the furnaces, but it is felt that if a furnace is properly designed, such coolers are unnecessary and wasteful.

In considering some of the mechanical parts of the furnace, power operated electrode clamps should be discussed first. Small clamps are now being constructed by all furnace builders. Some have sizes to cover from 4 to 24 in. diam electrodes. Today a furnace buyer can have his choice of several types of power operated clamps.

In top charge furnaces, any door lifting mechanisms which are operated from floor level should be well protected as well as sill plates and slag chutes to minimize trouble from spills.

The mast, roof structure and coolers must be designed to eliminate stray current losses. This source of power loss has never been given the study it deserves. Any current used outside the furnace is, to say the least, expensive and unnecessary.

For means of tilting and roof swing, furnaces are divided evenly between hydraulic and electric drives. Both have their advantages. The furnace operator's main interest is in trouble-free performance and simple maintenance.

Arc regulating devices should insure accurate control of the arc conditions for best use of power. To attain this, the electrode feeding mechanism must be capable of insuring quick and sensitive response to the regulator. Many operators and builders believe that the cable on electro-mechanical winch drive is superior. The stretch inherent in the cable is a good thing on electrode drive. The hydraulic control is a good control and does a splendid job. Hydraulic control can be tied in with rotating type control, such as Rototrol or Amplidyn, for the operation of pump motors. Therefore, it can take full advantage of the latest improvements from an electrical standpoint. An impartial comparison must be made between the winch and cable for direct drive of the electrode arms and the pump and oil driving the rise and fall masts. Here again maintenance and trouble-free operation are of prime consideration. Speed of hand control to raise and lower electrodes for charging and back charging is an item of importance with respect to melting rate.

Gas pressure is a problem in connection with high power input, as considerable gas pressure is generated at certain periods of the meltdown. Flame conditions are most severe and any attempt at opening up electrode gland clearances results in severe punishment of the electrodes, electrode clamps, and arms. As increases are made in furnace size and transformer size, consideration should be given to a method for relieving the gas pressure generated. Some work has been done toward using a water-cooled gland in the roof fitted over with a cover similar to the explosion doors long used in smelting operations. These glands and covers are designed to vent the gases when the pressure is increased. Another idea is to vent the furnaces through an opening in the furnace side wall. This opening should have a water-cooled frame and damper similar to a charging door. The opening would not only provide the necessary venting, but could also make possible the collection of fumes and dust, and even allow recovery of the metallics. A furnace pressure instrument could be used to operate the damper.

Fume and dust elimination devices are among the more important problems confronting the electric furnace operator. Much work has been done in certain localities, but so far equipment for this job has not been standardized. No doubt every operator eventually will be required to do something to overcome this serious drawback to electric furnace steelmaking.

Adequate power must be provided at a reasonable cost. Compared to other supplies, power has been relatively stable. This stability has been an important factor in improving the economic position of the electric furnace. Looking to the future, committees have been appointed to determine what can be expected from power plants located in the coal mining sections of the Ohio River Valley, southern Illinois, and other areas. Preliminary study indicates no increase in power cost, as might be the case with other fuels.

Transformer Size

Transformer size has been going up. There has been a marked increase in the capacity of transformers used to power a given sized furnace. Substation installations capable of delivering large amounts of power with a range of voltage suitable for the refining of higher grade steels are becoming more and more important. Transformers of 20,000 to 25,000 kva ratings are now being used, and one of 35,000 kva is to go into service this year.

The introduction of so much power into three electrodes has necessitated an increase in voltage. It was felt that on 60 cycles the maximum power that could be put into three electrodes at 70 pct power factor was 13,000 kw, which would figure 18,500 kva. Over the years there has been a gradual increase in secondary voltages, which is the obvious answer to increased power input. Increases up to 550 v already have been made.

A notable advancement is the elimination of guesswork in deciding what secondary voltages should be used. From 1920 through 1946 the increase in voltages was carried on by trial and error methods. Today it is possible to calculate the optimum voltage required for the introduction of a given amount of power at any set power factor.

To insure trouble-free operation of the big transformer, special attention must be given to features built into the unit and into the transformer house. Cooling is most important, and internal cooling coils long were standard. Forcing the oil through external water-cooled heat exchangers is proving very satisfactory. Recently a coolant spray type has been de-

veloped and this may prove superior to anything now in use. Hotestspot indicators for each phase are desirable. Dehydrator type breathers on the tank and tap changer for moisture control are important. Thermal syphon type oil conditioners on these components are also advantageous. Pressure relief devices have been installed on the tanks in recent years. An improved synthetic rubber seal around the secondary bus at the transformer tank is now in use. Tap changer mechanisms have been improved by the installation of tapered pins to offset the wear in rotating joints. The tapered pins are preferable to bolts. Brazed terminals are used wherever possible. Improvement of through type conductors between tap changer terminals and transformer terminals by providing through type stuffing boxes at the tap changer barrier eliminates stud type construction. It has been suggested that insulations of B and H classifications might lead to better and longer transformer life.

Regarding the transformer vault—air conditioning, where possible, is desirable. The room must have two door exits equipped with panic locks. Provision for heat under the transformer to be used during extended down periods is advisable. Permanent hinged type platforms with safety hand railings and removable access ladders for tap changer and transformer top inspection and servicing are important. Large dump valves on tap changers for fast oil removal and large capacity oil conditioners to return the reconditioned oil to the tanks are necessary when inspection and repairs are made. Ebony asbestos supports for transformer secondary bus at transformer house exit are superior to wood. Air circuit breakers have proven superior to oil for furnace switching duty at the transformer. Installation of equipment for adequate fire protection is essential.

Electrodes

Efficient and economical electric furnace operation depends in large measure on proper electrode performance for a low rate of consumption and a minimum of interruptions in production. It is essential that the design of the furnace and its associated equipment for handling and assembling electrodes be based on sound technical recognition of the electrode characteristics.

For greater economy, the head room of the furnace building, the crane clearances, and the beam clearances should allow the use of electrode sections up to 100 to 110 in. in length. To avoid overheating of the electrode ends and consequent oxidation and impairment of joints, the mast-arm travel should be sufficient to avoid need for clamping electrodes within about 10 in. of the end of the electrode.

Adding electrodes to the furnace columns can be done best with a device specifically designed for this operation. This hoist attachment should accurately locate the new electrode over the column, and should automatically lower the electrode at the correct pitch as it is screwed on to the nipple in the top of the column. This will enable the assembly of joints without damage to the threads, which is not possible with the main crane because of its fast travel and insensitive control.

To avoid electrode breakage on high-powered furnaces it is most desirable that the electrode joints be assembled with the tightening torque recommended by the electrode manufacturer. To attain this torque with electrodes larger than 12 in. diam requires a tightening mechanism with a greater leverage than possible with a simple chain or band wrench. Such tightening mechanisms are being developed at the present time and are under trial by several operators. To safeguard further against loosening of joints, it is helpful to use a joint cement which has been developed for this purpose. In order to obtain good joint performance, it is also very important that the socket and nipple be thoroughly cleaned before assembly.

The optimum diameter of electrode depends upon the overall balance of the electrical, mechanical, and metallurgical operating conditions, and can only be determined from actual service experience for the particular operating conditions. Electrode companies are producing 24-in. and 30-in. diam graphite electrodes and now have equipment to make up to 40-in. diam.

The pit area under the electric furnace has long been a trouble spot. Some operators pull slag pots for flush or slag-off slags up through the charging floor; other operators have mounted slag pots on transfer cars operated between tapping and slag-off side of the furnace. Slagging off in the back pit and pushing the slag through and under the furnace to the tapping pit with a bulldozer has proven very economical.

The top charging bucket must be designed as large as is practical for the volumetric capacity of the furnace. The old method of using rope to hold bottom segments is replaced by a latch that can be tripped by the crane. A clamshell type bottom that can be pulled open with an auxiliary hoist is considered most satisfactory. Bucket construction must be free from projections of any kind on the inside to insure free dumping of all grades of scrap.

A dolomite throwing machine for quick repairs to the furnace hearth between heats should be of great value, especially for large furnaces. It also has been suggested that a machine of similar design may be used for adding lime, ore, and other materials into the furnace.

Fast melting units, coupled with continuous casting mechanisms, are being considered favorably where tonnages are not sufficient to support a blooming mill. Billet type ingots also are produced economically by the smaller furnace.

Induction stirring is being introduced to this country by at least one producer. It will be interesting to note the merits of this device.

Conclusion

It is well known that the electric furnace is capable of producing rim steel and other open hearth grades by the single slag process, and because it provides better temperature and slag control, a more uniform product from a standpoint of analysis and quality is attainable.

Arc electric furnace shop layout, provided with the necessary auxiliary equipment for servicing the furnaces and with modern spectrographic and laboratory equipment for quick analysis, may be made to function on a production and quality control basis approaching automatic machine-like operation, precision and efficiency.

With improvements in design and the elimination of weaknesses that cause delays, it is believed that electric furnaces up to 150-ton capacity or larger are practical, and in the field of ordinary tonnage steel can compete with the large modern open hearth.

Recovery of Vanadium from Titaniferous Magnetite

by Sandford S. Cole and John S. Breitenstein

The recovery of over 80 pct of the vanadium values in titaniferous magnetite from MacIntyre Development, Tahawus, N. Y., was accomplished by an oxidizing roast with Na_2CO_3-NaCl addition. Process description is given for leaching of roasted ore and precipitation of V_2O_5 and Cr_2O_3 from leach liquor.

THE exploration and development of the MacIntyre orebody at Tahawus, N. Y., by the National Lead Co. provided a source of vanadium. Analyses of various composite sections of the drill cores of the MacIntyre orebody were made to establish whether or not the vanadium was constant throughout. Ten drill cores were sampled as 50 ft sections, crushed, and a portion magnetically concentrated. The head and concentrate were analyzed for total iron and vanadium. The results on the concentrates indicated that the vanadium is associated with the magnetite and maintains a close ratio to the iron content. The nominal ratio of 1:25:140 of V:TiO_2:Fe was found to exist in the concentrates. Typical value for the vanadium in the magnetite both from laboratory concentration and mill production is 0.4 pct.

The recovery of vanadium from the magnetite was investigated in 1942 to 1943. The research program encompassed both laboratory and pilot-plant work on sufficient scale to provide adequate data to establish the feasibility of a full scale plant.

The recovery of vanadium from various ores has been reported in the literature and has been the subject of many patents. The literature dealing with recovery from titaniferous ore by roasting is quite limited. Roasting with alkaline sodium chloride, sodium chloride or alkaline earth chlorides, and sodium acid sulphate have been claimed in various processes as effective means.[1-8] The reduction of the ore, followed by acid leaching, was another method proposed.[9-10] The use of various pyrometallurgical processes for recovery of vanadium in the metal or in the slag has also been extensively investigated, but the results had little application to the problem.[11-14] The separation of vanadium values from subsequent leach liquors and vanadium-bearing solution has been the subject of a considerable number of papers and patents. The most practical is by hydrolysis at a pH of 2 to 3 by acidifying a slightly alkaline solution. Data on solubility of V_2O_5 and V_2O_5 in water and in dilute sulphuric acid indicated a solubility of 10 g per liter in water.[16]

S. S. COLE, Member AIME, is Assistant Manager of Research, Titanium Div., National Lead Co., South Amboy, N. J., and J. S. BREITENSTEIN, Member AIME, Supervisor, Geochemical and Metallurgical Dept., Research Dept., Titanium Div., National Lead Co., South Amboy, is presently with National Lead Co. of Ohio, Cincinnati.

Discussion on this paper, TP 3177D, may be sent, 2 copies, to AIME by Feb. 1, 1952. Manuscript, Feb. 22, 1951; revision, Sept. 28, 1951. St. Louis Meeting, February 1951.

Laboratory Results

Magnetite Analysis: Adequate stock of magnetite was provided so that the laboratory and pilot-plant operation was on ore representative of the mill production. The ore was analyzed chemically and examined by petrographic methods to ascertain whether the vanadium was present in combined state or as an interstitial component between grain boundaries. No evidence was obtained which would indicate that the vanadium was in a free state as coulsonite.[15] The analysis of the ore was as follows: Fe_2O_3, 47.4 pct; FeO, 29.1; TiO_2, 10.1; V, 0.40; and Cr, 0.2.

The screen analysis of the ore on the as-received basis was: −20 +30 mesh, 28.8 pct; −30 +40, 18.9; −40 +50, 9.7; −50 +60, 15.1; −60 +100, 5.9; −100 +200, 11.2; −200 +325, 3.7; and −325, 7.2.

Roasting Conditions: The prior practice indicated that a chloridizing roast with or without an alkaline salt had been effective on other titaniferous magnetites. On this basis roasts with additions of sodium chloride, sodium carbonate and mixtures thereof were investigated varying the roasting temperature between 800° and 1100°C. Since the ore had shown no segregation or concentration of vanadium, the influence of particle size on the freeing of vanadium by the reagents during roasting was determined. The initial work was on silica trays in an electric resistance furnace with occasional rabbling of the charge. Subsequently, the roasting was carried out in a small Herreshoff furnace to establish the influence of products of combustion on the recovery of the vanadium.

The laboratory tests showed that this ore required an alkaline chloridizing roast, in conjunction with a reduction in particle size to less than 200 mesh. When roasted in air at 900°C with 5 pct NaCl and 10 pct Na_2CO_3, over 80 pct recovery of the vanadium was attained as a water-soluble salt. The presence of alkaline earth elements gave detrimental effects and care had to be exercised to avoid any contamination of the ore or roast product by such materials.

The solubilization of vanadium under the various conditions is given in a series of curves in Figs. 1 to

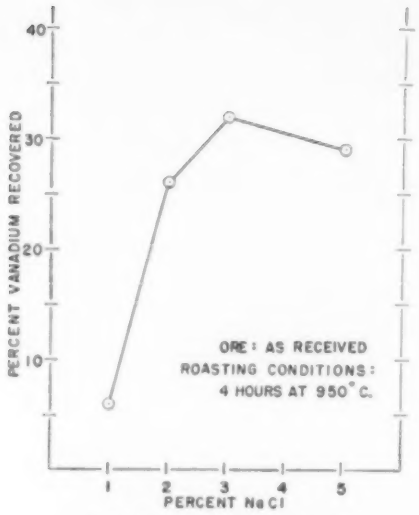

Fig. 1—Effect of roasting as-received ore with NaCl at 950°C.

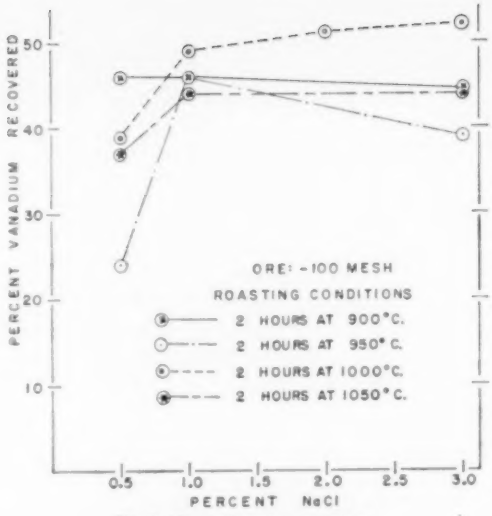

Fig. 2—Effect of roasting ground ore with NaCl at various temperatures.

6. The influence of the several factors is quite apparent. The general conditions for processing the ore as determined by the roasts are shown in Table I.

Leaching Conditions: Leaching of the roasted ore was varied using percolation and countercurrent washing. The retention of solution on the ore was not found to be critical since the vanadium-bearing salts were on the surface of the ore particle. The use of countercurrent stages for leaching was desirable since the concentration of vanadium could be increased to 10 to 20 g per liter, thus reducing the volume of liquor in process. Four to five stages of leaching removed 98 to 100 pct of the soluble vanadium. The increase in vanadium content of the leach liquor is shown in Fig. 7 when the leaching was carried out for six stages. Crushing the consolidated lumps to −10 mesh and avoiding forming of −100 mesh material yielded the optimum product. Large amounts of −100 mesh material gave a slow rate of filtration. The rate of diffusion of the leach liquor into lumps coarser than 10 mesh retarded the rapid removal of the soluble vanadium. The use of water at 80°C was found to give a slight improvement, especially in conjunction with suppression of aluminum salts.

Recovery of Vanadium and Other Values

The leach liquor from a chloridizing alkaline roast contained the vanadium as a sodium vanadate, sodium chromate, sodium aluminate, sodium chloride, sodium carbonate, and sodium sulphate. The cyclic recovery of sodium values was desirable and elimination of aluminum salts was necessary. The suppression of aluminum during leaching by a carbon dioxide atmosphere was found to be the most satisfactory.

Precipitation of vanadium as a calcium vanadate complex in presence of $CaCl_2$ and $Ca(OH)_2$ was satisfactory for leach liquors derived from salt roast or when the liquors were low in sulphur values. The optimum ratio by weight of reagents to vanadium was $2Ca(OH)_2$:V and $1\text{-}1.4CaCl_2$:2V without altering the pH of the leach liquor. This procedure had considerable merit when working with solutions having vanadium at low concentrations of the order of 0.5 to 5 g per liter.

Hydrolysis of vanadium from the leach liquor was based upon the use of nucleating conditions and adjusting the pH to 2.5 ± 0.2.[18, 19] The solution was acidified with sulphuric acid at room temperature and up to 80°C. The temperature was held at 95°C for 1 hr and then the solution was boiled for an additional hour. The acidification was done without agitation over a 10 min period. The slow formation of nuclei of V_2O_5 occurred and on subsequent heating and agitation large nodules or flocs of 1/16 to ¼ in. diam formed. No appreciable formation of V_2O_5 occurred below 85°C. This practice avoided the adherence of vanadium oxide to the side walls of the vessel and the product was easily filtered and washed. The removal of vanadium was over 99 pct.

The filtrate was reduced with SO_2 and the solution adjusted with Na_2CO_3 to a pH of 7.0, thereby hydrolyzing chromium as $Cr(OH)_3$. The filtrate from this step contained only sodium chloride and sodium sulphate which was readily crystallized and separated in pure state in accordance with published data.[20] The sodium chloride liquor containing some sodium sulphate could be returned to the process

Table I. Conditions for Processing Ores

		Mesh	Pct
Ore Grind		− 80 + 100	0.0
		− 100 + 200	1.0
		− 200 + 325	22.0
		−325	77.0
		Range	**Optimum, Pct**
Reagents	NaCl	3 pct min. 6 pct max.	8
	Na_2CO_3	6 pct min. 12 pct max.	10
Temperature		875°-925°C	
Atmosphere		Oxidizing	3.8-20.8 pct O_2
Vanadium solubilization		75-85 pct	

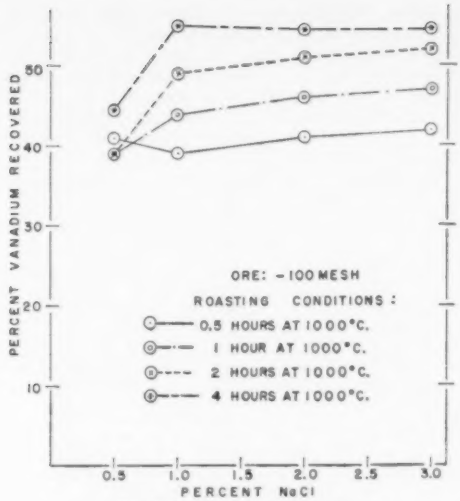

Fig. 3—Effect of roasting ground ore with NaCl at 1000°C.

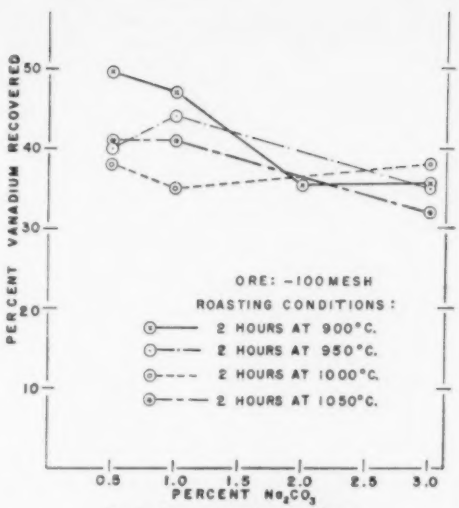

Fig. 4—Effect of roasting ground ore with Na_2CO_3 at various temperatures.

without adversely affecting the vanadium recovery since it contained only these compounds. The new salt makeup was 60 pct of the total requirement.

Pilot-Plant Operation

Based on laboratory results and procedures, process flowsheets were devised so as to adapt the existing pilot-plant equipment to the problem. In several instances improvisation was necessary and conditions indicated by laboratory practice were not met fully. This was particularly true in the case of leaching. Laboratory tests had indicated fast filtering equipment, but none was available so barrels were substituted and the solution transferred from one stage to the next. The roasting was done in a 3x30 ft rotary kiln, fired with Bunker "C" oil. The processing of roasted ore and leach liquor was on a scale comparable to a half ton of feed ore per 6 hr.

The flowsheet for the recovery of vanadium from the MacIntyre magnetite utilizing NaCl-Na_2CO_3 mixtures for the pilot-plant operation is given in Fig. 8. The specific conditions for each stage of the process are discussed in separate sections.

Ore Grinding and Blending: A small Raymond mill capable of grinding 500 to 600 lb per hr was used to prepare a feed for the rotary kiln which was comparable with ball mill ground ore. The differences in screen size were less than 2 pct of the product used for laboratory roasts.

The blending of the reagents with the ore was accomplished with a flight mixer using sufficient

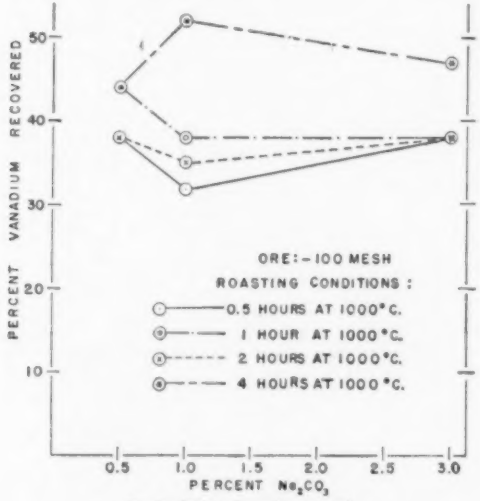

Fig. 5—Effect of roasting ground ore with Na_2CO_3 at 1000°C.

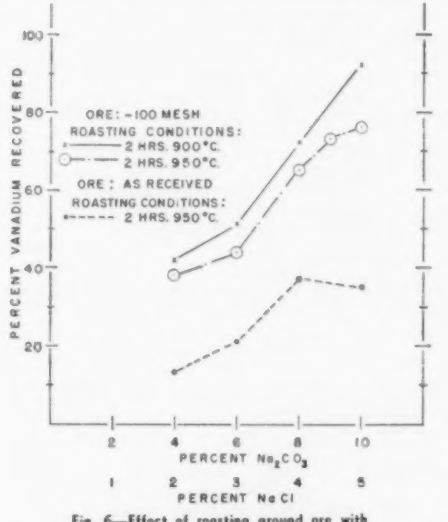

Fig. 6—Effect of roasting ground ore with Na_2CO_3-NaCl mixtures at 900° and 950°C.

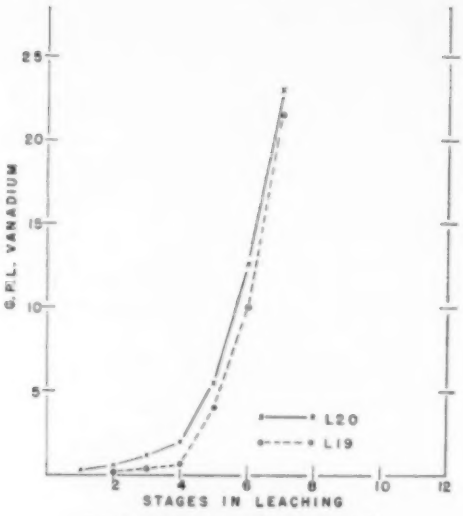

Fig. 7—Change in vanadium content of leach liquor at various stages of leaching.

water to prevent dust losses. This gave an even distribution of reagents through the ore. The mixture was then blended with water to produce a mass having 12 to 16 pct moisture. This served a dual purpose, since the reagents would be in better contact with the ore and the charge would form as balls or lumps in the kiln. The formation of lumps reduced the loss of sodium chloride during the roasting operation.

Roasting Operation: A bed of ore of 3 to 10 in. was maintained in the kiln which had 24 in. ID. The kiln temperatures were varied to determine what the optimum would be for pilot-plant as compared with laboratory scale. The results indicate 910° to 920°C with 1 to 2 hr retention time at that temperature. The lumps which formed about 90 pct of the discharge gave better recovery of vanadium. Table II shows the differences in retention time, temperature, and conditions of discharge.

The data obtained indicated that the general specification for kiln conditions would be as follows:

Temperature	910°-930° ± 10°C
Retention time	45-75 min
Bed thickness	6 in. minimum 12-24 in. maximum
Stack gas	2-7 pct O_2
Type of feed	Nodules ½-3 in. diam
Feed bulk	120-130 lb per cu ft

In order to determine what may have contributed to the differences in recovery of vanadium from the lumps vs. fines, a complete analysis was made from one 24-hr operation and partial analysis of several other shorter periods. The only difference observed was in the soluble NaCl content which was considerably lower in the fines, of the order of 0.9 to 1.0 pct while lumps gave 1.4 to 1.8 pct.

Analyses on dry basis of a typical composite before and after leaching of the furnace discharge are given in Table III.

Table II. Results of Roasting

Retention Time, Hr	Temperature, °C	Vanadium Recovery, Pct	
		Lumps	Fines
0.5	910	73	48
1.0	910	94	58
1.0	940	83	67
2.0	910	77	80
2.0	920	89	66
2.0	950	89	58

Table III. Analyses of Typical Composite of Leach

	Unleached, Pct	Leached, Pct
TiO_2	8.9	9.1
Fe_2O_3	69.5	73.4
FeO	1.0	1.0
V	0.36	0.08
SiO_2	3.88	3.96
Al_2O_3	4.87	6.14
CaO	0.82	0.92
MgO	1.10	1.2
Na_2O	6.53	3.52
NaCl	2.14	0.12
Cr_2O_3	0.34	0.15
MnO	0.29	0.28
S	0.22	0.036
	99.21	99.93

Leaching Roasted Ore: The lumps were crushed to pass a 6 mesh screen and 500 lb placed in wooden barrels equipped with drainage spouts. The initial water started through the leaching cycle was 80 gal per ton roasted ore with 34 gal per ton ore being recovered from the cycle due to porosity of the lumps and retention on the ore. The final liquor averaged 17 g per liter vanadium. Comparison of laboratory leaching efficiency with that of the pilot plant gave equivalent recovery of vanadium. Results of comparison of leaching recovery with first

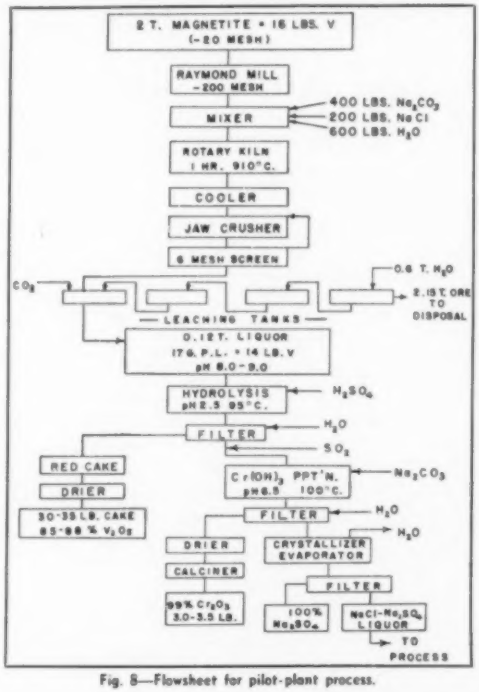

Fig. 8—Flowsheet for pilot-plant process.

and last stage showed 99.0 pct efficiency. Data on the leaching operation are as follows:

Comparison of First and Last Stages	
Vanadium in first stage liquor	20.458 lb
Vanadium in last stage liquor	0.444
Vanadium in solution held by ore	0.20
Vanadium lost in solution on ore	0.98 pct

Conditions for Leaching	
Ratio ore/water	3.3:1
Ratio ore/liquor	15:1
Stages of leaching	4-5
pH leach liquor after CO_2 acidification	8.8-9.2

Analysis of Leach Liquor	
Specific gravity	1.25-1.28 at 25°C
pH	8.8-9.0
V	16-20 g per liter
Al_2O_3	0-0.2 g per liter
Cr	2-4 g per liter
Na_2SO_4	120-140 g per liter
NaCl	75-120 g per liter
Temperature of leaching	80-80°C
Ore size, −4 mesh	100 pct
−100 mesh	<10 pct
Retention time, first stage	20 min
balance	1-5 min
Moisture, leached residue	14-18 pct

Recovery of Metal and Salt Values from Leach Liquor: A series of pilot-plant precipitations were made using composited lots of leach liquor. Analysis of the filtrates after each stage of vanadium and chromium removal showed over 99 pct effective removal.

Optimum conditions for recovery of the metal values based upon pilot-plant runs were found to be as follows:

V_2O_5 Precipitation	
H_2SO_4 concentration	66 pct
Temperature of solution	60°-90°C
pH after acid addition	2.5-2.75
Period for acid addition	>20 min
Agitation arrested	>40 min (including acid addition time)
Temperature for precipitation	95°-100°C
Rate of temperature rise	12°C per hr
Time at 95°-100°C	1-2 hr
Wash water for V_2O_5	Volume equal to starting liquor at pH 2.5-3.0
Floc volume	15-25 pct
Filtration rate of V_2O_5	5.4 g per sq cm per hr
Solids in cake	16.5 pct
Bulk volume	
Wet filter cake	22.0 lb per cu ft
Dry filter cake	10.9 lb per cu ft
Fused cake	180 lb per cu ft
Melting point	630°-650°C

Analysis of V_2O_5 Cake
85-88 pct V_2O_5
5-8 pct Na_2O
5-7 pct loss on ignition

Cr_2O_3 Precipitation	
SO_2 per kg Cr	3
Na_2CO_3 per kg Cr	4
Temperature for reduction	60°-90°C
pH after Na_2CO_3 addition	6.5-7.0
Temperature for Cr_2O_3 precipitation	70°-100°C
Rate of temperature rise	Not critical
Time at 95°-100°C	1-3 hr
Wash water for Cr_2O_3	¼-½ volume of filtrate
Floc volume	15 pct
Filtration rate for Cr_2O_3	0.15 g per sq cm per hr
Solids in cake	21.2 pct
Analysis of calcine	99 pct Cr_2O_3

Filtrate from Cr_2O_3 Precipitation

The filtrate available for sodium sulphate recovery had the following typical analysis from a 15 g per liter vanadium starting solution:

Volume increase	15 pct
pH	6.5
Na_2SO_4	200 g per liter
NaCl	63 g per liter
Cr	<0.01 g per liter
Specific gravity	1.2

Since this liquor could be concentrated and pure Na_2SO_4 crystallized in a standard unit, it was not considered necessary to follow out this step.

Summary

A process developed in the laboratory and carried through the pilot-plant for the recovery of vanadium values from MacIntyre magnetite containing 10 pct TiO_2 and 0.4 pct V has been described. Grinding the ore to pass 200 mesh screen is required. The addition of 3 to 5 pct NaCl and 6 to 10 pct Na_2CO_3 is made and roasting is under oxidizing conditions at 910° to 930°C. The effective release in soluble form of 75 to 90 pct of the vanadium contained and 50 pct chromium was accomplished by this roast.

The leaching of the roaster discharge in the presence of stack gases fixed the aluminum values in the leach cake. Conditions for precipitation of a fast filtering vanadium oxide by use of nuclei at a pH of 2.5 were established. The precipitation of chromium hydroxide after reduction of the solution with SO_2 at a pH of 6.5 to 7.0 yielded a sodium sulphate-sodium chloride liquor from which pure sodium sulphate was crystallized and the sodium chloride brine was returned to process. Recovery of vanadium and chromium values from the solutions was over 99 pct effective.

Acknowledgments

The authors wish to acknowledge the assistance given during the laboratory and pilot-plant phases by R. L. Holiday, W. F. Meister, C. H. North, and L. W. Rowe, Research Chemists of the Research Dept., and advice of J. L. Turner, Technical Director (deceased) and R. Dahlstrom, Technical Director, Titanium Div., National Lead Co.

References

[1] B. P. F. Kjellberg: *Engineering and Mining Journal* (1927) **123**, pp. 521-522; (1931) **131**, p. 460.

[2] A. D. Moro and H. S. Gibbs: *Journal Science Technology* (1938) **19**, pp. 523-526.

[3] B. P. F. Kjellberg: U. S. Patent 1,583,053 (May 4, 1926).

[4] H. T. Koenig: U. S. Patent 1,654,820 (January 3, 1928).

[5] L. M. Paul: U. S. Patent 1,696,923 (Janunry 1, 1929).

[6] B. P. F. Kjellberg: Swedish Paten: 80,681 (June 19, 1934).

[7] R. Asak: U. S. Patent 2,238,673 (April 15, 1941).

[8] J. Rockstroch: German Patent 683,083 (October 28, 1939).

[9] R. J. Traill, W. R. McClelland, and J. D. Johnston: Canada Dept. Mines Branch Report (1931) **720**, pp. 178-185.

[10] C. S. Parson, A. K. Anderson, and W. S. Jenkins: *Ibid.* (1934) **736**, pp. 213-218.

[11] I. M. Krasmokutskii: *Journal of Chemical Industry* (Moscow) (1935) **12**, pp. 281-284.

[12] Fried. A. G. Krupp: German Patent 671,943 (July 17, 1939).

[13] V. S. Gulyga: Sovet. Met. (1936) **8**, pp. 20-25.

[14] C. E. Wood, T. L. Joseph, and S. S. Cole: Bur. Mines, *RI* 3679 (1943).

[15] J. A. Dunn and A. F. Dey: *Trans.* Min. Geo. Inst., India (1937) **31**, pp. 117-194.

[16] C. S. Bohrer, O. E. Lanford, and S. J. Kiehl: *Journal* Amer. Chem. Soc. (1942) **64**, pp. 2810-2816.

[17] A. G. Rope: *Bull.* Acad. Sci. U.S.S.R. Classes Sci. Math., Nat. Ser. Chem. (1938) pp. 451-462.

[18] W. F. Meister: U. S. Patent 2,442,610 (June 1, 1948).

[19] S. S. Cole, R. L. Holiday, and J. S. Breitenstein: U. S. Patent 2,479,905 (August 23, 1949).

[20] W. C. Blasdale: *Industrial and Engineering Chemistry* (1918) **10**, pp. 344-353.

Low Grade Bauxites and Clays as Potential Aluminum Resources

by K. K. Kershner, C. W. Funk, and W. A. Calhoun

Future resources of aluminum may require the utilization of low grade ores to provide a more permanent protection for the nation. Aluminum minerals such as clay, shale, and high iron laterites may become important sources. An evaluation of reserves is given. New laboratory results are reported on the Vereinigte desilication process.

THIS report on future resources of aluminum metal emphasizes the necessity for investigating utilization of low grade potential ores to provide more permanent protection for the nation. Partial or complete interruption of the importation of high grade aluminum ores must be given consideration. Ultimately, aluminum minerals such as clay, shale, and high iron laterites may become the principal sources of aluminum. The development of extractive processes for treating these low grade materials is a step in long-range national preparedness that should receive more attention. In formulating such processes, the application of beneficiation methods for the purpose of classifying the several types of minerals before subjecting each type to the more expensive extractive procedures should be considered, and a careful survey of the basic factors of power sources, transportation facilities, and sources of raw material should be made.

Domestic Bauxite Resources

Of the domestic supply of current, treatable-grade bauxite, 95 pct comes from Arkansas. The present reserve of Arkansas bauxite suitable for metal production, including abrasive-grade, Bayer-grade, and modified Bayer-grade ores, is 34,000,000 tons. The total reserve of bauxite of all grades is approximately 75,000,000 tons. Reserves are estimated on a mined and dried basis. Data available to the Bureau of Mines in 1948 to 1949 were used in preparing Table I, which shows a breakdown by grades of bauxite for about a half of the reserves of the state.

The modified Bayer ore, 10,555,500 long dry tons, is based on a cutoff of 8 to 15 pct silica. The submarginal 10,074,700 long dry tons is assumed to contain more than 40 pct gibbsite, more than 15 pct silica, and less than 32 pct available alumina. A considerable amount of this low grade material was consumed in 1949 and 1950.

Table I. Arkansas Bauxite Reserves in Deposits for which Data Were Made Available to Bureau of Mines as of Dec. 31, 1948

Grade	Wet Long Tons in Place	Mined Dry Long Tons
Abrasive	2,863,500	1,634,200
Bayer	9,653,500	5,422,000
Modified Bayer	18,497,900	10,555,500
Subtotals	31,014,900	17,611,700
Marginal metal	7,823,300	4,347,000
High iron	8,334,300	4,580,100
Chemical	1,829,600	1,145,000
Submarginal	17,777,500	10,074,700
Grand total	66,779,600	37,758,500

Additional tonnages of bauxitic and kaolinitic clays are indicated by the Bureau of Mines drilling project.[1] Applying a 50 pct factor to arrive at long tons mined and dried, the results of this project are approximately 31,500,000 tons kaolinitic clay at +35 pct Al_2O_3 and 11,800,000 tons kaolinitic clay at 20 to 35 pct Al_2O_3.

Total reserves of kaolinitic clays are probably quite extensive—several times the reserves shown in the Bureau's work. Total reserves of bauxitic and high iron clays from the drilling program and previously established figures are 63,980,000 tons.

The mineral dressing methods,[2] the lime-sinter process,[3] the lime-sinter modification of the Pederson process,[4] the lime-soda sinter process,[5-8] and the Alcoa combination process[9, 10] have been described in the literature and will not be elaborated upon here. The less familiar Vereinigte Aluminium-Werke process used by the Germans during World War II may require some amplification. It was used to beneficiate boehmite ores containing 12 to 18 pct silica for a feed to the European Bayer process. Ore was

K. K. KERSHNER, Member AIME, is Chemist, C. W. FUNK, Junior Member AIME, and W. A. CALHOUN, Member AIME, are Metallurgists, U. S. Bureau of Mines, Rolla, Mo.

Discussion on this paper, TP 3178D, may be sent, 2 copies, to AIME by Feb. 1, 1952. Manuscript, Dec. 21, 1950; revision, May 4, 1951. St. Louis Meeting, February 1951.

Papers by authors of the U. S. Bureau of Mines Staff are not subject to copyright.

Table II. Desilication of Kaolinite

Temperature, °C	Time, Hr	Analysis of Calcine, Pct			Desilication Residue, Pct		Percent of Total Silica and Alumina				Percent Available Alumina, Desilication Residue
							Desilication Residue		Leach Solution		
		SiO_2	Al_2O_3	Ignition Loss	SiO_2	Al_2O_3	SiO_2	Al_2O_3	SiO_2	Al_2O_3	
700	4	49	43	0.8	35	29	75	72	25	28	0.1
900	4	49	44	0.3	36	42	70	83	30	17	0.1
950	4	50	44	0.1	13	65	15	90	85	10	29.0
1000	4	51	44		12	68	15	91	85	9	30.0

reported to be calcined at 900° to 1000°C (1652° to 1832°F) to decompose kaolin to amorphous silica and alumina. The calcine was crushed to 15 mm to be suitable for percolation and was leached with a recycled 10 pct sodium hydroxide solution at 90° to 95°C (194° to 203°F) to dissolve the silica. As much as 80 pct of the silica was extracted, and as little as 2 pct of the alumina was lost. Soda was regenerated by adding lime and precipitating dicalcium silicate. The desilicated residue was treated by the European Bayer process in the same reactor.[11, 12]

Bureau of Mines Research Work—1950

Preliminary laboratory tests on the percolation leaching of silica from bauxites by the Vereinigte process[11] were reported by Skow and Conley,[12] of the College Park laboratories. Approximately 65 to 80 pct of the silica and 8 to 11 pct of the alumina were removed from bauxites containing 11.9 to 22.2 pct silica.

This desilication process is being investigated at the Rolla, Mo., and Bauxite, Ark., laboratories of the Bureau of Mines. As the silica content of low grade bauxites and clay is largely in the form of hydrous aluminum silicates, the preliminary experiments have dealt with kaolinite and halloysite.

Differential thermal analysis curves made on samples of these materials showed endothermic and exothermic peaks at 595° and 596°C (1103° and 1105°F) and 965° and 969°C (1769° and 1776°F), respectively. These two peaks correspond to the loss of water of hydration[13, 14] and to a transitional or transformation reaction.[15, 16] The two samples contained 42 and 45 pct silica and 37 and 38 pct alumina, respectively.

The samples were dry-ground in a pebble mill to −100 mesh and calcined at different temperatures within a range of 400° to 1000°C (752° to 1832°F) for 2 and 4 hr periods. The calcines were agitated with 10 pct sodium hydroxide at 90° to 95°C (194° to 203°F) for 1 hr.

The distribution of silica and alumina in leach solutions and residues is summarized in Tables II and III. The available alumina, which is the quantity of the desilicated residue dissolved by pressure digestion with 10 pct caustic at 148°C for 10 min, and analyses of calcines also are given. The data are average values obtained from several tests.

These tables indicate that calcination above 900°C (1652°F) is required to extract an appreciable amount of silica. Below 900°C (1652°F) the silica extraction is less than 30 pct of the original content; simultaneously, approximately the same percentage of alumina is dissolved, part of which might be recovered by re-treating the leach solution. The amount of available alumina in the desilicated residues is substantially zero.

Calcination at 950°C (1742°F) affects a marked change in the percentage of soluble silica and alumina in the 10 pct caustic. It will be noted that 74 to 85 pct of the original silica is removed from calcines prepared at 950° and 1000°C (1742° and 1832°F) with the simultaneous solution of approximately 10 pct of the total alumina. In a cyclic process, a portion of this dissolved alumina would be returned as sodium aluminate with the sodium hydroxide liquor obtained from the causticization with lime to remove silica. The data also show a silica content of 12 pct in the kaolinite leach residues, as compared to 20 pct in those from the halloysite. The Vereinigte process shows reductions in silica content of 75 to 82 pct accompanied by alumina removals of 1 to 2 pct, and large-scale tower desilications produced desilicated material containing approximately

Table III. Desilication of Halloysite

Temperature, °C	Time, Hr	Analysis of Calcine, Pct			Desilication Residue, Pct		Percent of Total Silica and Alumina				Percent Available Alumina, Desilication Residue
							Desilication Residue		Leach Solution		
		SiO_2	Al_2O_3	Ignition Loss	SiO_2	Al_2O_3	SiO_2	Al_2O_3	SiO_2	Al_2O_3	
700	2	50	43	0.9	38	31	77	71	23	29	0.2
700	4	50	43	0.6	38	31	77	71	23	29	0.8
900	2	51	43	0.6	40	30	79	69	21	31	0.6
900	4				39	29	70	69	30	31	0.3
950	2	51	44	0.5	24	55	33	87	67	13	26.0
950	4	52	45	0.4	21	61	26	87	74	13	30.2
950	5½	52	45	0.4	23	58	30	90	70	10	
970	5½				20	64	23	89	77	11	28.7
990	5½				20	64	22	90	78	10	27.2
1000	2	51	44	0.4	22	59	27	88	73	12	28.0
1000	4	52	45		21	61	26	88	73	12	25.8

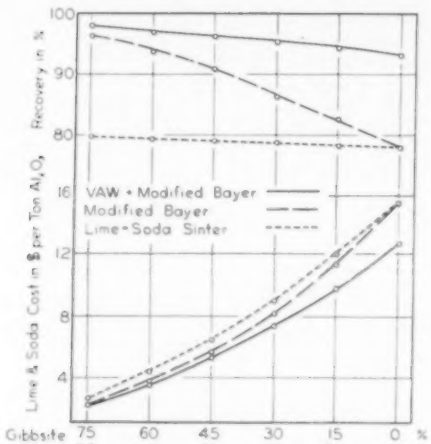
Recovery in %
Lime & Soda Cost in $ per Ton Al_2O_3
VAW • Modified Bayer
Modified Bayer
Lime-Soda Sinter
Gibbsite 75 60 45 30 15 0 %
Kaolinite 25 40 55 70 85 100
Al_2O_3 58.9 55.0 51.1 47.3 43.3 39.5 %
SiO_2 11.7 18.6 25.6 32.6 39.7 46.5

Fig. 1— Influence of silica content of ore on alumina recovery and reagent costs.

6 pct silica. The need for further investigation with variable leaching conditions is indicated by the removal of 10 pct alumina during desilication.

When calcination of the halloysite at 950°C (1742°F) was lengthened from 2 to 4 hr, silica extraction was improved without materially affecting the solubility of the alumina, and the alumina soluble by pressure digestion was increased. Raising the temperature of calcination of the kaolinite from 950° to 1000°C (1742° to 1832°F) decreased the alumina removal without affecting the silica extraction and somewhat increased the available alumina.

There are differences of opinion concerning the material resulting from the dehydration of hydrous aluminum silicates. Insley and Ewell[16] state that amorphous silica and amorphous alumina are formed; Vernadskii[17] says that kaolin anhydride is produced; and Hyslop[18] considers that kaolinite completely breaks down around 600°C (1112°F) to form a silicate stable to about 900°C (1652°F). X-ray examination of calcines and desilicated residues in this investigation shows that an amorphous condition follows dehydration. Calcines prepared at 600° to 800°C (1112° to 1472°F) were as resistant to increased silica extraction with 10 pct caustic as those produced at 400° and 500°C (752° and 932°F).

Experiments were conducted on the dehydration of halloysite under reduced pressures and lower temperatures in order to investigate the properties of the resulting products. It was thought that the release of chemically combined water under such conditions might yield a product more amenable to desilication. However, these calcines gave no definite X-ray patterns, and there was no material difference in their solubility from those produced under normal conditions.

X-ray patterns of calcines and leach residues showed the presence of mullite when calcinations above 900°C (1652°F) were made. Though quantitative measurements were not made, the amount of mullite appeared to increase with higher temperatures and longer calcination. The formation of mullite in the desilication process has not been reported previously, although its presence in fired kaolinite has been reported by other investigators.[19-21] Comofore, Fischer, and Bradley[22] describe the formation of mullite as due to the collapse of a noncrystalline skeletal anhydride to produce a more stable crystalline form when kaolinite is fired to approximately 1000°C (1832°F). The formation of mullite renders a portion of the silica resistant to the caustic treatment and probably causes some reduction in available alumina. X-ray diffraction also reveals the presence of γ alumina in the calcines and leach residues.

The results of the preliminary work on kaolinite show that by calcination and leaching with 10 pct caustic solution, 85 pct desilication may be expected with alumina losses of approximately 10 pct. Although the silica extraction is higher, the alumina losses are substantially greater than those reported for the Vereinigte Aluminium-Werke process. The desilicated product, which averages 68 pct alumina, with slightly less than half of it soluble by pressure digestion, cannot be considered a suitable feed for the Bayer process. Consideration may be given to this material as a feed to either the combination or lime-soda process. The desilication treatment is also open to speculation if applied to ores of lower silica content. The preliminary results are considered definite enough to warrant additional fundamental investigations with variable conditions of calcination to minimize the formation of mullite, and also with leaching procedures to reduce alumina losses in desilication.

In addition to kaolinite, bauxitic and kaolinitic clays with various amounts of gibbsite (both in naturally occurring ores and synthetic mixtures) will be included in future investigations. The calcination experiments will involve a more detailed consideration of heating rate as well as the temperature within the region of the exothermic reaction as determined by differential thermal analysis. Comparative tests will also be made on pelletized calcines, percolation, counterflow, and multiple-stage leaching, and determination of solution stabilities. These data will be necessary for a complete evaluation of the Vereinigte Aluminium-Werke process when applied to domestic high silica potential aluminum resources.

Process Comparison

A comparison of the potential position of the Vereinigte Aluminium-Werke desilication process relative to the modified Bayer, or Alcoa combination process, and the lime-soda sinter processes was evaluated in terms of the especially significant factors, alumina recovery and reagent cost. Although the less tangible factors of labor, plant installation, and fuel costs would appreciably influence any economic analysis, these considerations were not included in the comparison. The German and Alcoa procedures utilize stages of the Bayer and lime-soda sinter processes, and assumptions for these common stages were the same. Hypothetical feeds containing proportions of kaolinite and gibbsite were used to simplify the comparison.

The chemical and physical principles of the Vereinigte Aluminium-Werke process are not thoroughly established; therefore, the best results from the published German tests[15] were used in the evaluation. In this work, 80 pct of the silica was extracted with an alumina loss of only 2 pct, and a lime consumption of 3 mols per mol of silica ex-

tracted was assumed in the comparison. The Bayer digestion was assumed to recover 100 pct of the alumina that was not converted to insoluble sodium aluminum silicate. Corresponding portions of alumina and soda were considered to be rejected to red mud. Although alumina recoveries for the lime-soda sinter process of 86 to 89 pct have been obtained,[4] other authorities have expressed the opinion that commercial operations using high silica feeds would approach an alumina recovery of 80 pct. Although the latter figure may be slightly pessimistic, it was assumed for the calculations along with a rejection of 98 pct of the silica to the brown mud, a lime consumption of 200 pct, and a soda consumption equivalent to 7 pct of the silica removed.

The calculations are based on the treatment of the residue from the German desilication procedure by an appropriate Bayer digestion, the red mud from which would be re-treated by a lime-soda sinter and the leach liquor returned to the Bayer digestion. Calculations for the modified Bayer are on the normal flow circuit. Those for the lime-soda sinter are based upon the alumina being extracted by Bayer digestion. To provide a basis for comparison, lime requirements were converted to limestone at an assumed value of $2 a ton, and soda ash was valued at $24 a ton (f.o.b. August 1950). Trends resulting from these estimates are illustrated in Fig. 1, which plots alumina recovery and reagent costs against increasing silica content of the ore.

Estimated alumina recovery from the modified Bayer process decreases rapidly, and reagent cost increases over sixfold as the silica content of the ore increases. If ore is fed directly to a lime-soda sinter plant, alumina recovery is relatively unaffected by increased silica content in the ore, and recovery cannot be expected to exceed 80 pct due to a 20 pct aluminia loss in the first step of the process. Reagent costs for the direct lime-soda process are slightly higher than for the modified Bayer. Although alumina recovery for all processes decreases as the silica content of the ore increases, the recovery curve of the VAW process is the least affected. As a result of higher alumina recovery, the reagent costs of the VAW process are the most favorable.

Consideration may be given to the curves on the basis of an assumed alumina recovery in the lime-soda process of 90 pct. The recovery curve of the lime-soda sinter method would be displaced about 10 pct upward. As the modified Bayer and Vereinigte Aluminium-Werke calculations also depend on alumina recovery of the lime-soda sinter procedure, a proportional upward shift in these curves would also be obtained. Similarly, the reagent cost curves would be displaced downward for each process. It is then apparent that the absolute location of each curve depends on rather arbitrary assumptions, but the relative slope and relative position of each curve is inherently characteristic of the process.

Conclusions

Mineral-dressing methods are limited in their present technology by the colloidal character of the ore and the chemical association of alumina with silica in clays. When necessity requires the use of varied and complex ores, classification techniques that depend on physical differences of the materials may be useful for rejecting impurities to produce a smaller volume of feed of superior quality for subsequent extractive operations.

Any alkaline process will require large tonnages of high calcium limestone in the vicinity of the treatment plant to treat high silica ore. Direct feed of ore to a lime-sinter process is believed, by one school of thought, to be the best method currently available for treating high silica ore, as it avoids the large circulating load of soda.

Although there may be no technical limit to the modified Bayer process, as some authorities maintain, current economics dictate 13 pct as the maximum silica content in the ore unless soda is regenerated by carbonation, in which case 18 pct silica is the maximum. The increased tonnage of red mud caused by high silica ore reduces the tonnage of alumina that can be produced from an installation of a given sinter-plant capacity. If the VAW desilication procedure is capable of yielding a suitable feed to a Bayer process, the silica limit of aluminum ore could again be increased significantly with a subsequent expansion of available domestic resources.

An industrial and military preparedness program requires consideration of suddenly disrupted imports and ultimate depletion of domestic high grade bauxite. The technology of winning aluminum from domestic clays must be developed to meet such circumstances.

Further consideration of the Vereinigte process should include a more detailed study of conditions for calcination of kaolinitic and bauxitic clays to minimize mullitization, and an investigation of various leaching procedures to lessen alumina losses during desilication. Pilot-plant operations should follow promising laboratory experimental results and economic evaluations before commercial applications are considered.

Acknowledgments

The authors gratefully acknowledge the helpful suggestions and contributions regarding the economic and technical aspects of the extraction processes by R. B. Derr, General Manager, Aluminum Ore Co., St. Louis, Mo.; W. W. Binford, Manager, Reynolds Metals Co., Hurricane Creek Plant, Bauxite, Ark., and their staffs. Estimates of ore reserves were furnished through the cooperative efforts of B. M. Reynolds, Mining Engineer, and L. T. McElvenny, Chief, Mining Branch, Minerals Technology Division, Region VI, U. S. Bureau of Mines, Rolla, Mo.

References

[1] M. C. Malamphy, G. K. Dale, T. M. Romslo, A. H. Reed, A. Ollar, and J. I. Tracey, Jr.: Investigation of Arkansas Bauxite. Vol. 1. Bur. Mines *R. I.* 4251 (March 1948) 63 pp.

[2] S. M. Runke, E. G. Howe, J. S. Kennedy, and H. Kenworthy: Pilot Plant Concentration of Arkansas Aluminum Ores. Bur. Mines *R. I.* 4440 (April 1949) 38 pp.

[3] F. R. Archibald and C. F. Jackson: Alumina from Clay by the Lime Sinter Method. *Trans.* AIME (1944) **159**, p. 227.

[4] Raymond L. Copson, John H. Walthall, and Travis P. Hignett: Extraction of Alumina from Clays by the Lime Sinter Modification of the Pedersen Process. *Trans.* AIME (1944) **159**, p. 241.

[5] Frank J. Cservenyak: Recovery of Alumina from Kaolin by the Lime-Soda Sinter Process. Bur. Mines *R. I.* 4069 (May 1947) 59 pp.

[6] J. E. Conley, R. A. Brown, F. J. Cservenyak, R. C. Anderberg, H. J. Kandiner, and S. J. Green: Production of Metallurgical Alumina from Pennsylvania Nodular Diaspore Clays. Bur. Mines *Bull.* 465 (1947) 193 pp.

[7] R. A. Brown, F. J. Cservenyak, R. G. Anderberg, H. J. Kandiner, and F. J. Frattali: Recovery of Alumina

from Wyoming Anorthosite by the Lime-Soda Sinter Process. Bur. Mines *R. I.* 4132 (November 1947) 127 pp.

[8] John E. Conley and Milford L. Skow: Lime-Soda Sinter Process for Alumina from High-Silica Bauxites: Laboratory and Pilot Plant Tests. Bur. Mines *R. I.* 4462 (June 1949) 67 pp.

[9] Junius D. Edwards: The Combination Process for Alumina. *Trans.* AIME (1949) **182**, pp. 9-13; METALS TECHNOLOGY (April 1945).

[10] R. S. Sherwin: Extractive Metallurgy of Aluminum. *Trans.* AIME (1950) **188**, pp. 661-667; JOURNAL OF METALS (April 1950).

[11] O. C. Ralston: Abstract of Extraction of Silica from Bauxite. Dr. Bauermeister Pub. Board L 73502, FIAT Reel G-3, Frames 3704-3727.

[12] Milford L. Skow and John E. Conley: Laboratory Tests on Percolation Leaching of Silica from Bauxites. Bur. Mines *R. I.* 4649 (January 1950) pp. 1-38.

[13] Brown and Montgomery: U. S. Bur. Standards *Tech. Paper* 21 (1913).

[14] P. F. Kerr and J. L. Kulp: Multiple Differential Thermal Analysis. *American Mineralogist* (1948) **33**, p. 397.

[15] B. S. Shvetsov and Kh. O. Gevorkyan: Thermochemical Investigation of the Kaolin Heating Process. *Journal Applied Chemistry* (U.S.S.R.) (1942) **15**, pp. 302-318.

[16] Herbert Insley and R. H. Ewell: Thermal Behavior of the Kaolin Minerals. *Journal of Research* National Bur. Standards (1935) **14**, No. 5, pp. 615-627. R. P. 792.

[17] V. I. Vernadskii: The Behavior of Kaolin on Heating. *Trans.* Ceramic Soc. (English) (1922-1923) **22**, p. 398.

[18] J. F. Hyslop: The Constitutional Changes Occurring in Clays on Heating. *Trans.* Ceramic Soc. (English) (1924-1925) **24**, pp. 402-406.

[19] T. N. McVay and C. L. Thompson: X-ray Investigation of the Effect of Heat on China Clays. *Journal* Amer. Ceramic Soc. (1928) **11**, p. 838.

[20] P. P. Budnikov: Mullite Refractory from a Mixture of Kaolin and Alumina. *Compt. rend.* Acad. Sci. U.R.S.S. (1945) **49**, pp. 202-203.

[21] O. Krause: The Use of Röntgen and Fluorescence Rays in Fine Ceramics. *Ber. Deut. keram. Ges.* (1927) **8**, No. 5, p. 114.

[22] J. E. Comofore, R. B. Fischer, and W. F. Bradley: Mullitization of Kaolinite. *Journal* Amer. Ceramic Soc. (1948) **31**, pp. 254-259.

Technical Note

Crystallographic Angles for Tin

by J. F. Nicholas

THE angles between the crystallographic planes in cubic metals were originally given by Bozorth[1] and have been republished many times. Recently, Salkovitz[2] tabulated the angles for the hexagonal metals (magnesium, zinc, and cadmium). The most commonly used metal which does not fall into either of these groups is tin, which has a tetragonal structure with an axial ratio of $c/a = 0.54558$ (99.99 pct purity, 25°C).[3] Accordingly, Table I has been prepared giving the possible values for the angle, ϕ, between planes of the types $\{HKL\}$ and $\{hkl\}$. The formula used was:

$$\cos\phi = \frac{Hh + Kk + Ll\frac{a^2}{c^2}}{\left[\left(H^2 + K^2 + L^2\frac{a^2}{c^2}\right)\left(h^2 + k^2 + l^2\frac{a^2}{c^2}\right)\right]^{1/2}}$$

All angles are given correct to the nearest minute as this is sufficient for all practical purposes. Every angle depends in a different way on variations in the value of c/a, but even in the worst cases a variation of about 0.0003 in this ratio is needed to vary an angle by 1′, which corresponds to a temperature change of 20°C or can be caused by impurities.

References

[1] R. M. Bozorth: *Physical Review* (1925) **26**, p. 390.

[2] E. I. Salkovitz: JOURNAL OF METALS (January 1951), *Trans.* AIME, p. 64; Correction (October 1951), p. 880.

[3] E. R. Jette and F. Foote: *Journal of Chemical Physics* (1935) **3**, p. 605.

J. F. NICHOLAS is Research Officer, Div. of Tribophysics, Commonwealth Scientific and Industrial Research Organization, University of Melbourne, Carlton, Vic., Australia.

TN 95E. Manuscript, Sept. 25, 1951.

Table I. Angles between the Crystallographic Planes in Tetragonal Tin

{HKL}	{hkl}	Angles between Planes of Types {HKL} and {hkl}		
001	100	90°		
	101	28° 37′		
	110	90°		
	111	37° 39′		
	112	21° 6′		
	211	50° 40′		
	301	58° 35′		
	113	14° 25′		
	311	59° 54′		
100	100	0°	90°	
	101	61° 23′	90°	
	110	45°		
	111	64° 24′		
	112	75° 15′		
	211	46° 14′	69° 46′	
	301	31° 23′	90°	
	113	79° 51′		
	311	34° 50′	74° 7′	
101	101	0°	39° 35′	
		57° 14′		
	110	70° 12′		
	111	25° 36′	60° 47′	
	112	19° 48′	45° 48′	
	211	27° 24′	43° 46′	
		67° 0′	76° 59′	
	301	29° 58′	62° 46′	
		87° 12′		
	113	20° 51′	40° 1′	
	311	33° 34′	55° 10′	
		71° 39′	87° 19′	
110	110	0°	90°	
	111	52° 21′	90°	
	112	68° 54′	90°	
	211	42° 48′	75° 51′	
	301	52° 53′		
	113	75° 35′	90°	
	311	39° 18′	67° 14′	
111	111	0°	51° 11′	75° 18′
	112	16° 33′	42° 23′	58° 45′
	211	18° 11′	49° 22′	69° 22′
		86° 55′		
	301	38° 37′	87° 28′	
	113	23° 14′	39° 56′	52° 5′
	311	29° 34′	50° 42′	80° 45′
		85° 40′		
112	112	0°	29° 29′	42° 11′
	211	31° 11′	47° 12′	59° 46′
		70° 53′		
	301	45° 17′	74° 23′	
	113	6° 40′	25° 22′	35° 31′
	311	41° 43′	52° 37′	70° 48′
		79° 5′		
211	211	0°	28° 19′	40° 28′
		66° 18′	78° 41′	85° 36′
		87° 32′		
	301	22° 57′	51° 16′	74° 57′
		87° 58′		
	113	37° 11′	47° 33′	56° 25′
		64° 27′		
	311	11° 24′	37° 43′	65° 38′
		69° 51′	77° 6′	81° 4′
301	301	0°	63° 51′	74° 14′
	113	49° 4′	69° 14′	
	311	15° 53′	60° 20′	63° 58′
		88° 24′		
113	113	0°	20° 17′	28° 51′
	311	47° 17′	54° 24′	67° 5′
		72° 58′		
311	311	0°	31° 43′	45° 32′
		60° 12′	69° 41′	75° 26′
		78° 36′		

Mechanism of Grain Refinement in Aluminum Alloys

by F. A. Crossley and L. F. Mondolfo

The mechanism of grain refinement by the addition of small amounts of titanium, molybdenum, zirconium, tungsten, and chromium to aluminum was investigated. The results indicate that the grain refinement is caused by the peritectic reaction which, by transforming the intermetallic compound into crystals of aluminum solid solution, seeds the melt with nuclei above the freezing point of aluminum.

THE feasibility of reducing the grain size of aluminum alloy castings by the addition of small amounts of titanium, zirconium, molybdenum, tungsten, columbium, boron, and chromium has been known for a long time, and the use of some of these elements as grain refiners is common practice in the aluminum foundry industry. The purpose of the present investigation was to determine the mechanism by which these additions produce the grain refinement.

Asato et al.,[1-5] on the basis of extensive work on copper, antimony, and silver alloys, presented a theory of grain refinement based on the occurrence of the peritectic reaction. Briefly, this theory states that during cooling of the melt crystals of the primary phase form, which react peritectically with the liquid upon further cooling. The peritectic reaction transforms at least partially the primary crystals into crystals of the secondary phase, which then act as nuclei for solidification of the remaining melt. As the peritectic reaction takes place the primary crystals break in pieces, and each piece acts as a nucleus. Fine dendritic crystals which can easily break are the most effective for grain refinement.

Sicha and Boehm,[6] in investigating the refining effect of titanium on an Al-Cu alloy, concluded that $TiAl_3$ crystals serve as nuclei to initiate crystallization, but did not offer further information on the mechanism of refinement. Bonsack in the discussion of their paper suggested that refinement was due to clouds of some solid in the melt, probably TiO_2 which hindered grain growth.

Eborall,[7] after studying the effect of titanium, zirconium, vanadium, tungsten, columbium, chromium, and boron on some alloys, concluded that the peritectic reaction was not an essential feature of grain refinement. Her conclusion was based mainly upon the observation that under her experimental conditions (sand casting) the Al-Cr alloys, which undergo a peritectic reaction, did not show appreciable refinement.

Cibula[8] investigated the mechanism of grain refinement and reported that two types of grain refinement exist: 1—Grain refinement produced by restriction of grain growth by the concentration gradient mechanism proposed by Northcott.[9] 2—Grain refinement produced by the presence of particles in the melt, upon which the melt crystallizes easily. He further concluded that very marked grain refinement results from a combination of the two mechanisms. Since TiC was found present in aluminum alloys refined by the addition of titanium, it was identified as the nucleating agent. In the case

F. A. CROSSLEY, Junior Member AIME, is Head, Dept. of Foundry Engineering, Tennessee Agricultural and Industrial State College, Nashville, Tenn., and L. F. MONDOLFO, Member AIME, is Professor of Metallurgical Engineering, Illinois Institute of Technology, Chicago.

Discussion on this paper, TP 3179E, may be sent, 2 copies, to AIME by April 1, 1952. Manuscript, March 14, 1951; revision, Sept. 4, 1951. New York Meeting, February 1952.

This paper represents part of a thesis by F. A. Crossley submitted in partial fulfillment of requirements for the degree of Doctor of Philosophy in Metallurgical Engineering to the Illinois Institute of Technology.

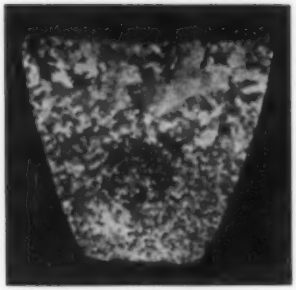

Fig. 1—Typical section of an ingot. Natural Size.

of the other refiners the identification of the nuclei as carbides was based on indirect evidence.

Experimental Technique

The metals used in this investigation were high purity aluminum (99.90 pct) and other metals (at least 99 pct). In the experimental melts the alloying elements were so diluted that any impurity introduced by them was negligible.

The master alloys were prepared in zircon crucibles using an induction furnace, and the experimental melts were made in alumina crucibles at the start, but the less expensive clay crucibles, coated with sodium aluminate to prevent contamination, were later used for most of the investigation. Graphite crucibles were used for the alloys to which carbon was to be added. The experimental melts were made in electric resistance furnaces. For fluxing the alloys and wetting of the addition elements, Dow Chemical No. 230 was used. Argon gas of commercial purity, containing small amounts of oxygen and nitrogen, was introduced in some melts through alumina tubes.

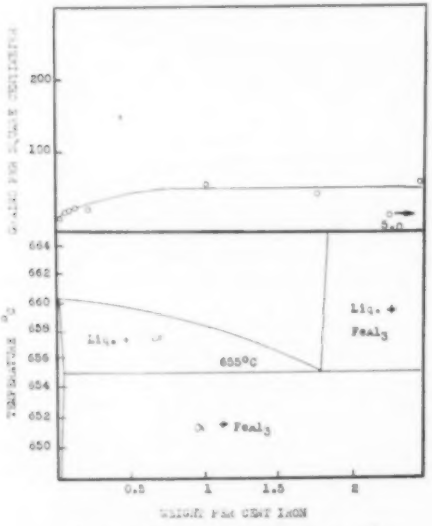

Fig. 2—Al-Fe equilibrium diagram and plot of grain size vs. composition of melt, series 3.

Table I. Composition and Analysis of Alloys

Sample No.	Average Analysis	Analysis of Grain Measurement Zone	Grain Size Grains per Sq Cm	Notes
00			0.75	Pure aluminum, furnace cooled from 100°C above the liquidus
00a			0.70	Pure aluminum, treated with argon 100°C above liquidus, furnace cooled
1-1	0.02 Zr		3	Furnace cooled from 100°C above the liquidus, alumina crucibles
1-2	0.04 Zr		2	
1-3	0.08 Zr		3.5	
1-4	0.12 Zr		9.5	
1-5	0.12 Zr		32	
1-10	0.14 Zr		38	
1-9	0.15 Zr		28	
1-6	0.40 Zr	0.41	314	
1-11	1.02 Zr		58	
2-1	0.05 Ti		36	Furnace cooled from 100°C above the liquidus, graphite crucibles
2-2	0.09 Ti		56	
2-3	0.14 Ti		94	
2-4	0.19 Ti		117	
2-5	0.23 Ti		238	
2-6	0.28 Ti		164	
2-7	0.47 Ti	0.462	168	
2-8	0.94 Ti	1.12	92	
3-9	0.01 Fe		13	Furnace cooled from 100°C above the liquidus, coated clay crucibles
3-8	0.04 Fe		21	
3-7	0.07 Fe		22	
3-6	0.10 Fe		23	
3-5	0.20 Fe		17	
3-4	1.00 Fe	0.995	53	
3-3	1.80 Fe		36	
3-2	2.50 Fe		63	
3-1	5.01 Fe	5.07	9	
4-1	0.20 Cr		20	Furnace cooled from 100°C above the liquidus, coated clay crucibles
4-2	0.30 Cr		28	
4-3	0.40 Cr		34	
4-6	0.78 Cr	0.81	205	
4-7	1.55 Cr		88	
5-4	0.17 W		24	Furnace cooled from 100°C above the liquidus, alumina crucibles
5-3	0.30 W		38	
5-5	0.39 W		101	
5-2	0.55 W	0.57	234	
5-1	1.23 W		48	
6-4	0.08 Mo		16	Furnace cooled from 100°C above the liquidus, coated clay crucibles
6-3	0.20 Mo		52	
6-2	0.41 Mo		167	
6-1	0.79 Mo	0.84	211	
7-1	0.03 Ti	0.029	6.2	Furnace cooled from 100°C above the liquidus, melts 1 to 7 in alumina crucibles, others in coated clay crucibles
7-17	0.07 Ti	0.073	26	
7-2	0.10 Ti	0.096	50	
7-3	0.13 Ti	0.118	66	
7-4	0.15 Ti	0.146	139	
7-15	0.18 Ti		211	
7-13	0.20 Ti		256	
7-16	0.22 Ti	0.191	248	
7-12	0.24 Ti	0.238	354	
7-14	0.30 Ti	0.280	418	
7-10	0.32 Ti	0.323	576	
7-11	0.37 Ti	0.384	1080	
7-8	0.39 Ti	0.385	840	
7-9	1.10 Ti	1.27	754	
7-7	1.75 Ti	2.29	222	
7-1a	0.07 Ti	0.068	21	Treated with argon at 100°C above the liquidus, then furnace cooled in coated clay crucibles.
7-2a	0.13 Ti		28	
7-3a	0.22 Ti		88	
7-4a	0.29 Ti		158	
7-5a	0.40 Ti		263	
7-6a	0.75 Ti	0.82	445	
7-8a	1.53 Ti		56	
2-1c	0.32 Ti		60	Held ½ hr at 850°C, Al_4C_3 stirred in melt, furnace cooled, graphite crucible
2-2c	0.32 Ti	0.314	71	Same as above, except that graphite instead of carbide
2-3c	0.52 Ti		56	Held at 900°C 2½ hr, furnace cooled, graphite crucible

The experimental melts were prepared by adding the required amount of master alloy to molten aluminum. When the melt reached a temperature 100°C above the liquidus it was stirred for a few minutes and then allowed to cool in the furnace. The rate of cooling was determined to be 6° to 7°C per min.

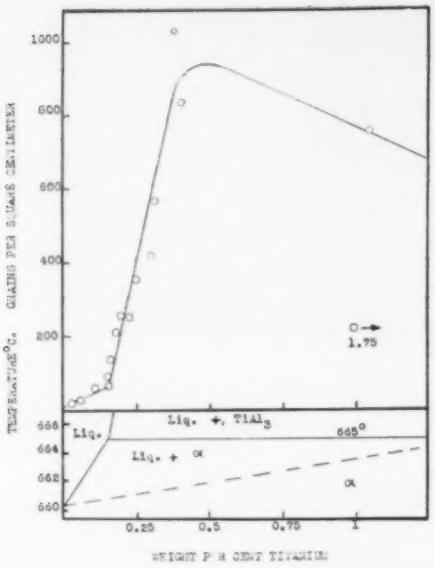

Fig. 3—Al-Ti equilibrium diagram and plot of grain size vs. composition of melt, series 7.

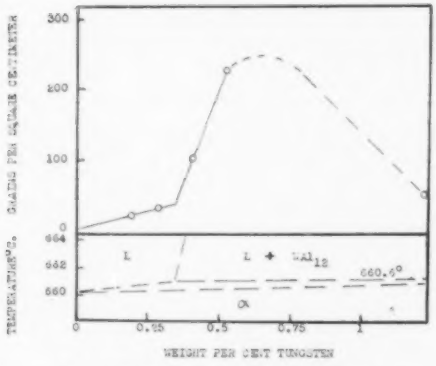

Fig. 4—Al-W equilibrium diagram and plot of grain size vs. composition of melt, series 5.

Five series of alloys were run this way, one for each of the alloying elements. Another series of Al-Ti alloys was treated with argon at the maximum temperature. The argon gas was bubbled through the melt for 30 sec, then the alloys were furnace cooled as usual. A third series of Al-Ti alloys was run in graphite crucibles, using the same technique as for the alloys discussed before. In addition three more melts were made in graphite crucibles using special techniques to increase the amount of carbon in the alloys. One melt containing 0.32 pct Ti was held at 850°C (approximately 100°C above the liquidus temperature) for 30 min. During this time aluminum carbide was stirred into it. This was followed by furnace cooling. The second melt, also containing 0.32 pct Ti, was treated in a similar way, but

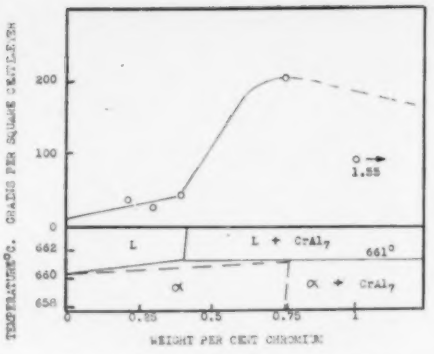

Fig. 5—Al-Cr equilibrium diagram and plot of grain size vs. composition of melt, series 4.

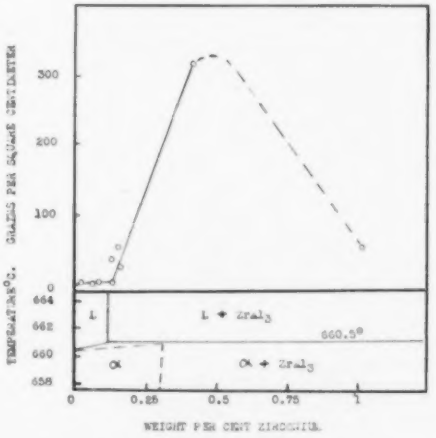

Fig. 6—Al-Zr equilibrium diagram and plot of grain size vs. composition of melt, series 1.

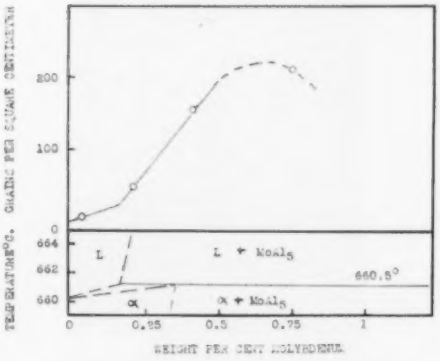

Fig. 7—Al-Mo equilibrium diagram and plot of grain size vs. composition of melt, series 6.

Fig. 8—Nucleation by $TiAl_3$. Etched with 1 pct HF-1.5 pct Ti, slow cooled in furnace. X25.

Fig. 9—Nucleation by $CrAl_7$. Etched with 1 pct HF-1.79 pct Cr, slow cooled in furnace. X50.

Fig. 10—Nucleation by $TiAl_3$. Etched with 1 pct HF-1.75 pct Ti, slow cooled in furnace. X5.

graphite, instead of carbide, was stirred into it. The third melt, containing 0.50 pct Ti, was held at 900°C for 2½ hr in a graphite crucible, stirred thoroughly, and then furnace cooled.

The solidified specimens from all these melts had the approximate size and shape shown in Fig. 1.

Some of the grindings that resulted when the specimens were cut and faced were analyzed by wet methods. In most alloys the difference between these analyses and the nominal ones was within the error of analysis (approximately 0.01 pct). The zirconium-bearing alloys, however, showed large losses of zirconium, and for this reason all of them were analyzed. The nominal compositions or, when available, the actual analyses are reported in col. 2, Table I.

After the melts had solidified and they were examined for grain size, other spot checks for composition were run. The grain size count was done in all specimens at the same distance from the bottom, along a horizontal line. Drillings were then taken along this line with a ⅛-in. drill and analyzed. This was done because segregation of primary crystals was evident in some alloys. These analyses revealed that segregation was appreciable only in the alloys with an alloying content above 1 pct. For the other alloys the difference between the nominal analysis and the analysis of the zone where the grain determination was done was within the error of analysis. These analyses are reported in col. 3 of Table I.

The ingots were sectioned vertically at the center, and the grain size of the specimens was measured by counting the grains intercepted by a line running horizontally on the polished face 0.3 in. from the bottom. Great care was taken to position this line exactly on the specimens, since variations of grain size were found from top to bottom of the melts, as shown in Fig. 1.

Fig. 11—Shape of primary crystals of $TiAl_3$ when rapidly frozen 1.3 pct Ti poured in water. Etched with 1 pct HF. X700.

Results and Discussion

In Figs. 2 to 7 are shown the effects of increasing additions of the elements on the grain size, as related to the equilibrium diagrams. Dashed lines have been used when the data are uncertain.

In the Al-Fe alloys, as the iron content was increased, the grain size decreased slightly with the first additions of iron, remained fairly constant over a wide range, well past the eutectic point, and then slowly increased. At the lower concentrations the other alloys behaved similarly, but when the composition was reached, at which the peritectic reaction occurred, a marked grain refinement appeared; and there was a sharp change in the slope of the grain size curve. With increasing additions beyond the start of the peritectic reaction, the grain refinement reached a maximum and then decreased.

At the point where the first change in slope of the grain size curve took place, primary crystals of intermetallic compound were formed. However, the presence of primary crystals per se could not be the cause of grain refinement, since in the hypereutectic Al-Fe alloys the same effect could not be noticed. Thus, the evidence points to the peritectic reaction as the cause of the grain refinement.

The above supposition found good confirmation from the microexamination. As shown in Figs. 8 to 10, the primary crystals of intermetallic compound were found inside the crystal, and the dendrites of aluminum solid solution appeared to center on them. Some of the dendrites did not show primary crystals. However, this can be explained by assuming that either the primary crystal was not in the plane of

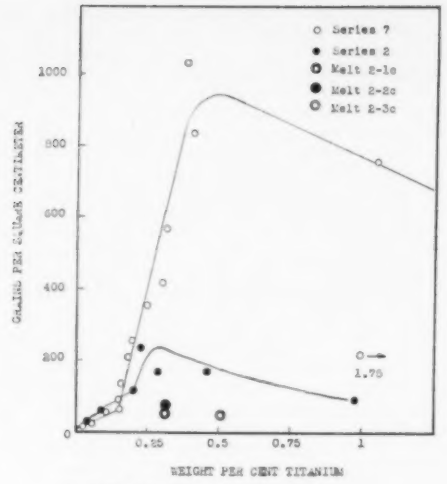

Fig. 12—Effect of carbon additions on the grain size of Al-Ti alloys.

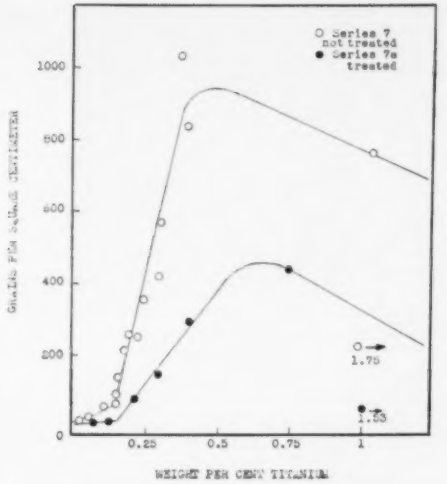

Fig. 13—Effect of treating with argon gas on the grain size of Al-Ti alloys.

the section, or the peritectic reaction was completed and the primary crystal was consumed. Fig. 10 shows the same type of distribution of primary crystals and in addition shows that, when the number of primary crystals was sufficient, practically every grain surrounded a primary crystal. The micrographs shown are all of alloys with amounts of alloying element well above the beginning of the peritectic reaction. This was necessarily so, because with lower contents the primary crystals were completely consumed and disappeared. This explains the relatively coarse grain size in the micrographs.

The same type of evidence for nucleation was also found in the other systems (with the exception of the Al-Fe), although in some cases the evidence was not as clear as in the examples shown. In the Al-Zr and Al-W alloys it was not possible to develop the dendritic structure well enough to photograph it, although evidence of nucleation around the primary crystals was visible when the alloys were strongly over-etched.

Extensive microexamination was conducted to determine if fragmentation of the primary crystals played a significant role in the refinement. It was found that the intermetallic compounds formed by the grain refiners investigated tended to have a platelike (needles in section) structure, rather than the dendritic structure deemed necessary for fragmentation by Asato et al. Even very rapid cooling did not appreciably change the form of the primary crystals, as evidenced by Fig. 11. Cracking of the primary crystals was sometimes observed (Fig. 8) and there was some evidence that occasionally the pieces of a primary crystal, when broken, nucleated two or more grains. However, this phenomenon was found in very few cases and did not seem to play an important part in the grain refinement.

In Fig. 12 are plotted the results of experiments run in the presence of carbon. Three sets of results are plotted: 1—melts in which the introduction of carbon was carefully avoided (series 7); 2—melts in which some carbon was absorbed from the graphite crucibles (series 2); and 3—melts in which an effort was made to introduce large amounts of carbon (melts 2-1c, 2-2c, 2-3c). The grain size of the alloys in which no peritectic reaction occurred was not appreciably affected by the addition of carbon. In the alloys undergoing the peritectic reaction the effect of carbon additions was very pronounced and the grain refining effect was greatly reduced, and even disappeared when sufficient carbon was present. These results are in direct opposition to Cibula's statement that TiC is the agent responsible for grain refinement, because if this were true, grain refinement should have increased with increasing carbon content. Instead, the suggestion is further substantiated that the peritectic reaction of $TiAl_3$ with the liquid was responsible for the grain refinement. The addition of carbon, by tying up the titanium as TiC, prevented the formation of $TiAl_3$.

Holiomon and coworkers[11] and others[12-15] have demonstrated that solid impurities in a melt can act as

Fig. 14—Effect of number of primary crystals on grain size.
At the bottom large amount of fine primary crystals, above few coarse primary crystals. Etched with 1 pct HF-1.5 pct Ti, slow cooled in furnace. X5.

centers for crystallization. Any treatment that reduces the amount of the solid impurities must result in a coarsening of the grain. This is clearly shown in Fig. 13. The alloys in which argon treatment had removed impurities solid above the liquidus temperature showed a much coarser grain than the nontreated alloys. However, the shape of the grain size curve was the same, thus indicating that, although the number of $TiAl_3$ particles was reduced, their effect as nucleating agents was not lost. The dependence of the grain size on the number of primary crystals is also shown in Fig. 14. Because of gravity segregation a large number of primary crystals were concentrated in the bottom layer and the grain size there was very small, the layer above it contained only a few large primary crystals, and the grain size was coarse.

Conclusions

Grain refinement in aluminum alloys by the addition of titanium, zirconium, molybdenum, chromium, and tungsten is associated with the peritectic reaction. The primary crystals of intermetallic compound which form, react with the liquid and become sheathed with a solid having the crystal structure of the phase that is going to be formed from the liquid. These solid particles act as nuclei for the crystallization of the melt, thus eliminating the necessity for undercooling to provide spontaneous nucleation.

In the case of the above elements, fragmentation of the primary crystals during peritectic reaction was not observed to an appreciable extent and consequently does not seem to play an important part in the grain refinement.

The final grain size appears to be mainly dependent on the number of primary crystals that form, and any factor which affects the number of these crystals will alter the grain size.

The addition of carbon to Al-Ti alloys reduces the grain refining effect, and the effect of the grain refining agent is lost if sufficient carbon is added.

Some grain refinement can be obtained by additions of the above elements in amounts insufficient to produce the peritectic reaction, or by the addition of other elements, but the effect is not as pronounced as when the peritectic reaction occurs.

Summary

The mechanism of grain refinement by the addition of chromium, titanium, tungsten, molybdenum, zirconium, and iron was investigated. The first five elements, when present in sufficient amounts, formed primary crystals which reacted peritectically with the liquid. The resulting solid particles acted to nucleate the solidification of the remaining liquid. This extra source of nucleation produced decided grain refinement in many cases. It was found that lesser amounts of the five elements and even large additions of iron only slightly reduced the grain size. No evidence of nucleation by primary crystals of $FeAl_3$ was found. Upon these findings it was concluded that the peritectic reaction was necessary for decided grain refinement. No evidence was found that fragmentation of the primary crystals was of importance in producing the grain refinement, as reported by Asato et al. Removal of solid impurities and additions of carbon to the melt were found to decrease decidedly the grain refining effect.

Acknowledgment

The authors gratefully acknowledge their indebtedness to the Apex Smelting Co. and to the Reynolds Metals Co. for the chemical analyses, to the Aluminum Co. of America for the high purity aluminum, to the Titanium Manufacturing Co. for the titanium and zirconium of high purity and the zircon crucibles. The authors also wish to thank the members of the staff and the students of the Department of Metallurgical Engineering of Illinois Institute of Technology, whose aid and suggestions were helpful in the course of this research.

References

[1] J. Asato: *Kinzoku no Kenkyu* (1932) **9**, p. 392.
[2] J. Asato: *Kinzoku no Kenkyu* (1933) **10**, p. 488.
[3] J. Asato: *Kinzoku no Kenkyu* (1934) **11**, p. 317.
[4] K. Iwase, J. Asato, and N. Nasu: *Kinzoku no Kenkyu* (1936) **13**, p. 213.
[5] K. Iwase, J. Asato, and N. Nasu: *Sci. Rep.* Tohoku Imp. Univ., Honda Anniversary Volume (1936) p. 652.
[6] W. E. Sicha and R. C. Boehm: *Trans.* Amer. Foundrymen's Soc. (1948) **56**, p. 398.
[7] M. D. Eborall: *Journal* Inst. Metals (1949) **17**, p. 295.
[8] A. Cibula: *Journal* Inst. Metals (1949) **17**, p. 321.
[9] L. Northcott: *Journal* Inst. Metals (1938) **62**, p. 101.
[10] A. Cibula: *Journal* Inst. Metals (1949) **17**, p. 354.
[11] J. H. Hollomon and D. Turnbull: *Solidification of Metals and Alloys.* The Nucleation of the Solid. AIME (1951) pp. 1-19.
[12] C. S. Smith: *Trans.* AIME (1949) **185**, p. 204; JOURNAL OF METALS (March 1949).
[13] D. Turnbull: *Journal of Applied Physics* (1949) **20**, p. 817.
[14] B. Vonnegut: *Journal of Colloid Science* (1948) **3**, p. 363.
[15] C. C. Wang and C. S. Smith: *Trans.* AIME (1950) **188**, p. 136; JOURNAL OF METALS (January 1950).

Technical Note

Surface Effect in the Cleavage of Zinc Monocrystals

by John J. Gilman

SURFACE effects in the brittle fracture of materials such as glass and in the plastic slip of zinc and cadmium crystals are well known.[1] Recently, another surface effect has been found for zinc monocrystals. It has been observed that certain normally ductile zinc monocrystals become extremely brittle when their surface is coated with a layer of oxide or copper plate.

J. J. GILMAN, Junior Member AIME, is associated with the School of Mines, Columbia University, New York.
TN 90E. Manuscript, Aug. 23, 1951.

This phenomenon was first observed in a triangular zinc crystal which had been grown in a graphite mold surrounded by an atmosphere of air. The lowering rate during growth was 1 in. per hr and the temperature gradient in the furnace at the melting point was approximately 24°C per in. The raw zinc was chemically pure (99.999+ pct Zn). This crystal had a fairly thick (perhaps ½ mil thick) porous oxide coating as grown. Although its orientation was favorable (χ, 46°;* λ, 48°; θ, 47°) for ductile bending, it cleaved without prior plastic deformation when loaded in bending. The load required for cleavage was appreciably greater when the maximum tensile stress was at the apex of the triangular cross-section nearest the slip direction than it was when the base of the triangle was in tension. The cleavages were good basal cleavages. However, the crystal was "optically mosaic," see Fig. 1 and Ref. 2; that is, the cleaved basal planes were not absolutely plane. They consisted of two or more very slightly disoriented regions as shown for a typical cleavage in Fig. 1.

In order to render this extremely brittle crystal very ductile it was only necessary to etch away the oxide layer. This was accomplished by a 10 min etch in 15 pct HCl. After this treatment the crystal could be bent completely around a 2 mm diam rod without cleavage.

A very similar effect was observed for two copper-plated crystals. These crystals were also triangular and of the same size (base of triangle is 0.210 in.), but they were grown in molds sealed inside evacuated pyrex tubes. They had the following orientation angles: crystal *A*—χ, 50°; λ, 50°; θ, 49°; and crystal *B*—χ, 56°; λ, 56°; θ, 63°.

Crystal *A* was cleaned with dilute HCl and then plated with a thin coating of copper for half of its length (7 in.). This copper coating was very fine grained and approximately 2200Å thick. When the crystal was loaded in tension the clean portion began to deform plastically at a resolved shear-stress of 32 g per sq mm, while the plated portion began to deform when the resolved shear stress reached 52 g per sq mm. Further loading caused additional plastic deformation until the plated portion of the crystal cleaved when the resolved normal stress was approximately 93 g per sq mm and the elongation in the plated portion was 2.5 pct. When the crystal was loaded in bending several days later the two portions of the crystal exhibited markedly different amounts of ductility. The amounts of bending which each portion could stand is shown in Fig. 2. The basal cleavages shown in Fig. 2 were optically mosaic just as those of the oxidized crystal.

Crystal *B* was cleaned with HCl and then plated with a film of copper approximately 5000A thick. This crystal was very ductile when loaded in bending prior to the plating treatment. When it was loaded in bending a few hours after it had been plated it was very brittle. It had less ductility than crystal *A* after it had been plated. After the plate had been etched off with 25 pct HCl, the crystal was again ductile. In this case, also, when the basal cleavages were examined they were found to be optically mosaic.

These effects have not been found in all zinc crystals and, therefore, are tentatively associated with optically mosaic ones. However, the extreme change in ductility is produced by a change in the surface of the same crystal and to this extent is reproducible.

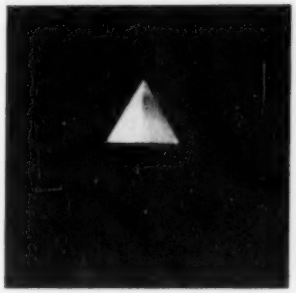

Fig. 1—Optically mosaic basal cleavage of a brittle triangular zinc crystal.

Fig. 2—Showing the difference in ductility between the copper-plated portion of crystal A and the clean portion. On the left is the plated half of the crystal.

The phenomenological explanation of the effect might be as follows: The oxide or copper coating is very fine grained and therefore has little ductility. When the crystal is loaded in bending, brittle failure of the film creates a rift at the surface which starts cleavage along the basal plane of the zinc. Basal cleavage then propagates readily even though the crystal is ductile, just as it does if a razor blade is used as a wedge along a basal plane of a ductile zinc crystal. Another possible explanation is that the oxide coating or the copper plating inhibits slip so strongly that the critical normal stress for cleavage is reached before much slip can occur. The reason why some crystals do not behave in this way is not known. It may be that the surface effect is more subtle than those which are outlined above, but the present observations leave this as an open question.

Acknowledgment

This work was supported by the Office of Naval Research, Contract N6onr 27128.

References

[1] S. Harper and A. H. Cottrell: Surface Effects and the Plasticity of Zinc Crystals. *Proc.* Phys. Soc. (May 1950), Sec. B.

[2] C. A. Cinnamon and A. B. Martin: Growth Conditions for Single and Optically Mosaic Crystals of Zinc. *Journal of Applied Physics* (1940) **II**, p. 87.

* The angles are defined as follows: χ is the angle between slip plane and specimen axis; λ, the angle between slip direction and specimen axis; and θ, the angle between slip direction and one surface normal.

Constitution of Titanium-Aluminum Alloys

by H. R. Ogden, D. J. Maykuth, W. L. Finlay, and R. I. Jaffee

Aluminum has been found to be soluble in α titanium to about 26 pct, and to raise the temperature range of transformation from α to β. Two intermediate phases exist in the system, a new face-centered tetragonal phase, designated as γ, which occurs between 34 and 46 pct Al, and $TiAl_3$. Metallographic and X-ray diffraction data were used to determine the diagram.

ALUMINUM is one of the useful alloying additions for titanium-base alloys. It is an important constituent in two commercial alloys released in 1950, one containing 4-pct-Al and 4 pct Mn, and the other containing 3 pct Al and 5 pct Cr as the metallic alloy content. It is probable that, in the future, other titanium alloys containing aluminum will be released. In the course of alloy development work, some of the features of the constitution of titanium-rich Ti-Al alloys have been developed. These are described in the present paper.

The only available information on the Ti-Al system concerns the aluminum-rich end of the diagram. In summarizing the early work, Hansen[1] indicated that there is little solubility of titanium in aluminum, and that a two-phase region exists up to the intermediate compound, $TiAl_3$ (37.2 wt pct Ti), which has a congruent melting point at 1355°C. Fink[2] has reported that a peritectic reaction occurs at 665°C between the melt and $TiAl_3$ to form the terminal solid solution of titanium in aluminum. The solubility of titanium in aluminum has been established at 0.24 pct at 510°C and is estimated to be between 1 and 1.5 pct at the peritectic temperature.

No information has been published on the diagram above $TiAl_3$, other than a statement[3] that aluminum raises the α to β transformation temperature of titanium.

H. R. OGDEN, Junior Member AIME, is Assistant Supervisor, D. J. MAYKUTH, Junior Member AIME, is Research Metallurgist, R. I. JAFFEE, Member AIME, is Supervisor in Nonferrous Physical Metallurgy, Battelle Memorial Institute, Columbus, and W. L. FINLAY, Member AIME, is Research Manager of Rem-Cru Titanium, Inc., Midland, Pa.

Discussion on this paper, TP 3185E, may be sent, 2 copies, to AIME by April 1, 1952. Manuscript, July 5, 1951. New York Meeting, February 1952.

Table I. Analysis of Raw Materials Used

Element	Analysis, Pct	
	Iodide Titanium	Aluminum
Fe	<0.04	0.002
Si	<0.03	0.002
Cu		0.002
Mg		0.001
N	0.005	
O	0.01	
C	0.03	
Al	<0.05	99.99+
Ti	99.85	

Materials and Preparation of Alloys

Iodide-type titanium and high-purity aluminum were used in this investigation. Typical analyses of these materials are given in Table I. Alloys were prepared by arc melting on a water-cooled copper hearth, using the techniques described previously for contamination-free melting.[4] Weight losses during melting were very low, ranging from 0 to 0.02 g in a 10 to 15 g charge, indicating that little or no loss of aluminum occurred during melting. This permitted the use of nominal compositions for these alloys.

Alloy ingots containing from 0 to 7.5 pct Al were rolled in air at 850°C to 0.040 in. sheet. Alloys containing from 7.5 to 16 pct Al could only be rolled about 25 pct reduction at temperatures up to and including 1200°C. Alloys containing above 16 pct Al

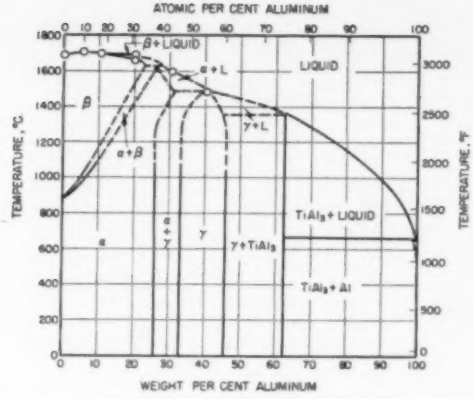

Fig. 1—Tentative diagram of the Ti-Al system.

were evaluated using cast ingots. The fabricated alloys were annealed for 3½ hr at 850°C in a vacuum of 1×10^{-4} mm Hg pressure before testing. After casting, the high aluminum alloys were given an homogenization anneal of 24 to 48 hr at 1000° to 1100°C before evaluation.

Methods of Investigation

Alloy constitution was determined mainly by metallographic methods, supplemented by X-ray diffraction. For a few alloys, transition temperatures were checked using the inverse-rate method of thermal analysis. Melting temperatures of the titanium-rich alloys were obtained by observing the melting of an ingot with a hole drilled in it.

Heat treatments were done in a resistance furnace using an atmosphere of gettered argon. Temperature control was maintained at ± 3°C during the heat treatment. Iodide-titanium control samples showed no hardness increase after several hours at 1050°C, which indicated no contamination during heat treatment. The specimens were quenched into water from the heat-treatment temperature.

The metallographic specimens were mounted in bakelite, ground through 600X paper, and given a final polish with either diamond paste or jeweler's rouge on a wool lap. Etching was done with an aqueous solution of 3 pct HNO_3, 1½ pct HF.

All X-ray diffraction work was done on powder

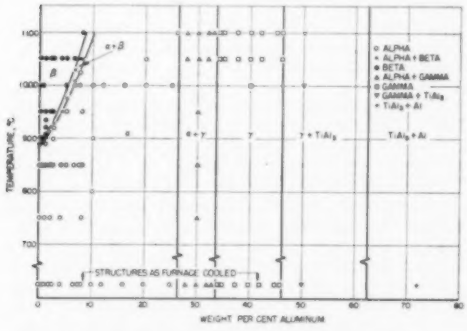

Fig. 2—Section of Ti-Al diagram showing data points.

samples. To avoid contamination during heat treatment, the alloy filings were kept in a hole drilled into a short length of as-deposited iodide-titanium rod, and capped with a titanium plug. This, in turn, was encapsulated in vacuum in Vycor. After heat treatment for the desired time and temperature, the Vycor capsule was quenched and broken under water.

The X-ray diffraction patterns on the powders were obtained using cobalt K radiation in a 57 mm Debye camera of the Buerger type with a Straumaius setting. An aluminum filter was inserted between the sample and the film to absorb scattered radiation. The lattice constants were calculated by the method of simultaneous equations from the quadratic form of the Bragg equation using the angular position of the (12.1) and the (11.4) K-α doublets, and, in alloys containing up to 7.5 pct Al, the (12.3) K-β reflection.

In the melting point work, ingot samples were used which had a ⅛ in. hole drilled in them. These were supported by a molybdenum lining in a beryllia crucible and heated by induction in a vacuum furnace, using a graphite sleeve inductor. The temperature of the hole was observed continually with

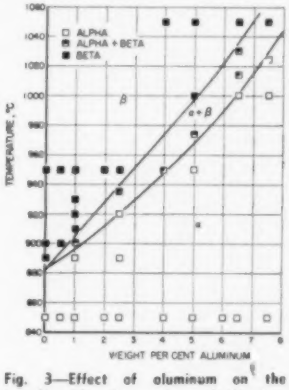

Fig. 3—Effect of aluminum on the transformation temperature of titanium.

an optical pyrometer, and the temperature at which the hole filled with molten metal was taken as the liquidus temperature. Solidus temperatures could be approximated by observing the temperature at which the edges of the hole started to round off.

Constitution Diagram

A tentative diagram of the Ti-Al system is given in Fig. 1. The solid lines indicate the phase boundaries that have been established by this investigation between 0 and 50 pct Al and by others[1, 6] between 50 and 100 pct Al. Dashed lines indicate the probable equilibria in the areas not covered in this investigation, based on extrapolation of known data and pertinent observations discussed later in this paper. The solid equilibria section of the diagram covered by the present work is shown in Fig. 2, where data points indicate the results of microscopic examination. Fig. 3 shows the effect of aluminum on the transformation temperature of titanium between 0 and 7.5 pct Al in more detail. Aluminum is seen to cause a marked increase in the temperature range of the α-β transformation.

Thermal analysis produced an arrest at 888°C for

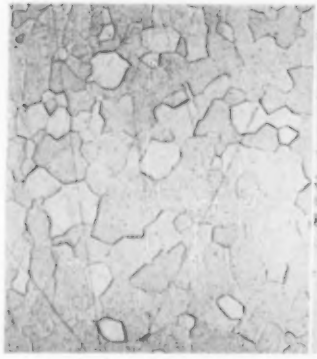

Fig. 4—Ti-5 pct Al alloy. X100.
Annealed 3½ hr at 850°C and furnace cooled. Equiaxed α grains.

Fig. 5—Ti-5 pct Al alloy. X100.
Quenched after 30 min at 1000°C. Transformed β structure.

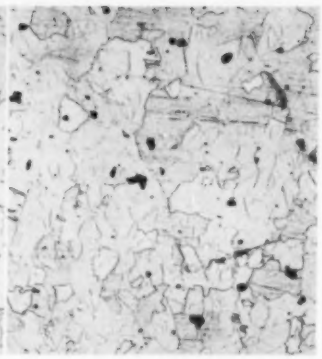

Fig. 6—Ti-5 pct Al alloy. X100.
Quenched after 30 min at 975°C. Transformed β plus equiaxed α structure.

Fig. 7—Ti-16 pct Al alloy. X75.
Rolled 25 pct at 1050°C and annealed 24 hr at 1000°C. Equiaxed α grains.

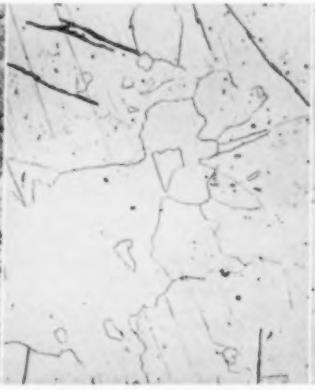

Fig. 8—Ti-20 pct Al alloy. X75.
As-cast plus 24 hr at 1000°C. Serrated Widmanstätten plates of α.

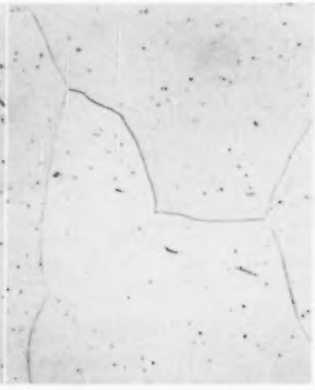

Fig. 9—Ti-25 pct Al alloy. X75.
As-cast plus 24 hr at 1000°C. Equiaxed α grains.

unalloyed titanium, at 964°C for a Ti-5 pct Al alloy, and at 1051°C for a Ti-8 pct Al alloy. These data confirmed the results of the metallographic work.

The melting point data obtained are given in Table II. The melting point obtained for pure titanium is considerably below the 1725°C melting point observed by De Boer.[5] This may have been the result of contamination from the carbon inductor. The melting point data obtained on the Ti-Al alloys fit better with 1725°C for the melting point of titanium. Also, they indicate a very slight decrease in melting point imparted by aluminum up to 20 pct Al. Above 20 pct Al, the melting point drops off much more rapidly.

Table II. Melting Point Data

Wt. Pct Al	Incipient Melting, °C	Completely Molten, °C
0	1690	1690
5	1710	1710
10	1700	1700
20	1670	1690
30		1600
40		1480

The limit of solubility of aluminum in α titanium has been established at about 26 pct between room temperature and 1100°C. The raising of the α-β transformation range by aluminum results in an extensive, but restricted, β field. With more than 26 pct Al, a new phase appears, and two-phase structures are found up to about 33 pct Al. Between 33 and 46 pct Al, a single-phase region occurs which has a face-centered tetragonal structure. This has been designated as the γ phase. The composition corresponding to TiAl, 36 wt pct Al, is located within the γ-phase field. Above 46 pct Al, the $TiAl_3$ phase appears, which indicates that the two-phase region of γ-plus-$TiAl_3$ extends up to the composition limits of $TiAl_3$.

The section of the diagram above 1050°C has been sketched in to show the probable equilibria at the higher temperatures. Since the melting point of titanium was found to be depressed only slightly by initial additions of aluminum, the extrapolation of the α and β solvus lines would indicate a peritectic reaction occurring at a high temperature, at about 25 pct Al. The marked lowering of the melting point for the 30 and 40 pct Al alloys indicates that there

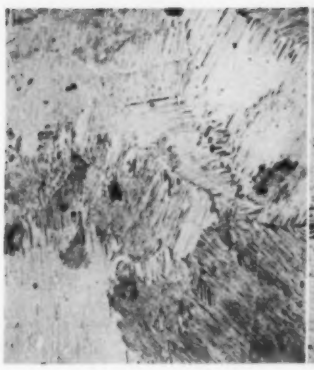

Fig. 10—Ti-28 pct Al alloy. X100. As-cast plus 24 hr at 1100°C. Banded structure of precipitated γ in α.

Fig. 11—Ti-30 pct Al alloy. X500. As-cast plus 24 hr at 1000°C. Banded structure of precipitated γ in α.

Fig. 12—Ti-32 pct Al alloy. X100. As-cast plus 48 hr at 1100°C. Banded structure of γ precipitated in α and γ grains.

Fig. 13—Ti-34 pct Al alloy. X100. As-cast plus 48 hr at 1100°C. γ phase.

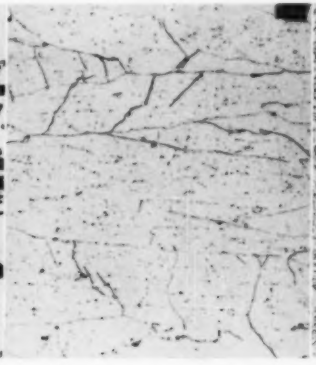

Fig. 14—Ti-46 pct Al alloy. X100. As-cast plus 48 hr at 1100°C. Cored γ structure.

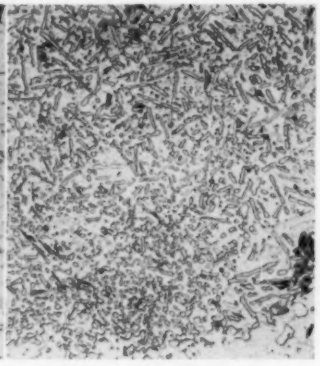

Fig. 15—Ti-50 pct Al alloy. X75 As-cast plus 48 hr at 1100°C. γ and $TiAl_3$.

is a second peritectic reaction between α and liquid to form the γ phase. The melting point of the Ti-40 pct Al alloy has been established at about 1480°C, which is probably fairly close to the peritectic temperature. The increase in solubility of aluminum in α titanium at the γ peritectic temperature has been based on the microstructure of the α-plus-γ alloys, wherein an α decomposition product is obtained.

Microstructures

The microstructures of Ti-Al alloys at low aluminum contents are similar to those of titanium. Alloys rolled and annealed at temperatures within the α field have equiaxed α grains similar to those found in high purity titanium given the same treatment. A typical structure of this type is shown in Fig. 4 for a Ti-5 pct Al alloy annealed at 850°C. Quenching the alloys from the β field results in a transformation structure of large, serrated Widmanstätten plates, very similar to that found with iodide titanium. This structure is shown in Fig. 5. The microstructure of alloys quenched from the α-plus-β field consists of a mixture of equiaxed α grains and serrated Widmanstätten plates. This structure is difficult to interpret because of the similarity between the two types of grains. A typical structure is shown in Fig. 6 for a Ti-5 pct Al alloy quenched from 975°C. In the composition range of 8 to 16 pct Al, where the alloys had been rolled about 25 pct reduction at 1000°C, annealing for 24 hr at 1000°C produced an equiaxed α structure, as shown in Fig. 7. Alloys containing above 16 pct Al, which could not be fabricated, were examined after an homogenizing anneal of 24 hr at 1000°C. At 20 pct Al, Fig. 8, the structure consists of large Widmanstätten plates, indicative of a β to α transformation structure. These plates probably existed in the as-cast alloy and were not overcome by the homogenizing anneal. Several cracks can be seen in the structures of the 16 and 20 pct Al alloys, illustrative of the inherent brittleness of the high aluminum-content α range. At 25 and 26 pct Al, Fig. 9, equiaxed α grain structures were obtained which showed no evidence of a transformation from the β phase. These data indicate that the solubility limit of aluminum in β titanium lies between 20 and 25 pct Al, probably quite close to 20 pct.

In the α-plus-γ field, the alloys have a banded

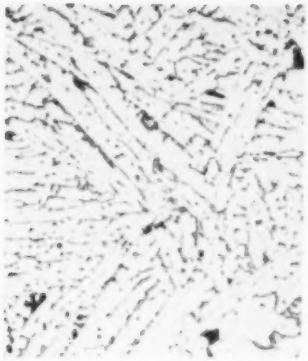

Fig. 16—Ti-72 pct Al alloy. X50. As-cast structure. $TiAl_3$ and Al.

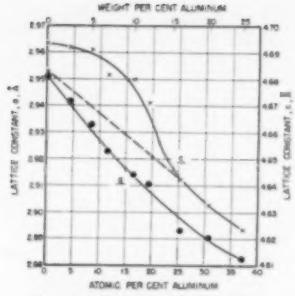

Fig. 17—Effect of aluminum on the lattice constants of titanium.

structure, suggesting that the α phase has precipitated the γ phase on cooling. This is shown in the Ti-28 pct Al and Ti-30 pct Al alloys, Figs. 10 and 11, where the entire grain is banded. This indicates that the maximum solubility of aluminum in the α phase is at least 30 pct at the γ peritectic temperature. At 32 pct Al, the banded structure still exists, but separate γ grains are beginning to appear. This structure is shown in Fig. 12.

Figs. 13 and 14 show microstructures of the γ-phase alloys after a homogenization treatment of 48 hr at 1100°C. The Ti-34 pct Al alloy has an equiaxed grain structure rather similar to that found in face-centered cubic metals. This structure persisted to 40 pct Al. From 42 through 46 pct Al, somewhat different structures, shown for the Ti-46 pct Al alloy in Fig. 11, were obtained. The fine structure shown there is not believed to be grain-boundary precipitation, but is more likely the result of coring derived from a long freezing range. If it is assumed that the composition of the γ phase at the peritectic temperature occurs at about 40 pct Al, then the differences in microstructure are readily understandable. A longer freezing range on the aluminum-rich side of this point could account for the heavily cored structure of these alloys.

The microstructure of a γ-plus-$TiAl_3$ alloy is shown in Fig. 15, and that of a $TiAl_3$-plus-aluminum alloy is shown in Fig. 16. The Ti-50 pct Al alloy consists of needles of $TiAl_3$ in a matrix of γ phase, while the Ti-72 pct Al alloy consists of dendrites of $TiAl_3$ with aluminum present as the dendritic filler. The $TiAl_3$ phase has been identified in both of these alloys by X-ray diffraction using lattice spacings reported by Fink, Van Horn, and Budge.[6]

X-Ray Diffraction

The lattice-constant curves showing the effect of aluminum on the lattice constants of titanium are given in Fig. 17. To obtain these data, powder samples of alloys containing up to 7.5 wt pct Al were heat treated for 1 hr at 800°C and alloys containing 10 to 25 wt pct Al were heat treated 20 min at 850°C. The lattice constant a_o decreases almost linearly with increasing aluminum content. However, the c_o curve shows a hump at low aluminum contents, which may be indicative of oxygen and/or nitrogen contamination in the powder samples. Clark[7] has shown that both oxygen and nitrogen cause an increase in the c_o constant of titanium, but they do not significantly affect the a_o constant. However, even assuming some contamination of the low aluminum-content alloys, the c_o values in this range seem much higher than would be expected. Using the actual values, the axial ratio c/a increases almost linearly, 1.591 at 0 pct Al to 1.604 at 20 atomic pct Al. Above 20 atomic pct Al, the axial ratio remains constant at 1.604.

It was also found that the annealing treatment given to powder samples had a direct bearing on the lattice constants obtained. Filings of alloys containing 10 to 25 wt pct Al annealed in vacuum in the titanium-block holder for 24 hr at 1000°C had lattice constants corresponding to about 2.5 wt pct Al, and gave very diffuse patterns. This was probably caused by diffusion of the aluminum from the filings into the titanium capsule, or diffusion of titanium from the capsule into the filings. Similarly, powder samples of alloys containing 30, 35, and 40 wt pct Al, which had been identified microscopically as α-plus-γ and γ-phase alloys, had lattice constants of the α phase corresponding to 2.5 pct Al with no γ-phase lines present when annealed 24 hr at 1100°C. These alloys were checked by X-ray diffraction examination of filings made from solid samples given the same annealing treatment. The patterns obtained were diffuse, because of the cold work present in the filings, but both the γ and α phases could be identified in the 30 wt pct Al alloy and only the γ phase in the 35 and 40 wt pct alloys. Therefore, the technique of first homogenizing block samples of α-plus-γ and γ-phase alloys followed by low temperature annealing of the powder samples was adopted for these alloys.

Using the lattice-parameter curves in Fig. 17, an attempt was made to determine the effect of temperature on the solubility of aluminum in α titanium.

Table III. Alpha Lattice Constants of a Ti-30 Pct Al Alloy Quenched from Various Temperatures

Heat Treatment (Water Quenched)		Lattice Constant, A*		
Time, Hr	Temperature, °C	a_o	c_o	Wt Pct Al
16	650	2.934	4.635	23 ± 1.5
8	750	2.931	4.637	20 ± 1.5
4	850	2.927	4.642	21.5 ± 1.5
½	900	2.927	4.636	21.5 ± 1.5
¼	1050	2.886	4.633	22 ± 1.5

* Degree of accuracy: $a_o \pm 0.003$A, $c_o \pm 0.007$A.

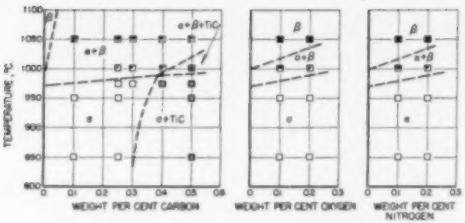

Fig. 18—Effect of carbon, oxygen, and nitrogen on the transformation range at the level of 5 pct Al.

Powder samples of a Ti-30 pct Al alloy were quenched from several temperatures, and lattice constants of the α phase were determined. The lattice constants and corresponding aluminum solubilities at the various temperatures are given in Table III. The α solubilities of aluminum calculated from the X-ray diffraction data are of the same order of magnitude but are 2 to 3 wt pct Al lower than the value determined microscopically. The lower solubilities are believed to be caused by the diffusion effect noted before. Therefore, it is considered that the metallographic observations on the terminal solubility of aluminum in α titanium are more reliable than those using X-ray diffraction.

Diffraction patterns of γ-phase alloys (33 to 46 wt pct Al) were diffuse, and precision lattice constants could not be obtained. Filings for this work were taken from block samples homogenized for 48 hr at 1100°C and then given a short-time strain-relief anneal. The diffuse patterns may have been caused by either an insufficient homogenization treatment, or an insufficient strain-relief anneal. However, good patterns were obtained of the γ phase from alloys in the α-plus-γ and γ-plus $TiAl_3$ fields, so that the lattice constants of the upper and lower limits were obtained. These are given in Table IV. The crystal structure has been established as face-centered tetragonal with an axial ratio c/a of 1.012 to 1.018. It is interesting to note that the lattice constants of the γ phase are very close to the lattice constant of aluminum, 4.0408A.[6] It has also been established that the γ phase has an ordered structure, probably of the CuAu type with alternate layers of titanium and aluminum atoms. Superlattice lines were observed in all alloys containing from 30 to 50 wt pct Al, and, although precision lattice constants could not be determined for γ-phase alloys, the superlattice lines were still discernible. Quenching alloys containing 35 to 40 wt pct Al from temperatures up to 1050°C did not overcome the ordered structure, indicating either that no order-disorder transformation exists at least up to 1050°C, or that it cannot be suppressed by quenching.

Effects of Carbon, Oxygen, and Nitrogen

Because carbon, oxygen, and nitrogen are the major impurities present in commercial grades of titanium, it is important to know their effects in small quantities on the Ti-Al diagram. Fig. 18 shows the effect of carbon, oxygen, and nitrogen on the transformation range at the 5 pct Al level. All three of the interstitial additions raise the α and β transus temperatures markedly, which is what might be expected from the previous data on the binary alloys of these elements with titanium.[4] In all three cases, the slopes of the α and β transus lines have been estimated from the quantity of β present at temperatures within the α-β field. Precise determinations of the exact location of these lines have not been made.

Table IV. Lattice Constants of Gamma Phase

Aluminum Content		Lattice Constants, A		Other Phases Present
Wt Pct	Atomic Pct	a	c	
30	43.25	4.0155	4.0625	α
50	64	3.976	4.049	$TiAl_3$

Summary

The titanium-rich portion of the Ti-Al diagram has been surveyed between room temperature and 1100°C. Very limited data were taken above 1100°C, and the diagram in this region has been sketched in chiefly to conform with melting point data and microstructural appearance of cast alloys. The main features of the diagram may be summarized as:

1—The solubility of aluminum in α titanium is about 26 wt pct.

2—The temperature of α to β transformation is increased by aluminum additions, resulting in a two-phase field where β solubilities are less than α solubilities. This is the first documented case of a metallic α-stabilizing addition for titanium.

3—A new phase designated as γ occurs between 34 and 46 pct Al. This phase has an ordered face-centered tetragonal structure with an axial ratio close to unity and with lattice constants very close to the lattice constant of aluminum.

4—Aluminum additions up to 20 pct do not appreciably lower the melting point of titanium. Above 20 pct Al, the melting point is markedly lowered.

In addition, the effects of small amounts of carbon, oxygen, and nitrogen on the transformation range of Ti-Al alloys have been surveyed.

Acknowledgments

The authors are grateful to Rem-Cru Titanium, Inc., for permission to publish the results of this work which was done at Battelle Memorial Institute under their sponsorship. They also wish to thank B. W. Gonser, of Battelle, for valuable suggestions and discussion, which greatly aided the progress of the experimental work, and J. R. Doig, of Battelle, for the X-ray diffraction measurements reported in this paper.

References

[1] M. Hansen: *Aufbau der Zweistofflegierungen*. pp. 158-159. (1936) Berlin, Julius Springer.

[2] W. L. Fink: *Physical Metallurgy of Aluminum Alloys*. A.S.M. (1949) pp. 69-70.

[3] D. I. Brown: Two New Titanium Alloys Now in Production. *Iron Age* (1950) **166**, pp. 85-88.

[4] R. I. Jaffee, H. R. Ogden, and D. J. Maykuth: Alloys of Titanium with Carbon, Oxygen, and Nitrogen. *Trans.* AIME (1950) **188**, pp. 1261-1266; JOURNAL OF METALS (October 1950).

[5] A. E. von Arkel: *Reine Metalle*. p. 168 (1939) Berlin, Julius Springer.

[6] W. L. Fink, K. R. Van Horn, and P. M. Budge: Constitution of High-Purity Aluminum-Titanium Alloys. *Trans.* AIME (1931) **93**, p. 421.

[7] H. T. Clark: The Lattice Parameters of High Purity Alpha Titanium; and The Effects of Oxygen and Nitrogen on Them. *Trans.* AIME (1949) **185**, pp. 588-589; JOURNAL OF METALS (September 1949).

[8] *Metals Handbook*. A.S.M. (1948) p. 21.

Model for Dendrite Growth Form in Metals and Alloys

by R. B. Pond and S. W. Kessler

Metal specimens were solidified through a measured thermal gradient so a free surface and the liquid-solid interface could be examined. A line structure was observed on the surface and a hexagonal structure on the interface. A model to explain these forms is proposed.

NUMEROUS observations of the dendrite form have been made both in nonmetallic and metallic systems. From these, extrapolations have been made as to the probable dendrite form in pure metals. Observations of the dendrite form in pure metals, nevertheless, have been scanty. In general, these observations have been made on the skeleton dendrite after the mother liquid has been drained from around it, and a mechanism of the formation of the dendrite has been postulated from this solid form. Recent investigations have been conducted in an endeavor to make a study of the formation of the dendrite in several pure metals and the effect of several variables on this mechanism and final form. For these investigations, an apparatus was designed and constructed as shown in Fig. 1. It consists of a talc block containing a half-cylindrical depression, the end of which terminates in the conical recess of a copper block having an external attachment for cooling. A heating coil extends the length of the mold just beneath the lower limits of the cavity. The entire cavity for holding metal is coated with a thin film of graphite. Six thermocouples are equally spaced in the cavity and under the graphite, and six microammeters indicate the temperatures at the particular thermocouple stations. Readings were taken of all meters at the same instant time measurements were taken by photographing the panel of microammeters and a stop watch which was started at the beginning of the run.

It was possible with this apparatus to solidify metals through a measured thermal gradient and to observe the progression of the liquid-solid interface with time by following the formation of the dendrite markings in the surface of the solid material. These

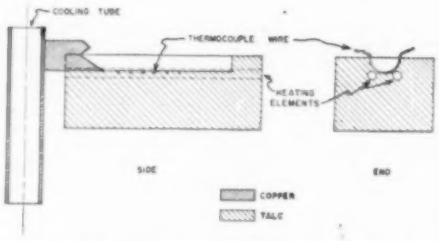

Fig. 1—Schematic drawing of mold used in studies of growth form.

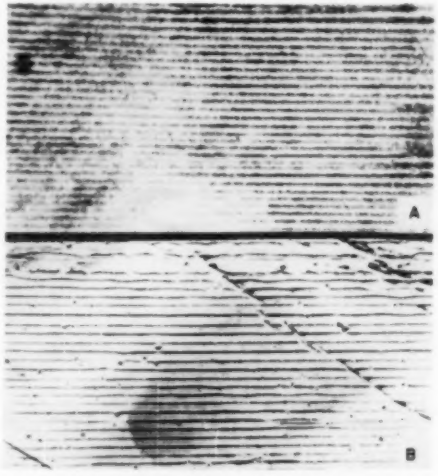

Fig. 2A—Reproduction of Graf's picture[7] of layer structure in copper. Estimated X1000. B—Longitudinal striae in pure indium. X450.

R. B. POND is Assistant Professor, and S. W. KESSLER, Student Associate, AIME, is a graduate student, Metallurgy Section, Department of Mechanical Engineering, The Johns Hopkins University, Baltimore.

Discussion on this paper, TP 3159E, may be sent, 2 copies, to AIME by April 1, 1952. Manuscript, June 21, 1951; revision, Sept. 14, 1951. New York Meeting, February 1952.

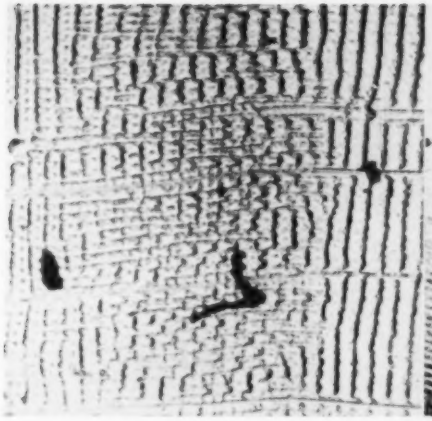

Fig. 3—Typical longitudinal and transverse striae witnessed in the surface of solidified pure tin. X50.

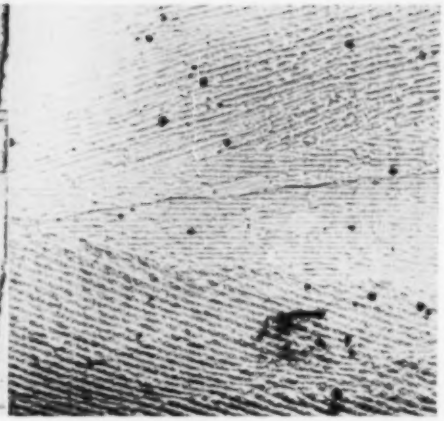

Fig. 4—Longitudinal striae delineating grain boundaries in pure tin. X50.

dendrite markings apparently were caused by the unequal and progressive growth of the dendrite segments and shrinkage of the liquid between these segments. When the residual liquid solidified, it was at this new level; and the dendrite was then marked out in relief. The dendrite in relief gave a frosted appearance to the solid as described by Turnbull and Cech,[1] while the liquid maintained a shiny mirror-like surface.

During the course of investigation, it was desired to observe the shape of the total liquid-solid interface in order to determine if the surface trace was characteristic of the total interface. This was accomplished by sucking the metal from the molten part of the bath at an extremely rapid rate after partial solidification. This process allowed another view of the dendrite form which was witnessed on the surface.

The dendrite form as witnessed on the surface was a stria or line structure aligned parallel, or roughly parallel, to the direction of growth (longitudinal striae), as well as a coarser line structure which was aligned roughly perpendicular to the longitudinal striae (transverse striae). The longitudinal striae were observed to be almost identical in form with that structure reported by Graf[2] as a layer-type structure, as can be seen in Fig. 2 by comparing his structure with the longitudinal striae. The transverse striae were not so easily witnessed and proved most difficult to photograph at the same time as the longitudinal striae. Fig. 3 shows the presence of both striae, and Fig. 4 shows the predominant appearance of the longitudinal striae and their delineation of the grain boundaries. The transverse striae in Fig. 4 appear only by faint light bands across the structure.

The longitudinal striae are of crystallographic origin, i.e., parallel within each grain but different from grain to grain. The transverse striae, on the other hand, often would be found to be parallel across all grains. It has been shown that this transverse striae is not a true dendrite marking however, but is a shrinkage mark. This is explained with reference to Fig. 5. If the original volume of material $S + L$ is liquid and solidification proceeds from 1 to 5, the first volume of material to solidify at 1 will be at the liquid level, A. As the rest of the material decreases in temperature, the liquid level drops to B; and as the volume of material 2 solidifies, it will be at level B. This process is repeated, thereby giving a step-like surface to the solid, S, which will show as striae when viewed from above. This model points to the fact that the transverse striae should be more prominent in portions of the specimens where the liquid-solid interface existed when the liquid solidified under the most rapid rate of cooling. This was found to be the case. Fig. 6 is a micrograph of polycrystalline pure tin which was solidified from a point source and shows the transverse marking as arcs emanating from this point. Since these marks have a definite curvature in each grain, they cannot be classed as crystallographic or dendritic markings.

The bled face showed a hexagonal network similar to the hexagonaloid structure shown by Buerger.[3] Fig. 7 indicates that the longitudinal striae is the impression of the tops of the hexagons in the surface. A higher magnification of this structure shows a characteristic array of almost perfect hexagons, cf. Fig. 8. Fig. 9 shows the hexagonaloid to be a three dimensional unit with a breastlike shape; consequently, the name mammiform is assigned to it since this is the noun form of the word given by Dana[4] to describe such imitative shapes. A check to determine if these forms represented different grains was made by examination under polarized light. Fig. 10 shows three grains, each containing mammiforms, the grain boundaries being mammiform boundaries, and shows the mammiform in any one grain to be consistent in orientation with the rest of the grain. The specimen was deformed to produce twin bands which can be seen crossing the mammiforms and terminating at

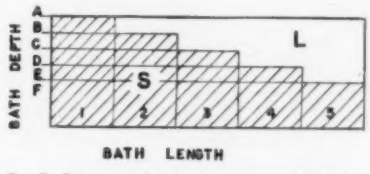

Fig. 5—Schematic sketch of step-like solidification.

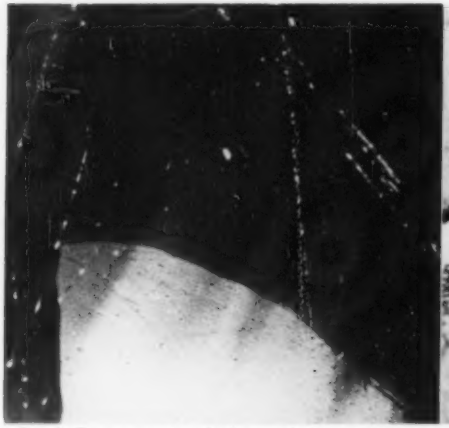

Fig. 6—Transverse striae showing as circular marks in pure tin. X40.

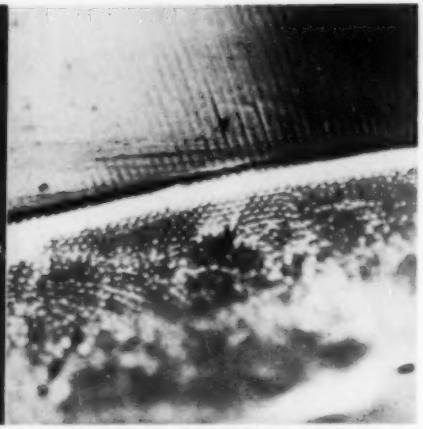

Fig. 7—Billet of pure indium showing the correlation of the mammiforms in the bled face with the longitudinal striae in the surface. Approximately X15.

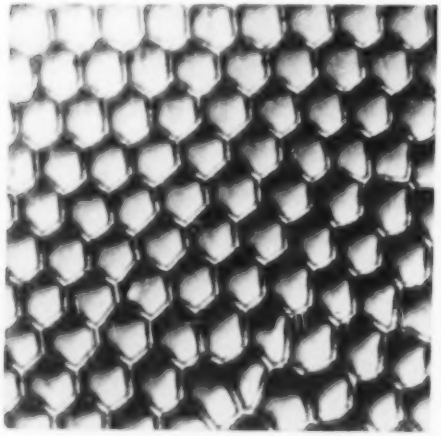

Fig. 8—Ends of the longitudinal striae in pure tin showing the characteristic hexagonal array. X125.

the grain boundaries. It is to be noted that this structure is not the same as the cellular structures reported by Bengough,[7] and referred to as a double ture, the formation of which is described by Desch.[6] The cells of these structures are individual grains. The observed structure is probably the same as that reported by Bengough,[7] and referred to as a double cellular network, as well as by Smialowski[8] and Buerger.[9]

In an attempt to explain the hexagonal shape of the rod of the dendritic structure, consider an array of identical cones situated on a plane so that the axes of the cones are perpendicular to the plane, and are in a close-packed arrangement. If the cones are made sufficiently large so that their sides will everywhere intersect the sides of neighboring cones, these intersections will describe a net of hexagons,

Fig. 9—Typical three dimensional structure of the mammiform in pure indium. X400.

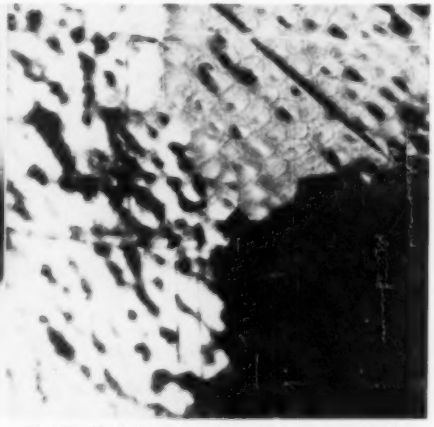

Fig. 10—Grain boundaries in pure tin portrayed under polarized light follow mammiform boundaries. X50.

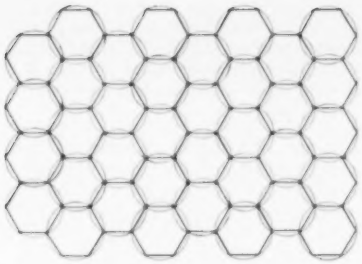

Fig. 11—Development of array of hexagons by the intersection of cone bases.

Fig. 12—Sharp nosed pentagons developed by omitting one cone from the array.

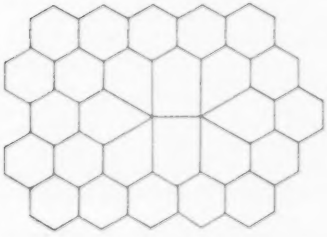

Fig. 13—Square nosed pentagons developed by omitting two cones from the array.

cf. Fig. 11. It should be noted in Fig. 8 that there are other than six-sided figures. Using the model shown in Fig. 11, the misshapen figures can be explained by omitting a selected nucleus from the structure. Fig. 12 illustrates sharp-nosed pentagons obtained by omitting one nucleus, and Fig. 13 indicates square-nosed pentagons obtained by omission of two nuclei. Mammiforms were also observed where no great uniformity of shape existed, as in Fig. 14. Such nonuniform shapes can be constructed by omission of a sufficient number of selected nuclei.

Two major explanations are necessary relative to the inherent hexagonal shape of the rods. One, by what mechanism is the hexagonal close-packed site selected for growth of the mammiforms; and two, why the particular shape of the mammiform? In an endeavor to answer the first question reference is made to Fig. 15.

The assumption is made that the block of material XYZ is solid material which has been solidified from the melt, and in which the face X represents the liquid-solid interface. The control gradient (or the gradient which controls the flow of heat from the liquid) along this block of material is expressed by line 1 and the solidification temperature of the material by line 2 on the temperature-distance curve adjacent to the block material. It will be noted that the temperature at the interface in this static condition is the solidification temperature of the metal. It is assumed, for the moment, that a block of material of mass A adjoins itself to the solid structure at A and transforms from a liquid into a solid. The latent heat of fusion of this mass A may be given up in three ways: 1—It may be conducted into the already solid material in accordance with the control gradient. 2—It may be diffused into the liquid in accordance with the temperature gradient in the liquid and the conductivity of the liquid. 3—It may be diffused in the surface X toward the boundaries of this face.

The thermal diffusivity of the metal in the surface X will determine the rate at which this heat is conducted away from point A. Consider, now, the heat dispersion in plane X at time t_1. For simplicity's sake, plane X is assumed to be thermally isotropic. It will be noted that the temperature at point A has been increased to A_1, as shown on the temperature-distance curve. If the mass A is to remain solid at the temperature A_1, either the small solid particle can be heated to A_1 without melting, or A_1 is the true solidification temperature and supercooling to the noted solidification temperature curve 2 is necessary to cause this initial solidification. The surface thermal gradient from point A_1 is expressed by curve 3, and that closest point at which another mass of material can solidify is to be found on that loci of points represented by the surface gradient curve 3 crossing the solidification temperature curve 2. If it is now assumed that solidification occurs at some random point B of this loci of points, the latent

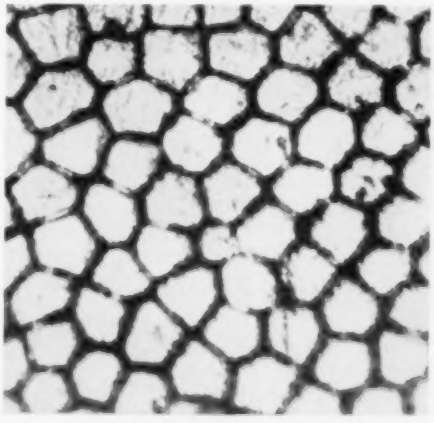

Fig. 14—Mammiforms in pure lead showing no extensive uniformity of shape. X50.

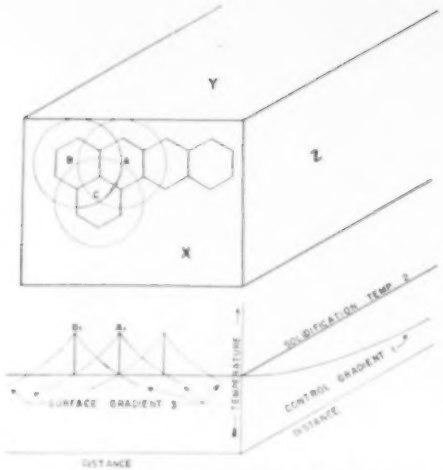

Fig. 15—Model for explaining mammiform site selection.

heat of fusion as noted before for *A* will be dispersed in a like manner; and a new loci of points will exist at which another mass of material can solidify. The possible positions of solidification determined by mass *A* are still imposed. The closest approach to *A* and *B* for this newest point will be at C, assuming that there is a proper balance of heat flow in the surface gradient and the control gradient. It is noticed that these *A*, *B*, and *C* points are in a close-packed arrangement, or that the angles between lines connecting these points are 60°. If, however, the balance of heat flow in the surface gradient and control gradient are not properly adjusted, point *C* may be removed away from points *A* and *B* or toward points *A* and *B*, thereby increasing or decreasing the closeness of packing.

If the solidification of masses *A*, *B*, and *C* should occur simultaneously and in a random fashion, so that any one mass is within the surface control gradient of another mass, then one of the masses must liquefy, since it will be above the solidification temperature. Consequently, the simultaneity of solidification is improbable unless the control gradient is sufficiently steep so that heat is removed from all masses at a rate such that the surface control gradient areas are very small. In this case, the masses may be solidified in random distribution. It should

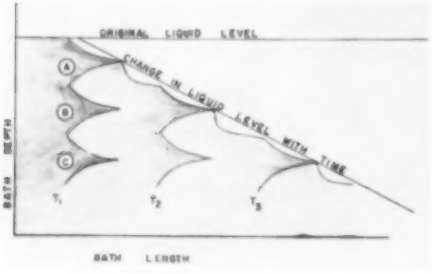

Fig. 16—Model for explaining step-like solidification.

be noted that if the entire surface *X* is at the temperature of solidification, the deposition process may start from a multiplicity of points; and that although a close-packed array may exist in each area, the zones between these areas need not show a continuance of the order.

With this model for the selection of growth sites and the accompanying order of growth sites, there will be growth from these points in accordance with the growth vectors of the materials being solidified; i.e., the shape of the liquid-solid interface will be determined by the orientation of the crystal. However, this shape will be determined for every growth site, and consequently the liquid-solid interface for each site will approximate a cone projecting into the liquid if growth proceeds in a symmetry direction. Since the cone projected into the liquid will be entering areas of different temperature, or since a temperature gradient will exist down the axis of the cone, the shape of the cone cannot be expected to be extremely regular; and it will more nearly approach a mammiform structure. If this particular shape has grown out from the original plane *X*, a time will be reached when the bases of these mammiform figures will intersect. These intersections will form hexagons if the sites are in close-packed array. If the site *C* is removed from sites *A*

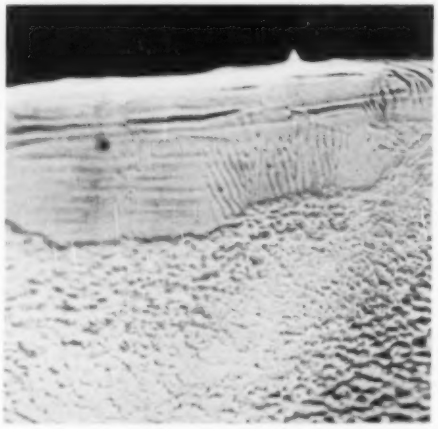

Fig. 17—Liquid-solid interface in pure tin which was not progressing when liquid was sucked off. Note absence of mammiforms. X500.

and *B*, as previously described, the shape of the intersection figures will be flattened hexagons. If a mass site is erased by being situated too close to another site, as described above, and yet exerts its influence on a third site prior to its eradication, then a vacant site may exist and the figures in this locale will be irregular pentagons, cf. Fig. 12. If the two sites are so erased, there will be two zones of irregular pentagons of different shapes. By making various sites disappear, almost any type figure can be made to exist, cf. Fig. 13, or if the sites are laid down at random as may occur if the control gradient is sufficiently steep, the figures will present themselves in many devious designs.

If growth from one site occurs before growth from other sites due to local differences in the control thermal gradient, then the size of the particular fig-

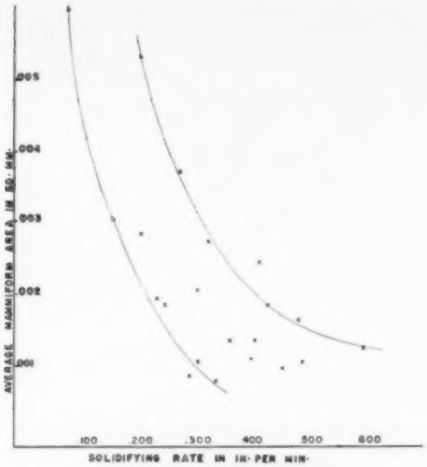

Fig. 18—Plot of average mammiform size vs. solidification rate.

ure around this site will be relatively larger than its neighbor; but its geometry will remain unchanged. Conversely, a site which is delayed in its growth will have a relatively small size, and its geometry will be changed, cf. Fig. 12.

The transverse markings might be formed by the following mechanism: In Fig. 16, the original liquid level and the change in liquid level with time are represented at various positions of the bath; a series of mammiforms *A*, *B*, *C*, etc., are growing; and at time t_n the tip of mammiform *A* has reached the liquid level and cannot propagate further into the liquid. The upper side of the form will continue to grow as long as there is metal available to feed it; but it must be remembered that the liquid can flow off around the sides of the form, and consequently it will never be able to utilize the entire volume of metal available to it at t_n. The lower side of the form will also continue to grow until it grows out of the liquid so that at t_n, the tip of mammiform *B* will have reached the liquid surface and mammiform *A* will have terminated its growth in the profile shown. As the mammiforms *A*, *B*, *C*, etc., continue to follow this procedure, the step-like shrinkage marking, previously described, is developed.

In the above models, the mammiform is a growth form and would not be present if growth were not proceeding. The liquid-solid interface was held in one position for an hour by establishing a steady-state condition of heat flow and then all of the liquid was sucked off. No mammiforms could be observed, as seen in Fig. 17. The background structure may be explained by the rapid solidification of that liquid metal which was wetting the solid metal and which could not be drawn off. Near the top edge of the specimen where drainage was more complete, an absence of this fine structure may be noted. This experiment was repeated with the exception that after the interface had been stopped for an hour growth was allowed to continue and the liquid immediately sucked off. The characteristic mammiform structure was found.

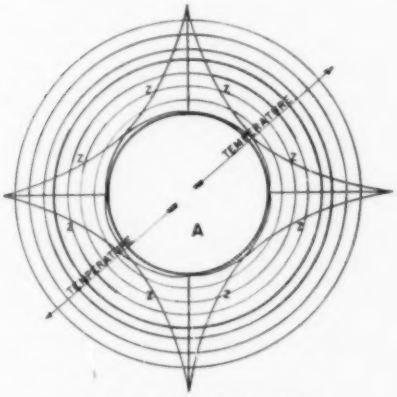

Fig. 20—Model for explaining radial distribution of dendrite arms.

By the above model, it was speculated that the steeper the control gradient in the solid, the greater would be the quantity of heat conducted into the solid per unit time and the smaller would be the available heat from the nucleus to be distributed in the liquid-solid interface. This means that the area influenced by a nucleating mass will be smaller or that the base area of the mammiform would be smaller. Since the steepness of the control gradient was found to be roughly proportional to the rate of solidification, the average mammiform sizes in specimens which had been solidified at various rates were determined and plotted vs. rate of solidification, Fig. 18. The envelope including the points shows the tendency for decrease in mammiform size with an increase in growth rate as predicted from the proposed model.

Since the first observations and investigations of the mammiform were made in specimens produced

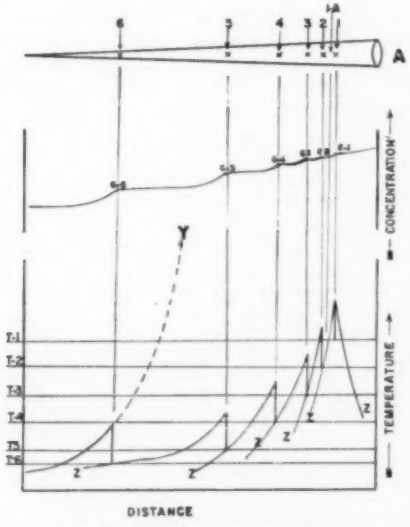

Fig. 19—Model for explaining the tree-like dendrite of solid-solution alloys.

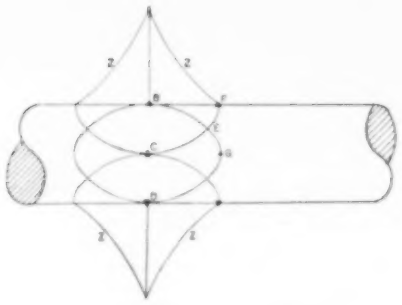

Fig. 21—Model for explaining alignment of mammiform sites along axis of original form.

Fig. 22—Schematic drawing of growth of the mammiform bases together to form webs.

as described above, it seemed necessary to check the existence of the mammiform when the metal was solidified in other ways. Polycrystalline metal masses were solidified in deep and shallow pots from the bottom, and in hollow tubes from the outside. In every instance, mammiforms were witnessed. The mammiforms were observed in all metals investigated, i.e., 99.997 pct pure Sn, 99.99+ pct pure Pb, 99.998 pct pure Bi, 99.999 pct pure In, 99.8+ pct pure Sb, and 99.997 pct pure Al.

An application of the proposed mammiform model in the case of the solid-solution alloys may be made in an endeavor to explain the mechanism of formation of the tree-like dendrite form. This is done by the imposition of a concentration gradient on the model, Fig. 19. The assumption is made that a relatively long mammiform *A* has grown onto the liquid-solid interface, that the temperature of the surface of this mammiform is (over microscopic segments) constant, and that with a given core temperature of the mammiform, the thermal gradient curve of this material is represented as curve *Y*. If a mass of concentration c-1 of solidification temperature *T*-1 deposits on site 1, the local temperature will be increased and the surface temperature gradient *Z* will be established so that the closest approach of the next mass c-1 to be deposited will be at 1-*A*. However, with reference to the concentration curve, it is seen that the concentration at point 1-*A* is c-2 and its solidification temperature *T*-2 and a solid mass of c-2 will not deposit at 1-*A*. However, at site 2 the solidification temperature *T*-2 has been reached and so c-2 will deposit there. The latent heat of fusion of c-2 will be given up and the process repeated. Since the temperature achieved by mass c-2 is less than that attained by c-1, the slope of the thermal gradient curve is less and so the site 3 where c-3 will deposit will be further from site 2 than site 2 is from site 1. This indicates that as growth proceeds, the concentration is changed, longer time is required for solidification because of the decrease in the temperature difference between the mammiform core temperature and the site temperature, and the cross arms should get farther and farther apart. This variation of distance between dendrite cross arms and speed of solidification as dependent on progression of growth was noted by Alexander and Rhines.[9] They also noted that the dendrite spacing in any one alloy system varied in the same manner as the ratio of the heat of fusion to the thermal diffusivity. In the proposed model, it is noted that the slope of the surface control gradient curve *Z*, which determines the closeness of approach of the dendrite arms, will vary directly with the latent heat of fusion of the metal being deposited and inversely with the thermal diffusivity of the metal already deposited.

Reference to the probable temperature distribution curves *Z* around the mammiform, Fig. 20, indicates that the mammiform sites will be distributed 90° around the original mammiform. Fig. 21 shows how the mammiform sites are maintained in alignment along the length of the original form. After the masses *B*, *C*, and *D*, Fig. 21, have been deposited, it appears that *E* would be the next site to be occupied. However, the solute element has been diffusing toward *E* from both *B* and *C*, and point *E* will therefore be replete in the solute and have a lower solidification temperature than either *G* or *F*, so the points *G* and *F* will be selected as mammiform sites prior to *E*. As the mammiforms are continually formed in a line parallel to the original mammiform axis, their bases will grow together to form a web between the forms, Fig. 22. Cross arms on the cross arms can be developed in the same manner.

Acknowledgment

Special acknowledgment is due to the Office of Air Research for their support of this investigation of solidification mechanics.

References

[1] D. Turnbull and R. E. Cech: Microscopic Observation of the Solidification of Small Metal Droplets. *Journal of Applied Physics* (1950) **21**, pp. 804-810.

[2] Ludwig Graf: About the Structure of the Real Crystal—The Formation of Mosaic Structure in Cast, Plastically Deformed, and Recrystallized Materials. *Ztsch. f. Physik* (1943) **73**, p. 121.

[3] M. J. Buerger: The Lineage Structure of Crystals. *Ztsch. f. Kristallo* (1934) **89**, pp. 195-242.

[4] E. S. Dana: *A Textbook of Mineralogy*. 4th edition by W. E. Ford (1932) p. 205.

[5] C. O. Bannister: Studies on the Crystallization of Gold from the Liquid State. *Journal* Inst. Metals (1929) **42**, pp. 141-147.

[6] C. H. Desh: The Solidification of Metals from the Liquid State. *Journal* Inst. Metals (1919) **22**, pp. 241-263.

[7] G. D. Bengough: Discussion ref. 6. *Journal* Inst. Metals (1919) **22**, p. 269.

[8] M. Smialowski: On the Mosaic Structure of Metal Crystals. *Journal* Inst. Metals. *Abstracts* (1937) **4**, p. 94.

[9] B. H. Alexander and F. N. Rhines: Dendritic Crystallization of Alloys. *Trans.* AIME (1950) **188**, pp. 1267-1273; JOURNAL OF METALS (October 1950).

A Survey of the Sulphur Problem Through The Various Operations in the Steel Plant

by T. E. Brower and B. M. Larsen

A perspective is presented of the steel plant sulphur distribution and elimination problem from coal to liquid steel ready for teeming, giving distributions of sulphur over a range of coke sulphur content, and some methods of sulphur control, in the blast furnace, external desulphurization between blast furnace and open hearth, distribution between fuel, slag, and metal, and methods and limitations of control of sulphur in the open hearth furnace.

AS a part of the 1951 AIME symposium on sulphur in steelmaking, it was thought that a discussion of the distribution of sulphur throughout the whole series of operations, from coal and ore to finished steel ingots, might have some value in giving a perspective on the whole problem. The following discussion is an attempt to present such an overall picture. The order is that of the actual plant operations, beginning with a very brief consideration of the coking process.

Sulphur in Coal and Coke

Since by far the largest source of sulphur entering the steelmaking cycle is in the coal used to make coke for the blast furnace, it would seem reasonable to eliminate some of it, either from the coal, or the coke, or during the coking process. This has appeared impracticable up to the present, at least, for two main reasons: the low activity of the organic sulphur in either coal or coke, and because of price limitations involved in treating a low cost material such as coke.

A variable portion, usually ½ or less, of the sulphur is present in coal in the form of pyrites or similar compounds, and a large part of this sulphur may be removed in the coal washery. Most of the sulphur, however, is normally present as "organic" sulphur, intimately associated with the coal structure. Its distribution prevents any separation by mechanical means. Its low activity makes improbable any rapid chemical removal, although hydrogen will remove sulphur from both coal and coke. Thus, prolonged recirculation of coke oven gas in the coking process would tend to leave a smaller percentage of the total sulphur in the coke residue. Table I shows a typical distribution of sulphur from coal into products in the coking process. As the sulphur in the coal increases, the sulphur in the coke tends to increase in about the same proportion.

Sulphur in the Blast Furnace

The best picture of the situation in the blast furnace is provided by a sulphur balance of raw materials entering, and of products leaving, the furnace. The difficulties in accurate weighing and sampling of the variable solid materials entering this process, and the number of hours required for the raw materials to descend through the furnace under variable operating conditions, make it difficult to obtain an accurate balance. However, balances made over periods of weeks or months tend to average out some of these uncertainties.

Table II presents three typical sulphur balances similar to a number that the writers have calculated. In most of these the slag volume calculated from the sulphur balance is, in some instances more, and in other instances less, than the value corresponding to the best input and output balances of the other slag constituents (lime, silica, alumina, etc.). Probably the greatest source of error in these calculations is the sulphur content of the slag. Despite some possible inaccuracies the balances of Table II show rather definitely the following points:

1—That 87 to 95 pct of the total sulphur input is in the coke and 95 to 97 pct of the total sulphur output is in the slag. Also, that if any sulphur leaves the furnace with the gas it is relatively small, amounting to a possible 1 pct or less.

2—At the lower sulphur coke level of 0.86 pct the total amount of sulphur charged is 15 lb of sulphur per ton iron increasing to 26 lb per ton at the higher sulphur, intimately associated with the coal strucrare burdens containing sulphur-rich ores will the total sulphur burden fail to be nearly proportional to the content in the coke used.

3—The 7 to 9 pct of the total sulphur input from the limestone of furnaces B and C is due to the relatively high sulphur content of the stone, 0.226 and 0.265 pct, respectively. In the case of furnace A, the sulphur content of the limestone was only 0.06 pct which resulted in only 3 pct of the total sulphur input coming from this source.

It is rather interesting to compare the sulphur balances of a typical ferromanganese furnace with

T. E. BROWER and B. M. LARSEN, Members AIME, are associated with the Research Laboratory, U. S. Steel Co., Kearny, N. J.

Discussion on this paper, TP 3191C, may be sent, 2 copies, to AIME by Feb. 1, 1952. Manuscript, June 25, 1951. St. Louis Meeting, February 1951.

Table I. Distribution of Sulphur from Coal During the Coking Process

Coal, Pct S	Lb S per Ton Coal	Coke, Pct S	Lb S per Ton Coal	Gas, Grains S per 100 Cu Ft	Lb S per Ton Coal	Tar, Pct S	Lb S per Ton Coal
0.80	16	0.56	8.1	240	2.9	0.40	0.6
1.20	24	0.87	12.5	420	5.0	0.61	0.9
1.60	32	1.15	16.6	600	7.2	0.81	1.2

the iron furnaces of Table II. Briefly the comparisons are as follows:

1—The percentage distribution of the items of the total sulphur input of both types of ore smelting is practically identical. That is, in the ferromanganese furnace 92 to 94 pct of the total sulphur is in the coke. Since the coke consumption of the ferromanganese furnace is approximately double that of the iron furnace, the total sulphur input is in the neighborhood of 40 to 45 lb sulphur per ton of ferromanganese for a 1.06 pct sulphur coke. (Compare with the iron furnace B of Table II which has a total input of 20.5 lb sulphur per ton iron.)

2—The output side of the sulphur balance of the two smelting processes is somewhat different. In the case of manganese smelting about 1 pct or less of the total sulphur is in the ferromanganese and approximately 80 to 85 pct is in the slag. The remaining 14 to 19 pct of the total sulphur was probably carried in the fine fume passing out the top of the furnace.

Since nearly all the sulphur burden in iron smelting can be attributed to the coke, the sulphur content of this raw material becomes of prime importance. In this country, coke with relatively low sulphur contents (0.70 to 1.00 pct) is becoming less common; we are having more and more to use cokes containing normally 1.20 and 1.30 pct, with periods of wide variations which occasionally reach values as high as 1.80 and 2.00 pct.

Table II. Sulphur Balance of Blast Furnaces Over One Month's Operation

Item	A Coke S = 0.86 Pct		B Coke S = 1.08 Pct		C Coke S = 1.12 Pct	
	Lb S per Ton Iron	Pct of Total S	Lb S per Ton Iron	Pct of Total S	Lb S per Ton Iron	Pct of Total S
Input						
Coke	14.18	94.1	18.12	88.3	23.45	89.8
Limestone and dolomite	0.45	3.0	1.76	8.6	1.79	6.9
O.H. slag			0.26	1.3	0.39	1.5
Ore, sinter	0.39	2.6	0.37	1.8	0.45	1.7
Scale and scrap	0.05	0.3			0.04	0.1
Total	15.07	100.0	20.51	100.0	26.12	100.0
Output						
Flue dust	0.08	0.5	0.11	0.5	0.27	1.0
Iron	0.48	3.2	0.66	3.2	0.84	3.2
Slag	14.51	96.3	19.74	96.3	25.01	95.8
Total	15.07	100.0	20.51	100.0	26.12	100.0

Sulphur distribution as determined by slag volume, calculated from other materials balances, is as follows:

CaO Balance					
S in slag	14.43	95.8	20.46	96.4	
S unaccounted for	0.08	0.5	—0.72 (input side)	3.4	
Al_2O_3 Balance					
S in slag	14.14	93.8	19.37	94.4	
S unaccounted for	0.37	2.5	0.37	1.8	
Average pct S in slag	1.74		2.01		2.49

Accordingly the sulphur problem of the blast furnace becomes one of distributing the total sulphur input between slag and iron so as to leave the iron with minimum sulphur content. Obviously this becomes more and more important as the total input increases due to the necessary usage of higher sulphur cokes.

With a process capable of leaving only about 3 pct of its total sulphur burden in the iron produced, desulphurization in the blast furnace is a problem only because the open hearth has such a limited capacity for sulphur removal. This is illustrated by the sulphur balances of the open hearth which will be discussed in more detail later. It is sufficient to mention that this small amount of sulphur remaining in the iron usually becomes, in turn, the largest single item of the sulphur input to the open hearth furnace. The slag-metal distribution follows the simple distribution law, not exactly perhaps, but closely enough to serve as a good guide in practice. That is, if the total sulphur input is doubled, the percentages in both slag and metal will be approximately twice as large. Since measured distribution ratios of sulphur in slag to sulphur in metal ((S)/[S]) vary from about 15 to 150, it would seem possible to compensate for a large increase in total sulphur burden, but there are limitations in practice:

Increasing the slag volume also increases the coke consumption, which, in addition to lowering production rate, causes the effect to be partially offset by the accompanying increase in total sulphur, since most of this comes from the coke. According to Steudel[1] each increment of 100 lb of slag requires approximately 50 lb of extra coke. This estimate agrees with that indicated by differences which existed in former years between northern and southern blast furnace practice. The lower iron content of southern ores gave approximately 2400 lb coke and 2400 lb slag per ton of iron. The richer iron ore of the north gave approximately 1800 lb coke and 1200 lb slag per ton of iron (both practices using about the same average blast temperature). Heat calculations based on Steudel's value of 50 lb extra coke indicate 275,000 Btu of extra input of heat are needed. Nearly half of this heat is consumed in melting the extra slag and burning the extra limestone, part of the remainder being available for processes in the shaft. It must be remembered that, unless the amount of sulphur held by this extra 100 lb slag is substantially greater than that carried in by the 50 lb coke, it is useless to increase slag volume as a means of obtaining low sulphur iron.

Ideally, the silicon content of basic iron should be only 0.7 pct or less, but nearly all low silicon practices show low sulphur ratios of around 15 to 40. These, in general, increase with silicon content, running as high as 100 to 140 at the 1.20 to 1.60 pct Si range. Of course, the increased silicon is in general accompanied by higher coke consumption, partially neutralizing the gain by an increased sulphur burden and lowered production rate.

Increased slag basicity as a very effective means for obtaining higher sulphur ratios also tends to involve a higher coke rate, larger flux requirements, and decreased production. Substitution of MgO for CaO, up to an optimum range of about 6 to 8 pct MgO, is one method which seems to involve no loss in production rate in most cases. If the increased basicity is achieved by the increase of only the CaO, the viscosity of the slag tends to be increased, which

Table III. Comparison of Practices and Sulphur Content of Iron with Increasing Sulphur Content of Coke

Period of time	Furnace D 1 Month	Furnace E 1 Month	Furnace F 1 Month	Furnace G 1 Month	Furnace H 1 Month	Furnace I 1 Week	Furnace I 1 Week
Coke sulphur, pct	0.80	0.95	1.30	1.37	1.42	1.66	1.83
Coke rate, lb per ton iron	1910	1799	1980	1890	1671	1680	1665
Slag, pct SiO_2	35.1	36.1	34.2	33.1	34.2	33.0	33.2
Al_2O_3	14.3	12.3	12.8	14.3	12.7	13.4	13.5
CaO	44.5	38.3	45.0	42.9	44.6	45.5	44.6
MgO	3.2	8.9	4.4	5.6	5.7	5.0	5.8
(S)	1.59	1.30	2.37	2.39	2.49	2.53	2.71
Iron, pct Si	0.71	0.83	1.07	0.98	1.10	0.99	1.18
Mn	2.36	0.31	2.85	2.12	2.19	1.87	1.83
[S]	0.036	0.042	0.029	0.037	0.042	0.030	0.033
Pct of casts above 0.050 pct S	6.6	18.9	0.8	11.0	22.4	0.0	2.0
Ratio (S) slag/[S] metal	44	31	82	65	59	83	82
Slag basicity: Mols (CaO) + Mols (MgO) / Mols (SiO_2)	1.49	1.50	1.60	1.64	1.64	1.70	1.70
Slag basicity: Pct (CaO) + Pct (MgO) / Pct (SiO_2)	1.36	1.31	1.44	1.47	1.47	1.53	1.52
Slag weight, calculated Lb per ton iron	1090	1135	1140	1050	1005		

in turn requires a higher temperature to maintain a free running slag. However, if the MgO content is raised to about 6 to 8 pct of the final slag composition, the slag then becomes more fluid over a wide range of temperatures, as shown by McCaffery.[2] It was also shown in an earlier paper[3] that MgO in the range of 6 to 8 pct gave a good correlation with lower sulphur in the iron, with one molecule of MgO equal to or better than one molecule of CaO up to this limit.

Any trend toward lower coke consumption by higher blast temperature, or by factors such as sized ores and other charge materials which give greater regularity in operation, will of course favor sulphur removal with no penalty on production rate. Indeed, output rate is usually increased by such methods.

Better contact between metal and slag in the furnace would favor sulphur elimination, but this cannot be controlled by any method now known, except, perhaps, as shown by Steudel,[1] that longer retention of slag favors sulphur absorption, and this is severely limited by the space available below the tuyere level.

In spite of the fact that the theory is yet in dispute, it does appear that in practice a high manganese content in the iron favors increased sulphur ratios as indicated in the paper[3] mentioned above. Even though higher manganese practice does tend to decrease production rate to some small extent, this may be more than offset by the improved sulphur elimination.

As shown in Table III, however, in spite of limitations, the blast furnace can handle a considerable increase in sulphur burden with little or no increase in sulphur content in iron produced. In the cases listed here, the coke-sulphur contents range upward from 0.80 to 1.83 pct, yet all the averages for sulphur in iron remain within the limits of 0.029 to 0.042 pct. Certain points in this group of data may be worth noting, as follows:

Furnaces D and E both used relatively low sulphur coke, 0.80 and 0.95 pct, respectively. Both furnaces produced relatively low silicon iron, 0.71 and 0.83 pct, respectively. Both had approximately the same basicity ratio, 1.49 and 1.50, calculated as mols CaO + mols MgO/mols SiO_2. However, this relatively low basicity ratio resulted in a moderately low sulphur distribution ratio of 44 for furnace D and 31 for furnace E. An interesting question raised by the comparison is why furnace D had on the average 13 units higher sulphur ratio and hence produced 0.006 pct lower sulphur iron (0.036 as compared to 0.042 for furnace E) despite a 0.12 pct lower silicon iron. The probable reason is the high manganese content of the iron, 2.36 pct, as compared to 0.31 pct for furnace E. It is possible that even greater desulphurization could have been obtained in the case of furnace D if the MgO had been 6 to 8 pct instead of 3.2 pct.

Furnaces F, G, and H had a charge of much higher sulphur coke, 1.30 to 1.42 pct. All three furnaces had comparable silicon contents in iron, 0.98 to 1.10 pct. The three furnaces also had nearly the same basicity, 1.60 to 1.64 mol basis. This basicity ratio is higher than that for the two preceding furnaces discussed above and results in higher sulphur distribution ratios, 59 to 82. Again it is interesting to find that furnace F which had the highest manganese content in the iron (2.85 pct) also had the highest sulphur ratio (82) and hence the lowest sulphur content of iron (0.029 pct) as compared with 0.037 and 0.042 pct for the other two furnaces.

Finally, the two separate weekly tabulations of furnace I represent a charge of still higher coke sulphur, 1.66 and 1.83 pct. Despite these high values the iron averaged relatively low in sulphur content (0.030 and 0.033 pct) with fairly high sulphur ratios (83 and 82). These values resulted mainly from the very high basicity, 1.7 mol basis. This is the highest basicity ratio of all the data listed in Table III. Also contributing to this high degree of desulphurization was the medium silicon (0.99 and 1.18 pct) and manganese (1.87 and 1.83 pct) contents together with a medium magnesia content of 5.0 and 5.8 pct. Probably even greater desulphurization would have resulted if the manganese in the iron had been higher.

In the paper by Kennedy and Thornton[4] a series of slag compositions were studied with respect to sulphur removal. In going from 0 to 100 pct dolomite flux charge it was found that the 35 pct dolomite, 65 limestone charge produced the maximum desulphurization. In Table I of their paper is shown the average results of 70 bessemer iron casts of this charge. Briefly the results can be summarized as follows:

The average sulphur distribution ratio was 101, which resulted in 0.018 pct sulphur in the iron. This high degree of desulphurization was achieved: 1—by a high basicity ratio (1.66 mol basis or 1.50 percentage basis) accompanied with 6.1 pct MgO in the

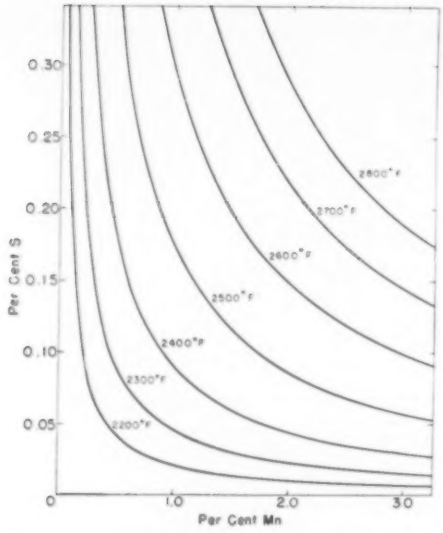

Fig. 1—Solubility of manganese and sulphur in hot metal as a function of temperature.

slag, and 2—with a high silicon content of the iron (1.53 pct) which indicates a high hearth temperature (2750°F average flush slag temperature). It is interesting to note that the manganese in the iron was only 0.50 pct, which illustrates how high slag basicity, temperature, and silicon content can overbalance the countereffect of a low manganese level.

In Fig. 9 of this same paper[4] is shown the distribution curve of the sulphur distribution ratio for the individual casts which varies from 70 to 160. These upper values of 150 and 160 represent about the maximum values that we have obtained on individual casts. The usual range of observed values of this ratio vary from 20 to 125 based on composites of 12 and 24 hr samples (2 to 4 casts).

External Desulphurization of Iron

It has been suggested that the problem of sulphur in iron can best be solved by operating the blast furnace without reference to the sulphur, which is then brought down to a satisfactory level by some special treatment of the liquid iron after it has been removed from the furnace.

External desulphurization has been accomplished mainly with alkalies. This method has been employed in many foundries for some time as well as a number of blast furnace plants for the treatment of off-casts high in sulphur. As a result, a number of papers have been written on this subject.

Various methods for external desulphurization may be listed and discussed briefly as follows:

The use of alkalies or mixtures as follows: soda ash (Na_2CO_3) with 58 pct Na_2O; caustic soda (NaOH) with 76 pct Na_2O; soda ash and caustic soda mixtures; and soda ash, limestone, and fluorspar mixtures. The alkalies are produced in granular or briquette form. The advantage of the latter is that boiling action is prolonged by slower melting of the lumps. These alkalies are commonly added to the bottom of the ladle before casting or to the iron stream flowing into the ladle. Sometimes a combination of both methods is used. Obviously contact between alkali and metal is obtained by the stirring action of the falling iron stream and the boiling action of the desulphurizing material. Such a means of making contact is bound to be erratic from one addition to another. Hence a variable amount of sulphur reduction results from cast to cast. It has also been found that a high sulphur content in the iron can be lowered quite consistently to the 0.040 to 0.050 pct range, but considerable difficulty is encountered in attempting to bring it down near 0.030 pct or below. Further complications arise from the reaction of this alkaline slag with the silica refractory of ladles and mixer. This in turn results in increased refractory costs. Finally, if proper separation of this desulphurizing slag and kish is not made at the ladles or mixer, it will be charged into the open hearth furnaces. How much of this extra sulphur is oxidized and removed in the gas phase, or passes out with flush slag in heats using a runoff practice, is quite debatable. An elaborate layout of ladles equipped with facilities for the separation of the spent desulphurizing slag is discussed by Evans.[5] This method eliminates some of the variation in sulphur reduction but it will not aid in the desulphurization to a low sulphur level.

The desulphurization of iron has also been accomplished with calcium carbide. Laboratory experiments on the method of adding this material were made by Wood[6] and coworkers. It is interesting to note that by rapid stirring in of fine calcium carbide below the iron surface a sulphur elimination ranging from 63 to 93 pct was obtained. This illustrates the intimate contact that must be made between surfaces of liquid metal and the desulphurizing media.

It has been reported by Warren[7] that the sulphur content of iron decreased somewhat during an abnormally long interval between casting into transfer ladles and delivery to the mixer in the open hearth shop. A detailed study of metal and kish samples from Warren's practice, which also included X-ray diffraction patterns, indicated the presence of MnS. These data tend to confirm the reality of MnS separation from iron. However, this should occur only when manganese and sulphur contents are high enough, and the final temperature low enough, to cause supersaturation. For illustration, Fig. 1 presents a family of solubility curves of manganese and sulphur in liquid iron for various temperatures based on Joseph and Holbrook's findings.[8] If the analyses of the above mentioned samples are compared to this chart the effects indicated are as follows:

When cast into the ladle at the blast furnace the iron contained 0.085 pct S and 1.90 pct Mn. The iron cooled during the 3 to 4 hr travel to the mixer and when it reached a temperature of approximately 2490°F solid MnS began to separate. This continued until the final composition at the mixer was 0.042 pct S and 1.82 pct Mn. On this diagram this corresponds to approximately 2380°F. On the basis of the solubility diagram, it would usually be possible to reduce the sulphur on high sulphur casts by cooling the ladles of metal to approximately 2400°F. The final sulphur content, at this temperature, would obviously depend on the manganese content of the iron. For example, if the manganese content were below 1.0 pct the final sulphur content would not be reduced below 0.090 pct. However, if the manganese content were 1.75 pct, the final sulphur would then be down to 0.05 pct; and if the manganese content

were further increased to 2.8 pct, the sulphur would be reduced to 0.03 pct.

Prerequisites for this method of sulphur reduction are high manganese iron, longer delivery time to the mixer, and lower temperature iron entering the mixer. The two latter requirements are the most objectionable from the standpoint of speed of operation. Besides these three requirements a good separation of the solid MnS and kish should be made before the iron enters the mixer.

In general, it appears evident at this time that future developments in desulphurization between blast furnace and open hearth should trend toward improved and better controlled contact between metal and desulphurizing agent; minimum costs of material and labor; and less cooling of the metal. Increased dependence on lime, as the cheapest and most effective sulphur absorber, seems probable. If the desulphurizing unit could be incorporated in, or take the place of, the regular iron mixer, this would be best adapted to the flowsheet of the normal steel plant.

Sulphur Problem of the Open Hearth

The reduction of sulphur in the open hearth bath is more difficult and is limited to much smaller amounts than the reduction in the blast furnace. This is exemplified by: 1—the difference in sulphur distribution ratios, with observed values of from about 2 to 12 in the open hearth, whereas in the blast furnace the range is from 15 to 150; 2—the inherent nature of the open hearth, with its pattern of heat flow largely from above through the slag layer, limits the practical slag weight to from 8 to 18 pct of the metal weight as compared to a range of 40 to 150 pct in various blast furnace practices.

Consequently the sulphur burden or total sulphur input into the individual open hearth heats becomes of primary importance. Before discussing various specific sulphur balances and burdens, it might be well to consider briefly the different items that make up the input side of the sulphur balances. These items are listed as follows:

Liquid Iron or Hot Metal: The amount of sulphur introduced into the open hearth charge in the liquid iron usually accounts for 27 to 50 pct of the total sulphur input. This of course depends mainly on the amount of liquid iron addition which usually corresponds to from 40 to 70 pct of the total weight of scrap and hot metal. Open hearth shops making much of their product to rather low sulphur specification may desire the percentage of sulphur in the hot metal to average below 0.030 pct. Shops producing steel with a less critical sulphur specification frequently average 0.040 pct S or higher in the liquid iron.

There is another source of sulphur which is introduced with the hot metal and is commonly called kish. This material is heterogeneous and erratic in both physical and chemical makeup. It consists of oxidized metal shot, coke fines (thrown on the top of the iron ladles), fire clay, silica (from ganister refractories and sand of the runner and cast house floor), separating particles of MnS, and frequently blast furnace slag. The primary components of the kish which contribute sulphur are the coke fines, the slag, and the MnS phase, and they represent a wide range of sulphur contents (see Table IV). The rather high silica content (10 to 35 pct) of kish has a deleterious effect on the sulphur removal from the open hearth bath because it counteracts the basicity of the slag. These detrimental effects of kish are obviously most serious in the case of open hearth heats without runoff slags. The kish probably tends to float on the slag in the open hearth as the iron is charged. Some rather recent samplings of runoff slags have indicated that the first portions of the runoff are often higher in sulphur than would be expected from slag-metal equilibria. These data suggest that much of the kish entering the open hearth is floated or carried out by the runoff slag, at least in those heats having the start of flush immediately or shortly after the time of the hot metal addition.

Table IV. Typical Ranges of Sulphur in Some Charge Materials

Materials	S, Pct
Limestone	0.03-0.20
Burnt lime	0.02-0.25
Raw dolomite	0.02-0.40
Single burned dolomite	0.02-0.25
Double burned dolomite	0.01-0.20
Fluorspar	0.10-2.00
Kish	0.30-0.80

Scrap: The amount of sulphur introduced into the open hearth charge from scrap is somewhat variable, obviously depending on its sulphur content and the amount charged (governed largely by the hot metal percentage of the particular shop). The sulphur content of the scrap that is produced in a given shop should be known reasonably well, especially if steps are taken to separate the high sulphur steel scrap from the ordinary scrap lower in sulphur. However, the sulphur content of purchased scrap is practically unknown; this is especially true of the miscellaneous scrap. This introduces considerable uncertainty in the sulphur burden if large quantities of purchased scrap are charged.

Recent findings of Osborne[5] indicate that the rust attached to the scrap may have a sulphur content 15 to 18 times greater than the base metal. From Table I of his paper, the average sulphur content of the base metal was 0.0206 pct and that of the rust accompanying this scrap was 0.324 pct. In this connection, we have collected different rust samples from various scrap piles of our plants. These rust samples had been formed over a period of one to seven years and gave sulphur contents varying from 0.20 to 1.10 pct with an average of 0.50 pct. It is interesting to note that if we assume that the scrap averaged 95 pct metal with 0.030 pct S and 5 pct rust with 0.50 pct S, the aggregate sulphur content of the scrap would then be 0.054 pct. This would result in a very appreciable increase in sulphur burden if an appreciable amount of rust were charged on some heats. However, it is difficult to know what percentage rust is present in most scrap and there is also the possibility that the sulphur in the rust would be vaporized out during melting, although Fig. 2 of Osborne's[5] paper does not tend to substantiate this idea.

From this discussion it can be seen how difficult it is to obtain a representative sulphur content for the scrap to be used in calculating a sulphur input balance. To obtain such a value good clean scrap free of rust and of known composition must be used.

Limestone, Burnt Lime, and other Fluxes: The chemical analyses of numerous shipments of the various fluxes (see Table IV) have revealed a wide variation in sulphur content. This variation usually represents differences between quarries, although considerable variation sometimes exists in shipments

Table V. Comparison of the Ladle Sulphur Content of Heats Charged with High and Low Sulphur Limestone Content

Time	No. of Heats	Avg. S Content of Limestone	Avg. Pct Ladle S
First six months	616	0.160	0.0285
Second six months	872	0.045	0.0245
Difference		0.115	0.0040

from the same quarry. Table IV gives typical ranges from a large number of individual determinations.

The users of fluxes high in sulphur content are very likely to pay a penalty in the form of higher final sulphur contents. This is illustrated by the following example which is a comparison of heats for similar low carbon grades made over two consecutive six-month periods. The open hearth fuel was natural gas (hence there was no sulphur pickup from the furnace gases). The steel was made on a runoff practice with comparable limestone charge, scrap, and iron analysis. The main difference was the sulphur content of the limestone as shown in Table V.

This is quite understandable when it is realized that the ratio of weight of steel to the weight of tap slag varies from about 7:12, whereas the slag to metal sulphur ratio at tap is most commonly about 4:7. Even on heats with maximum sulphur specifications of 0.04 to 0.05 pct, limestone with more than around 0.25 pct S may add more sulphur to the burden than it can remove; in heats for steel with maximum sulphur of 0.020 pct or below, this critical value may be down toward 0.10 pct S or lower. For the same reason the sulphur content of burnt lime and dolomite should be kept as low as possible.

It is worth remembering that the moderate amount of sulphur removed in runoff slag may come from charge ore, scrap, hot metal, or dolomite on banks, but all the sulphur in the charged limestone contributes to the sulphur carried in the final slag and metal at tap. Higher sulphur in dolomites used may contribute sulphur to both runoff and tap slags.

Ore, Sinter, and Miscellaneous Additions: The sulphur content of ore, sinter, and alloy additions should be kept as low as possible. It is realized that often only one type of ore, sinter, or other material is available at the particular plant and must be used. However, when a choice can be made between similar materials that are reasonably comparable in other respects except sulphur contents, then the one which has the lowest sulphur content should be used.

Fuel: The total amount of sulphur charged from all the sources just discussed above, from hot metal to ore, usually varies from a low of 0.65 lb to a high of 1.25 lb S per ton of steel.

In considering open hearth fuels it is found that the total amount of sulphur available from this source varies widely with the different types of fuels. Also that all the fuels except natural gas have an amount of sulphur that exceeds the total from all other input sources. This is illustrated in Table VI which represents typical values for present day fuels.

It is very fortunate that this relatively high sulphur potential of the fuel is transferred to the slag-metal system at a very low efficiency. With fuels having lower sulphur contents (similar to fuels used 12 to 17 years ago), it is doubtful whether any appreciable amount of sulphur enters the metal. This point will be discussed in more detail a little later. The studies of Diehl[4] and others of the sulphur equilibrium between metal and sulphur-containing gases show that an increase in oxygen pressure decreases the tendency toward sulphur absorption from the gas. During the melting of scrap in the open hearth the scrap is piled fairly high in the furnace and is bathed by portions of the flame containing incompletely combusted fuels to give a low oxygen pressure, favoring sulphur pickup from the fuel.

Conversely the factors which minimize the sulphur pickup from a high sulphur fuel during scrap melting may be enumerated as follows: 1—rapid scrap charging, 2—maintenance of a high ratio of air to fuel with a short oxidizing flame, 3—rapid melt down, and 4—avoidance, as much as possible, of a high pile of scrap that remains for a considerable period of time in the direct path of the flame.

It has frequently been found, when calculating sulphur balances, that the input side was less than the output. This difference has often been captioned "unaccounted for (from furnace gases)." It is thus assumed that the unaccounted for sulphur represents the sulphur absorbed from the fuel during the scrap melting. Actually, however, the amount of unaccounted for sulphur which can be attributed to the fuel is rather difficult to estimate. For example, under our discussion of the sulphur content of scrap it was pointed out that 5 pct rust on the scrap would increase the aggregate sulphur content approximately 80 pct. Sulphur contents in such rust, in kish spilled in with hot metal, and in eroded dolomite are frequently overlooked. The point is that an error in the sulphur content of some of the charged materials could easily account for all or nearly all the missing sulphur of the balance in most cases. The fact that, when the sulphur content of the fuel is relatively low, or only moderately high, the amount of sulphur absorbed during scrap melting is rather small tends to be substantiated by data obtained approximately 15 years ago when the sulphur content of fuels was lower than that in present fuels.

These data from several plant practices are tabulated in Table VII and, for each plant, represent an average of ten heats of the same grade of steel. All 50 heats were carefully made with complete details of weights and analyses of incoming materials and outgoing products. It is believed they represent a very good set of data for calculating balances. Table VII is confined to the sulphur balance data.

As nearly as could be ascertained, all the heats were charged with fairly clean scrap and the amount of rust introduced with the scrap was rather insignificant, consequently the sulphur content of the base scrap metal was probably close to the true value. Hence it would seem that the amounts of sulphur charged into these heats are truly representative. Thus for these particular heats the unaccounted

Table VI. Average Amount of Sulphur Available in the Various Fuels

Materials	Lb S per Ton Steel	Equivalent Pct S in Steel
All other input materials	0.65 to 1.25	0.033-0.063
Natural gas	0	0
Tar and natural gas	1.25	0.063
Oil	2.15	0.108
Tar	2.50	0.125
Tar and coke oven gas	4.25	0.213
Coke oven gas	6.00	0.300

for sulphur probably represents a fairly good estimate of the sulphur pickup from, or loss to, a group of fuels with low to moderate content of sulphur.

In discussing the results of Table VII, consider first the data from plants A and B:

In the case of plant A, the fuel was a mixture of 62 pct natural and 38 pct coke oven gas with a relatively low total sulphur content of 0.79 lb per ton (from the coke oven gas). The unaccounted for sulphur amounted to only 0.01 lb per ton or 1.5 pct of the total sulphur charged and is on the output side of the balance, indicating a loss of sulphur from the slag-metal system to the gas phase.

In the case of plant B, a mixed fuel was used which consisted of 58 pct natural gas and 42 pct tar. Again this fuel had a relatively low total sulphur content of 0.70 lb per ton (from the tar). The unaccounted for sulphur of the balance amounted to 0.11 lb per ton or 12.9 pct of the total sulphur, once more on the output side of the balance. The unaccounted for sulphur of the balance (0.11 lb per ton) seems rather high and could be due, in part, to some other errors of the sulphur contents of input or output materials. In any case, the data of this plant indicate a net loss of sulphur to the gas phase.

In discussing the remaining data of Table VII the result of plants C, D and E will be considered together as follows:

Two plants (C and D) used producer gas whereas the third plant (E) used 80 pct tar and 20 pct coke oven gas. The sulphur content of these fuels varied from 1.80 to 2.17 lb S per ton steel, or more than double the sulphur content of fuels of plants A and B. The unaccounted for sulphur, of the balance, varied from 0.01 to 0.03 lb S per ton steel or 1.5 to 4.4 pct of the total sulphur of the balance. In all three cases the unaccounted for sulphur is on the input side of the balance indicating a pickup of sulphur from the fuel. If we consider the fuel as contributing all the unaccounted for sulphur, it will be noted that this is fairly small and amounts to only 1.5 to 4.4 pct of the total sulphur burden. If this unaccounted for sulphur is compared with the sulphur content of the fuel, the low efficiency of the sulphur transfer is apparent:

Plant C

$$\frac{\text{0.03 lb S per ton unaccounted for}}{\text{1.84 lb S per ton in fuel}} \times 100 = 1.6 \text{ pct}$$

Plant D

$$\frac{\text{0.03 lb S per ton unaccounted for}}{\text{2.17 lb S per ton in fuel}} \times 100 = 1.4 \text{ pct}$$

In other words it appears that a maximum of 1.0 to 2.0 pct of the sulphur of the fuel is absorbed by the slag-metal system during melting at these intermediate levels of fuel sulphur content.

In some of the present day higher sulphur fuels (4.0 to 6.0 lb S per ton steel) which some of the plants are forced to use from time to time, a larger transfer and absorption of sulphur from the fuel is noted. To illustrate this point the experience of several plants may be noted briefly as follows:

One plant normally had a supply of open hearth fuel oil that averaged 1.0 pct S. With this fuel the desired ladle sulphurs were obtained with an average slag basicity of approximately 2.6. For a period of one to two months this plant had to use a fuel oil containing over 3.0 pct S. It was soon found that

Table VII. Comparison of the Sulphur Content of the Fuel with the Unaccounted for Sulphur of the Sulphur Balance

	Plant A		Plant B		Plant C		Plant D		Plant E	
Item	Lb	Pct	Lb	Pct	Lb	Pct	Lb	Pct	Lb	Pct
S in all charged material	0.66	100.0	0.81	100.0	0.73	95.6	0.87	96.1	0.64	98.5
Unaccounted for					0.03	4.4	0.03	3.9	0.01	1.5
Total input	0.66	100.0	0.81	100.0	0.76	100.0	0.90	100.0	0.65	100.0
S in liquid steel	0.46	69.7	0.45	56.3	0.50	66.2	0.47	52.1	0.46	70.7
S in runoff slag	0.09	13.7								
S in final slag	0.10	15.1	0.25	30.8	0.26	33.8	0.43	47.9	0.19	29.3
Unaccounted for	0.01	1.5	0.11	12.9						
Total output	0.66	100.0	0.81	100.0	0.76	100.0	0.90	100.0	0.65	100.0
Type fuel	62 pct natural gas 38 pct coke oven		58 pct natural 42 pct tar		Producer gas		Producer gas		80 pct tar 20 pct coke oven	
S in fuel, lb per ton	0.79		0.70		1.84		2.17		1.80	

in order to finish the heats with the same ladle sulphur as before, the slag basicity had to be increased to 3.5 to 3.8. After the plant again returned to its regular oil supply containing 1.0 pct S the lime and limestone consumption decreased to its regular value. Several sulphur balances were made on another plant using coke oven gas with high sulphur contents (4.0 to 5.0 lb S per ton steel). These particular sulphur balances are fairly accurate but probably not as good as those shown in Table VII. Consequently, we cannot be sure that all the unaccounted for sulphur came from the fuel, though it is quite possible that a large fraction was contributed by the fuel. This will be discussed further a little later in connection with some other data. Returning to the sulphur balances, the unaccounted for sulphur varied from 0.17 to 0.34 lb S per ton steel. Comparing these values with the sulphur content of the fuel the following variation is noted:

For one balance:

$$\frac{\text{0.17 lb S per ton unaccounted for}}{\text{4.0 lb S per ton in fuel}} \times 100 = 4.3 \text{ pct}$$

For another balance:

$$\frac{\text{0.34 lb S per ton unaccounted for}}{\text{4.8 lb S per ton in fuel}} \times 100 = 7.1 \text{ pct}$$

Thus it appears from these data that a maximum of 4.0 to 7.0 pct of the sulphur in the fuel was transferred to, or absorbed by, the slag-metal system during melting, at these high levels of sulphur content of the fuel. This gain of sulphur from the fuel is of sufficient magnitude to raise the ladle sulphur content by approximately 0.006 to 0.010 pct S. Other experiments with high sulphur coke oven gas have shown that a substantial reduction in final ladle sulphur contents can be obtained if desulphurized coke oven gas is used during the scrap melting period of the heat. One or more erratic conditions probably exist in normal practice, causing variability in sulphur absorption from gases; further study is needed here.

The sulphur problem of the open hearth, as discussed so far in this paper, has been centered on the input of the sulphur balance including the various types of fuel. The remainder of this discussion will

Table VIII. Average Sulphur Balance for Groups of 10 Heats. No Runoff Practice

Item	Plant D		Plant E	
	Lb S per Ton Steel	Pct of Total	Lb S per Ton Steel	Pct of Total
S charged in scrap	0.35	39.0	0.30	46.1
S charged in liquid iron	0.26	28.3	0.25	38.5
S charged in limestone	0.14	15.6	0.09	13.9
S charged in fluorspar	0.12	13.2		
Unaccounted for	0.03	3.9	0.01	1.5
Total input	0.90	100.0	0.65	100.0
S in liquid steel	0.47	52.1	0.46	70.7
S in final slag	0.43	47.9	0.19	29.3
Total output	0.90	100.0	0.65	100.0
Limestone and equivalents, lb per ton	172		152	
Weight of final slag, lb per ton	192		167	
Basicity ratio	3.94		2.32	
Pct S in metal	0.024		0.023	
Ratio $\frac{\text{Pct S in Slag}}{\text{Pct S in Metal}}$	9.3		5.1	
Pct S in slag	0.223		0.117	

deal with the output side of the sulphur balance and with the metallurgical problems that arise when it is desired to lower the sulphur content of the bath during the refining period. The situation can best be outlined by tabulating a couple of sulphur balances and referring to certain points of interest. For this purpose the complete sulphur balances of plants D and E of Table VII are repeated more in detail in Table VIII.

It will be noted that a difference exists between the total input sulphur of the two plants. Plant D has a heavier sulphur burden input, largely due to the higher sulphur content of the fluorspar and limestone. The larger sulphur input of plant D required a larger slag volume and heavier limestone charge to give the higher sulphur ratio of 9.3 as compared to 5.1 for plant E. The most interesting point in the practice at plant D is that the high slag basicity of 3.94 produced a sulphur content of only 0.024 pct, whereas plant E obtained 0.023 pct S in the metal with a slag basicity of only 2.32. Obviously such a practice as that used by plant D is uneconomical both in cost of material and increased time of heat. At a later period, plant D obtained new sources of these materials with lower sulphur contents and was able to decrease slag volume and basicity without changing the sulphur content of the final steel.

It is generally agreed by most investigators that the open hearth process is a poor desulphurizer, so that a small amount of excess sulphur requires a relatively large excess of basic materials (CaO and MnO) and large slag volumes. It is further agreed that the observed sulphur ratio (of sulphur in slag to sulphur in metal) is increased by free CaO (that CaO remaining after the SiO_2 and the P_2O_5 have been chemically satisfied) and free MnO in the open hearth slag.

There is some disagreement among various investigators on the method of calculating the sulphur ratio between slag and metal from the ordinary open hearth slag analysis. One method of calculation has been proposed by Darken and Larsen[11] and another by Grant and Chipman.[12] Somewhat different results from the two methods illustrate the difficulties that arise with a multicomponent system such as an open hearth slag.

The sulphur balances of Table VIII were for heats of a no-runoff practice, with a relatively low percentage of liquid iron in the charge, in the range of 35 to 45 pct. In recent years it has been the practice for a number of plants to operate with much higher liquid iron percentages in the range of 50 to 70 pct. Such a practice necessitates running or flushing off the early premelt slag prior to the lime boil. Obviously such a practice has both advantages and disadvantages. However, these will be discussed only with respect to the sulphur problem.

The advantages are that if the runoff practice is properly executed to give a maximum runoff slag, approximately 55 to 65 pct of the total silica and 14 to 20 pct of the total sulphur is eliminated.

The disadvantages are as follows: In a good runoff slag practice approximately 55 to 65 pct of the total Mn is eliminated as MnO. As a result, the refining slag is lower in MnO which in turn produces a lower sulphur ratio between slag and metal. A further disadvantage occurs when a poor slag runoff is obtained. In such cases only about 30 to 50 pct of the total silica and 8.0 to 13.0 pct of the total sulphur is removed from the system. The extra silica, and also the sulphur that is not flushed off, are added to the refining slag. This additional silica requires practically all the extra charged limestone to neutralize it. Consequently the slag after melting is not very basic and requires variable, and frequently large, additions of extra burned lime to produce the desired desulphurization of the bath. Such a condition causes poor control of slag shaping and lowered production rate.

The importance of maintaining a good runoff of slag from heat to heat cannot be overemphasized. This requires constant supervision from the foreman and furnace operator.

Sulphur Problems After Tap

Ordinarily there is no appreciable change in sulphur content of steel as it is tapped from the furnace and teemed into the ingot mold. Occasionally heats are encountered in which the final steel sulphur has increased 0.002 to 0.004 pct. It will be found that in such cases the tap slag is of low basicity ratio, nearly on the acid side. In addition such heats are usually blocked and silicon killed. Consequently the furnace slag, already low in basicity as it enters the ladle, becomes more acid because of the extra silica from the ferro-silicon ladle addition and because of the ladle refractory erosion, the resultant effect being to cause a reversion of both sulphur and phosphorus to the metal.

In contrast we have found that silicon-killed steel to which calcium-silicon ladle additions have been made show a decrease in final sulphur. We have carefully checked nearly a dozen heats to which 3.5 to 5.0 lb CaSi per ton of steel was added and find that sulphur content of the steel has decreased 0.002 to 0.004 pct from the tapping to the teeming operation.

Summary

In the steelmaking cycle the largest source of sulphur is in the coal used to make coke for the blast furnace. Efforts to remove any appreciable amount of sulphur from the coal or the coke have so far been impracticable because of the low activity of the organic sulphur in the coal and coke and because of the price limitations involved in treating a low cost material such as coke.

Sulphur balances of the blast furnace indicate that 88 to 94 pct of the sulphur input is from the coke and 94 to 96 pct of the total sulphur is carried out in the blast furnace slag.

Cokes with average sulphur content in the range 0.80 to 1.80 pct have been charged in the blast furnace and iron with sulphur content of 0.036 to 0.042 pct has been produced. This was possible with an increase in slag basicity, addition of dolomite to produce a slag with 5 to 8 pct MgO, and by increasing the manganese content of the iron with increased open hearth slag additions.

External desulphurization of the iron has been accomplished by the use of alkalies and calcium carbide. Also iron with high manganese content can be desulphurized by holding the ladles for an extra 2 to 4 hr and thereby lowering the iron temperature to allow the separation of MnS.

The reduction of sulphur in the open hearth is more difficult than in the blast furnace. This is illustrated by the sulphur distribution ratios which are 10 to 12 times lower in the former process. For this reason the sulphur content of each raw material charged should be kept to the absolute minimum. This is especially true of limestone, burnt lime, the various dolomites, fluorspar, kish, and also rusty scrap. Evidence is presented to show that the charging of fluxes high in sulphur results in several points increase in the final ladle sulphur analysis.

The total amount of sulphur available from the open hearth fuels varies widely with the different types of fuels. All the fuels except natural gas carry in an amount of sulphur that exceeds the total from all other input sources. Although the percentage of this sulphur which is transferred to the slag metal system is generally rather poor, it tends to increase at the higher fuel sulphur levels, so that those fuels highest in sulphur content do contribute an appreciable amount. The amount of this sulphur absorption is variable with furnace operating conditions during scrap charging and melting.

Complete sulphur balances of open hearth heats are shown; these indicate the importance of minimum weight of $SiO_2 + P_2O_5$ in the tap slag, also the need to both increase basicity and increase manganese oxide of the slag to further lower the sulphur content of the bath during the refining period.

References

[1] G. E. Steudel: Effect of Volume and Properties of Bosh and Hearth Slag on Quality of Iron. *Trans.* AIME (1940) **140**, pp. 65-86.

[2] R. S. McCaffery and coworkers: Effect of Magnesia on Slag Viscosity. *Trans.* AIME (1932) **100**, pp. 122-135.

[3] T. E. Brower and B. M. Larsen: Some Correlations Between Variables Affecting Sulphur in Blast Furnace Iron. *Trans.* AIME (1948) **176**, pp. 330-342; METALS TECHNOLOGY (October 1948).

[4] T. H. Kennedy and A. W. Thornton: Studies Relating to the Control of Sulphur in the Production of Pig Iron. *Year Book* Amer. Iron and Steel Inst. (1949) pp. 222-242.

[5] G. S. Evans: Desulphurizing Pig Iron by Ladle Treatment with Soda Ash or Caustic Soda and a Nontechnical Discussion of the Reaction of Alkali Slags. *Trans.* AIME (1938) **131**, pp. 145-161.

[6] C. E. Wood, E. P. Barrett, and W. F. Holbrook: Desulphurization of Pig Iron with Calcium Carbide. *Trans.* AIME (1940) **140**, pp. 87-105.

[7] H. E. Warren: Sulphur in Basic Iron and Steel. JOURNAL OF METALS (August 1949) pp. 6-10.

[8] T. L. Joseph and W. F. Holbrook: Bureau of Mines *RI* 3240 (1934).

[9] A. H. Osborne: Effect of Charging Variables and Additions on Sulphur Elimination. AIME *Open Hearth Proceedings* (1949) **32**, pp. 66-71.

[10] A. N. Diehl: Action of Sulphur in Basic Open Hearth Steel Practice. Amer. Iron and Steel Inst. (1926) pp. 404-453.

[11] L. S. Darken and B. M. Larsen: Distribution of Manganese and of Sulphur Between Slag and Metal in the Open Hearth Furnace. *Trans.* AIME (1942) **150**, pp. 87-112.

[12] N. T. Grant and John Chipman: Sulphur Equilibria between Liquid Iron and Slags. *Trans.* AIME (1946) **167**, pp. 134-154; METALS TECHNOLOGY (April 1946).

Technical Note

Useful Etchants for Electron Metallography

by William L. Grube

SPECIMEN preparation for electron metallography involves several steps, such as polishing, etching, replicating, mounting, and shadowing. Although each step must be done with care, the operation requiring the utmost attention is etching.

Proper etching is important because the relief pattern developed on the surface of the specimen by the etchant, and reproduced as minute differences in thickness of the replica, determines entirely the amount of detail seen in the final micrograph. The characteristic colored stains, sometimes used in light metallography to simplify identification of certain microconstituents, cannot be tolerated because there is danger of introducing artifacts in the replicating operation. It is also quite difficult to remove plastic replicas from stained specimens. A suitable etchant for electron metallography must, therefore, in all cases exhibit a preferential attack upon each of the microconstituents present sufficient to result in a difference in surface elevation.

When only two microconstituents are present, it is not too difficult to find a suitable etchant since their physical or chemical properties are generally sufficiently different to result in a marked difference in attack by the etchant. For example, picral (a saturated solution of picric acid in methanol used as an immersion etch) is a satisfactory etchant for the specimen shown in Fig. 1 consisting of iron carbide particles embedded in a ferrite matrix.[1]

W. L. GRUBE is associated with the Research Laboratories Div., General Motors Corp., Detroit.

TN 91E. Manuscript, Sept. 4, 1951.

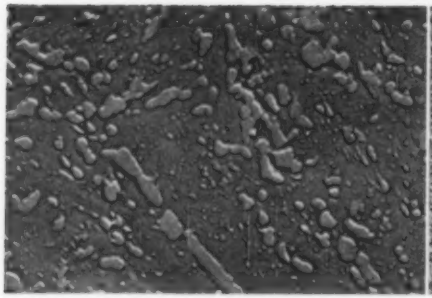

Fig. 1—Tempered martensite. 1100°F, 1 hr. Etched in 4 pct picral. X5000.

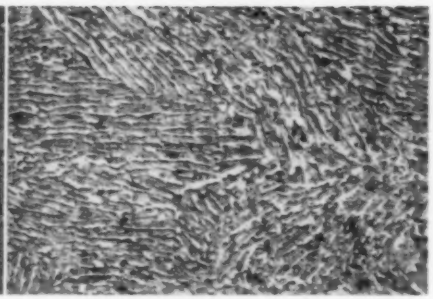

Fig. 2—Fine pearlite. I.T. 1100°F. Etched in 4 pct picral. X5000.

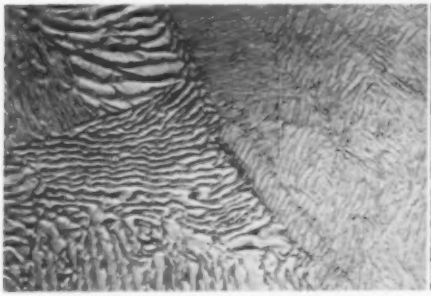

Fig. 3—Fine pearlite. I.T. 1100°F. Etched in $FeCl_3$-HCl. X5000.

Fig. 4—Martensite as-quenched. Etched in 4 pct picral. X5000.

Fig. 5—Martensite as-quenched. Etched in 2 pct nital plus zephiran chloride. X5000.

Fig. 6—Martensite as-quenched. Etched in Allten's reagent. X5000.

Fig. 7—S.A.E. 52100 steel. Etched in 2 pct nital. X5000.

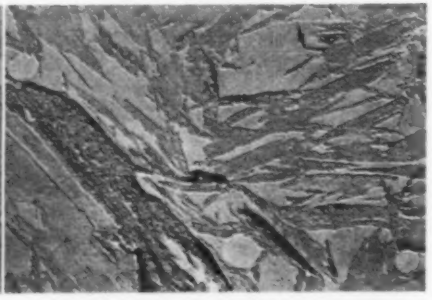

Fig. 8—S.A.E. 52100 steel. Etched in 2 pct nital plus zephiran chloride. X5000.

Fig. 9—Cemented tungsten and tantalum carbides. Composite electrolytic alkaliferricyanide and 3 pct nital etch. X5000.

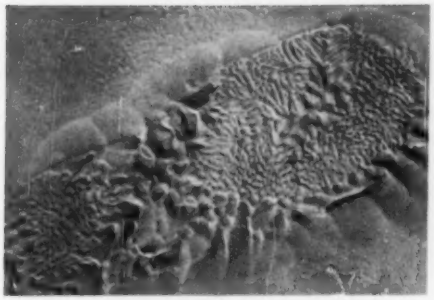

Fig. 10—Carbide in Vitallium. Vacuum-cathodic etch. X5000.

Picral is less satisfactory when used to etch fine lamellar pearlite shown in Fig. 2. Although the relief is sufficiently developed, the etchant has left a residue upon the surface as indicated by the presence of small opaque particles. Moreover, some irregularities appearing in the carbide lamellae indicate that the replica adhered to the specimen tightly and suffered some disturbance upon removal.

A more satisfactory etchant for fine pearlite is ferric chloride-hydrochloric acid (1 pct HCl; 2 pct FeCl, in methanol). As shown in Fig. 3, this etchant leaves a cleaner surface for replicating. Also differences in orientation of the pearlite colonies are more clearly resolved.[1]

As pointed out earlier by Ellis[2] it is quite difficult to etch the harder microstructures of steel (those containing martensite as-quenched, slightly tempered, or both) satisfactorily for electron metallography. For as-quenched steels, the etchant must, essentially, differentiate between martensite and retained austenite. This picral will not do, as indicated in Fig. 4. A modified nital etchant[3] consisting of 2 pct nital containing 0.5 to 1.0 pct zephiran chloride is almost ideal for this structure as shown in Fig. 5. Etchants which develop the retained austenite to this extent yield micrographs suitable for making quantitative measurements. Allten's reagent[4] is also very satisfactory for developing retained austenite as shown by Fig. 6. For simple structures, there is no particular advantage in using Allten's reagent. For more complicated structures containing smaller amounts of retained austenite it shows promise of being more satisfactory because, being used electrolytically, it can be controlled more effectively. It should be pointed out, however, that electrolytic etches may prove unsatisfactory for electron metallography because it has been found that a residue is sometimes left at phase boundaries. This residue is difficult to remove and often covers up much detail.

In structures containing more than two microconstituents it often becomes imperative to use a modified etchant. For example, Fig. 7 shows the microstructure of a specimen of S.A.E. 52100 steel etched in 2 pct nital. The undissolved carbide and tempered martensite are well developed, but there is no differentiation between the untempered martensite and retained austenite. When this structure is etched with 2 pct nital containing zephiran chloride, the complete structure as shown in Fig. 8 is developed.

In cases where it is not possible to develop the microstructure completely with a single etchant, a composite etch (two etchants in succession) may be used. Such is the case with cemented carbide compositions containing both tungsten and tantalum carbide. An electrolytic alkaliferricyanide etch (equal parts 10 pct potassium hydroxide and 10 pct potassium ferricyanide at 4 volts) develops only the angular shaped tungsten carbide grains. If an additional 3 pct nital etch is used after the above etch, the complete structure as shown in Fig. 9, is developed. The nital etch effectively reveals the smooth, round-contoured grains of tantalum carbide by attacking the cobalt binder.

When a satisfactory composite etch cannot be found, the only recourse is to use two or more etches independently. Such a procedure is not entirely satisfactory, but it is sometimes the only way to study the complete microstructure. For example, an electrolytic, 5 pct hydrochloric acid etch is effective in developing the secondary carbide precipitate in high temperature alloys. The primary carbide "aggregates," however, are either unattacked or etched so deeply that a faithful replica cannot be obtained, thereby precluding the possibility of interpreting the microstructure. On the other hand, a vacuum-cathodic etch[5] develops the structure of the primary carbide well as shown in Fig. 10. The secondary carbide particles which surround the primary carbide phase, however, are only faintly visible. Neither etchant is completely satisfactory, but the use of both permits a more accurate interpretation of the structure. In summary, results of the use of various etchants on typical metallographic specimens have been shown. From the results, it is evident that the success of a particular etchant in electron metallography cannot always be predicted from previous experience in light metallography. However, the etchants found to be satisfactory in light metallography should serve as starting points for the development of etchants more suitable for electron metallography.

References

[1] First Progress Report, Sub-Committee XI on Electron Microstructure of Steel, Committee E-4, A.S.T.M. (1950).

[2] A. L. Ellis: The Electron Microscope in Metallurgy. Paper presented before A.I.S.I. (May 24, 1950).

[3] B. L. Averbach and M. Cohen: *Trans.* AIME (1948) **176**, p. 401; METALS TECHNOLOGY (February 1948).

[4] A. E. Nehrenberg: The Growth of Austenite as Related to Prior Structure. *Trans.* AIME (1950) **188**, p. 162; JOURNAL OF METALS (January 1950).

[5] D. M. McCutcheon and W. Pahl: Cathodic Vacuum Etching of Metals. *Metal Progress* (November 1949) **56**, No. 5, p. 674.

Solubility of Gaseous Nitrogen in Gamma Iron and the Effect Of Alloying Constituents — Aluminum Nitride Precipitation

by L. S. Darken, R. P. Smith, and E. W. Filer

The solubility of nitrogen gas in purified iron and low alloy steels is determined for the γ region (930° to 1350°C). The diffusivity of nitrogen is estimated from the rate of approach to equilibrium. The investigation of aluminum-killed steels, held in nitrogen, discloses precipitation of aluminum nitride, the solubility of which is determined.

ALTHOUGH several investigations of the solubility of nitrogen gas in γ iron have been reported, all have made use of the method adopted by Sieverts in his classic work, whereby the solubility is determined by the pressure or volume change of the gas. The agreement between different investigators* is rather poor, particularly as compared to the self-consistency of results of several individual investigators. The present report represents a portion of our investigation of the equilibrium of nitrogen and nitrogenous atmospheres with iron and steels. The method adopted in this temperature region (910° to 1400°C) consists of holding the specimen in gaseous nitrogen, quenching (or cooling), and determining the nitrogen content by direct analysis (solution in acid followed by distillation and titration of the ammonia).**

Up to 1050°C a 20 in. vertical wire-wound (Kanthal) furnace was used; this was wound in three sections so that by proper adjustment of relative currents, and use of a modulator[1] and a commercial controller (using a chromel-alumel control couple), a zone almost 6 in. long could be maintained uniform within a few tenths of a degree. Since the temperature coefficient of the nitrogen solubility is low, the full precision was not utilized and a variation of 1° to 2° was tolerated; a variation of a similar amount also occurred occasionally between the beginning and end of the experiment. At higher temperature a vertically mounted, tubular Globar furnace and control unit was used; the zone of uniformity (1° to 2°C) was here limited to about 2 in.; fluctuations with time were comparable to those in the wire-wound furnace. Reported temperatures were measured by use of a platinum-platinum-rhodium thermocouple, which was frequently compared with a similar standard couple which was calibrated at the gold and palladium points and also compared with one certified by the Bureau of Standards; error from this source is believed to be less than 1°C.

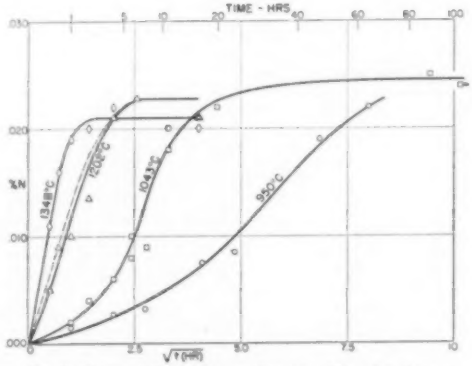

Fig. 1—Nitrogen absorption as a function of time for electrolytic iron suspended in nitrogen gas (+1 pct H_2). The dashed curve and that for 1348°C have the theoretical form for a diffusion controlled process with constant surface concentration.

Nitrogen gas from a commercial cylinder was mixed with slightly over 1 pct H by use of a gas mixer described previously.[2] This mixture was passed over hot copper and through ascarite and phosphorus pentoxide to remove oxygen and water vapor. The purified gas contained 1.05 pct H. This procedure was adopted to prevent the formation on the specimens of oxide film, which is well known to be nearly impervious to nitrogen; its success was attested by

L. S. DARKEN, Member AIME, R. P. SMITH, and E. W. FILER are associated with the Research Laboratory, U. S. Steel Co., Kearny, N. J.

Discussion on this paper, TP 3205E, may be sent, 2 copies, to AIME by April 1, 1952. Manuscript, Aug. 3, 1951. New York Meeting, February 1952.

* One of the difficulties of this method lies in the determination of the so-called "hot volume"—that is the amount of nitrogen (or other substance) in the gaseous phase. This subject was investigated and discussed by M. H. Armbruster, *Journal* Amer. Chem. Soc. (1943), **65**, p. 1043.

** The authors are greatly indebted to Glenn W. Momeyer for the analytical work of this investigation.

Table I. Composition of Samples

Iron or Steel	C	Mn	P	S	Si	Al†	N
1*	0.011	<0.001			0.008	None	<0.001
2*	0.012	<0.001	0.004	0.003	0.002	<0.001	<0.001
3	0.10	0.41	0.011	0.024	0.01	<0.001	0.003
4	0.10	0.44	0.010	0.024	0.01	<0.001	0.003
5	0.10	0.44	0.011	0.024	0.01	0.005	0.003
6	0.10	0.42	0.011	0.025	0.01	0.013	0.003
7	0.75	0.55	0.025	0.032	0.020	0.038	
8	0.10	0.43	0.10	0.025	0.01	0.047	0.004
9	0.051	0.35	0.006	0.033	0.006	0.054	
10	0.79	0.62	0.011	0.025	0.023	0.062	
11	0.10	0.44	0.012	0.023	0.01	0.144	0.004
12	0.064	0.26	0.052	0.021	0.21		
13	0.073	0.28	0.020	0.022	0.57		
14	0.074	0.28	0.012	0.015	1.26		
15	0.052	0.24	0.010	0.015	2.55		
16					3.5		
17	0.028	0.24	0.010	0.013	4.8		
18	0.10	0.43	0.010	0.034	0.007		
19	0.10	0.53	0.010	0.043	0.006		
20	0.20	1.46	0.027	0.022	0.205		
21	1.40	12.98	0.048	0.019	0.32	<0.001	
22		0.028	0.014	0.029	0.003		0.0036

* Irons 1 and 2 are carbonyl and electrolytic respectively. Spectographic analysis indicated the presence of no other metallic elements in excess of 0.001 pct except for 0.02 pct Ni in each and 0.05 pct Cu in the electrolytic iron.

† Metallic aluminum; this is believed negligibly small in the steels which were not aluminum-killed and for which no value is tabulated.

the fact that specimens pulled up and cooled in the glass head of the furnace exhibited no tarnish except in the case of the high silicon steels. In this latter case a "getter" of transformer steel was ultimately suspended beneath the specimens. The purified gas was led through glass tubing (with two butt joints of treated rubber) and introduced into the porcelain furnace tube (¾ or 1 in. ID) through a mercury seal at the bottom. At the top was a ground pyrex joint, the male portion of which was sealed to the porcelain. The gas was discharged to the atmosphere through a long glass tube to prevent any breathing of air into the furnace. Although barometric readings were taken, these are not reported since the effect of departures from 760 mm was negligibly small. Similarly the effect of the 1 pct H on the nitrogen solubility is negligible; by Sievert's law this lowers the nitrogen solubility by only ½ pct—for example by 0.0001 pct out of 0.02 pct.

The composition of the irons and steels used is given in Table I. Except as noted below these were in sheet form; specimens were cut about ½ in. wide and 4 or 2 in. long, depending on the uniform zone of the furnace used. They were pickled and sanded. Several specimens were frequently run simultaneously; small porcelain rings were used as spacers in this case. The suspension wire was of iron. The series of aluminum steels were initially in bar form (¾ in. diam); half disks were used as specimens. The ingot iron used in an attempt to determine the diffusivity was a cylinder 4 in. long and ⅝ in. diam.

Table II. Solubility of N_2 in Purified Iron and Low Alloy Steels

Temperature, °C	Iron or Steel	Thickness, Mm	Time, Hr	Pct N
933	1	0.34	16	0.026, 0.026
923	3	3.2	93	0.023
923	4	3.2	93	0.028
918	12	1.6	65	0.025
918	12	1.6	134	0.029
923	Average of above			0.026_0
923	solubility from smooth plot of Fig. 2			0.026_1
1045	2	2.2	89	0.025
1047	2	2.2	68	0.024
1045	12	1.6	89	0.025
1047	12	1.6	68	0.023
1048	3	3.2	65	0.024, 0.025
1048	4	3.2	65	0.023, 0.027
1051	18	1.5	16	0.025
1051	19	2.0	16	0.024
1048	Average of above			0.024_6
1048	solubility from smooth plot of Fig. 2			0.024_6
1202	2	2.2	6½	0.023
1203	2	2.2	16	0.021
1203	12	1.6	16	0.022
1200	3	1.6	16	0.024
1200	4	1.6	16	0.024
1202	Average of above			0.022_8
1202	solubility from smooth plot of Fig. 2			0.022_8
1348	2	2.2	4	0.022
1342	2	2.2	16	0.020
1342	12	1.6	16	0.020
1348	3	1.6	16	0.021_5
1348	4	1.6	16	0.021_5
1345	Average of above			0.021_0
1345	solubility from smooth plot of Fig. 2			0.021_0

Solubility of Nitrogen in γ Iron

It was originally thought that the slow step in achieving equilibrium between specimen and atmosphere would be the diffusion of nitrogen through the specimen. It was hoped that both the solubility and the diffusivity could be determined by a time series. Electrolytic iron was used for this purpose and the results are shown in Fig. 1. Also shown in this figure is the form[1,4] of the theoretical curve that would be expected if the surface of the specimen were saturated rapidly and remained so. The square root of time is used as abscissa in this figure to facilitate comparison with the theoretical curve (dashed) which is linear and of finite slope in the vicinity of the origin, becoming concave downward as saturation is approached, and eventually leveling off. At the lower temperatures the experimental data do not even approximate this form; the boundary condition is undoubtedly not satisfied and the diffusivity cannot reliably be computed from these data. It would seem that surface adsorption rather than diffusion is the slow step in attaining equilibrium. Even at 1200°C the same conclusions would seem to apply though to a lesser extent. This may be seen by comparison of the experimental data with the theoretical curve for diffusion into a slab under the condition of constant surface concentration. For the data at 1348°C, the curve in Fig. 1 is drawn with the theoretical form and corresponds to the diffusivity:

$$D = 3.1 \times 10^{-4} \text{ sq cm sec}^{-1}$$

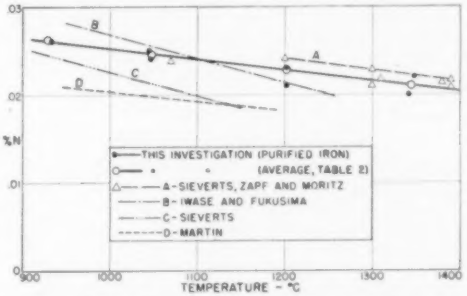

Fig. 2—The solubility of nitrogen gas (at atmospheric pressure) in γ iron.

These time series at least indicate the minimum time required for approximate equilibration. In each case, except for the lowest temperature, two specimens were run for a substantially longer time. At the lowest temperature a much thinner specimen was used to achieve equilibrium. The solubility of nitrogen gas in iron, as thus determined, is given in

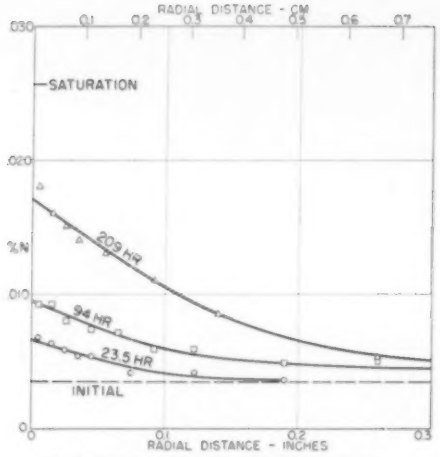

Fig. 3—Penetration curve for nitrogen in iron rod.

Table II. The solubility in several low alloy steels is also included. As indicated here and substantiated later, the extraneous constituents have a negligibly small effect; hence all these results at or near a given temperature are averaged. These averages, as well as the individual results for iron, are plotted in Fig. 2 and compared with the results of other investigators.[2-5] The results are represented remarkably well by a straight line, whose equation is:

$$[\text{Pct N}] = 0.0404 - 1.2\text{x}10^{-4}\,T$$

Approximate Diffusivity at 955°C

In order to verify the previous conclusion that the slowness in the lower temperature region is due to failure to establish surface saturation and to determine the diffusivity, another series of experiments was run. An ingot iron cylinder (4 in. long, $^5/_8$ in. diam) was suspended in the furnace in the same manner as before. After a predetermined time ($23^1/_2$, 94, or 209 hr) the cylinder was quenched and subsequently turnings were taken on a lathe, after discarding the ends. The nitrogen content of the layers is shown in Fig. 3. It is quite apparent that the surface layer did not become saturated even in 209 hr. The diffusivity of nitrogen may be determined directly from its definition. By graphical integration the mean nitrogen content was computed for each time. The rate of entrance of nitrogen per unit area, as determined therefrom, divided by the concentration gradient (at the surface) at the corresponding time gives a mean:

Table III. Effect of Manganese on the Solubility of N_2 in Austenite

Temperature, °C	Specimen No.	Time, Hr	Pct Mn	Pct N
1051	(From Fig. 2)		0	0.024[2]
	18	16	0.43	0.025
	19	16	0.53	0.024
	20	6	1.46	0.025
	20	16	1.46	0.025
	21	16	12.98	0.066
1203	(From Fig. 2)		0	0.022[2]
	21	16	12.98	0.046
1342	(From Fig. 2)		0	0.021
	20	16	1.46	0.020

Table IV. Effect of Silicon on the Solubility of N_2 in Austenite

Temperature, °C	Specimen No.	Time, Hr	Pct Si	Pct N
1046	(From Fig. 2)		0	0.024[2]
	12	89	0.20	0.025
	12	157	0.20	0.023
	13	89	0.58	0.023
	13	157	0.58	0.022
1203	(From Fig. 2)		0	0.022[2]
	12	16	0.20	0.022
	13	16	0.58	0.020
1342	(From Fig. 2)		0	0.021
	12	16	0.20	0.020
	13	16	0.58	0.018

$$D = 1.9\text{x}10^{-7} \text{ sq cm sec}^{-1}$$

The same result was obtained using a more complicated method. The precision leaves much to be desired, but it is believed that the error probably does not exceed 20 pct.

Effect of Alloying Constituents

The effect on the solubility of nitrogen in austenite of the amounts of carbon, manganese, sulphur, and phosphorus usually present in plain low carbon steels is seen from Table II to be negligible. The effect of increasing amounts of manganese is shown in Table III. Up to 1.5 pct Mn, the effect is seen to be well within the error of analysis; from the previous data on time required (allowing for decreased thickness) as well as the agreement of the 6 and 16 hr specimens, there seems little doubt that these specimens were equilibrated with the atmosphere. The 13 pct Mn steel unquestionably absorbed considerably more nitrogen except at the highest temperature; no checks were run to determine whether it would have absorbed still more in longer time. Since 1.5 pct Mn does not observably affect the solubility and since

Table V. Nitrogen Absorbed by Aluminum-Killed Steels

Temperature, °C	Specimen No.	Thickness, Mm	Time, Hr	Pct Al	Pct N
1048		(From Fig. 2)		0	0.0247
	3	3.8	21	<0.001	0.020
	3	3.8	65	<0.001	0.024, 0.025
	4	3.8	21	<0.001	0.019
	4	3.8	65	<0.001	0.023, 0.027
	5	3.8	21	0.005	0.021
	5	3.8	65	0.005	0.024, 0.025
	6	3.8	21	0.013	0.021
	6	3.8	65	0.013	0.025, 0.027
	8	3.8	21	0.047	0.033
	8	3.8	65	0.047	0.048, 0.048
	11	3.8	21	0.144	0.045
	11	3.8	65	0.144	0.078, 0.082
1042	11	(millings)	64	0.144	0.091, 0.092
1051	7	1.6	17	0.038	0.037
	7	1.6	40	0.038	0.038
	10	1.6	17	0.062	0.049
	10	1.6	40	0.062	0.051
1200		(From Fig. 2)		0	0.022[2]
	3	1.6	16	<0.001	0.024
	4	1.6	16	<0.001	0.024
	5	1.6	16	0.005	0.024
	6	1.6	16	0.013	0.023
	8	1.6	16	0.047	0.034
	11	1.6	16	0.144	0.073
	11	(millings)	16	0.144	0.078, 0.081
1348		(From Fig. 2)		0	0.021[2]
	3	1.6	16	<0.001	0.022
	4	1.6	16	<0.001	0.021
	5	1.6	16	0.005	0.020
	6	1.6	16	0.013	0.020
	8	1.6	16	0.047	0.021
	11	1.6	16	0.144	0.031
1350	9	1.6	5	0.054	0.023

the effect of high manganese appears to decrease with temperature, it was thought that there might be a nitride precipitate in the high manganese steel. However, metallographic examination disclosed a completely austenitic structure free of observable precipitate.

The effect of silicon on the solubility of nitrogen is shown in Table IV. At each temperature the nitrogen content was lowered slightly by silicon. Difficulty was experienced in equilibrating higher silicon steels with the nitrogen atmosphere; for example a specimen of a 1.2 pct Si steel (a member of the series tabulated) contained 0.016 pct N after 89 hr treatment at 1046°C, and a similar specimen contained only 0.009 pct N after the longer treatment of 157 hr. A dynamo grade steel (3.48 pct Si) behaved even more erratically. The highest nitrogen content attained was 0.012 pct at 1203°C; this steel, however, is partially ferritic. It seems probable that this difficulty is due to an oxide film in spite of the aforementioned precautions and the fact that such film was not directly observable in the case of specimens cooled in the head of the furnace. Such difficulty was avoided by using a higher hydrogen content and higher temperature, which procedure places the series in the δ region beyond the range of the present report.

Precipitation of Aluminum Nitride

To investigate the effect of small amounts of per cent Al, principal use was made of steels from a series of ingots from the same heat (Nos. 3, 4, 5, 6, 8, and 11 of Table I); the aluminum addition was 0, ¼, ½, 1, 2, and 4 lb per ton, respectively. A few other aluminum-killed steels were also used. The nitrogen content of all samples treated above 1000°C is given in Table V. Equilibrium is believed to have been substantially attained in at least one run for each specimen at each temperature. This statement is based on checks of shorter and longer time runs or comparison of the time requirement with Fig. 1 (noting agreement of shorter time runs), taking into account any difference in thickness and the extra nitrogen absorbed; millings were used in two cases to hasten equilibrium.

The equilibrium nitrogen content is plotted against aluminum in Fig. 4. At each temperature the nitrogen content was independent of aluminum up to a critical amount thereof, above which the nitrogen rose abruptly. The small amount of aluminum present would not in any case be expected to influence observably the solubility of nitrogen in homogeneous austenite; the behavior of the lower aluminum specimens particularly at higher temperature verify this expectation. The abrupt rise in nitrogen content at higher aluminum is typical of the behavior encountered in the case of a phase change. If such is the case then this straight rising line is a tie line connecting the compositions of the two phases in equilibrium and should have a slope equal to the ratio of nitrogen to aluminum in the new phase.† The observed slope corresponds, well within the experimental error,‡ to a one to one atom ratio of nitrogen to aluminum. Since the only known nitride of aluminum[9, 10] corresponds to the chemical formula AlN,

† Strictly, the slope is the ratio of the difference of nitrogen and of aluminum in the two phases, but as both are so small in the austenite there is negligible error in the above statement.

‡ The experimental error is believed to be principally in the analytic determination of aluminum. The analyses here reported and used were performed in this Laboratory, and the precision as judged by checks and prior experience is about 0.003 pct. Check analysis by an outside laboratory varied by twice this amount.

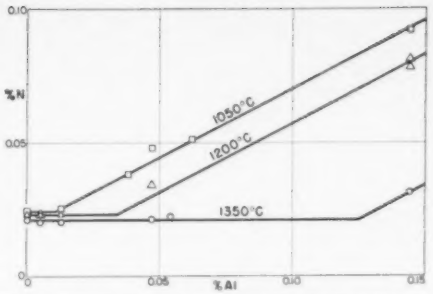

Fig. 4—Nitrogen content of aluminum-killed steels equilibrated with nitrogen gas.

it seems almost certain that it is the precipitation of this phase which gives rise to the nitrogen contents (Fig. 4) which are in excess of the solubility in austenite; the lines of the figure are drawn with this theoretical slope.

The equilibrium constant (solubility product) for the reaction:

$$\text{AlN (solid)} = \underline{\text{Al}} + \underline{\text{N}}$$

may be determined from the position of the break in each curve of Fig. 4. This point corresponds to the composition of austenite in equilibrium with AlN. The values of K (which is [pct Al] [pct N]) thus found are plotted against the reciprocal of the absolute temperature in Fig. 5. The line drawn may be represented by the relation:

$$\log K = -\frac{7400}{T} + 1.95$$

The heat of formation of AlN from dissolved nitrogen and aluminum is thus found to correspond to $\Delta H = -34{,}000$ cal. This heat may also be estimated from Kelley's compilation,[9] in which, for the formation of AlN from metallic aluminum and gaseous nitrogen, ΔH is selected as $-54{,}700$ cal (at 1200°C); the data reviewed exhibit discrepancies of over 10,000 cal. Subtracting from this $\Delta H = -500$ cal for the solution of nitrogen gas in austenite, and $\Delta H = -15{,}000$ for the solution of aluminum in ferrite[11] at 20°C (which is here considered to apply approximately to aluminum in austenite at 1200°C), the computed value for ΔH of formation of AlN from aluminum and nitrogen dissolved in austenite is

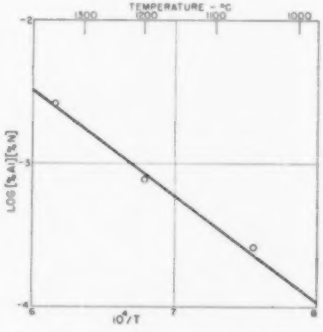

Fig. 5—The solubility product of aluminum nitride in γ iron.

Fig. 6—Aluminum-killed steel (0.144 pct Al) held in nitrogen for 93 hr at 923°C.
Aluminum nitride precipitate and grain refinement in rim zone permit its recognition even by naked eye. Rim-core boundary is indicated by arrows. Picral etch. X18.

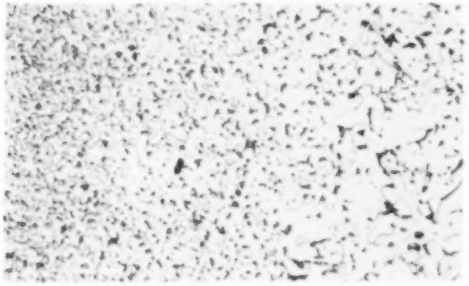

Fig. 7—Same specimen as Fig. 6. Rim-core boundary at X65.

found to be −39,200 cal. as compared to the above experimental value of −34,000 cal. The discrepancy is within the many errors involved in the two determinations and lends support to the foregoing general interpretation of our results.

Several of the specimens of Table V, as well as some treated at 923°C, were examined metallographically. Specimens containing 0.047 and 0.144 pct Al, for which the time of treatment at 923° and 1048°C was insufficient to achieve complete equilibrium, exhibit a definite "rim" and "core" which

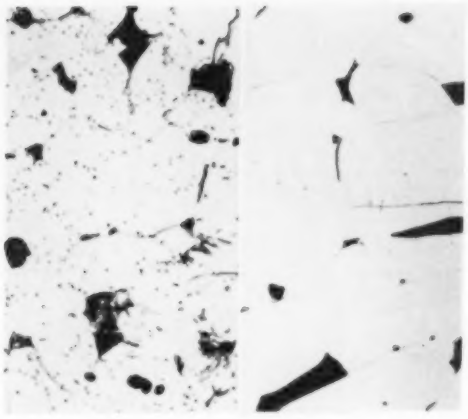

Rim Core

Fig. 8—Same specimen as Fig. 6. Rim and core at X650.

were obvious, on the polished sample, even to the naked eye. Examination of the specimens disclosed that the rim differs from the core in two distinct respects: 1—the rim contains a copious fine precipitate which the core does not; 2—the ferrite grain size of the rim was considerably smaller (by about 2 A.S.T.M. sizes) than that of the core. Obviously, the nitride here forms a subscale similar to that found, for example, by Rhines[12] in the case of some oxides. The difference between the subscale (rim) and central (core) zones is illustrated for a typical specimen by the micrographs of Figs. 6 to 8. Even at X650 (Fig. 8) the precipitate is barely resolvable. However, it is shown clearly in the electron micrograph of Fig. 9.

Subscale thickness for a few specimens is given in Table VI. The fact that precipitation occurred throughout one specimen furnishes added evidence that this specimen (the composition of which is used in Fig. 4) is substantially equilibrated with the atmosphere. The final entry in the table is for a specimen in which the subscale has penetrated 90

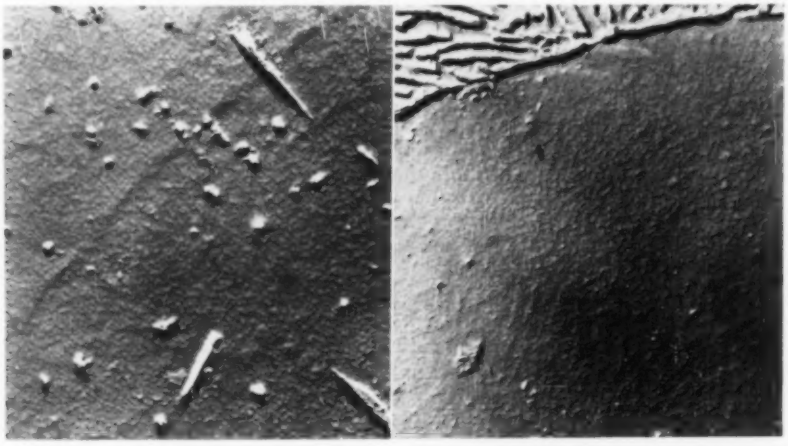

Rim Core

Fig. 9—Same specimen as Fig. 6. Electron micrograph at X9000 of rim showing aluminum nitride precipitate and core.

Table VI. Subscale Thickness

Temperature, °C	Pct Al	Time of Treatment, Hr	Pct N	Subscale Thickness, Mm
923	0.047	40½	0.021	1.0
	0.144	40½	0.036	0.5
	0.144	93	0.051	0.7
1048	0.047	21	0.033	1.4
	0.047	65	0.048	(Complete)
	0.144	21	0.045	0.65
	0.144	65	0.080	1.7

pct of the way to the center; this is in rough agreement with what would be expected by comparing its nitrogen content (0.080 pct) with that (0.091 pct) of the equilibrated milled specimen of Table V.

In general, the observed subscale thickness is somewhat less than the thickness computed from the diffusivity on the assumption that the surface of the specimen is saturated with nitrogen. This is not surprising since it has been shown, Fig. 3, that surface saturation is not achieved in this temperature range. It may be worthy of comment that in one case (the final entry of Table VI) the subscale or zone of precipitation extended much further than the zone of fine grains. This may be associated with the fact that aluminum nitride is by no means "insoluble" and hence the transition from rim to core is not sharp. Grain refinement undoubtedly depends on the number and size of the precipitated particles both of which vary somewhat. However, in all other cases, within the error of measurement, the grain size change occurred at the inner boundary of the subscale.

Summary

The solubility of nitrogen gas in iron and low alloy steels has been measured in the γ region from 930° to 1350°C. The specimens were equilibrated with the gas and analyzed. The diffusivity of nitrogen in iron is reported at 955° and 1348°C (D = 1.9×10^{-7} and 3.1×10^{-6} sq cm per sec, respectively). The solubility in plain low carbon steels is the same as that in iron and may be represented by the equation:

$$[\text{Pct N}] = 0.0404 - 1.2 \times 10^{-5} T$$

Manganese up to 1.5 pct has no observable effect. Silicon (0.58 pct) appears to lower the solubility slightly. Steels killed with sufficient aluminum exhibit a precipitate of aluminum nitride (AlN) which, for incompletely equilibrated specimens is in the form of a subscale. The solubility product of aluminum nitride has been determined. This solubility product or equilibrium constant may be represented by the relation:

$$\log K = \log [\text{Pct Al}] [\text{Pct N}] = -(7400/T) + 1.95.$$

References

[1] L. S. Darken: *Review of Scientific Instruments* (1949) **20**, p. 323.
[2] L. S. Darken and R. W. Gurry: *Journal* Amer. Chem. Soc. (1945) **67**, p. 1398.
[3] D. H. Andrews and J. Johnston: *Journal* Amer. Chem. Soc. (1924) **46**, p. 640.
[4] A. B. Newman: *Trans.* Amer. Inst. of Chem. Engr. (1931) **27**, p. 310.
[5] A. Sieverts: *Ztsch. für Physik. Chem.* (1931) **155A**, p. 299.
[6] A. Sieverts, G. Zapf, and H. Moritz: *Ztsch. für Physik. Chem.* (1938) **183A**, p. 19.
[7] E. Martin: *Archiv für das Eisenhütten.* (1929) **3**, p. 407.
[8] K. Iwasé and M. Fukusima: *Sci. Repts.* Tohoku (1939) **27**, p. 162.
[9] K. K. Kelley: Bur. Mines *Bull.* No. 407 (1937).
[10] M. Hansen: *Der Aufbau der Zweistofflegierungen.* (1936) Berlin.
[11] F. Körber: *Stahl und Eisen* (1936) **56**, p. 1401.
[12] F. N. Rhines: *Trans.* AIME (1940) **137**, p. 246.

Technical Note

Change in Yield Strength During Aging in Iron

by C. A. Wert

THE change in mechanical properties accompanying quench aging of carbon in α iron has been known for a number of years. Since the amount of carbon involved is rather small, however, no measurements could be made to correlate the property change with the state of precipitation of the carbide. Indeed, until a few years ago it was not plain which property might be used to indicate the state of the progress of precipitation. Some years ago the internal friction of solid solutions of carbon in α iron was demonstrated, and the use of this phenomenon to ascertain the amount of carbon in solid solution at any given time was developed. Shortly afterward the author made a number of measurements in which changes in electrical resistance, thermoelectric emf, and hardness were determined simultaneously with the internal friction (and hence with the precipitation).[1] A little later Dijkstra and Wert measured the change in magnetic coercive force accompanying aging.[2]

The present work was undertaken to inquire into the changes in yield strength accompanying aging. The work was done on specimens made of Puron. These specimens were 0.05 in. in diam and about 6 in. long. Though specimens of this small size are not ideal for yield strength measurements, such specimens are desirable for internal friction meas-

C. A. WERT is Research Associate Professor of Physical Metallurgy, University of Illinois, Urbana, Ill.
TN 89E. Manuscript, Aug. 27, 1951.

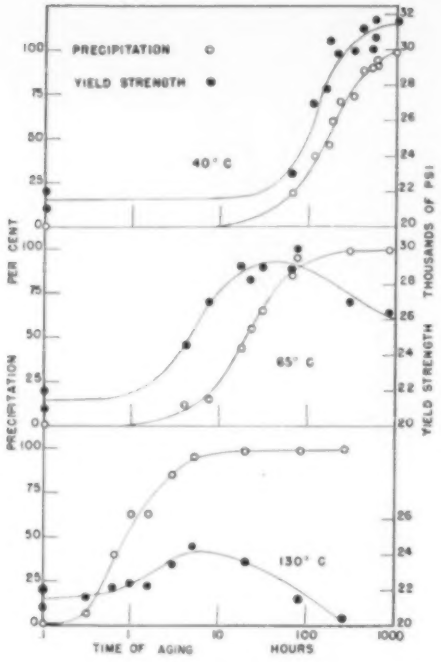

Fig. 1—Change in yield strength accompanying precipitation of carbide in α iron.

urements. The tensile machine used was essentially the same as that used previously by the author in a similar type of investigation.[2] Specimen grips were made which would fit into both the torsion pendulum apparatus and the load bearing supports of the tensile machine. These grips were silver soldered to the ends of the specimen. Numerous attempts were made to attach the grips after all heat treatments (decarburization, carburization, and aging) just prior to the tensile measurement, but these attempts were all futile because the soldering operation invariably produced softening sufficient to cause failure of the sample at the grips. By soldering the grips in place before these heat treatments however, this was avoided except for an occasional sample which had a very high yield strength. Elongation of the sample during loading was measured by running a single strand of 0.001 in. resistance wire along a 2 in. section in the center of the sample. This strain-gage wire served as one arm of a Wheatstone bridge.

Measurements were made on three groups of samples; these groups were aged at 40°, 65°, and 130°C, respectively, after having been carburized to about 0.015 pct C. The yield strength data and the precipitation data (the latter as deduced from internal friction measurements) are shown in Fig. 1. The significant points to be noticed are:

Table I. Calculation of Particle Diameter for Fully Aged Specimens

Temperature, °C	d (Angstroms)	d′ (Angstroms)
40	160	1000
65	210	1300
130	500	3000

1—The peak yield strength becomes higher as the aging temperature is lowered. This was perhaps to be expected from previous knowledge of behavior of hardness during quench aging.

2—The increase in yield strength occurs simultaneously with the precipitation. The peak is not reached until near the end of the precipitation process, after which the decline in yield strength is fairly rapid. Overaging is seen to manifest itself in yield strength just as it does in hardness. It is not clear from these measurements (nor does it seem clear from any other measurement) what is the detailed mechanism of overaging.

By methods previously described,[1] a calculation of particle diameter, d, for fully aged specimens (and hence of mean particle distance, d') was made.[4] These calculations give the results shown in Table I.

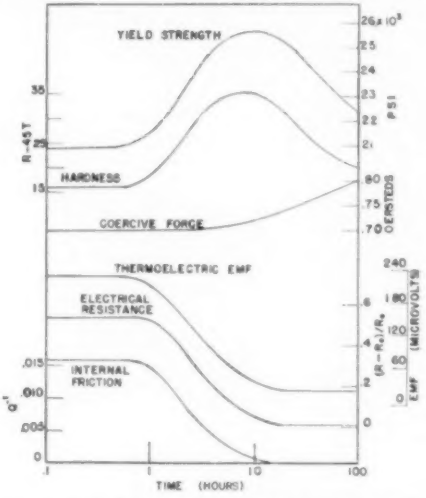

Fig. 2—Change in various properties during aging of carbon in iron at 100°C.

This plot represents yield strength, hardness, and coercive force measurements at 20°C; internal friction at 40°C; electrical resistance at —195°C; and thermoelectric emf (relative to decarburized iron) between —195° and 0°C.

If the peak yield strength be plotted as a function of log d' (after Gensamer, Pearsall, Pellini, and Low[4]) a straight-line function is obtained though with a much different magnitude and slope from the work of Gensamer et al.

This measurement adds to the growing list of physical properties that have been correlated to the precipitation of carbide in α iron. Fig. 2 shows schematically how these properties change during a typical heat treatment at, say, 100°C. With the exception of magnetic coercive force, where a striking critical-size-effect was observed, all these properties change steadily during the precipitation, the major change in property coming during the most rapid formation of the carbide.

References

[1] C. Wert: *Thermodynamics in Physical Metallurgy.* (1950) Cleveland. A.S.M.

[2] L. J. Dijkstra and C. Wert: *Physical Review* (1950) **79**, p. 979.

[3] C. Wert: *Trans.* AIME (1950) **188**, p. 1242; JOURNAL OF METALS (October 1950).

[4] Gensamer, Pearsall, Pellini, and Low: *Trans.* A.S.M. (1942) **30**, p. 983.

Effect of Varying the Rate of Reduction on the Magnetic Properties, Ultimate Tensile Strength, and Resistivity Of 18/8 Stainless Steel Wire

by Samuel Storchheim

IT was noted that variations existed in the magnetic properties, namely, coercive force, *Hc*, and remanence, *Br*, of 18/8 stainless steel wires of the same analysis when these wires were given the same percentage of reduction of area at different rates of reduction. In order to determine the extent of these variations, a program was initiated whereby commercial 302 and 304 stainless steels were drawn with a wide variation of speeds. Ultimate tensile strengths and specific resistances, as well as the *Hc-Br* measurements, were determined. If variations of considerable magnitude were found, it was thought that the knowledge accrued from the investigation could probably aid in determining the particular drawing speed required to obtain desired properties for a given specification for a particular analysis of wire.

Drawing Procedure

Two specimens (set I, No. 302 and No. 304), the chemical analyses of which are given in Table I, were drawn at different speeds, namely, 45 to 3900 ft per min, directly from 0.016 in. diam wire to 0.004 in. diam wire, a 93.7 pct reduction of area. To obtain this high percentage of reduction, the wire at 0.016 in. was softened by annealing at 1150°C. It was then strung in a No. 16CF variable speed Vaughn drawing unit and passed through 13 B.&S. gage dies of successively smaller diameter, as shown in the accompanying table.

Following this step, several hundred feet of the wire was drawn, at a particular speed, through the dies and wound upon a spool. Once the sample of wire was drawn at the desired speed, the spool with the finished sample was removed, tagged for later identification, and an empty spool was placed in the machine. Another wire sample was drawn at a different speed, after making the necessary adjustments upon the Vaughn unit. At the greater speeds, several thousand feet of sample were drawn to insure that the wire to be used for testing would be uniform. This was done because the desired speed was not reached instantly; the wire taking a short while to attain the required drawing rate. All speed measurements were made by placing a tachometer against one of the machine's pulleys during the actual drawing of the specimens.

S. STORCHHEIM, formerly Metallurgical Engineer, Wilbur B. Driver Co., Newark, N. J., is now Senior Metallurgical Engineer, Metallurgical Laboratories, Sylvania Electric Products Inc., Bayside, N. Y.

Discussion on this paper, TP 3181E, may be sent, 2 copies, to AIME by April 1, 1952. Manuscript, June 15, 1951; revision, Aug. 3, 1951. New York Meeting, February 1952.

To broaden the extent of the investigation, two additional specimens (set II, No. 302 and 304), analyses for which are given in Table I, were studied for variations in properties. However, these were drawn at heavier starting sizes directly through nine dies in a 12 HF Vaughn wire drawing unit. The B.&S. gage numbers and die diameters used were as given in the accompanying table which shows an

Set I, No. 302 and 304		Set II, No. 302 and 304	
B.&S. No.	Die Diam, In.	B.&S. No.	Die Diam, In.
26	0.0159	13	0.072
27	0.0142	14	0.064
28	0.0126	15	0.057
29	0.0113	16	0.051
30	0.010	17	0.045
31	0.0089	18	0.040
32	0.008	19	0.036
33	0.0071	20	0.032
34	0.0063	21	0.0285
35	0.0056		
36	0.005		
37	0.0045		
38	0.004		

84.4 pct reduction of area. The 0.072 in. diameter wire was also annealed at 1150°C. The process of obtaining samples was the same as described above. The only difference between the two was that the rates involved were not as extensive, set II covering a range of 625 to 1150 ft per min.

Tensile tests were carried out for the 0.004 in. diam wires on a horizontal Scott Tensile Tester, while tensile tests for the 0.028 in. diam wires were made on a vertical Scott Tensile Tester. Each value listed in the tables represented the average of five samples with a maximum deviation of approximately 3 pct among the samples. Resistance per foot of the wires was determined by use of standard bridges accurate to the nearest hundreth of an ohm for the 0.004 in. wire, and to the nearest thousandth of an ohm for the 0.028 in. wire. The resistances per foot were then converted to resistivities by use of the following equation:

$$P = R \times CM$$

where R is the resistance per ft in ohms per ft; CM, the area in circular mils; and P, the resistivity in ohms—$\frac{CM}{\text{ft}}$. The values listed in the tables likewise represented the average of five samples among which there was a maximum deviation of about 2 pct.

The magnetic measurements, *Hc-Br*, were made with a Hysteresis Loop Tester[1] which projected the

[1] W. W. Wetzel: Review of the Present Status of Magnetic Recording Theory. Part I. *Audioengineering* (November 1947) 31, No. 10.

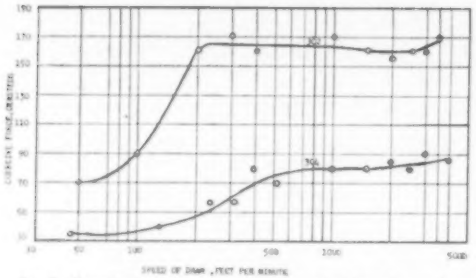

Fig. 1—Coercive force as a function of speed of draw for set I.

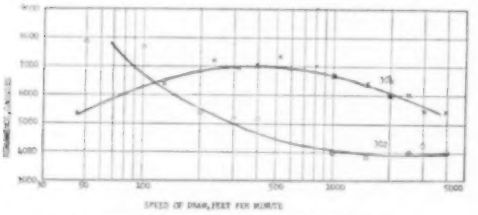

Fig. 2—Remanence as a function of speed of draw for set I.

image of the hysteresis loop on a previously calibrated cathode ray oscilloscope screen. The results obtained were the average of five samples with a maximum deviation of 5 pct for the *Hc* readings and 10 pct for the *Br* readings.

The data obtained using these sets of stainless steel types are tabulated in Tables II to V, and from these tables curves were drawn depicting the general nature of the various relationships between the log of the rate of reduction vs. other properties, Figs. 1 to 4.

Discussion of Results

Rate of Reduction vs. Coercive Force: For set I, the two analyses exhibited similar coercive force curves with the exception that they were displaced from each other, see Fig. 1. For the 302 analysis, the curve indicated that the *Hc* values were low at low rates of draw, but rose quickly at moderate rates of draw to a value approximately 143 pct greater than that initially obtained. Once this "ultimate" value was obtained, there was little deviation from it except that caused by scatter. The 304 curve showed an initially lower *Hc* value than the 302 curve at low speeds. This value also rose as did the 302 curves, but more slowly. As in the case of the 302 curve, the final *Hc* of the 304 curve increased over its initial value by approximately 143 pct.

The limited spread of rates of reduction for set II did not warrant a similar plotting. However, these data plus those of set I indicated that an increase in the percentage of nickel content caused an upward displacement in the relative positions of curves; i.e., the *Hc* was increased for the same speed of draw when the nickel content was higher.

Rate of Reduction vs. Remanence: When the remanence curves for the two analyses of set I were plotted, they did not follow similar patterns as was the case with the coercive force curves, see Fig. 2. The 302 curve indicated a high *Br* value at low drawing speeds which gradually fell off at increasing speeds and then levelled off at high rates of draw and remained relatively constant as in the case of the *Hc* values. The 304 curve behaved differently in that the initial values of *Br* at low drawing rates were low. As the rates increased these values increased and then decreased gradually.

The data from set I together with that from set II indicated that higher nickel contents at moderate-to-fast rates of draw exhibited lower values of *Br*. However, set I showed that the higher nickel 302 at slow rates of draw exhibited values of *Br* about 45 pct greater than the lower nickel 304, in fact 9 pct higher than any other obtained with the lower nickel analysis regardless of drawing speed. The variation of *Br*, within the higher nickel (set I, 302) specimens, was greater over the range of drawing speeds investigated than the lower nickel (set I, 304), namely, 51.0 pct as against 27.2 pct, respectively.

Rate of Reduction vs. Ultimate Tensile Strength: Plotting the ultimate tensile strengths of both the 302 and 304 vs. the rate of reduction gave two curves similar in appearance, but, as in the *Hc* set, dis-

Table I. Analyses of Stainless Steels Used, Pct

Type	C	Mn	P	S	Si	Mo	Ni	Cr
Set I								
302	0.08	0.91			0.59	0.08	9.41	18.39
304	0.070	1.07	0.030	0.018	0.40	0.10	8.47	18.91
Set II								
302	0.12	1.50	0.025	0.019	0.70		9.40	18.04
304	0.071	0.97	0.034	0.030	0.45	0.25	9.85	18.04

Table II. Set I, 302

No.	Rate of Reduction, Ft per Min	*Hc*, Oersted	*Br*, Gausse	Ultimate Tensile, 10^3 Psi	Resistivity, Ohm-cm per Ft
1	50	70	7850	395	555
2	100	90	7700	325	540
3	200	160	5450	372	500
4	300	170	5180	360	500
5	400	160	5180	372	500
6	1000	170	4000	372	490
7	1500	160	3850	369	500
8	2000	155	4250	356	510
9	2500	160	4000	365	500
10	3000	160	4250	372	490
11	3900	170	4000	372	485

Table III. Set I, 304

No.	Rate of Reduction, Ft per Min	*Hc*, Oersted	*Br*, Gausse	Ultimate Tensile, 10^3 Psi	Resistivity, Ohm-cm per Ft
1	45	35	5330	372	615
2	130	40	6400	357	610
3	235	55	7200	361	600
4	315	55	6930	361	595
5	395	80	7070	357	585
6	510	70	7330	357	590
7	1000	80	6870	357	580
8	1500	80	6400	357	570
9	2000	85	6000	350	560
10	2500	80	6000	357	560
11	3000	90	5460	357	555
12	3900	85	5460	357	555

Table IV. Set II, 302

No.	Rate of Reduction, Ft per Min	*Hc*, Oersted	*Br*, Gausse	Ultimate Tensile, 10^3 Psi	Resistivity, Ohm-cm per Ft
1	625	220	1290	271	465
2	710	220	1270	279	460
3	815	210	1450	279	460
4	885	195	350	275	475
5	1000	240	2090	288	470
6	1120	220	2560	270	485

placed from each other, see Fig. 3. Initially, the values were high at slow drawing rates but decreased gradually to a value which remained relatively constant from moderate to very fast drawing rates; i.e. constant from about 200 ft per min up to 3900 ft per min. The maximum decrease in tensile strength obtained at fast rates of draw for the "constant" tensile value over the initially high (slowest speed of draw) value was approximately 6 pct for the 302 and 4 pct for the 304. In the cases investigated the higher carbon 302 specimen of both sets I and II exhibited the higher tensile values, about 4 pct higher for set I and 10 pct higher for set II. The low carbon content 304 tensile value at 50 ft per min was equivalent to the higher carbon containing 302 drawn between 300 and 3900 ft per min. The low tensile value obtained for the 302 curve at 100 ft per min was believed caused by a possible improper sampling; i.e., sufficient wire may not have been drawn to obtain a true representation of that particular drawing speed. The "dips" in the two curves at 2000 ft per min possibly were the results of a mechanical fluctuation of the drawing unit while the wire was being drawn.

Rate of Reduction vs. Resistivity: The resistivity/rate curves generally were not too alike except that they showed a trend to decrease as the speed increased, see Fig. 4. For the 302 curve of set I, the strongly decreasing trend stopped at about 300 ft per min where the resistivity partially levelled off to a slowly decreasing value. Between 50 to 300 ft per min a maximum drop of 10 pct was experienced. The curve for 304 of set I showed a gradual decrease through the entire range of speeds investigated. The maximum decrease in resistivity obtained again was about 10 pct. In both sets of curves, the highest values of resistivity were found at the slowest drawing speeds.

Using both groups of data from sets I and II, it was seen that the resistivities were lowered by an increase in nickel content; i.e., for the same rate of drawing speed, an analysis of higher nickel content exhibited a lower specific resistance. The lower nickel 304 curve of set I at very slow rates of draw exhibited a value of resistivity approximately 10 pct greater than the higher nickel 302 for the same low rate of draw, namely, 50 ft per min. A maximum difference of almost 20 pct was obtained between the two analyses over the range of speeds investigated.

Explanation of Effects of Drawing Speed

A possible explanation of the effects found on the properties of 18/8 stainless steel by varying the rate of drawing speed could be as follows: Cold working a metastable austenitic 18/8 stainless steel produces martensite, provided the temperature during working is not much higher than room temperature.[2] During the process of drawing wire through a die or a series of dies, an increase in temperature of the wire occurs, because of the dual processes of deformation and friction. The wire generally will be cooled off by the coolant to approximately room temperature in the time that it travels the distance from one die to the next. Should the temperature become greater, less martensite will be formed. Thus, if the speed of draw is increased to the point where the lubricant can no longer cool the wire fast enough, the temperature of the wire will rise above the room temperature. Therefore, the higher the drawing speed, the higher the temperature, and less martensite will be formed; consequently, the *Br*, resistivity, and tensile strength will be lower and the *Hc* will be higher.

Table V. Set II, 304

No.	Rate of Reduction, Ft per Min	*Hc*, Oersted	*Br*, Gausse	Ultimate Tensile, 10^3 Psi	Resistivity, Ohm-cm per Ft
1	630	250	1440	251	455
2	740	235	1130	251	450
3	815	255	1130	248	445
4	915	240	1270	251	455
5	1050	240	1440	237	455
6	1150	235	1270	253	450

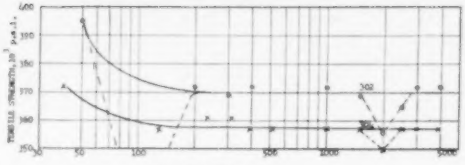

Fig. 3—Ultimate tensile strength as a function of speed of draw for set I.

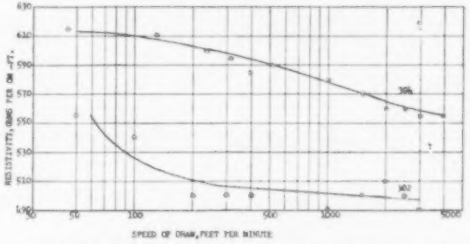

Fig. 4—Resistivity as a function of speed of draw for set I.

Conclusion

It was determined that variations did exist in magnetic properties, ultimate tensile strength, and specific resistance of commercial 18/8 stainless steel wires when the rate of reduction of these wires was varied. With increasing drawing rates it was found that coercive force increased, while remanence, tensile strength, and resistivity decreased. The changes in coercive force and remanence were quite extensive, while those of tensile and specific resistance, although significant, were less. A higher nickel content caused, for the same rate of draw, an increase in *Hc* and a decrease in *Br* and resistivity. Higher carbon contents exhibited higher tensile values for the same rate of draw.

From the above results and by possible further future investigation, it would appear that an 18/8 stainless steel analysis, which might normally have been considered inferior for a particular specification, could be salvaged by the correct choice of drawing speed. This could be of special value when the present critical situation regarding the availability of almost all metals and alloys is considered.

Acknowledgment

The author should like to express his appreciation to the Wilbur B. Driver Co. for permission to publish this article.

[2] Thum: *Book of Stainless Steels*. A.S.M., Cleveland.

Correlation Between Electrical Conductivity and Temperature Coefficient of Resistance of Solid-Solution Alloys

by M. Hansen, W. R. Johnson, and John M. Parks

AS part of a research project sponsored by the Signal Corps Engineering Laboratories, which had the objective of obtaining a magnet wire of good conductivity and low temperature coefficient of resistance, a comprehensive literature survey, supplemented by experimental work, revealed that a linear relationship exists for solid-solution alloys between the electrical conductivity, κ, and the temperature coefficient, α, as expressed by the equation:

$$\kappa = \alpha\beta$$

where β is constant for the solvent metal and $\alpha = \frac{\Delta R}{\Delta t R_o}$ per °C.

It has long been known that the electrical conductivity at a given temperature and the temperature coefficient of resistance of binary alloys are related to their constitution by the LeChatelier-Guertler rules, as illustrated by Figs. 1 and 2:

Rule 1—In alloy systems consisting of a heterogeneous mixture of two phases, the electrical conductivity and temperature coefficient vary as a straight line, if the composition of the alloys is given in volume percentage, Fig. 1.

Rule 2—In solid solutions, the electrical conductivity and temperature coefficient are always lower than those of the solvent metal, and usually a considerable decrease occurs with the first small percentage additions of the solute metal, Fig. 2b. If the two components form a continuous series of solid solutions, the electrical conductivity and temperature coefficient curves take the form of a U-curve, Fig. 2a.

That some kind of proportionality exists between electrical conductivity and temperature coefficient of resistance is implied by the LeChatelier-Guertler rules and by study of data such as those given by Smith and Palmer,[1] Fig. 3. Dellinger[2] in 1910 first recognized this relationship in a number of commercial copper wires, ranging in conductivity from 94 to 100.7 pct I.A.C.S. He gave the ratio of temperature coefficient to the percentage of conductivity as a constant, $C = 0.003939$. A year later, Lindeck[3] observed that the linear relationship was valid for a wider range of conductivity in "various sorts of copper," and concluded that the product of resistivity and temperature coefficient was $6.78 \times 10^{-6} \pm 1.5$ pct. Since then, this relationship seems to have been entirely ignored.

Conductivity-Temperature Coefficient Relationship

If the electrical conductivity of copper solid-solution alloys with phosphorus, silicon, arsenic, antimony, aluminum, nickel, manganese, and iron is plotted against the temperature coefficient of these alloys, the diagrams in Figs. 4 and 5 are obtained. Similar data were found with copper-rich solid solutions containing magnesium, cobalt, and titanium,[4] as shown in Fig. 6. In all cases, a linear relationship exists. The point representing the highest

M. HANSEN, Member AIME, is Chairman, W. R. JOHNSON is Research Metallurgist, and J. M. PARKS, Member AIME, is Supervisor of Welding Research, Metals Research Dept., Armour Research Foundation of Illinois Institute of Technology, Chicago.

Discussion on this paper, TP 3189E, may be sent, 2 copies, to AIME by April 1, 1952. Manuscript, July 12, 1951. New York Meeting, February 1952.

Fig. 1

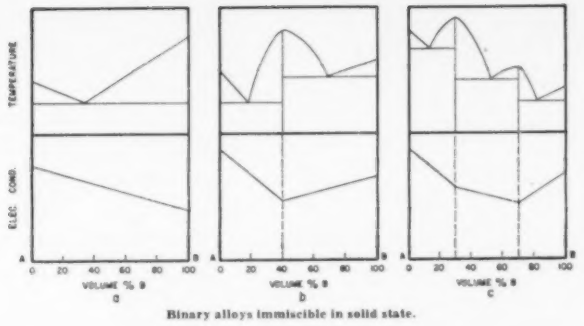

Binary alloys immiscible in solid state.

Fig. 2

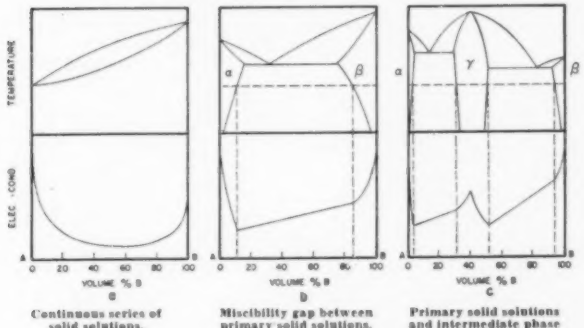

Continuous series of solid solutions.

Miscibility gap between primary solid solutions.

Primary solid solutions and intermediate phase of variable composition.

Figs. 1 and 2—Electrical conductivity of binary alloy vs. constitution.

conductivity and temperature coefficient is that of pure copper; as increasing percentages of solute elements are added, both the electrical conductivity and the temperature coefficient of resistance decrease along the straight line, until the solubility limit is reached. Beyond that composition, a deviation from the straight line results as illustrated by the Cu-P and Cu-Al data presented in Figs. 4 and 5.

If the low conductivity end of these plots is examined in detail, it may be seen that, in the case of the solid solutions with phosphorus, arsenic, and antimony, the extrapolated line almost intersects the origin of the plot. With Cu-Si and Cu-Al solid solutions, the straight line cuts the abscissa slightly to the right of the origin; whereas with Cu-Ni, Cu-Mn, and Cu-Fe, it cuts the abscissa to the left of the origin, nickel, manganese, and iron being transition elements. However, with all of these addition agents to copper, there is no appreciable deviation from the straight line conductivity vs. temperature coefficient of resistance relationship except for the low conductivity, low temperature coefficient range of Cu-Mn and Cu-Ni solid solutions. In Cu-Mn solid solutions, a negative temperature coefficient of resistance is reached between 4.5 and 9.5 pct Mn, Fig. 3.

Copper and nickel form a continuous series of solid solutions. According to Feussner and Lindeck,[11] the temperature coefficient becomes negative between 30 and 40 pct Ni and, with increasing nickel contents, positive again between 46 and 49 pct Ni. This finding agrees with that of Smith and Palmer, Fig. 3, who found that a negative temperature coefficient will be attained at about 33 pct Ni. On the

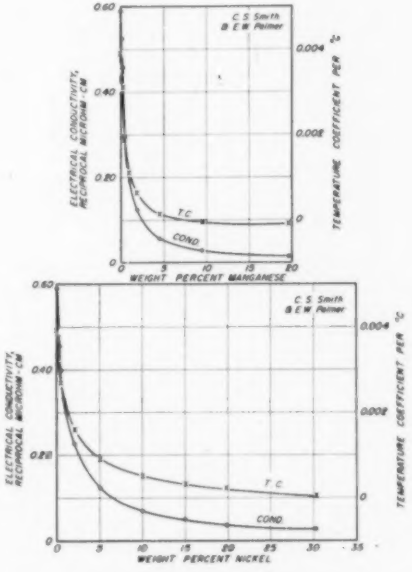

Fig. 3—Electrical conductivity and temperature coefficient of resistance of Cu-Mn and Cu-Ni solid solutions.

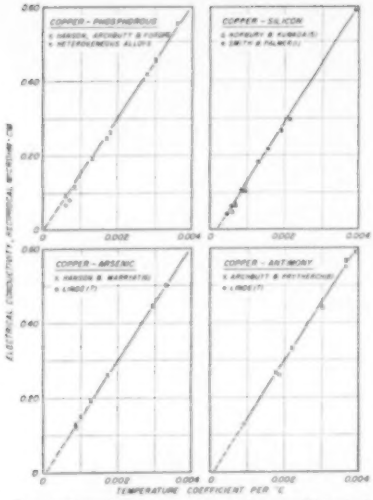

Fig. 4—Electrical conductivity vs. temperature coefficient of resistance of solid solutions of copper with phosphorus, silicon, arsenic, and antimony.

other hand, Krupkowski[14] found a negative temperature coefficient around 45 pct Ni. As the nickel content is increased further, the conductivity vs. temperature coefficient plot follows a curve which approaches the point representing pure nickel ($\kappa_{20°C} = 14.62$; $\alpha_{0-100°C} = 0.0069$).[14] As shown in Fig. 5, this curve is not a straight line, probably because alloys with more than 69 pct Ni are ferromagnetic at room temperature. The temperature coefficient curve for the Cu-Ni system, as determined by Krupkowski, shows a large deviation from the ideal U-curve in this composition range, which indicates that the temperature coefficient is considerably affected by the electronic transitions which produce ferromagnetism.

Fig. 6 summarizes the data on various copper-base solid solutions plotted on the same basis; it indicates a slight spread in the data for these alloys. This linear relationship also holds for ternary copper-base solid solutions, Fig. 7, as well as for silver-base and gold-base solid solutions, Figs. 8 and 9. Furthermore, all data available on solid-solution additions to other metals, such as aluminum, magnesium, zinc, platinum, palladium, tin, lead, molybdenum, and tungsten, indicate that this linear relationship is a fundamental property of solid-solution conductors.

It appears justified, therefore, to draw a conductivity vs. temperature coefficient of resistance curve for the various solvent metals, such as shown in Fig. 10. The slope, β, of each of these straight lines gives a constant which is a characteristic of the solvent metal, as indicated in Table I.

The capacity of each metal to form solid solutions with other metals, and their specific influence on the

Table I. Electrical Constants of Metals

Metal	Pure Metal Constants: κ_0 Reciprocal microhm-cm	Pure Metal Constants: α_0 per °C	Solvent Metal Constant: β value, °C per microhm-cm
Silver	0.629	0.00410	153
Copper	0.5896	0.00392	150
Gold	0.4502	0.00294	114
Aluminum	0.3766	0.00429	87.8
Magnesium	0.2243	0.0042	53.5
Zinc	0.169	0.00419	40.3
Platinum	0.0943	0.00393	24.0
Nickel	0.1462	0.0069	21.2
Tin	0.0870	0.00447	19.5
Iron	0.1030	0.00651	15.8
Lead	0.0484	0.004	12

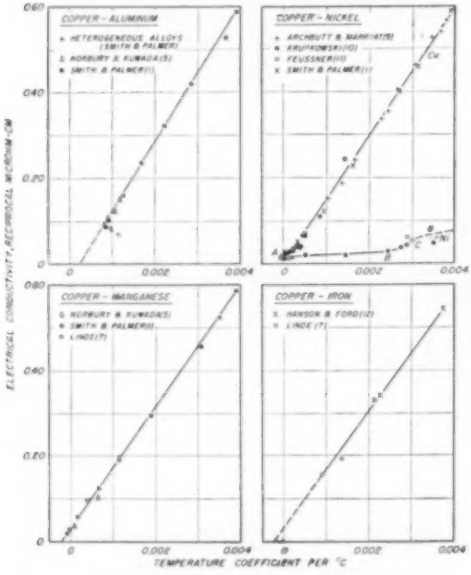

Fig. 5—Electrical conductivity vs. temperature coefficient of resistance of solid solutions of copper with aluminum, nickel, manganese and iron.

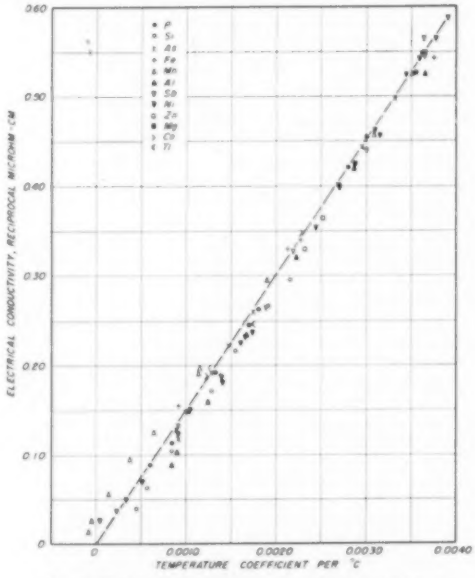

Fig. 6—Electrical conductivity vs. temperature coefficient of resistance of binary copper-base solid solutions.

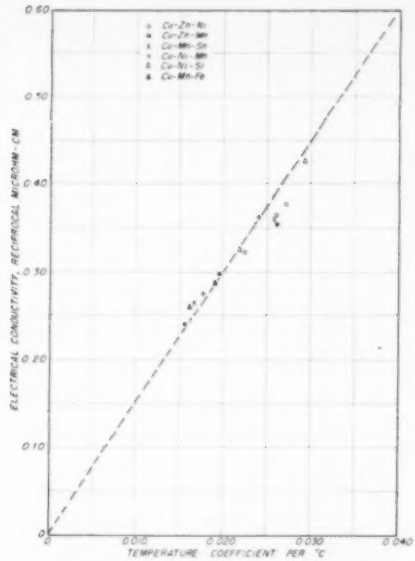

Fig. 7—Electrical conductivity vs. temperature coefficient of resistance of ternary copper-base solid solutions.

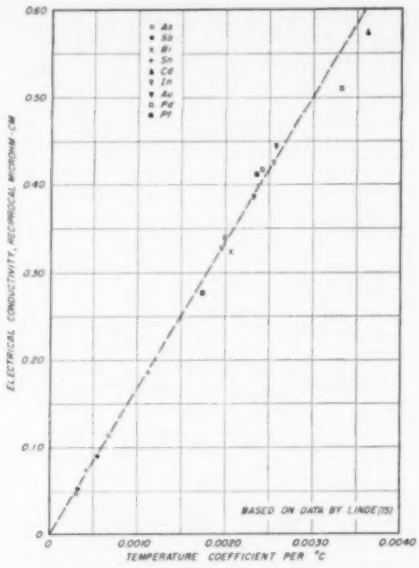

Fig. 8—Electrical conductivity vs. temperature coefficient of resistance of binary silver-base solid solutions.

electrical properties of the base metal determine how far the straight line for the respective binary, ternary, or more complex solid solutions extends from the point representing the pure solvent metal toward the point of origin of the diagram. The linear plots of Fig. 10 should be considered for approximate purposes only, especially in the low conductivity-low temperature coefficient range, as slight deviations occur for certain solute metals as indicated by Fig. 6. A slight deviation will also occur in solid solutions which undergo a magnetic transformation, as shown for the nickel-rich Cu-Ni solid solutions, Fig. 5.

The existence of the linear correlation between electrical conductivity and temperature coefficient of resistance of solid-solution alloys provides a simple means to predict, within certain limits, temperature coefficients of any single-phase alloy if the conductivity is known, and vice versa. Or if it is desired to achieve a certain electrical conductivity and corresponding temperature coefficient in a given base metal, a large number of alloying components may be used. For example, to achieve 60 pct of the conductivity of standard copper, and its corresponding temperature coefficient of 0.0023 per °C, the various elements listed in Table II can be added to copper in the percentages indicated. Or to obtain the same conductivity, and the corresponding temperature coefficient of 0.0021 per °C for a silver-base alloy, various elements in the percentages also given in Table II may be added to silver.

Table II. Composition of Copper-Base and Silver-Base Solid Solutions Having Conductivities of 60 Pct I.A.C.S. and Temperature Coefficients of 0.0023 and 0.0021 per °C, Respectively

Copper-Base Alloys, Wt Pct	Silver-Base Alloys, Wt Pct
0.075 P	0.12 As
0.14 Si	(0.2 Al)
0.15 Fe	0.21 Sb
0.20 As	0.33 Sn
0.33 Mn	0.35 Bi
0.39 Al	(0.4 Ag)
0.42 Sb	0.53 Pb
0.80 Sn	0.55 Mg
0.90 Ni	1.33 Zn
	4.0 Cd

Linear Relationship in Binary Systems

For binary systems with a continuous series of solid solutions, two straight lines are found when the conductivity is plotted against the temperature coefficient. Fig. 11 shows such diagrams for the systems

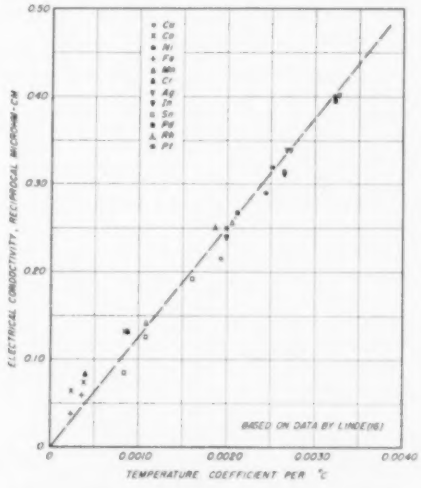

Fig. 9—Electrical conductivity vs. temperature coefficient of resistance of binary gold-base solid solutions.

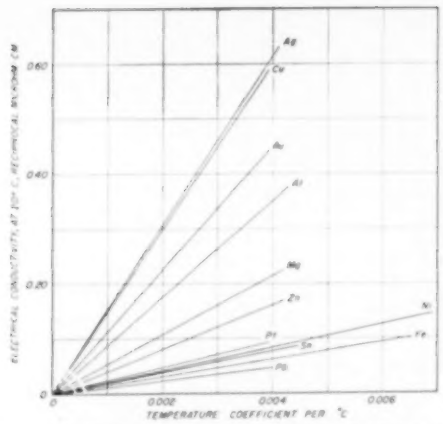

Fig. 10—Electrical conductivity vs. temperature coefficient of resistance of solid solution alloys with various elements as base metals.

Ag-Pd, Au-Pd, and Pd-Pt, based on the data given by Geibel.[12-13] The two branches of the Ag-Pd and Au-Pd alloys represent the conductivity vs. temperature coefficient plot of the silver-rich and gold-rich solid solutions, on one hand, and the palladium-rich solid solutions, on the other. The point of intersection represents—considering possible experimental errors—approximately 50 atomic pct; the actual atomic percentage of palladium of the alloys is indicated beside each point on the diagram. The lines representing the silver-rich and gold-rich solid solutions intersect very close to the origin, whereas the extrapolation of the line representing the palladium-rich solid solutions cuts the abscissa to the left of this point. This may be related to the fact that palladium is a transition metal. Both branches of the conductivity vs. temperature coefficient plot of Pd-Pt solid solutions practically coincide, since the conductivity and temperature coefficient of pure palladium and platinum are almost identical. Again, the lowest point of the plot is about 50 atomic pct.

For binary alloy systems in which the component metals are soluble in each other to a limited extent and do not form an intermediate phase, the conductivity-temperature coefficient diagram consists of two straight lines representing the electrical properties of the primary solid solutions and a third straight line joining the points representing the saturated solid solutions for each phase. This is illustrated in Fig. 12 by data for the Cu-Co[20] and Cu-Ag[21] systems.

Norbury and Kuwada Relationship

Norbury and Kuwada[3] tried to find a correlation between electrical resistivity and temperature coefficient of resistance of copper-base alloys. The temperature coefficient they used was defined as $\alpha' = \frac{\Delta R}{\Delta t}$, rather than as $\alpha = \frac{\Delta R}{\Delta t R_o}$, which is normally used. On the basis of resistivity measurements of copper alloys containing aluminum (up to 3.8 pct), tin (up to 3.9 pct), and silicon (up to 2.7 pct) at various temperatures between −191° and 438°C, they claimed that a linear relationship between resistivity at 0°C and $\alpha' = \frac{\Delta R}{\Delta t}$ (for that temperature range) exists, which may be expressed by the equation:

$$\alpha' = (0.0064 + R_o \times 0.0002) \text{ microhms-cm per °C} \quad [1]$$

Their data are shown in Fig. 13, together with those of some Cu-Ni and Cu-Mn solid solutions. The values for the latter do not follow the linear correlation, as their resistivity does not change linearly between −191° and 438°C.

In order to throw further light on Norbury and Kuwada's relationship, data obtained by other authors have been similarly evaluated. Fig. 14 shows resistivity vs. $\frac{\Delta R}{\Delta t}$ based on data by Smith and Palmer[5]; the $\frac{\Delta R}{\Delta t}$ values were calculated using resistivity values for 20°C and $\alpha = \frac{\Delta R}{\Delta t R_{20°C}}$ values determined from resistivity data at 200° and 20°C. It follows from Fig. 14 that the curves for Cu-Si and Cu-Al solid solutions deviate substantially from each other, and do not obey the relationship of eq 1. The solid solutions with the transition elements manganese and nickel behave very differently; with relatively low nickel contents, the $\frac{\Delta R}{\Delta t}$ values are

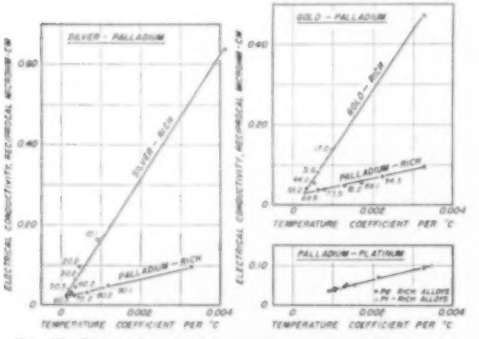

Fig. 11—Electrical conductivity vs. temperature coefficient of resistance diagrams of the systems Ag-Pd, Au-Pd, and Pd-Pt.

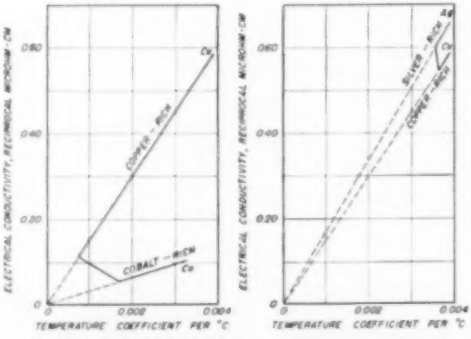

Fig. 12—Electrical conductivity vs. temperature coefficient of resistance diagrams of the systems Cu-Co and Cu-Ag.

somewhat larger, and above 20 pct Ni they become smaller, than that of pure copper.

In a similar way, data given by Linde[7] have been evaluated; the $\frac{\Delta R}{\Delta t}$ values were based on resistivities at $-183°$ and 0°C. The results for the solid solutions with arsenic and antimony did not obey Norbury and Kuwada's relationship. Again, the alloys with manganese, and also with iron, behave quite differently, although their temperature coefficient of resistance is constant between −183°C and room temperature.

In general, it can be said that eq 1 does not hold for all copper-base solid solutions, even if the transition elements are excluded as solvents. Hence, this relationship cannot be regarded as a means of predicting resistivity of copper-rich solid solutions if $\frac{\Delta R}{\Delta t}$ is known, and vice versa. On the other hand, the linear relationship between electrical conductivity and the temperature coefficient of $\alpha = \frac{\Delta R}{\Delta t R_o}$ essentially holds for all solid-solution alloys, regardless of the base metal.

Conclusions

1—A linear relationship has been found to exist between the electrical conductivity and temperature coefficient of resistance $\left(\alpha = \frac{\Delta R}{\Delta t R_o}\right)$ for all solid-solution components added to a given metal solvent.

2—Each solvent metal has its own distinctive β value—defined as the slope of the electrical conductivity-temperature coefficient of resistance plot.

3—Of the common metals, the β value is highest for silver, and progressively smaller for copper, gold, aluminum, magnesium, zinc, platinum, nickel, tin, iron, and lead.

4—Knowledge of this relationship permits quick approximation of the temperature coefficient of resistance of a solid-solution alloy by measurement of its conductivity, or vice versa.

Acknowledgments

The authors wish to thank the U. S. Signal Corps Engineering Laboratories, Fort Monmouth, N. J., for sponsoring this work and permitting publication of this paper—specifically, L. Reiss, V. Kublin, and E. Both. In addition, the authors acknowledge the assistance of E. Evaneskes in making some experimental determinations.

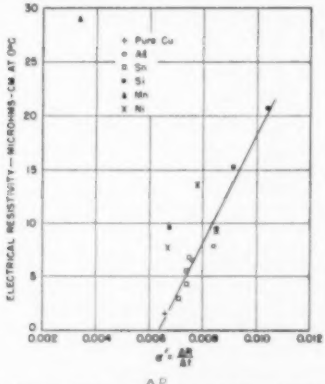

Fig. 13—Values of $\frac{\Delta R}{\Delta t}$ vs. resistivity at 0°C of solid solutions of copper with various elements (based on data by Norbury and Kuwada).

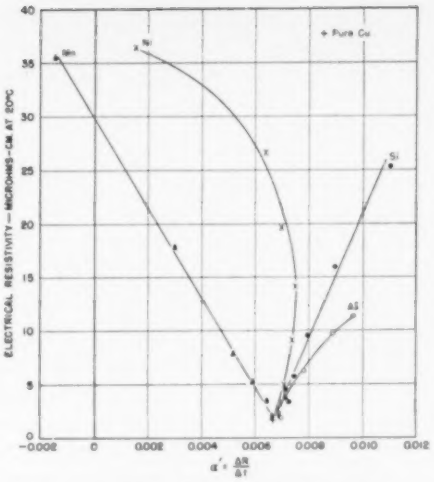

Fig. 14—Values of $\frac{\Delta R}{\Delta t}$ vs. resistivity at 20°C of solid solutions of copper with various elements (based on data by Smith and Palmer).

References

[1] C. S. Smith and E. W. Palmer: *Trans.* AIME (1935) **117**, p. 225.
[2] J. H. Dellinger: *Journal* Franklin Inst. (1910) **170**, pp. 213-216.
[3] S. Lindeck: *Verhandlungen der Deutschen Physikalischen Gesellschaft* (1911) **13**, pp. 65-71.
[4] D. Hanson, S. L. Archbutt, and G. W. Ford: *Journal* Inst. Metals (1930) **43**, pp. 41-72.
[5] A. L. Norbury and K. Kuwada: *Philosophical Magazine* (1927) **4**, pp. 1338-1341.
[6] D. Hanson and C. B. Marryat: *Journal* Inst. Metals (1927) **37**, pp. 121-168.
[7] J. O. Linde: *Ann. Physik* (1932) **15**, pp. 219-232.
[8] S. L. Archbutt and W. E. Prytherch: *Journal* Inst. Metals (1931) **45**, pp. 265-305.
[9] S. L. Archbutt and C. B. Marryat: see S. L. Archbutt and W. E. Prytherch, Effect of Impurities in Copper. London (1937) (Brit. Nonferrous Met. Res. Assn. Monograph No. 4).
[10] A. Krupkowski: *Rev. Métallurgie* (1929) **26**, pp. 131-153, 193-208.
[11] K. Feussner and S. Lindeck: *Wiss Abh. Physik.—techn. Reichsanstalt* (1895) **2**, pp. 503-516.
[12] D. Hanson and G. W. Ford: *Journal* Inst. Metals (1924) **32**, pp. 335-365.
[13] Unpublished work by the authors.
[14] *Metals Handbook*, 1948 Edition. A.S.M. Cleveland.
[15] J. O. Linde: *Ann. Physik* (1932) **14**, pp. 353-366.
[16] J. O. Linde: *Ann. Physik* (1931) **10**, pp. 52-70; (1932) **15**, pp. 233-237.
[17] W. Geibel: *Ztsch. anorg. Chem.* (1911) **70**, pp. 240-242.
[18] W. Geibel: *Ztsch. anorg. Chem.* (1911) **69**, pp. 43-46.
[19] W. Geibel: *Ztsch. anorg. Chem.* (1911) **70**, pp. 242-246.
[20] G. Reichardt: *Ann. Physik* (1901) **6**, p. 832.
[21] N. S. Kurnakow, N. Puschin, and N. Senkowski: *Ztsch. anorg. Chem.* (1910) **68**, pp. 123-140.

Metallurgical Mechanism for Mercury Stress Cracking Of Copper Alloys

by W. D. Robertson

SINCE the comprehensive paper of Moore, Beckinsale, and Mallinson,[1] little consideration has been given to the mechanism of mercury stress cracking of copper-base alloys, apart from extensive work on metallurgical and fabrication variables employing mercurous nitrate as an evaluation test. However, with the phase diagrams now available and the recent considerations of interfacial tension at grain boundaries, developed by Smith,[2] it appears that the elements of a detailed solution to the problem are available.

The facts that require explanation are:

1—Pure copper is not embrittled by mercury, with or without an applied or residual stress.

2—Cu-Zn and other copper-base alloys, in excess of some undefined solute concentration, are embrittled provided an external or residual stress is acting; cracking is not observed in the absence of stress.

3—The path of fracture is invariably intergranular.

4—Copper and copper-base alloys do not dissolve readily in mercury at room temperature.[1]

Consideration of the Cu-Hg phase diagram[3] shows that, at room temperature, solution of copper in mercury is probably limited by the formation on the surface of a microscopically thin layer of intermetallic compound, CuHg, having a very limited range of solubility which effectively restricts diffusion of copper and mercury. But, above 150°C (the highest peritectic temperature) copper solid solution is in equilibrium with a liquid Hg-Cu solution and, consequently, copper should dissolve freely in a large volume of mercury with the formation of an equilibrium dihedral angle at grain boundaries in contact with the liquid phase. Depending on the magnitude of this angle, mercury will or will not penetrate the solid phase along grain boundaries and spread over grain faces. Thus the measurement of the dihedral angle of grain boundaries in equilibrium with the liquid phase above 150°C should indicate whether copper is intrinsically resistant to embrittlement by mercury. In view of the fact that mercury is appreciably soluble in copper, it may also be anticipated that diffusion of mercury will take place at higher temperatures in the absence of the intermetallic compound and possibly at a more rapid rate along grain boundaries than through the grains, resulting in a Cu-Hg alloy of unknown properties.

In the case of brass, the ternary system Cu-Zn-Hg is involved and, from the resistance of brass to general solution in mercury at room temperature, it is probable that a compound of limited solubility range also exists, similar to the binary Cu-Hg system. Also, compared with copper, a change in the dihedral angle at grain boundaries in contact with mercury may be expected to result from the addition of zinc to copper. The preceding generalizations appear to be confirmed by the following experiments.

W. D. ROBERTSON, Member AIME, is associated with Hammond Metallurgical Laboratory, Yale University, New Haven, Conn.

Discussion on this paper, TP 3186E, may be sent, 2 copies, to AIME by April 1, 1952. Manuscript, July 11, 1951. New York Meeting, February 1952.

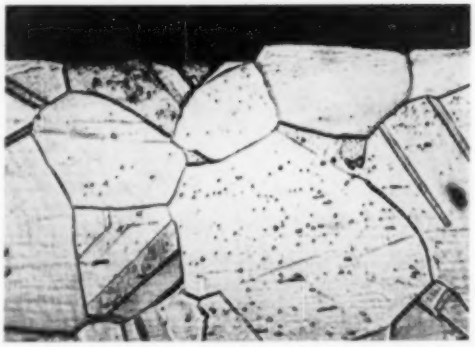

Fig. 1—Copper annealed at 700°C, immersed in mercury at 170°C. X300.

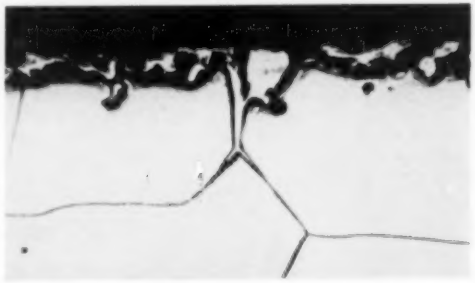

Fig. 2—Brass (69 pct Cu) annealed at 850°C, immersed unstressed in mercury at 350°C. X150.

Experimental Results

Oxygen-free copper wire, annealed at 700°C for 3 hr in copper foil, was immersed in mercury at 170°C, with and without an applied stress. After 24 hr immersion, specimens which were spring loaded to a nominal stress of 10,000 psi had not failed, and there was no apparent embrittlement as indicated by a 180° bend around a diameter approximately equal to the diameter of the wire (0.125 in.): General solution of the surface had taken place, indicated by a change in diameter of the wire, and the resulting structure of the surface is shown in Fig. 1. It is apparent that angles have developed at grain boundaries and examination at a high magnification indicates that the angle is in excess of 120°, completely excluding penetration of mercury. In view of the measurements made by Smith[2] on the

Cu-Pb system, it may be assumed that the dihedral angle does not vary greatly with temperature and, therefore, the value obtained at 170°C is applicable at room temperature. It may also be assumed that the applied stress will not appreciably affect the angle, and examination of both stressed and unstressed specimens indicates that the apparent angles are similar in both cases which is, in part, confirmed by the fact that none of the stressed specimens failed.

Brass sheet (69 pct Cu), after annealing at 850°C for 3 hr followed by slow cooling, was immersed, unstressed, in mercury at 170°C for 40 hr. A 90° bend at room temperature, after evaporation of the mercury at a low pressure, showed embrittlement at grain boundaries, but angles were not well developed and there was no significant general solution of the alloy. Consideration of the possible ternary system now involved indicated that a higher temperature might be required, and a second test was conducted, unstressed, at 350°C for 18 hr. Complete embrittlement resulted together with general solution of the brass. The microstructure, Fig. 2, reveals the cause of embrittlement. It is apparent that a layer of a second phase has formed, probably on cooling to room temperature, and the dihedral angle has changed from the large value characteristic of copper to something much less than 60° as a result of the addition of zinc to the alloy. Instead of the alloy dissolving in mercury with the formation of a large dihedral angle, extensive penetration of the grain boundaries by the phase present on the surface has taken place.

These experiments apparently lead to the following conclusions regarding the mechanism of stress cracking of copper-base alloys in mercury.

1—Copper is not susceptible to mercury cracking because the equilibrium dihedral angle formed at grain boundaries in contact with mercury is such that penetration is impossible.

2—Cu-Zn alloys, above some zinc concentration to be determined by quantitative measurement of the angles as a function of zinc concentration, may be embrittled by mercury because the dihedral angle formed by the solid solution and liquid mercury is less than 60° leading to penetration under equilibrium conditions and in the absence of an applied or residual stress.

3—At room temperature, equilibrium between brass and liquid mercury is not attained owing to the formation of an intermetallic compound which prevents continued penetration. If, however, an external or residual stress is present, the brittle compound formed at the surface is fractured allowing further contact of the alloy with mercury and continued penetration in accordance with the small dihedral angle.

Fig. 3 shows the initial stage in the fracturing of the brittle phase by bending the brass sheet after cooling to room temperature and evaporating mercury at a low pressure. Fig. 4 shows that a grain, which was surrounded at the higher temperature in the absence of stress, can be completely separated from the matrix by bending at room temperature. It is apparent that the path of fracture is through the brittle phase formed in the grain boundaries.

Thus the function of stress is apparently defined as a mechanical aid to the continued contact of the alloy with mercury. Basically, the problem is resolved in terms of the equilibrium dihedral angle. The limiting zinc concentration above which Cu-Zn alloys may be embrittled by mercury is, to a first approximation, defined by the alloy in which the dihedral angle is less than 60°; measurements are now being made to determine quantitatively the equilibrium angle as a function of zinc concentration and temperature.

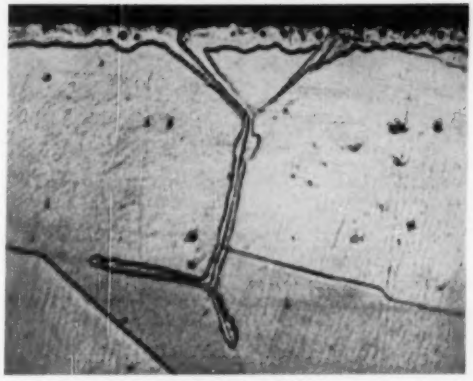

Fig. 3—Brass (69 pct Cu) annealed at 850°C, immersed unstressed in mercury at 350°C, and bent at room temperature after evaporation of mercury at a low pressure. Initial stage of fracture passing through brittle phase at grain boundaries.

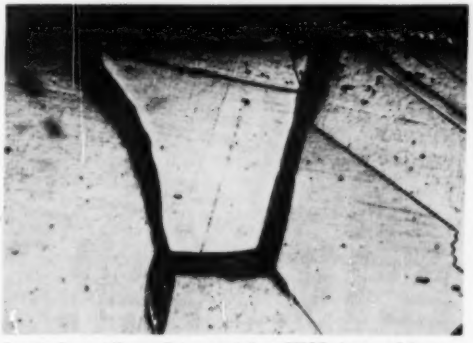

Fig. 4—Brass (69 pct Cu) annealed at 850°C, immersed in mercury at 350°C, and bent at room temperature after removal of mercury by evaporation at a low pressure. Final stage of fracture passing through brittle phase at grain boundaries.

Mercury stress cracking appears, therefore, as a problem in interfacial tension and intermetallic compounds, and no special properties of grain boundaries need be invoked, other than interfacial energy relationships and their dependence on alloying and orientation.

Acknowledgment

The author would like to express his appreciation to Arthur Phillips, Chairman of the Department of Metallurgy, for his interest and suggestions which have contributed to this work. Partial financial support of the Office of Naval Research under Contract NONR-305(00) is gratefully acknowledged.

References

[1] H. Moore, S. Beckinsale, and C. E. Mallinson: *Journal* Inst. Metals (1921) **25**, No. 1, p. 35.

[2] C. S. Smith: *Trans.* AIME (1948) **175**, p. 15; METALS TECHNOLOGY (June 1948).

[3] M. Hansen: *Der Aufbau der Zweistofflegierungen* (1936) Berlin. Julius Springer.

Rate of Evaporation of Zinc at Low Pressures

by H. W. St. Clair and M. J. Spendlove

An automatic surface-follower mechanism was used to measure the surface temperature and the rate of evaporation of molten zinc while undergoing distillation at low pressure. At pressures of 50 to 100 microns Hg, the rate of evaporation may be 60 to 80 pct of the theoretical maximum corresponding to the measured temperature. The rate decreases rapidly at pressures above 100 microns Hg, to only 7 pct of the theoretical maximum at 2000 microns Hg. Measured temperature gradients at the surface are in agreement with theoretical gradients calculated from the heat of vaporization, rate of evaporation, and thermal conductivity of molten zinc.

THIS paper covers a series of careful measurements of the rate of evaporation of molten zinc at low pressures, undertaken as a part of a general investigation on the separation of metals by distillation.[1] Preliminary results on the rate of evaporation of zinc were described in a previous publication.[2] The results of the preliminary study are as follows:

1—The observed rates of evaporation of zinc were as high as 0.60 g per sq cm per min, corresponding to 75 pct of the maximum rate as determined by the temperature of the metal.

2—The evaporation rate was decreased from 0.30 g per sq cm per min at a pressure of 25 microns to only 0.09 g per sq cm per min when the pressure was increased to 5 mm.

3—The temperature of the surface during rapid evaporation may be 35° to 100°C less than the main mass of metal. Observed temperature gradients at the surface are consistent with those calculated from the heat of vaporization and the thermal conductivity of liquid zinc.

In the preliminary experiments, the rate of evaporation was determined from the loss in weight of the metal in the crucible during the test. This was compared with the weight of the condensate. Obviously, this method was subject to error because of some uncertainty as to the period of evaporation that should correspond to the loss in weight. Furthermore, this method did not permit taking into account probable variations in the rate of evaporation during the test. A more serious shortcoming was that the temperature at the evaporating surface was not known, so the maximum theoretical rate of evaporation could not be calculated accurately.

To improve the precision of rate measurements and to allow accurate measurements of the surface temperature, a refined experimental technique was developed whereby the temperature and position of the surface could be measured accurately. This was done by an automatic surface-follower mechanism that gave a continuous record of the surface temperature and the amount of zinc evaporated. These data permitted an instantaneous determination of the actual rate of evaporation and the surface temperature throughout the test. Pure zinc (99.99 pct Zn) was used in all experiments.

Description of Distillation Furnace

The details of construction of the distillation furnace are shown in Fig. 1. The furnace is enclosed in a large quartz tube open at one end. The open end of the quartz tube is sealed by means of a water-cooled head. The entire enclosure is vacuum tight. The connection between the water-cooled head and the quartz tube is sealed by means of a rubber gasket which fits tightly against the smooth end of the tube. The metal is heated by induced current set up in the molten zinc and the walls of the graphite crucible by means of a water-cooled induction coil outside the quartz tube. High frequency current is passed through the induction coil from a 6 kw mer-

H. W. ST. CLAIR, Member AIME, is Metallurgist, U. S. Bureau of Mines, Washington, and M. J. SPENDLOVE, Associate Member AIME, is Electrical Engineer, Minerals-Technology Div., U. S. Bureau of Mines, College Park, Md.

Discussion on this paper, TP 3176D, may be sent, 2 copies, to AIME by Feb. 1, 1952. Manuscript, Feb. 19, 1951; revision, July 23, 1951. St. Louis Meeting, February 1951.

Papers by authors of the U. S. Bureau of Mines staff are not subject to copyright.

cury-spark-gap frequency converter. The enclosure is evacuated by means of a rotary vacuum pump connected to the water-cooled head by a 2 in. pipeline. The condenser projects inside the quartz tube and is supported above the crucible by two cooling-water tubes that connect the condenser cooling coil to the condenser flange. The condenser insert sleeve extends from the condenser into the annular groove in the top of the crucible wall to prevent the escape of zinc vapor from between the crucible and the condenser. The flange on the condenser assembly fits tightly against the flange section at the upper end of the head. Coupling between the two flanges is likewise sealed by a rubber gasket. The atmospheric pressure acting against the flanges is sufficient to insure a vacuum-tight system.

The temperature of the main mass of metal in the crucible is measured by a thermocouple that projects up through the rubber stopper at the bottom of the quartz tube into a thermocouple well in a reentrant dome at the bottom of the graphite crucible. Thermocouple wires in the base of the crucible are electrically shielded by the graphite crucible and the metal it contains. The surface-follower thermocouple wires are shielded by the water-cooled condenser. The absence of induction heating in the thermocouple wires was verified by measuring the melting point of zinc with power on the induction furnace and then observing the same temperature for the freezing point with the power turned off.

Pressure within the enclosure is measured by an ionization vacuum gage. A McLeod gage is used to verify all pressure-reading instruments at frequent intervals.

The zinc vapors evaporating from the surface of the molten metal rise to the water-cooled condenser, where they are collected on the cylindrical iron insert sleeves, which are removed from the condenser when the condensate is to be stripped.

Operation of the Follower Unit

To measure the surface temperature of the metal during the course of an evaporation experiment, a special surface-follower mechanism was designed. It is schematically illustrated in Fig. 2. The surface-follower mechanism is mounted on a base plate that fits against the water-cooled condensing head (6) shown in Fig. 1. The surface-follower electrode (16) is supported by a movable carriage (7). The carriage is raised and lowered by means of a pair of vertical screws driven by a dc motor through a reduction gear. The motor runs continuously and is coupled to the carriage mechanism by means of a magnetic clutch (3). The clutch is energized through a set of contacts on a low-voltage relay. At the instant the follower electrode touches the metal surface, the relay circuit is closed and contacts for the magnetic clutch are opened. The de-energized clutch then slips, and the downward motion of the carriage stops, leaving the electrode and the thermocouple exactly at the metal surface. The downward motion starts again when the surface of the metal is lowered sufficiently by evaporation so that electrical contact with the surface-follower electrode is broken. This mechanism permits the follower electrode to indicate the rate of evaporation of the metal very accurately. During an evaporation test, the magnetic clutch engages and disengages with great rapidity.

A thermocouple for measuring the surface temperature is mounted on the same carriage as the surface-follower electrode. The position of this

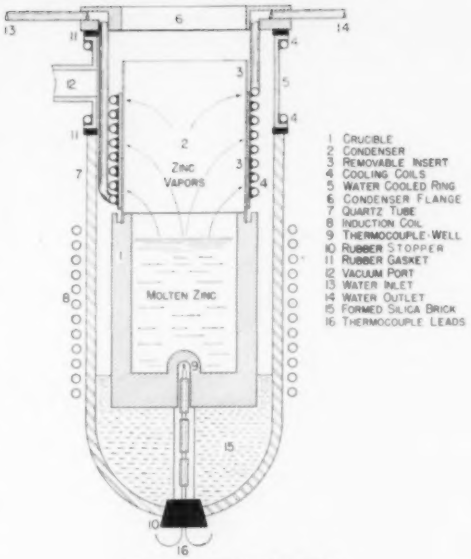

Fig. 1—Vacuum distillation unit.

thermocouple is adjusted carefully at the beginning of the test by means of the thumb screw (9). The wall thickness of the protection tube is made very thin at the closed end where the thermocouple junction is located. The temperature indicated by the thermocouple is quite sensitive to the relative position of the thermocouple tube. The indicated temperature increases as the thermocouple is immersed below the surface and decreases above the surface, but there is a marked discontinuity in the temperature gradient at the surface. This discontinuity serves to indicate the proper position for the thermocouple to give an accurate indication of the surface temperature. It was found that the tube was in

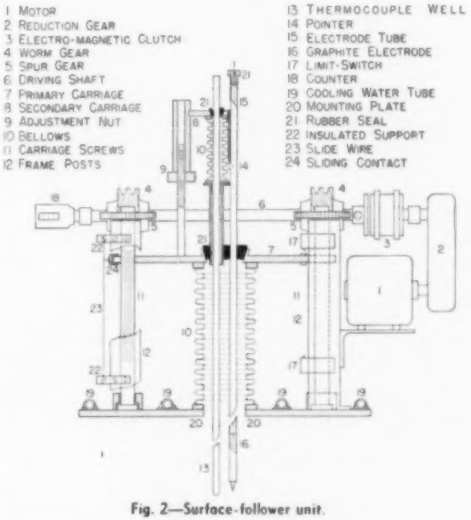

Fig. 2—Surface-follower unit.

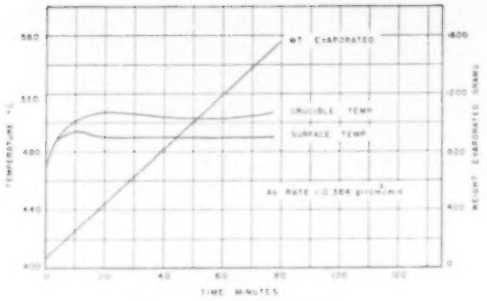

Fig. 3—Typical distillation test.

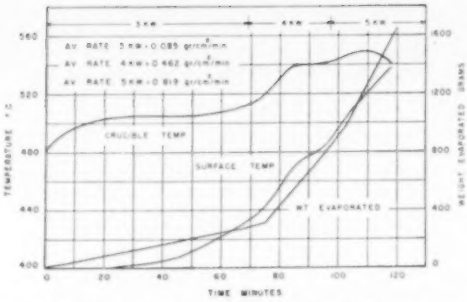

Fig. 4—Typical test on the distillation of zinc at different rates of evaporation.

proper position when the tip of the protection tube projected approximately 1 mm into the liquid metal. Preliminary sensitivity tests revealed that the probable maximum departure from this position is 0.019 cm. The thermocouple response to such a variation in depth of immersion is negligible.

Movement of the carriage is permitted by sylphon bellows soldered to the carriage and base plate. Another smaller bellows is provided for the thermocouple support. The thumb screw and small bellows permit movement of the surface thermocouple to determine the variation of temperature above and below the evaporating surface during a test.

The position of the follower electrode is indicated by a counter attached to the shaft of the screw mechanism. The position is also recorded automatically by means of a sliding contact (24) upon the carriage, which picks up a voltage from the potentiometer (23). A constant low voltage is applied to the ends of the wire (22). The potential of the sliding contact is linearly related to the distance the carriage is above the zero position. This voltage is recorded on the strip-chart potentiometer and is easily calibrated to read in terms of weight of metal evaporated. The slope of the voltage-time curve is therefore proportional to the rate of evaporation. More accurate determination of the surface displacement is obtained by the revolution counter on the main drive shaft. The automatic surface follower thereby provides a means for simultaneously determining the surface temperature and the rate of evaporation at any time during the test.

A complete description of the mechanical and electrical characteristics is beyond the scope of this paper, but a detailed discussion of these is presented elsewhere.[6]

Experimental Procedure

The general procedure followed in most of the evaporation tests was to evacuate the system to a pressure of the order of 25 microns and then raise the metal temperature to start evaporation. Evaporation begins shortly after the temperature exceeds the melting point. The follower electrode was lowered to the metal surface after the metal was completely melted but before appreciable evaporation had occurred. It was necessary to keep the electrode above the surface until after the metal was melted to avoid breaking the electrode tip on the solid metal when the electrode made contact.

In some experiments the metal was heated before evacuation. Evaporation was started by suddenly reducing the pressure in the system. In this way it was possible to obtain better control over the exact time at which evaporation started, but precautions had to be taken because of the sudden release of absorbed gas. The rapid evolution of the gas from the metal sometimes caused droplets of the metal to become entrained in the out-rushing gas and thereby were carried to the condenser by mechanical means rather than by true evaporation. Although the metal surface could not be observed visually in these experiments, the condition was determined by supplemental tests. A window section was put in the place of the follower unit and the metal surface was visually observed throughout the distillation period. Details of these observations are reported in another paper.[7] Early in the evaporating period a heavy film of fine material collects over most of the surface and then gradually disappears as the system comes up to temperature. The surface remains clean for the remainder of the test. Only slight turbulence of the zinc bath could be noted. The same conditions are assumed for experiments with the automatic surface follower.

Results of Distillation Experiments

The results of a typical distillation test are shown in Fig. 3, in which the weight of metal evaporated, the crucible temperature, and the temperature of the surface of the metal are represented graphically against the duration of the test. It will be observed that there is a fairly constant rate of evaporation even at the beginning of the test when the temperature has not quite risen to maximum. The crucible temperature rises sharply to about 500°C, after which it levels off and becomes fairly constant. The surface temperature is about 15° to 20° lower than the crucible temperature.

During this test, the loss in weight of the crucible amounted to 1542 g, as compared to 1523 g, the weight of the condensate collected in the condenser. The weight of zinc indicated by the counter on the surface-follower mechanism was 1544 g, which agreed very well with the loss in weight of the crucible. The average rate of evaporation for the entire test per unit area of surface of the metal exposed to low pressure amounted to 0.384 g per sq cm per min. These data are typical. The weight of zinc evaporated as indicated by the counter usually approximates very accurately the loss in weight of the crucible. Weight of the condensate is usually about 10 to 20 g less than the weight of metal evaporated. This small amount of zinc vapor is lost by diffusion to other parts of the evacuated enclosure.

In test 24, Fig. 4, evaporation was started at a

power input of 3 kw. During this time the rate of evaporation was fairly constant, even though the crucible temperature was rising at the beginning and near the end of this part of the test. After about 70 min, power was increased to 4 kw. Shortly afterward, the rate of evaporation increased rather abruptly. The crucible temperature likewise increased and leveled off at 540°C. After 30 min, the power was increased further to 5 kw, and again the rate of evaporation increased proportionally. Tests shown in Figs. 3 and 4 were made at a pressure of 15 to 20 microns.

The interesting fact brought out by this experiment is that the rate of evaporation is more definitely related to the power input than to the crucible temperature or the surface temperature as recorded by the thermocouple on the surface follower. The surface temperature, as shown in this experiment, is abnormally low throughout most of the test, and it is likely that it does not represent the average surface temperature.

Theory of Rate of Evaporation

The principal advantage of evaporation at reduced pressure is that high rates of evaporation are attained at relatively low temperatures. Evaporation at atmospheric pressure is retarded because the preponderance of gas molecules above the evaporating metal greatly impedes the diffusion of vapor molecules away from the surface. Under equilibrium conditions, such as exist when vapor-pressure measurements are made, the rate of evaporation from the molten metal is equal to the rate of condensation back onto the evaporating surface. The following expression has been derived from the effusion formula to express the theoretical maximum rate of evaporation into a perfect vacuum:[2]

$$W_o = p_o \alpha \sqrt{\frac{M}{2RT}} \qquad [1]$$

where M is the molecular weight; R, the gas constant; p_o, the vapor pressure at temperature T; and α, the coefficient of condensation. As the value of α is virtually unity for metals, the maximum rate of evaporation of zinc can be given by:

$$W_o = \frac{28.30\, p_o}{T^{1/2}} \qquad [2]$$

in which W_o is expressed in g per sq cm per min. This equation has been used to calculate the maximum rate of evaporation as given in this paper.

At very low pressures, the vapor molecules themselves offer the only impedance to the diffusion of vapor away from the surface. Their presence above the evaporating surface causes many molecular collisions, which cause some condensation back onto the surface. There is, however, a net rate of evaporation and recondensation. If, under these conditions, the partial pressure of the zinc vapor is p, the net rate of evaporation will be:

$$W = W_o \frac{28.30\, p}{T^{1/2}} \qquad [3]$$

which, combined with eq 2, gives:

$$W = \frac{28.30}{T^{1/2}} (p_o - p) \qquad [4]$$

Table I. Rate of Evaporation of Zinc at Various Pressures. Power 3.5 kw

Test No.	Pressure, Microns	Avg Surface Temperature, °C	Rates: G per Sq Cm per Min			Vapor Saturation,* $\frac{p}{p_o}$
			Max. W_o	Observed W	$\frac{W}{W_o}$	
1a	100	489	1.05	0.625	0.596	0.404
1b	300	496	1.24	0.625	0.504	0.496
1c	800	511	1.80	0.417	0.232	0.768
2a	100	494	0.93	0.768	0.826	0.174
2b	300	497	1.27	0.645	0.508	0.492
3a	1500	513	1.90	0.272	0.143	0.857
4a	500	498	1.27	0.385	0.303	0.697
4b	1000	524	2.45	0.253	0.104	0.896
4c	1500	537	3.45	0.123	0.036	0.964
5a	1000	457	0.46	0.336	0.730	0.260
5b	1500	511	1.80	0.320	0.178	0.822
5c	2000	525	2.50	0.177	0.071	0.929
6a	50	457	0.46	0.647		
6b	100	485	0.95	0.647	0.680	0.320
6c	500	485	0.95	0.444	0.468	0.532
6d	1000	487	1.00	0.251	0.251	0.749

* Vapor pressure of zinc for this calculation from U. S. Bureau of Mines, *Bull.* 383, p. 109.

As the observed rate of evaporation is W at a temperature for which the maximum rate of evaporation is W_o, it may be concluded that the zinc vapor is partly saturated. The degree of saturation represented by p/p_o is equal to:

$$p/p_o = 1 - W/W_o \qquad [5]$$

Variation of Evaporation Rate with Residual Gas Pressure

The rate of evaporation was measured for several tests in which the residual gas pressure was regulated at various assigned values while the power was held constant at 3.5 kw. The results of the tests are summarized in Table I. Variation of the observed rate of evaporation with respect to residual gas pressure is illustrated graphically by the solid line in Fig. 5. The rate of evaporation falls rapidly as the pressure is increased. A similar trend is shown by data obtained in previous experiments at lower rates of evaporation. These data are represented by the two dotted lines, representing evaporation at 1.9 and 1.2 kw, respectively.

The regulation of pressure at pressures of 100 microns or below was difficult because of the greater

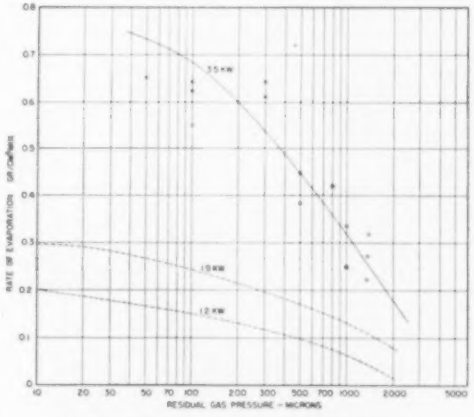

Fig. 5—Rate of evaporation vs. residual gas pressure.

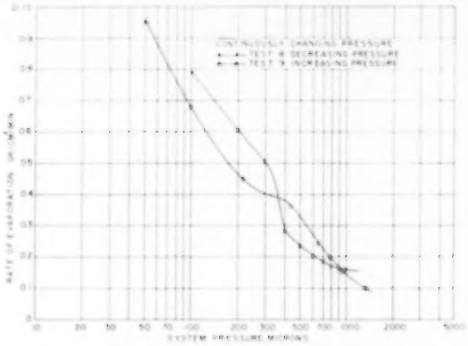

Fig. 6—Rate of evaporation in relation to continuously changing residual gas pressure.

time required for the vacuum pump to reduce the pressure, if it should momentarily be allowed to become too high. Therefore, no attempt was made to regulate the pressure below 100 microns. However, the rate of evaporation at 50 to 100 microns is of the order of 60 to 80 pct of the maximum rate, so that reducing the residual gas pressure below 100 microns will have much less effect than a corresponding decrease at higher pressures. It should be pointed out that the residual gas pressure as measured by the vacuum gage does not represent either the total gas pressure or the partial pressure of the residual gas at the evaporating surface. The partial pressure of the zinc may be many times the residual gas pressure. Furthermore, the partial pressure of the residual gas at the metal surface may be many times less than that in the condenser, because the evaporating zinc vapor sweeps the permanent gas molecules away. In other words, the evaporating zinc vapor has the same effect as mercury vapor in a diffusion pump.

At lower pressures there is greater freedom for effusion of vapors away from the molten metal surface, and the observed rate of evaporation becomes correspondingly nearer the calculated maximum rate as determined from the measured surface temperature. A comparison of the observed and maximum rate of evaporation is given in Table I under the heading W/W_m. In one instance the observed rate of evaporation is about 83 pct of the maximum at 100 microns. At 2000 microns it is about 7 pct of the maximum. The theoretical maximum rate of evaporation cannot be reached at high rates of evaporation even at extremely low pressures, because the greater concentration of vapor molecules above the surface will partly obstruct the flow of other vapor molecules from the surface.

The effect of an increase in pressure of the residual gas in the system is to impede the diffusion of molecules of zinc vapor away from the surface, thereby increasing the partial pressure of zinc. The degree of saturation of the zinc vapor at the surface may be calculated from the observed rate of evaporation and the maximum rate corresponding to the surface temperature as shown in eq 5. The saturation as thus determined was as low as 17 pct at 100 microns pressure but increased to 96 pct at 2000 microns.

Two experiments were run in which the rate of evaporation was measured while the residual gas pressure was being continuously increased or decreased. In experiment 8, the pressure was gradually reduced at a uniform rate from 1000 to 100 microns. In experiment 9, the pressure was increased in the same manner at approximately the same rate from 50 to 1500 microns. These pressure adjustments were made by manually manipulating vacuum valves to throttle the vacuum pump. A careful record of the pressure measurements was kept throughout each test. Rates of evaporation corresponding to many different pressure measurements were calculated for each experiment. Two values for the rate of evaporation were thus obtained for each pressure. These data are represented graphically in Fig. 6.

In both experiments, an anomalous change in rate of evaporation occurs at pressures in the range of 300 to 400 microns. There is a sudden rise in the observed rate when the pressure decreases through this range, and the rate becomes more nearly constant when the pressure is increased through this range. No satisfactory explanation for this phenomenon has yet been determined.

The temperature decreased gradually from 489° to 447°C in test 8 and increased from 447° to 482°C in test 9. Temperature variations for the two tests are so nearly identical that curves are omitted for reasons of simplicity.

A series of tests was made to observe the rate of evaporation at several different power levels. These tests were continued for relatively long periods. The results are presented in Table II.

These data show that the total weight of the metal evaporated can be measured rather accurately by the surface-follower mechanism, the greatest error being about 2 pct in test 23. The relation between total power and the rate of evaporation is illustrated graphically in Fig. 7. It shows the total power required to evaporate at the observed rate. The curve is extrapolated to zero rate of evaporation and indicates that about 1.5 kw is needed to hold the system temperature at a point where evaporation starts. The power required for vaporization of zinc at the observed average rate of evaporation also is shown. The difference between the two curves represents the power losses.

It has been stated previously that starting evaporation by suddenly reducing the gas pressure above the molten metal is likely to result in an apparent rate of evaporation that is higher than the true rate would be. This is brought about by the rapid escape of absorbed gas, which carries droplets of metal from the molten surface into the condenser, where it solidifies as though it had actually been evaporated. Only five such tests were considered to give dependable rates of evaporation. Averages of the results for these five tests are as follows: The theoretical maximum rate of evaporation was 1.77 g per

Table II. Rate of Evaporation of Zn in Relation to Power

Number	Zn Evaporated from Crucible, G	Zn Condensate, G	Zn Accounted for by Level Difference	Power, Kw	Avg Rate of Evaporation, G per Sq Cm per Min
19	1542	1523	1544	3.0	0.384
20	1629	1610	1632	4.75	0.706
21	1910	1905	1933	4.0	0.419
22	1276	1264	1254	3.0	0.230
23	1927	1907	1975	4.0	0.370
				5.0	0.634
24	2186	2173	2185	3.0	0.085
				4.0	0.462
				5.0	0.819

sq cm per min, and the observed rate was 0.577 g per sq cm per min, or 35 pct of the maximum. The average residual gas pressure was about 50 microns, and the zinc vapor near the surface was about 66 pct saturated.

Temperature Gradient Near the Surface

The temperature of the metal at the surface, where evaporation is taking place, may be much cooler than the temperature of the main body of metal, as indicated by the crucible temperature. The difference between the crucible and surface temperatures is illustrated in Figs. 3 and 4. The difference is due to the cooling effect of rapid evaporation. The heat required to evaporate 1 g of zinc at 500°C is about 440 cal. The thermal conductivity of liquid zinc is 0.138 cal per sq cm per cm per sec per °C.[4] The temperature gradient required to evaporate W g of zinc per sq cm per min[2] is given by:

$$\frac{dt}{dx} = \frac{440\ W}{60 \times 0.138} = 53W \qquad [6]$$

This means that a temperature gradient of about 50°C per cm is required to evaporate zinc at a rate of 1 g per sq cm per min. The temperature distribution in the metal is determined by the flow of heat from the crucible walls and the adjacent metal where it is generated to the surface from which the metal is evaporated.

The surface-follower unit was used to measure the temperature gradient in the metal while evaporation was proceeding at a high rate. The follower automatically established the exact location of the surface as a reference while the thermocouple tube was manually adjusted. The results of this experiment are given in Fig. 8. The observed rate of evaporation as determined by the surface follower was 0.570 g per sq cm per min. The temperature

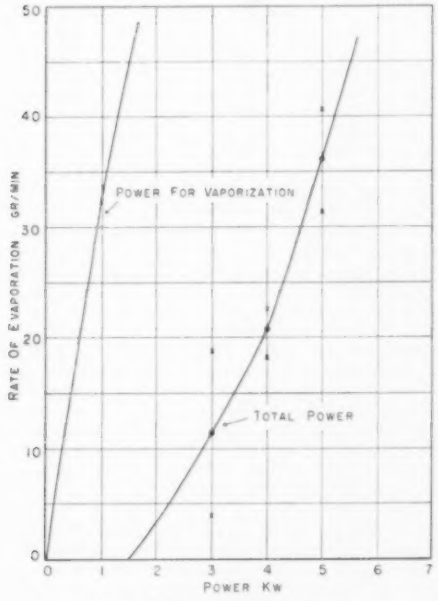

Fig. 7—Rate of evaporation vs. power.

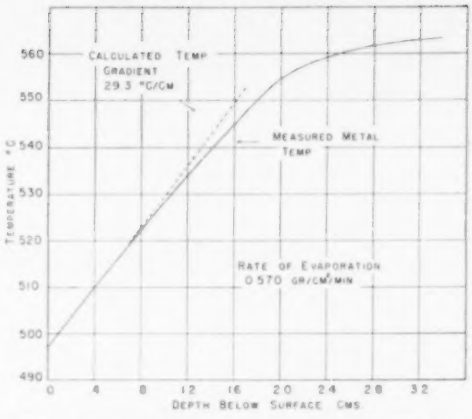

Fig. 8—Temperature distribution near surface of evaporating zinc.

of the metal at the surface was 497°C, for which the thermal conductivity is 0.1381 (cal per sq cm per cm per sec per °C). The calculated temperature gradient necessary to evaporate zinc at the observed rate would therefore be 29.3°C per cm. It will be observed that this value is in very close agreement with the measured gradient.

Previous gradient measurements[2] were made at lower rates of evaporation. At a rate of 0.264 g per sq cm per min, the gradient was calculated to be 13.85°C per cm, and it too was in fairly good agreement with the observed temperature distribution.

Summary and Conclusions

By means of an automatic surface-follower mechanism, careful measurements were made of the surface temperature and rate of evaporation of molten zinc while undergoing evaporation at a rapid rate at very low pressures. At pressures of 50 to 100 microns, the rate of evaporation may be 60 to 80 pct of the maximum theoretical rate. As the pressure of the residual gas increases above 100 microns, the rate decreases; at a pressure of 2000 microns the observed rate of evaporation was only 7 pct of the theoretical rate corresponding to the observed surface temperature.

The surface temperature during rapid evaporation is much lower than the average temperature of the metal because of the large amount of heat abstracted from the surface by the evaporating molecules. Measurements of the temperature gradient at the surface were in good agreement with the theoretical gradient calculated from the heat of vaporization, rate of evaporation, and thermal conductivity of molten zinc.

References

[1] M. J. Spendlove and H. W. St. Clair: Low Pressure Distillation of Zinc from Al-Zn Alloy. *Trans.* AIME (1949) **185**, pp. 553-560; JOURNAL OF METALS (September 1949).

[2] H. W. St. Clair and M. J. Spendlove: Rate of Evaporation of Zinc at Low Pressures. U. S. Bur. Mines *R. I.* 4710 (June 1950).

[3] H. W. St. Clair and M. J. Spendlove: An Automatic Surface Follower for Measuring the Rate of Evaporation of Molten Metals Undergoing Vacuum Distillation. Unpublished.

[4] N. Winter: *Reine Metall.* P. 432 (1939) Berlin. Julius Springer.

Vapor Pressures of Zinc Over AgZn Alloys

by E. E. Underwood and B. L. Averbach

The vapor pressure of zinc in equilibrium with solid β AgZn alloys has been measured by the dew-point method. The thermodynamic activities of silver, and the molar heats of formation have been calculated. Similar measurements have been made for the ternary alloys formed by adding gold to AgZn. An apparent particle size effect has been observed for AgZn filings. The vapor pressure of zinc over filings is 15 to 20 pct higher than over the solid alloys.

STATISTICAL methods have been used to interpret the thermodynamic activities of the components of a solid solution in terms of average equilibrium atomic configurations. In some cases, the atomic arrangements can be measured by X-ray methods, and the results are usually expressed in terms of short range order parameters. Only in the cases of Cu_3Au and AgAu have there been sufficient X-ray and thermodynamic data to verify the assumed correlation between the X-ray and the thermodynamic measurements. In Cu_3Au the agreement is good; negative deviations from Raoult's law are observed and the number of Cu-Au nearest neighbor pairs predicted on the basis of the thermodynamic treatments agrees quite well with the number of such pairs observed by the X-ray methods.

The β brass alloys present a different set of conditions. The ordering is so rapid in these alloys that the disordered state cannot be retained on quenching. In contrast, the disordered state in Cu_3Au is easily retained on quenching. On heating, the ordered β brass loses its long range order continuously as the critical temperature is approached; in Cu_3Au the order decreases slightly on heating and then drops discontinuously to zero at the critical temperature. These differences indicate that the short range order configurations in β brass systems may be of a different character than in Cu_3Au systems. However, X-ray measurements of local order cannot be made in the Cu-Zn alloys because of the similarity in scattering factors. The alloy AgZn is isomorphous with CuZn, however, and recent experiments have indicated that there is a good possibility of observing short range order in this system.

Another complication arises in the case of β AgZn. The disordered body-centered cubic structure exists above 280°C. On quenching from above this temperature an ordered structure of the cesium-chloride type is formed. On slow cooling, however, a complex hexagonal structure, the ζ phase, is produced; and if an ordered quenched alloy is reheated the ζ phase begins to form above 80°C. It is thus difficult to study local order by X-ray methods in single crystals of AgZn since the ζ phase formed on heating does not necessarily return to a single crystal of the original orientation. This problem has been met, however, by adding a few percent of gold to the AgZn. The gold suppresses the formation of the ζ

E. E. UNDERWOOD, Associate Member AIME, is Research Assistant, Dept. of Metallurgy, and B. L. AVERBACH, Member AIME, is Assistant Professor of Metallurgy, Massachusetts Institute of Technology, Cambridge, Mass.

Discussion on this paper, TP 3184E, may be sent, 2 copies, to AIME by April 1, 1952. Manuscript, July 3, 1951; revision, Aug. 24, 1951. New York Meeting, February 1952.

This paper represents a part of a thesis by E. E. Underwood submitted in partial fulfillment of the requirements for the degree of Master of Science to the Massachusetts Institute of Technology. This research program was sponsored in part by the Atomic Energy Commission under contract No. AT-30-1-GEN-368.

phase, without otherwise altering the structure, and this made it possible for Muldawer[1] to study the long range order in β AgZn as a function of temperature.

Local order measurements are being undertaken in the gold-bearing β AgZn alloys. In order to investigate the correlation between thermodynamic activities and short range order, the vapor pressures of zinc in equilibrium with various alloys of β AgZn and β AgZn plus Au were measured. These thermodynamic data are reported in this paper.

Several attempts have been made to detect the excess free energy associated with the formation of new surfaces. These experiments have, in general, been unsuccessful, and there has been no direct experimental verification of the Thompson equation which relates the practical size with the excess free energy. In this paper the vapor pressure of zinc in equilibrium with fine filings of β AgZn was measured and found to be measurably higher than the vapor pressure in equilibrium with a bulk sample of the same alloy. This excess vapor pressure was associated with the large local curvature present in the filings, although no experimental measurement of this local curvature was made.

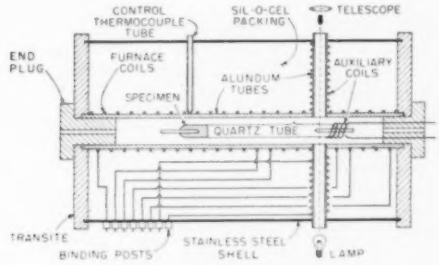

Fig. 1—Sketch of furnace cross-section.

Experimental Method

The Hargreaves[2] dew-point method was used to measure the vapor pressure of zinc over solid alloys. In this method an alloy is placed at one end of an evacuated clear quartz tube which has a deep thermocouple well at each end and a side arm for evacuation and sealing. The sample was a $\frac{3}{8}$ in. diam cylinder 1 1/16 in. long and contained a hole drilled into one end so that the sample could slip over the thermocouple well. The quartz tube was placed inside a tube furnace heated by three separately controlled resistance windings and so arranged that the end of the evacuated tube containing the alloy could be maintained at a constant temperature, T_h, while the temperature at the other end of the tube could be lowered to a selected temperature T_c. When T_c was below the dew point of the zinc vapor, droplets of liquid zinc were observed over the thermocouple well at the cold end, and the equilibrium value of T_c was taken as halfway between the closest temperatures of condensation and evaporation.

The furnace is shown schematically in Fig. 1 and a typical temperature gradient for this furnace is shown in Fig. 2. A small coil, independently controlled, was placed around the condensation end of the quartz tube for fine temperature control. The maximum fluctuation observed at the hot end of the tube was ±1°C. Chromel-alumel thermocouples,

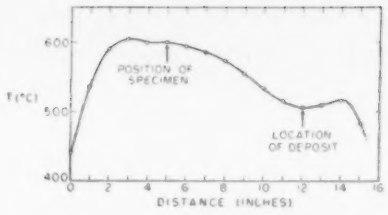

Fig. 2—Temperature gradient along furnace tube.

calibrated against a Bureau of Standards Pt-Pt-10 pct Rh thermocouple, were used.

The alloys were prepared from silver shot, more than 99.99 pct pure, and from zinc sticks of about 99.98 pct Zn; for the ternary alloys, gold of 99.96 pct purity was added. Melts were made in a graphite crucible in an induction furnace, and the crucible and melt were quenched into water to minimize segregation. The ingot was machined to a $\frac{3}{4}$ in. diam cylinder and annealed in an evacuated tube at 640°C for several days. The $\frac{3}{8}$ in. diam specimen was then prepared, thoroughly degreased, and sealed into the clear quartz tube.

Each specimen was held at temperature overnight in the quartz tube and observations were started on the following morning by lowering the temperature at the opposite end of the furnace. After the first deposit of liquid zinc droplets was observed, the temperature of the droplets was raised until they evaporated, then lowered slowly until they reappeared. This process was repeated until the equilibrium temperature was determined. At the higher vapor pressures the dew point could be determined within ±1°C, but at lower pressures only within ±2°C. Chemical analyses of the specimens before and after the dew-point determinations agreed closely and indicated that a negligible amount of zinc had been lost during the measurements.

It is believed that dezincification of the alloy surfaces did not occur to any noticeable extent. The vapor pressure measurements were performed at relatively high temperatures where the diffusion

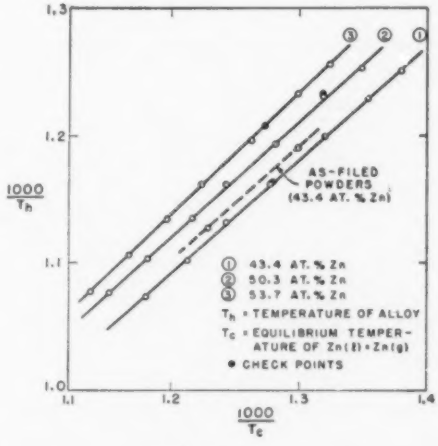

Fig. 3—Plot of $\frac{1}{T_h}$ vs. $\frac{1}{T_c}$ for binary alloys.

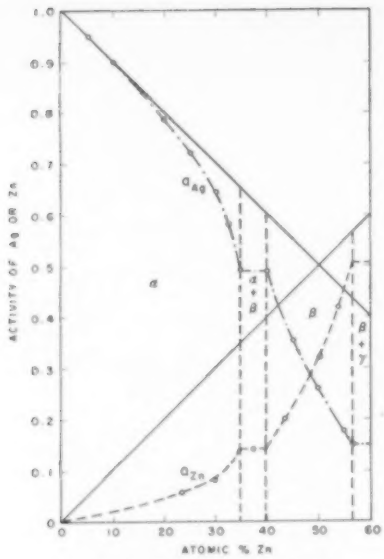

Fig. 4—Activities of silver and zinc in Ag-Zn alloys at 620°C. Activity of zinc referred to liquid zinc.

rates are quite large. In a closed system where no zinc is lost to the atmosphere, it would be expected that a steady state would be reached rather quickly and the specimen would attain a uniform composition.

The vapor pressure measurements were made on each sample at a series of temperatures. The experimental points shown in Fig. 3 were not taken in sequence and no systematic deviations of vapor pressure were noted during the long periods of time (10 to 14 days) during which the specimens were at temperature. Furthermore, the amount of zinc in the vapor phase is negligibly small. At the highest pressures encountered, about 0.001 g Zn would be in the vapor phase, while the weight of the sample was about 12 g.

In addition, check runs were made later with the same specimens, and the confirmation of the original data was quite satisfactory, see Fig. 3. Table I shows that the vapor pressures of zinc over the bulk alloys were the same, within experimental error, as those over the corresponding preheated powders. This would not be expected if dezincification had occurred. Finally, a comparison of the dew-point method for measuring vapor pressures over α Cu-Zn alloys[2] with the absorption spectra method,[9] the weighing method,[10] and the carrier-gas method[11] shows the dew-point method to good advantage.

A one degree error in T_s was found to introduce a relative error of 2.5 pct in the activity of zinc. Deviations in chemical analyses averaged between 1 to 2 pct and the overall error was estimated at 5 to 10 pct.

Experimental Results

The experimental values may be checked quickly for consistency by plotting $\frac{1}{T_b}$ vs. $\frac{1}{T_s}$. If the vapor pressure throughout the tube is considered to be the same, the Clausius-Clapeyron equation for each end may be written as:

$$\ln p = \frac{-\Delta H_v}{RT_b} + C = \frac{-\Delta H_v^\circ}{RT_s} + C' \qquad [1]$$

where p is the zinc vapor pressure within the tube; ΔH_v and ΔH_v° are the heats of vaporization of zinc from the alloy and from pure liquid zinc, respectively; R, the gas constant; and C and C', the integration constants. If ΔH_v, ΔH_v°, C, and C' are taken as independent of temperature:

$$\frac{1}{T_b} = K \cdot \frac{1}{T_s} + K' \qquad [2]$$

Fig. 3 shows such a plot of the experimental temperatures with the best straight lines determined by the method of least squares. The vapor pressures for pure zinc were obtained from the equations of Kelley.[8] The activities and activity coefficients of zinc with respect to liquid zinc are listed in Table I. The activities of silver at three temperatures were calculated by means of the Gibbs-Duhem equation. The activities for zinc and silver at 620°C are shown in Fig. 4, and the activities of zinc are indicated on the Ag-Zn equilibrium diagram in Fig. 5.

Birchenall and Cheng[4] obtained only one point within the β field and this is somewhat lower than the corresponding value obtained in this investigation. However, the vapor pressure of one alloy in the α region containing 31.3 atomic pct Zn was measured and showed good agreement with the Birchenall and Cheng data. These data, plus those of Schneider and Schmid[5] for liquid Ag-Zn alloys at 700°C, are shown in Fig. 6. The similarity to the data for solid alloys is quite striking. In order to compare the data for liquids with the data obtained in this research, the zinc activities for the solid alloys were extrapolated to the solidus at 700°C and compared with the corresponding value for the activity of the liquid in equilibrium with this composition. The activities (referred to liquid zinc) were 0.24 from the extrapolation of the solid values and 0.26 from the liquid data.

Partial molar heats of formation, relative to pure solid zinc or silver, were calculated for several com-

Table I. Activities of Zinc (referred to liquid zinc) in Various Alloys

	Temperatures, °C								
	500	520	540	560	580	600	620	640	660
Binary Alloys									
43.4 atomic pct Zn	0.145	0.154	0.163	0.173	0.182	0.192	0.202	0.211	0.221
50.3 atomic pct Zn	0.242	0.255	0.268	0.281	0.295	0.308	0.321	0.334	0.347
53.7 atomic pct Zn	0.361	0.371	0.381	0.390	0.399	0.408	0.417	0.425	0.434
Ternary Alloys									
43.9 atomic pct Zn (6.68 atomic pct Au)	0.131	0.140	0.149	0.158	0.166	0.175	0.185	0.194	0.204
47.8 atomic pct Zn (3.33 atomic pct Au)	0.167	0.176	0.187	0.196	0.208	0.217	0.227	0.238	0.249
Powders Filed and Preheated 2 days at 560°C									
43.4 atomic pct Zn				0.161	0.170	0.179	0.189	0.197	0.207
50.9 atomic pct Zn			0.270	0.282	0.295	0.305	0.318	0.330	0.342
53.4 atomic pct Zn			0.360	0.373	0.385	0.396	0.409	0.420	0.432
As-filed Binary Powders			567.9°C				613.8°C		
43.4 atomic pct Zn			0.204				0.236		

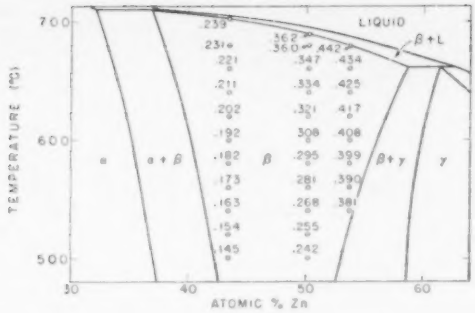

Fig. 5—Activities of zinc on the Ag-Zn equilibrium diagram, referred to liquid zinc.

positions in the β field from the slopes of the straight lines obtained by plotting ln a_{Zn} or ln a_{Ag} vs. $\frac{1}{T}$. The relative integral molar heat of formation at the composition AgZn was approximately −1880 cal per mol and the corresponding partial molar heats were $\Delta\overline{H}_{Zn} = -1590$ and $\Delta\overline{H}_{Ag} = -2170$ cal per mol.

Ternary Alloys: The addition of 3 atomic pct Au to β AgZn alloys is sufficient to suppress the formation of the ζ phase. The vapor pressure of zinc was measured for two alloys with 3.33 and 6.68 atomic pct Au and the data are summarized in Table I. The zinc vapor pressures of the two ternary alloys were less than those from corresponding binary Ag-Zn alloys at the same temperature. Schneider and Schmid[3] showed that the activities of zinc in liquid Au-Zn alloys were lower than in Ag-Zn alloys. Hargreaves[2] measured the zinc vapor pressures over solid Ni-Cu-Zn alloys and also found a decrease in vapor pressure in comparison with the Cu-Zn alloys.

Table II. Vapor Pressure of Zinc over β AgZn Filings 43.4 Atomic Pct Zn

Temperature, °C	Vapor Pressure of Zn Over Filings, p' (mm)	Vapor Pressure of Zn Over Bulk Alloy, p (mm)	$\frac{p'}{p}$
614	3.50	2.95	1.19
568	1.26	1.09	1.16

Powdered Alloys: Ag-Zn powders were prepared by filing from the same homogenized castings that were used to obtain specimens for the vapor pressure measurements. Clean files and a decreased vise were used, and iron fragments were removed with a permanent magnet. Only particles which would pass a 325 mesh screen were used. The powder was fed into one end of the cleaned quartz tube up to the point usually occupied by the solid specimens and packed as much as possible by tapping. After heating the as-filed particles, a light brown cloudy film appeared at the cold end of the tube but the liquid droplets could still be observed. Vapor pressure measurements were also made on filings which had been preheated at 560°C for two days. In these cases the brown film was not observed.

A significant increase in the vapor pressure was obtained over the as-filed powders in comparison with the bulk material. These differences have been summarized in Table II. The ratio of the zinc vapor pressure over the filings, p', to the pressure over the bulk alloys, p, is approximately 1.15 to 1.20.

According to the Thompson equation:

$$\ln \frac{p'}{p} = \frac{2\sigma \overline{V}}{RTr}$$

where σ is the specific surface free energy; $\overline{V}$, the partial molar volume; R, the gas constant; T, the temperature; and r, the effective radius of curvature. Assuming a value of 700 ergs per sq cm for σ at 800°K, the effective radius of curvature, r, is calculated to be approximately 0.03 microns.

This effect can be explained in terms of the shapes of typical filings observed under the microscope. The filings contain many sharp, jagged edges and the net effect of such peaks could produce this increase in vapor pressure, provided that the effective radius of curvature was small enough and that the radius of curvature of the valleys was much larger. The valleys need not necessarily cancel the increase in pressure due to the peaks, unless the valleys had much the same (negative) radius of curvature. The sharp edges of the as-filed powders were found to be somewhat rounded off after the runs had been completed. However, it can be said that when sharp-edged particles were introduced into the furnace, higher vapor pressures resulted than when rounded particles were used initially.

The zinc vapor pressures of the filings preheated

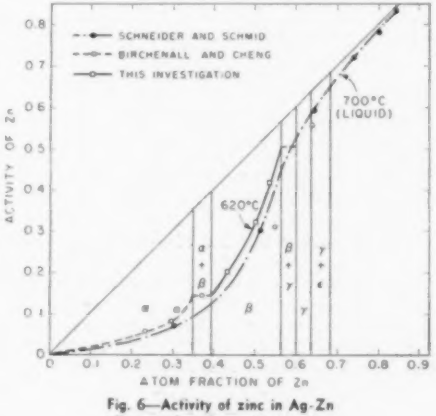

Fig. 6—Activity of zinc in Ag-Zn alloys, referred to liquid zinc.

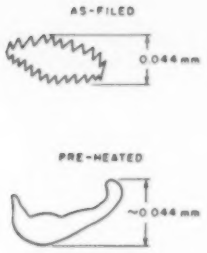

Fig. 7—Cross-sections of Ag-Zn filings.

for two days at 560°C were determined next. The activities of zinc for the preheated powders are essentially the same as those obtained for the corresponding bulk alloys and the values are listed in Table I. A metallographic examination of these preheated powders showed that the jagged edges had been rounded off approximately as shown in Fig. 7.

Neither powder showed any appreciable evidence of sintering as a result of the heating incidental to the vapor pressure measurements. Chemical analyses of the filings after the runs checked closely with the original analyses.

Discussion of Results

A correlation between the measured activity coefficients and the corresponding equilibrium atomic arrangement can only be made in an approximate fashion. As a starting point it may be assumed that the entropy of mixing for zinc and silver atoms in the body-centered cubic solution is ideal and the heat of mixing may be interpreted in terms of nearest neighbor interactions. For a regular solution it can be shown[8] that:

$$\frac{ZN_{av}(1-X_A)^2}{RT} = \ln \gamma_A \qquad [4]$$

where Z is the number of nearest neighbors, N_{av} Avogadro's number; X_A, the atomic fraction of component A; γ_A, the activity coefficient of component A; and $\nu = E_{AB} - \frac{1}{2}(E_{AA} + E_{BB})$, the interaction energy. This equation only applies to the case where the activity coefficients are referred to a pure metal A which has the same crystal structure as the alloy. However, in the β AgZn region, the activities of the zinc in the body-centered cubic alloy have been referred to the pure solid metal in the hexagonal close-packed form. A straightforward calculation of the interaction energy from the measured activity coefficients thus contains a structural contribution from the hypothetical phase change Zn(hexagonal close-packed) = Zn(body-centered cubic).

The activities for the 50.3 atomic pct Zn alloy were calculated with respect to solid zinc as a standard state and these values were used to evaluate ν. On plotting $\ln \gamma_{Zn}$ as a function of $\frac{1}{T}$ a straight line was obtained and the slope of this line gave a value of -790 cal per mol for N_{av}. Cowley[7] has derived an approximate relationship for β brass structures between the interaction energy ν and T_c, the critical temperature for long range order:

$$\frac{N_{av}}{R} = \frac{-T_c}{4} \qquad [5]$$

Recently the long range order was measured by Muldawer[1] in several ternary AgZn plus Au alloys. On extrapolating the critical temperatures to binary AgZn, a value of 270°C was obtained for T_c. This corresponds to -275 cal for N_{av}. The difference, -515 cal per mol, may be assigned to the hypothetical phase change Zn(hexagonal close-packed) = Zn(body-centered cubic). This value, however, cannot be verified experimentally.

It is difficult to reconcile the apparent higher vapor pressures observed over the filings in terms of a particle size effect alone. The 15 to 20 pct increase in vapor pressure corresponds to a local curvature of 0.03 microns, but the classical Thompson equation may not be valid for particles with such small radii of curvature. It is quite possible that surface contamination or the greatly disturbed surface due to the filing operation also contributed to the effect on vapor pressure.

Summary

The thermodynamic activities in three solid β AgZn alloys have been obtained over a temperature range of 500° to 660°C. The activities of silver and the molar heats of formation have been computed. Similar measurements have also been made for ternary AgZn-plus Au alloys.

An apparent particle size effect has been observed in the case of AgZn filings. The vapor pressures of zinc over -325 mesh filings were 15 to 20 pct higher than over solid alloys.

Acknowledgments

The chemical analyses were performed by W. M. Saunders and D. L. Guernsey. The advice and assistance of L. L. Seigle and D. A. Hay are also gratefully acknowledged.

References

[1] L. Muldawer: X-ray Measurement of Long Range Order in β-AgZn. *Journal of Applied Physics* (1951) **22**, p. 663.

[2] R. Hargreaves: The Vapour Pressure of Zinc in Brasses, *Journal* Inst. Metals (1939) **64**, p. 115.

[3] K. K. Kelley: Contributions to the Data on Theoretical Metallurgy. Bur. Mines *Bull.* 383, p. 108 (1935).

[4] C. E. Birchenall and C. H. Cheng: The Vapor Pressures of Zinc and Cadmium Over Some of Their Silver Alloys. *Trans.* AIME (1949) **185**, p. 428; JOURNAL OF METALS (July 1949).

[5] A. Schneider and H. Schmid: The Vapor Pressures of Zinc and Cadmium Over Their Binary Liquid Alloys with Copper, Silver and Gold. *Ztsch. Elektrochemie* (1942) **48**, p. 627.

[6] K. K. Kelley: Contributions to the Data on Theoretical Metallurgy. Bur. Mines *Bull.* 476, p. 192 (1949).

[7] J. M. Cowley: An Approximate Theory of Order in Alloys. *Physical Review* (1950) **77**, p. 669.

[8] C. Wagner: *Thermodynamik metallischer Mehrstoffsysteme* in *Handbuch der Metallphysik* edited by G. Masing, Vol. 1, Part 2, p. 31 (1940) Leipzig. Reproduced by J. W. Edwards, Edward Brothers, Inc., Ann Arbor, Mich.

[9] A. W. Herbenar, C. A. Siebert, and O. S. Duffendack: The Vapor Pressure and Thermodynamic Activities of Zinc in Solid Alpha Brasses. *Trans.* AIME, (1950) **188**, p. 323; JOURNAL OF METALS (February 1950).

[10] W. Seith and W. Krauss: Diffusion and Vapor Pressure of Zinc in Brass. *Ztsch. Elektrochemie* (1938) **44**, p. 98.

[11] K. Jellinek and G. A. Rosner: On the Vapor Pressures and Activities of a Volatile Component in Binary Metal Alloys at High Temperatures. *Ztsch. Physik. Chem., Abt. A*, (1931) **152**, p. 67.

Analytical Representation of Certain Phase Boundaries

by W. Rostoker

Using an expression for the free energy of a homogeneous phase as a function of composition, a relationship is derived which interrelates the phase boundaries extending from the allotropic transformation of the solvent metal. Comparisons between observed and calculated phase boundaries in the systems Fe-Ni, Fe-Mn, Fe-W, Ti-Mo, and Ti-Cb are presented.

IT is the purpose of this paper to illustrate how the general free energy equations for two phases in equilibrium may be used to derive an expression which interrelates the phase boundaries extending from the allotropic transformation of the solvent metal. The free energy per gram atom of a disordered solid solution may, for many purposes, be represented by the equation:[1]

$$F = \tfrac{1}{2}NZ\,[C \cdot V_{AA} + (1-C)\,V_{BB} + 2C\,(1-C)V] + K(T) + RT\,[C \cdot \ln C + (1-C)\ln(1-C)] \qquad [1]$$

where N is Avogadro's number; Z, the coordination number; C, the concentration of the solute element in atomic percent; the subscripts refer to concentrations at phase mixture boundaries; V_{AA}, V_{BB}, and V_{AB} are the bond energies between like and unlike adjacent atoms, respectively, at the interatomic spacing characteristic of the phase. The bond energies are usually assumed to be independent of small changes in the lattice parameter occasioned by solute additions and variations in temperature; $V = V_{AB} - \frac{V_{AA} + V_{BB}}{2}$; $K(T)$ is the sum of the heat content and heat entropy; R, the molar gas constant; and T, the temperature in degrees Kelvin.

The free energy of a homogeneous phase is therefore the sum of an internal energy, a specific heat, and a configurational entropy term, respectively. The compositions of two phases in equilibrium at a given temperature are governed by the minimum total free energy principle. Graphically, this is represented by the points of tangency of the tangent common to the free energy vs. concentration curves of the two phases.

Analytically, this may be expressed as:

$$\left(\frac{dF}{dc}\right)_\alpha = \left(\frac{dF}{dc}\right)_\beta \qquad [2]$$

Expanding both sides using eq 1, the following equation is obtained after convenient readjustment of the terms:

$$RT \ln \left[\left(\frac{C_\beta}{1-C_\beta}\right)\left(\frac{1-C_\alpha}{C_\alpha}\right)\right] = \tfrac{1}{2}N (V_{AA} - V_{BB})(Z_\alpha - Z_\beta) + NV [Z_\alpha(1-2C_\alpha) - Z_\beta(1-2C_\beta)] \qquad [3]$$

The following assumptions have been made at this point:

1—The specific heats of the two phases are independent of composition variations within the range under consideration. Accordingly, the $K(T)$ terms disappear on differentiation.

2—$(V_{AA})_\alpha = (V_{AA})_\beta$; $(V_{BB})_\alpha = (V_{BB})_\beta$; $V_\alpha = V_\beta$

The justification for these assumptions can lie only in the successful application of the resultant equation. It may be noted that Zener[2] has used assumption 1 in the calculation of the boundaries limiting the $(\alpha+\beta)$ phase mixture in the Cu-Zn system.

W. ROSTOKER is associated with the Metals Research Dept., Armour Research Foundation and is Assistant Professor of Metallurgical Engineering, Illinois Institute of Technology, Chicago.

Discussion on this paper, TP 3183E, may be sent, 2 copies, to AIME by April 1, 1952. Manuscript, July 2, 1951. New York Meeting, February 1952.

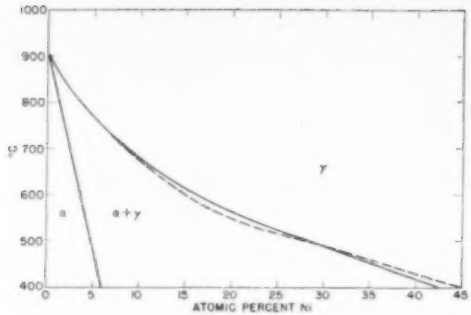

Fig. 1—Calculated, dashed line, and observed,[2] solid line, boundaries in the Fe-Ni system.

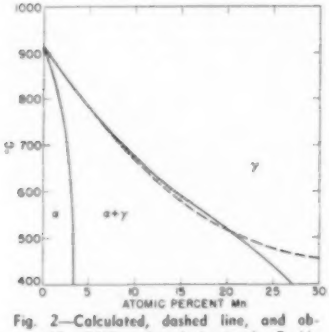

Fig. 2—Calculated, dashed line, and observed,[6] solid line, boundaries in the Fe-Mn system.

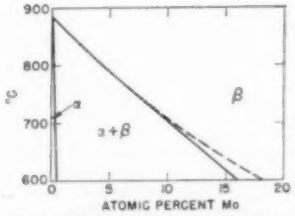

Fig. 3—Calculated, dashed line, and observed,[7] solid line, boundaries in the Ti-Mo system.

Eq 3 may be reduced to a more simplified form:

$$RT \ln \left[\left(\frac{C_\alpha}{1-C_\alpha}\right)\left(\frac{1-C_\gamma}{C_\gamma}\right)\right] = K_1[Z_\alpha - Z_\gamma] + K_2[Z_\alpha(1-2C_\alpha) - Z_\gamma(1-2C_\gamma)] \quad [4]$$

where $K_1 = \frac{1}{2}N(V_{AA}-V_{BB})$ and $K_2 = NV$. The values of the constants may be calculated from reliable data for C_α, C_γ at two temperatures. Eq 4 has been applied to several cases of phase mixture boundaries extending from the allotropic transformations of pure iron. Recent work on certain titanium-rich systems has permitted additional interesting examinations of the above relationship.

In the Fe-Ni system, the composition of the rejected α phase is isothermally invariant with time and consequently the accurate experimental location of the $\alpha/(\alpha+\gamma)$ boundary is much less difficult than the corresponding $(\alpha+\gamma)/\gamma$ boundary of the phase mixture. Using the data for the $\alpha/(\alpha+\gamma)$ boundary and two reliable values of $C_\gamma(T)$, the whole $(\alpha+\gamma)/\gamma$ boundary may be calculated by successive graphical solutions of eq 4.

The calculation for the Fe-Ni system may be summarized as follows: Using data from Owen and Sully,[2] constants K_1 and K_2 were evaluated as $K_1 = 703$ and $K_2 = 140$. Eq 4 becomes (since $Z_\alpha = 8$ and $Z_\gamma = 12$):

$$RT \ln \left[\left(\frac{C_\gamma}{1-C_\gamma}\right)\left(\frac{1-C_\alpha}{C_\alpha}\right)\right] = 2248 + 1128 [3C_\gamma - 2C_\alpha]$$

The value of C_γ corresponding to a given C_α may be found from the intersection of curves of:

$$RT \ln \left[\left(\frac{C_\gamma}{1-C_\gamma}\right)\left(\frac{1-C_\alpha}{C_\alpha}\right)\right] \text{ vs. } C_\gamma$$

$$2248 + 1128\,[3C_\gamma - 2C_\alpha] \text{ vs. } C_\gamma$$

Fig. 1 shows a good agreement between calculated and experimental boundaries.

Similar calculations have been applied to the same type of phase boundaries found in the systems Fe-Mn, Ti-Mo, and Ti-Cb. The results are graphically represented in Figs. 2, 3, and 4, respectively. Fig. 5 shows that the same treatment may be applied to the closed γ loop of the Fe-W system. The constants for the equations are summarized in Table I. It will be seen that the assumptions regarding the independence from composition of certain free

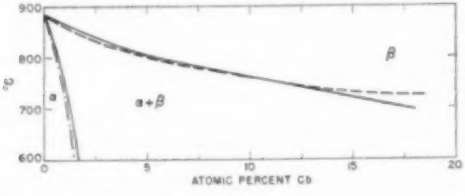

Fig. 4—Calculated, dashed line, adjusted, dash-dot line, and observed,[8] solid line, boundaries in the Ti-Cb system.

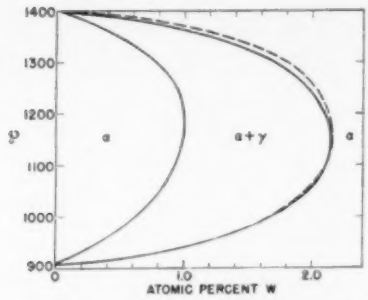

Fig. 5—Calculated, dashed line, and observed,[7] solid line, boundaries in the Fe-W system.

energy terms is valid in several cases for solute concentrations of as much as 30 atomic pct.

A useful application of this analytical method arose in the study of the phase boundaries for the titanium-rich Ti-Cb system. The $\alpha/(\alpha+\beta)$ boundary was first drawn as the best fit between brackets established by micrographic analysis at various temperatures. Using points from this boundary to calculate the $(\alpha+\beta)/\beta$ boundary yielded results widely divergent from the experimental work. By trial and error, it was found that a reasonable corroboration could be obtained if the $\alpha/(\alpha+\beta)$ boundary was redrawn in a new position which also lay within the confines of the brackets imposed by the data. It is suggested that eq 4 may be applied to experimental phase boundaries as a check of self-consistency.

It will be noted that the constant K_1 is represented as the difference between two terms which embody the molar cohesive energies of the pure components divided each by the coordination number. Using published data for molar cohesive energies[4] and the coordination number of the high temperature allotropic modification, calculated values for K_1 are presented in Table I for comparison with the observed values. For example, the calculation of K_1 for the Fe-Ni system proceeds as follows:

$$K_1 = \frac{1}{2} N(V_{Fe\text{-}Fe} - V_{Ni\text{-}Ni}) =$$

$$\left[\frac{\text{molar cohesive energy of Fe}}{12} - \frac{\text{molar cohesive energy of Ni}}{12} \right]$$

$$= \left[\frac{94000}{12} - \frac{85000}{12} \right]$$

$$= 750 \text{ cal}$$

The agreement in general is quite good, considering that no temperature corrections were made and that the published data pertains to cohesive energies at

Table I. Summary of Constants

System	K_1	K_2	K_1 (As Calculated from Eq 4)
Fe-Ni	+703	+140	+750
Fe-Mn	+1535	+257	+1670
Fe-W	−16,250	−9500	−18,410
Ti-Mo	+5085	−448	+7500
Ti-Cb	−4050	+2700	−4000

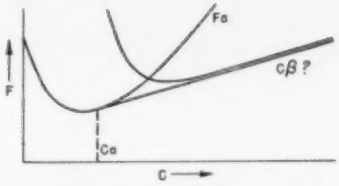

Fig. 6—Hypothetical free energy vs. concentration curves illustrating a possible origin of the indeterminate location of a phase boundary.

the interatomic spacings of the pure metals, rather than their acquired spacings in solid solution.

The calculated $(\alpha+\gamma)/\gamma$ boundary of the Fe-Ni system tends towards parallelism with the abscissa in the composition range which has always been the most difficult to study. The same effect may be noted in the cases of the Fe-Mn, Ti-Mo, and Ti-Cb systems (see Figs. 2, 3, and 4). This trend could be due to a breakdown of the assumptions upon which eq 4 are founded. On the other hand, the same effect could arise if the free energy vs. composition curve for the γ or β phase became approximately linear such that no unique tangent could be drawn. This is diagrammatically shown in Fig. 6. An examination of free energy data obtained by Kubaschewski and v. Goldbeck[8] indicate that this condition is possible.

There seems to be sufficient evidence that phase boundaries of the types considered can be represented by an equation derived from fundamental free energy relationships but involving certain ad hoc assumptions. An attempt to treat the $(\alpha+\beta)$ boundaries of the Cu-Zn system by the same method met with no success. This mention should serve to emphasize that eq 4 has limited application.

A much more elaborate development of this subject along classical thermodynamic lines has been published by Zener.[9] The writer feels justified in presenting this alternative treatment because of its greater simplicity and because the results, while not as widely applied, are at least as closely in agreement with experimental data.

Acknowledgment

This work was associated with a contract (Contract No. AF 33(038)-8708, E.O. No. 605-225) to the Armour Research Foundation from the Materials Laboratory, Engineering Division, Air Materiel Command, and is published with their permission. The writer wishes to express his appreciation to M. Hansen for stimulating discussions.

References

[1] A. H. Cottrell: *Theoretical Structural Metallurgy*. p. 154. Arnold.
[2] C. Zener: *Physical Review* (1947) **71**, p. 846.
[3] E. A. Owen and A. H. Sully: *Philosophical Magazine* (1939) **27**, p. 614.
[4] F. Seitz: *Modern Theory of Solids*: p. 3. New York. McGraw-Hill Book Co.
[5] O. Kubaschewski and O. v. Goldbeck: *Trans.* Faraday Soc. (1949) **XLV**, p. 948.
[6] A. R. Troiano and F. T. McGuire: *Trans.* A.S.M. (1943) **31**, p. 349.
[7] W. P. Sykes: *Trans.* AIME (1931) **95**, p. 307.
[8] M. Hansen, E. L. Kamen, H. D. Kessler, and D. J. McPherson: JOURNAL OF METALS (October 1951), *Trans.* AIME, p. 881.
[9] C. Zener: *Trans.* AIME (1946) **167**, p. 513.

Surface Tension of Solid Silver

by E. R. Funk, H. Udin, and J. Wulff

The surface tension of solid silver is measured by a refinement of the Udin, Shaler, and Wulff technique. The tests were made in a purified helium atmosphere at four different temperatures and various times. The average of the results is $\gamma = 1140 \pm 90$ dynes per cm for the range 875° to 932°C.

A SUCCESSFUL measurement of the surface tension of solid copper was reported by Udin, Shaler, and Wulff.[1] They performed experiments on copper held in vacuum within 100°C of the melting point. At these temperatures, the creep rate in 5 and 3 mil copper wires was sufficient to permit determination of a balance between the contractile force of surface tension and the extending force of small copper weights joined to the end of the wire specimens. By suspending a series of variously weighted specimens and measuring the change in a gage length during the test, the balancing applied load could be found. This point of zero strain is a measure of the surface tension. The mathematical formulation of this gives:

$$w = \pi r \gamma \qquad [1]$$

where w is the weight for zero strain; r, the radius of the wire; and γ, the surface tension.

A subsequent note by Udin[2] pointed out that eq 1 applies only to single-crystal specimens. Since the specimens used revealed a "bamboo" structure upon

E. R. FUNK, Junior Member AIME, H. UDIN and J. WULFF, Members AIME, are Instructor, Assistant Professor, and Professor of Metallurgy, respectively, Massachusetts Institute of Technology, Cambridge, Mass.

Discussion on this paper, TP 3188E, may be sent, 2 copies, to AIME by April 1, 1952. Manuscript, July 11, 1951. New York Meeting, February 1952.

Table I. Applied Stress and Resulting Strain for Each Specimen

Test No.	22		23		24		25		26	
Spec. No.*	$\sigma \times 10^{-5}$	$\epsilon \times 10^{5}$	$\sigma \times 10^{-5}$	$\epsilon \times 10^{5}$	$\sigma \times 10^{-5}$	$\epsilon \times 10^{5}$	$\sigma \times 10^{-5}$	$\epsilon \times 10^{5}$	$\sigma \times 10^{-5}$	$\epsilon \times 10^{5}$
1	0.68	−83	0.66	−181	0.69	−36	0.60	−58	0.56	−63
2	1.01	−43	Specimen damaged		1.11	−49	0.87	−57	1.07	−74
3	1.39	−41	1.36	−44	1.41	−44	1.31	6	1.33	−12
4	1.71	56	1.70	46	1.71	42	1.64	17	1.67	28
5	2.18	61	2.18	122	2.24	48	2.11	−8	2.15	45
6	2.95	181	2.92	211	2.93	72	1.96	30	2.88	121
7	3.53	216	3.37	417	3.48	29	3.31	43	3.45	96
8	4.10	298	4.10	328	4.06	148	4.03	34	4.03	120
9	4.79	383	4.80	457	4.67	170	4.62	32	4.65	71
10	5.73	413	5.67	652	5.90	311	5.63	119	5.77	232
11	8.49	626			9.02	534	8.44	288	8.93	475
13					0.10	−93	0.09	−40	0.08	−88
14	0.11	−154	0.12	−187	0.09	−70	0.08	−76	0.09	−52

* Specimens numbered according to the position occupied in the cell cover.

metallographic examination, the equation must be modified to take into account the grain boundary energy. Since the grain boundaries are perpendicular to the axis of the wire, eq 1 becomes:

$$w = \pi r \gamma - \left(\frac{n}{l}\right) \pi r^2 \gamma_{gb} \qquad [2]$$

where γ_{gb} is the interfacial tension of a grain boundary and n/l, the number of grains per unit length.

Greenough[2] has shown, and further experiments in this laboratory have confirmed, that for silver in an inert atmosphere, the grain boundary interfacial tension for the average grain boundary is one third the tension of the free surface. Therefore eq 2 may be rewritten as:

$$w = \pi r \gamma \left[1 - \frac{n}{l} \frac{r}{3}\right] \qquad [3]$$

For the special case of the wires in our experiments n/l is 60 ± 10 grains per cm and r is 0.0065 cm, so that the equation relating the surface tension to the balancing load for polycrystalline wires is then:

$$w = \pi r \gamma \, [0.87] \qquad [4]$$

The applied stress for zero strain is the balancing load divided by the cross-sectional area of the wire:

$$\gamma = \frac{\sigma_{z=0} r}{0.87} \qquad [5]$$

where $\sigma_{z=0}$ is the applied stress for zero strain.

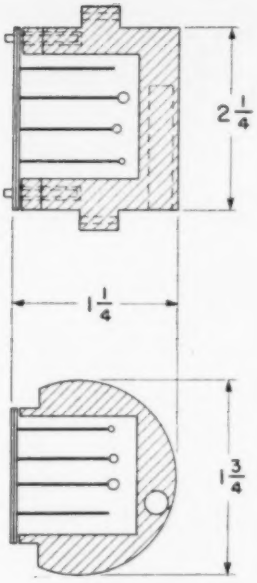

Fig. 1—Silver cell with thermocouple well.

Experimental Procedure

The techniques used by Udin, Shaler, and Wulff were used in modified form to measure the surface tension of solid silver. The wire was 0.00508 in. in diam and was drawn from a billet of high purity, vacuum cast silver. Preliminary experiments showed that commercially available fine silver wire was not suitable for this work because uninhibited grain growth did not occur, presumably due to the presence of oxides or other inclusions.

Two gage marks were cut into the wire approximately 1 cm apart so that the strain in the specimens could be measured. These marks were made by rotating the wire against the edges of spaced razor blades in an especially designed machine.[4] Each end weight, prepared from a length of the silver wire, was melted on a charcoal block and the end of the wire thrust into the molten ball as it solidified. In all the runs, 10 to 13 wires were used with external end weights ranging from 0 to 120 mg.

The wires were suspended from a silver cell cover and then the array was carefully transferred to a silver cell. The cover closed but did not seal the cell. The cell, shown in Fig. 1, was then transferred to a platinum wound Inconel tube furnace. This furnace has been described elsewhere.[4]

Preliminary runs were carried out in a vacuum of 5×10^{-4} mm Hg, but the evaporation of the silver wires at the test temperatures was so rapid that no reproducible results could be obtained. The runs reported here were therefore carried out in a purified helium atmosphere. A helium flow of 3 cu cm per sec was maintained in the furnace throughout the run. The helium was purified by passing it through an activated charcoal trap held at liquid nitrogen temperatures.

Due to the manipulation required for mounting, the wires were often slightly bent and cold worked. An anneal treatment of a few minutes at 600°C was sufficient to allow straightening of the wires.

The specimens were washed in alcohol and ether

Table I. (Continued)

Test No.	27		28		30		31		32	
Spec. No.	$\sigma \times 10^{-5}$	$\epsilon \times 10^{5}$	$\sigma \times 10^{-5}$	$\epsilon \times 10^{5}$	$\sigma \times 10^{-5}$	$\epsilon \times 10^{5}$	$\sigma \times 10^{-5}$	$\epsilon \times 10^{5}$	$\sigma \times 10^{-5}$	$\epsilon \times 10^{5}$
1	0.47	−83	0.52	−90	0.54	−57	0.64	−61	0.55	−159
2	0.84	−35	1.08	−66	1.09	−23	0.80	−31	0.79	−69
3	1.32	−7	1.32	−56	1.31	25	1.27	−27	1.31	−11
4	Specimen damaged		1.53	61	1.63	51	1.47	8	1.63	32
5			2.14	80	0.08	−86	1.97	60	2.16	71
6	Specimen damaged		2.93	200	2.92	115	2.62	120	2.94	250
7	3.27	143	3.41	285	3.42	196	3.78	182	3.42	332
8	Specimen damaged		4.04	323	4.03	262	4.02	259	4.02	433
9	4.59	172	4.65	172	4.62	350	4.36	264	4.64	429
10	5.55	344	5.78	277	5.88	705	5.47	411	5.80	695
11	8.40	417	8.89	1047	8.91	784	8.26	641	8.89	1078
12							0.10	−99		
13					0.09	−122				
14	0.07	−131	0.09	−319	0.09	−166				
16							0.09	−125	0.10	−201

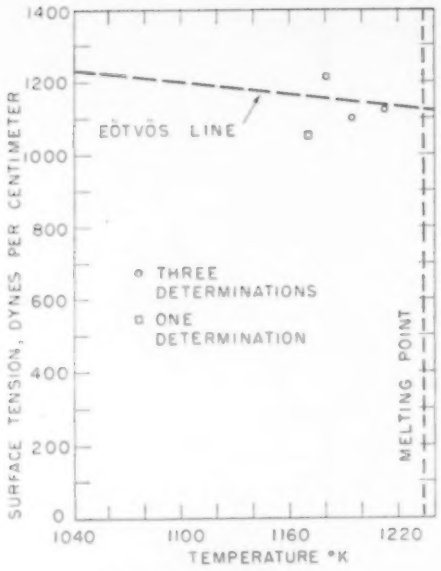

Fig. 2—Temperature dependence of the surface tension of solid silver.

to remove dirt and returned to the furnace for a high temperature anneal. This anneal lasted 1 hr at 940°C. The specimens were removed from the furnace after cooling, and the gage length of each wire was measured with a vertical traveling microscope with a screw accurate to ±0.00015 cm. This array was returned to the furnace for the run which lasted up to 116 hr for the lower temperatures and as short as 18 hr for the higher temperatures. Upon cooling the wires were removed from the furnace and the gage lengths again measured. The weights were clipped off at the weld and weighed to ±0.1 mg.

It was always possible to count the number of grains in each wire after a test was completed. This is possible because an equilibrium of surface forces exists where the grain boundary meets the free surface. The groove angle established at the grain boundary[5, 6] is distinctly visible under diffuse oblique illumination at X50. These grooves are often visible even after the short 940°C anneal. A grain count on a number of specimens after the anneal and also after the test itself showed that the grain size established during the anneal remains essentially unchanged.

Table II. Summary of Experimental Results

Test No.	Test Temperature, °C (± 1°C)	Duration of Test, Hr	Surface Tension, Dynes per Cm
22	938	18	1110
23	941	29	1150
24	923	18	1190
25	906	26	1265
26	923	36	1115
27	907	50	1210
28	907	108	1215
29	Run lost		
30	924	64.5	1005
31	876	116	1045
32	938	50.5	1070

The surface tension for all runs was calculated from eq 5. A straight line fits the data for applied stress between 0 and 4×10^5 dynes per sq cm. Points of larger applied stress were not included in the calculation. A least square calculation was used to determine the most probable stress at zero strain. The necessary but small (0.15×10^5 dynes per sq cm) correction to the ball weight for the weight of the wires between the lower gage mark and the weight was also made.

The values for the applied stress and the resulting strain for each specimen in each successful run are given in Table I. A summary of the experimental results is presented in Table II.

Discussion and Conclusions

Ten tests for the surface tension of solid silver in a purified helium atmosphere were made at four different temperatures and various times. The average of the results is $\gamma = 1140 \pm 90$ dynes per cm for the range 875° to 932°C. There is a tendency for short time runs to give slightly higher values for surface tension than runs of long duration. This trend seems to occur at all the test temperatures but is, in general, less than the experimental error. If it is a real phenomena, it may be attributable to one of several reasons. There may be a gradual adsorption of traces of metallic vapor contaminant. More likely, the average diameter of the wires decreases due to evaporation. This decrease would not have been detected if it was less than 5×10^{-5} in., and such a decrease would lead to a decrease of some 20 to 40 dynes per cm in the apparent value of the surface tension.

Fig. 2 shows the temperature dependence of the surface tension. In spite of the scatter of the data, probably attributable in a large part to the high sensitivity of silver to gaseous contamination, a least square calculation of the ten tests gives a temperature coefficient of −0.47 dynes per cm of °K. This is in good agreement with the coefficient theoretically predicted by the Eötvös rule. This rule says that the surface tension of a liquid decreases linearly to zero at the critical temperature. Assuming a critical temperature of 3330°K and, correcting for a liquid-solid interfacial tension of 200 dynes per cm,[6, 7] the Eötvös rule coefficient is −0.45 dynes per cm per °K. It is assumed that Antonow's rule holds at the melting point so that the sum of the liquid-vapor surface tension and the liquid-solid surface tension equals the solid-vapor surface tension.

Acknowledgment

The writers wish to acknowledge their indebtedness to the Office of Naval Research who made funds available for equipment and supplies used in this work under contract number N5ori-07841. We are also indebted to F. H. Buttner for his assistance in the experimental work.

References

[1] Udin, Shaler, and Wulff: *Trans.* AIME (1949) **185**, p. 186; JOURNAL OF METALS (February 1949).
[2] Udin: JOURNAL OF METALS (January 1951) *Trans.* AIME, p. 63.
[3] Greenough: Report to Ministry of Supply No. 52. London.
[4] Buttner: ScD Thesis, M.I.T. (1951).
[5] Smith: *Trans.* AIME (1948) **175**, p. 15; *Metals Technology* (June 1948).
[6] W. D. Kingery: Private communication.
[7] Turnbull: M.I.T. Colloquim. (May 1951).

Surface Tension of Solid Gold

by F. H. Buttner, H. Udin, and J. Wulff

Using a modified Udin, Shaler, and Wulff technique, the surface tension of gold in purified helium was found to be 1400 ± 65 dynes per cm for the temperature range 1017° to 1042°C.

IN the original Udin, Shaler, and Wulff technique for measuring the surface tension of copper,[1] variously weighted wires were allowed to extend or contract in a copper cell held at elevated temperatures in vacuum. By plotting stress vs. strain for a wire array in one test, the stress at zero strain is obtained. This is the point where the contractile forces resulting from surface tension are balanced by the applied load, according to the expression:

$$\gamma = \sigma_{\epsilon=0}\, r \qquad [1]$$

where γ is the surface tension in dynes per cm; $\sigma_{\epsilon=0}$ the stress at zero strain in dynes per cm; and r, the radius of the wire in cm. The assumption that the wires deform viscously permits the drawing of a straight line through the points on the stress-strain plot. Justification of the assumption has received further experimental support recently.[2-4]

The presence of grain boundaries in the wires requires a correction to the original expression used.[5] Thus:

$$\gamma = \sigma_{\epsilon=0} \cdot r\, [1 - (n/l)\, (ar)]^{-1} \qquad [2]$$

where, n/l is the number of grain boundaries per unit length, and a, the ratio of grain boundary tension to free surface tension.

Alexander, Kuczynski, and Dawson[6] in studying the creep of gold wire in vacuum were unable to obtain reproducible values of the surface tension of gold. In plotting stress vs. strain for progressively longer times, they found that the stress at zero strain drifted with time from positive stress values to negative values. Similarly, for the surface tension of silver, reproducible values were obtained only when a purified helium atmosphere was substituted.[5] Evidently the evaporation rate of silver in vacuum is too high at the temperatures employed to obtain solid-gas equilibrium even in a similar metal enclosure. Thus reproducibility of results is lost.

Experimental Procedure

The experimental procedure was much the same as that originally developed by Udin, Shaler, and Wulff with a few modifications and improvements. For greater accuracy in strain measurements, knots gave way to cut gage marks as shown in Fig. 1. These were made with a hand-driven lathe in which razor blades served as cutting tools. Also a more precise cathetometer with a screw accurate to 0.00015 cm was used. The tests were conducted in an atmosphere of purified helium rather than in vacuum in order to avoid possible evaporation difficulties. Five mil wire of high purity gold (99.98 pct) was used.

After cutting in the gage marks, each wire of a series of about 12 was differently loaded by welding a gold ball to one end. This was done by dipping the end of the wire in a cooling gold droplet, previously melted on a charcoal block with a No. 2 acetylene torch. The other end of the wire was strung through a hole in a gold lid and twisted over the edge to hold the wires fixed and in suspension from the lid. The lid and mounted wires were then dipped in pure ethyl alcohol to dissolve any skin oils and dirt on the surface of the wires due to handling. Finally the lid was put in place on an alundum crucible lined with gold so that the wires hung freely within the gold-lined chamber. This whole assembly was next heated in a quartz nichrome wound tube furnace and heated for a few minutes at 600°C to soften the wires. After this anneal the wires were easily straightened with tweezers.

The wire assembly was finally annealed 10° to 25°C above the subsequent test temperature for 2 hr. This treatment allowed the grains to grow to equilibrium size and shape. After the anneal, the lid was mounted in front of the cathetometer. The gage length was measured by sighting the 40 power microscope on the upper lip of the lower gage mark for the first reading, then traveling up to the lower lip of the upper gage mark for the final reading. This procedure was repeated four times to give an average gage length value. In this manner the annealed gage length and the final gage length could be measured to determine the strains. During all measurements, grain counts were made.

F. H. BUTTNER, Junior Member AIME, H. UDIN and J. WULFF, Members AIME, are Instructor, Assistant Professor, and Professor of Metallurgy, respectively, Massachusetts Institute of Technology, Cambridge, Mass.

Discussion on this paper, TP 3187E, may be sent, 2 copies, to AIME by April 1, 1952. Manuscript, July 11, 1951. New York Meeting, February 1952.

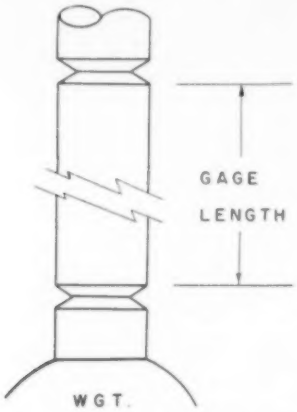

Fig. 1—Loaded wire with cut gage marks.

The furnace used was an 18 in. quartz tube, 2⅞ in. diam, wound with three nichrome tapered windings each controlled through a separate rheostat. The temperature was held to ±1°C over the 4 in. hot zone by a Celectray temperature controller. Two thermocouples, one for the temperature controller and the other a traveling thermocouple, were used to check the temperature distribution over the length of the furnace. The helium used as furnace atmosphere was passed through an activated charcoal trap held in liquid nitrogen. A getter boat containing titanium powder was also kept in the hot zone of the furnace. This last precaution was shown by run No. 5 to be unnecessary.

Nine tests were made in purified helium, while one test, No. 5, was carried out in air. The results of these tests are compiled in Table I, and shown graphically in Fig. 2. After a least square analysis of the data, the surface tension was calculated using eq 1. From these results the corrected surface tension was obtained with the aid of eq 2.

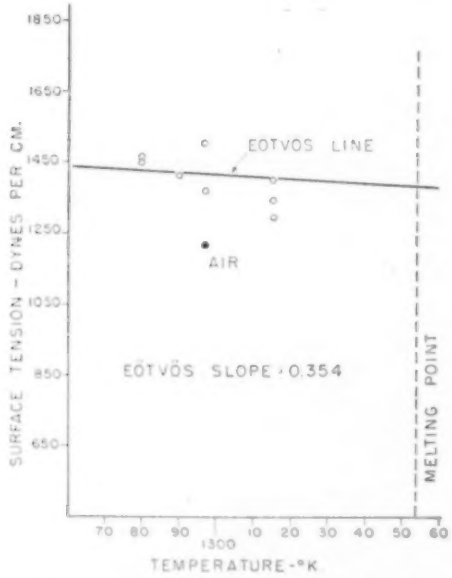

Fig. 2—Average surface tension vs. temperature °K showing Eotvos line.

Discussion and Conclusions

Test No. 5, run in air, gave a lower surface tension value than the tests run in helium. The result is however not sufficiently suppressed to indicate that oxygen adsorption is important as is the case in silver.[4] The short duration of run No. 9 at the lowest temperature exhibits so high a percentage of error that it was discarded.

The average value for the apparent surface tension was found to be 1250 ± 50 dynes per cm over the range 1280° to 1315°K. For the corrected value, eq 2 was used, where $n/l = 75$, and $a = 0.300$, which together give a correction factor of 0.889. The average corrected value over the same range of temperatures then becomes 1400 ± 65 dynes per cm. The value for n/l was computed from the average grain count with respect to the average annealed gage length of ten randomly chosen wires. The value for the constant, a, was computed from the average grain boundary angle for 250 readings by the reflected light method of Greenough and King[6] where the grain boundary angle averaged 163°.

The least square line drawn through the points of Fig. 2 has a slope of −0.433, which is in fair agreement with the Eötvös slope of −0.354. For silver[3] much closer agreement obtains.

Structure of the Gold Wires

The wires were of the typical bamboo or reed-like structures observed before.[1-3,7] An excellent series of micrographs of gold wires appear in a paper by Alexander, Dawson, and Kling,[7] showing kinking, offsetting, and what appears to be bulging. Similar effects were observed in the experiments reported here.

The phenomena of kinking and offsetting is critically discussed by Herring,[8] who predicts this behavior on the basis of his theoretical treatment. Kinking appears to be the result of rotation of the grains about an axis lying in the grain boundaries. Offsetting, which is seen only in heavily loaded wires, results from the normal viscous behavior of grain boundaries.

Concerning the matter of bulging, Zener[9] has shown theoretically that the surface tension forces in wires of this type should cause each wire to break up into a series of small connected spheres. Alexander, Dawson, and Kling conclusively demonstrated the reality of Zener's prediction by heating for 120 hr a gold wire lying in an alundum boat at 1055°C. It is thought that if this tendency is appreciable under the conditions of the experiments, accordingly appreciable error might be expected in the final results. As a matter of fact, Alexander, Dawson, and Kling attribute some erratic behavior in lightly loaded wires in their experiments to this phenomenon.

In the experiments reported here as well as those reported by Funk, Udin, and Wulff, dummy wires were attached to and never removed from the same lid used throughout all the tests. Some of the dummy wires were plastically strained so as to introduce artificial bulges at the restrained region of the grain boundaries, and waists at the regions of no restraint in the middle of grains. These dummy

wires accumulated at least 200 hr under the exact test conditions of these experiments. In no case was a visible incipient breakup in the unstrained wires observed nor was an aggravation of the bulged condition of the strained wires seen. Cut gage marks also introduce a start toward the expected breakup of the wires. But actually here the opposite effect is observed in that the gage marks over a period of time at the test temperatures tend to disappear by smoothing over.

Apparent bulges appear in mounted and polished specimens. A plane section as formed by polishing through a kink produces what appears to be a sizeable bulge as shown in the line drawing of Fig. 3. Also bulges may appear on polished specimens due to strains introduced by mounting the specimens in bakelite.

Even if bulges were to exist, they may not exert as strong an influence as might at first be thought. If it is assumed for the moment that the wires do change into what might be called an idealized string of small spheres, or series of waists and bulges, and if it is also assumed that the idealized condition evolves by removing a ring of material from the cylinder to form a waist, and then putting it back on the cylinder slightly above the waist to form a bulge—by doing this all along the wire a contoured bulge and waist condition is created. In this process, no elongation or contraction is effected. Comparing the strain of a contoured wire to a cylindrical wire after a period of time at the test temperature, excessive elongation at the waists will be offset by deficient elongation at the bulges. Thus, the overall elongation of the contoured shape should be the same as a uniform elongating cylinder. The sum of the vertical components of surface tension over the contoured surface equals the vertical tension of the original cylindrical surface. Thus, in this idealized condition, no difference in important behavior can be found from that of a cylindrical wire.

Although there is no reason to believe that the wires will assume the idealized condition, nevertheless any bulge and waist model would necessarily be some approach to the ideal. Only the departure of the actual from the ideal would introduce error into the results of the experiments.

The tendency of the wires to spheroidize is observed to be vanishingly small for the configuration of experiment described here. Visible beginnings of spheroidization would in themselves introduce only second-order errors, insofar as they depart from the above idealized picture. Thus, any errors due to a tendency to bulge are lost in the normal experimental uncertainties of the technique.

Table I. Thermal History and Results of Each Run

Run No.	Temperature °K (± 1°K)	Time, Hr	Dynes per Sq Cm x10⁶	Apparent Surface Tension, Dynes per Cm	Corrected Surface Tension, Dynes per Cm	Precision of Correction
1	1315	23.5	1.845	1190	1340	± 77
2	1297	18.0	1.882	1214	1367	± 53
3	1280	36.0	2.016	1300	1464	± 55
4	1315	31.5	1.779	1148	1293	± 40
5*	1297	30.0	1.660	1072	1207	± 75
6	1290	36.0	1.940	1252	1410	± 61
7	1315	9.0	1.923	1240	1396	± 94
8	1297	10.5	2.078	1334	1500	± 118
9	1280	10.5	2.405	1552		±158
10	1280	60.0	1.993	1286	1448	± 35

* Run No. 5 made in air, all other runs in purified helium.

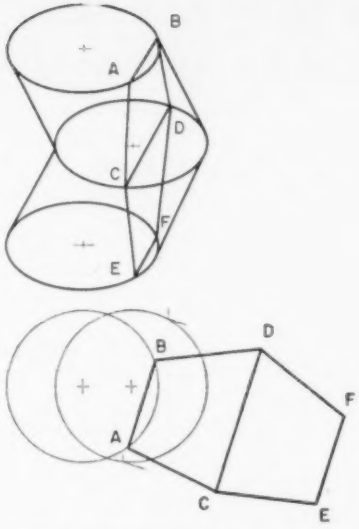

Fig. 3—Construction of the polished surface cutting through a kink.

Summary

Using a modified Udin, Shaler, and Wulff technique the surface tension of gold in purified helium was found to be 1250 ± 50 dynes per cm. Using the Udin correction for grain boundary energy, this becomes 1400 ± 65 dynes per cm for temperature range 1280° to 1315°K.

It has been observed that no spherical breakup of the wires is present in these experiments. Bulges appear on polished specimens, but this appears to be a spurious effect of the mounting and polishing technique. Ideas are presented indicating that the experiments could be carried out to the beginnings of visible spheroidization without introducing a significant error in either the value of surface tension or the rate of axial creep.

Acknowledgments

The authors wish to acknowledge their indebtedness to the Office of Naval Research for equipment and supplies purchased under contract number N5ori-07841, and to E. R. Funk for his assistance in carrying out the experimental work.

References

[1] Udin, Shaler, and Wulff: *Trans.* AIME (1949) **185**, p. 186; JOURNAL OF METALS (February 1949).

[2] Funk, Udin, and Wulff: This issue, p. 1206.

[3] Alexander, Kuczynski, and Dawson: *The Physics of Powder Metallurgy.* W. E. Kingston, Chap. II, pp. 202-213 (1951) New York. McGraw Hill Book Co.

[4] Buttner, Funk, and Udin: To be published in *Journal of Physical and Colloidal Chemistry.*

[5] Udin: JOURNAL OF METALS (January 1951) *Trans.* AIME, p. 63.

[6] Greenough: Report to Royal Aircraft Establishment, Met 52, (1950).

[7] Alexander, Dawson, and Kling: *Journal of Applied Physics* (1951) **22**, p. 439.

[8] Herring: *Journal of Applied Physics* (1950) **21**, p. 437.

[9] Zener: Private communication.

Technical Note

Eutectoid Decomposition of the Delta Phase of the Copper-Tin System

by C. C. Wang and M. Hansen

THE δ phase of the Cu-Sn system ($Cu_{31}Sn_8$ = 32.53 pct Sn) was considered to be stable down to room temperature until Owen and Iball[1] showed by X-ray analysis that it undergoes a eutectoid decomposition into the α and ϵ phases at a temperature near 300°C. Their findings have been confirmed by other investigators,[2-5] all of whom used X-ray diffraction studies of powdered specimens. The transformation temperature has been reported by various authors as lying between 300° and 380°C. To our knowledge, no microscopic evidence of the eutectoid reaction has been published, as yet.

It was in connection with other work that long-time annealings at 300°C were conducted with alloys containing 22, 32.6, and 35 pct Sn (nominal compositions) prepared from electrolytic copper and electrolytic tin and cast in a small iron mold. The specimens were first annealed at 700°C for 5½ hr and quenched from 400°C after cooling to, and annealing at, that temperature for 9½ hr. After this annealed 32.6 pct alloy, which was intended to consist entirely of δ phase. Due to some loss in copper on melting, the composition is slightly higher in tin. Accordingly, the sample after quenching from 400°C consisted of grains of the δ phase with the ϵ phase arranged along the grain boundaries and as a Widmanstätten precipitate within the δ grains. After an annealing time of 63 days, the eutectoid decomposition, $\delta \rightarrow \alpha + \epsilon$, is still in its early, initial state. The pearlitic type of eutectoid is nucleated at the ϵ crystals, preferably those surrounding the grain boundaries of the δ phase. The appearance of the $(\alpha + \epsilon)$-eutectoid in the 35 pct Sn alloy was very similar to that shown in Figs. 2 and 3. Again, the eutectoid decomposition nucleated at the ϵ phase and proceeded from there into the δ areas.

As is evident from Fig. 2, the rate of decomposition of the δ phase at 300°C is extremely sluggish: In the representative area shown only about 5 pct of the δ phase has undergone the eutectoid trans-

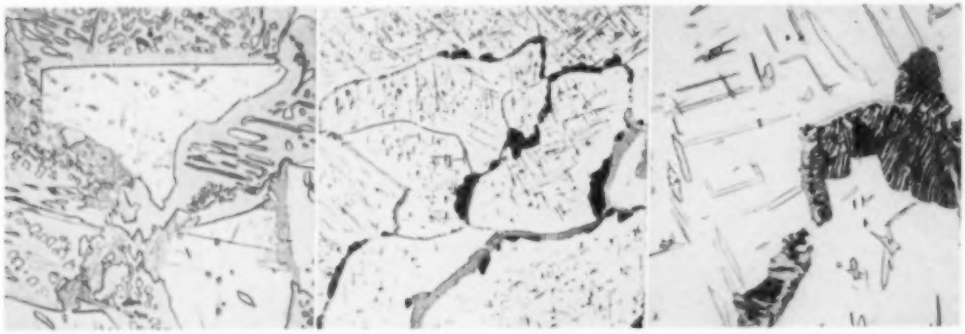

Fig. 1—About 22 pct Sn. X750. Fig. 2—About 33 pct Sn. X100. Fig. 3—About 33 pct Sn. X500.

Figs. 1 to 3—Microstructure of Cu-Sn alloys after annealing for 63 days at 300°C. Etchant, $FeCl_3$.

treatment the sample with 22 pct Sn was cold worked for 15 pct reduction in thickness; the 32.6 and 35 pct alloys were too brittle to be cold worked. The final anneal at 300°C was done in a sealed pyrex glass bulb for 63 days.

Fig. 1 represents the microstructure of the annealed alloy with 22 pct Sn. It shows primary α solid-solution crystals in a matrix of the $(\alpha + \delta)$-eutectoid formed at 520°C. The α crystals contain δ inclusions which precipitated from α due to the decrease in the solubility of tin in copper with fall in temperature. The decomposition of the δ phase into α (light) and ϵ (dark) can clearly be seen in some areas of the $(\alpha + \delta)$-eutectoid matrix. However, the decomposition is far from being completed, even after the long-time anneal used.

Figs. 2 and 3 depict the microstructures of the formation after annealing for 63 days. On the other hand, Owen and Williams[2] have reported that X-ray photographs of powdered samples with between 17.5 and 34 pct Sn did not show δ lines after annealing for only five to seven days at 300°C. This is in accordance with the fact that the rate of reaction in powdered samples is higher than in massive specimens, as a result of the excess free energy of the powder (due to its greater surface area).

The authors wish to express their thanks to C. A. Johnson for preparation of the micrographs.

C. C. WANG is associated with Massachusetts Institute of Technology, Cambridge, Mass., and M. HANSEN is with Armour Research Foundation of Illinois Institute of Technology, Chicago.

TN 94E. Manuscript, Sept. 17, 1951.

References

[1] E. A. Owen and J. Iball: *Journal* Inst. Metals (1935) **57**, p. 267.

[2] E. A. Owen and E. C. Williams: *Journal* Inst. Metals (1936) **58**, p. 283.

[3] C. Haase and F. Pawlek: *Ztsch. Metallkunde* (1936) **28**, p. 473.

[4] S. T. Konobeevsky and V. P. Tarasova: *Acta Physicochim.* U.R.S.S. (1937) **6**, p. 781.

[5] M. Hamasumi and K. Morikawa: *Nippon Kinzoku Gakkai-Si* (1938) **2**, p. 39.

AIME OFFICERS:
President—Willis McG. Peirce
Vice-Presidents—A. B. Kinzel, Philip Kraft, R. W. Thomas, J. L. Gillson, M. L. Haider
Vice-President and Treasurer—Andrew Fletcher

AIME STAFF:
Secretary—E. H. Robie
Ass't. Secretaries—E. J. Kennedy, Jr., Ernest Kirkendall, J. V. Beall, J. B. Alford, R. E. O'Brien
Ass't. to Secretary—H. N. Appleton
Ass't. Treasurer—H. A. Maloney

aime NEWS

Metals Branch Outlines Topics For Annual Meeting Technical Sessions

The annual meeting of the American Institute of Mining and Metallurgical Engineers will be held at the Statler Hotel, New York City, Feb. 18 to 21, 1952. The annual banquet will be held Wednesday, Feb. 20, 1952 in the Grand Ballroom of the Waldorf Astoria Hotel.

Institute of Metals Div.—In addition to the usual technical sessions are the following features: Monday afternoon, Symposium on High-Temperature Alloys; Tuesday, Seminar on the Electron Theory of Metals; Wednesday afternoon, Research in Progress; Thursday, Powder Metal Symposium. Dr. William Shockley, research physicist, Bell Telephone Laboratories, Inc., will deliver the annual lecture on Wednesday at 11 a.m.

Iron and Steel Div.—Two symposiums, one on oxygen, the other on manganese (joint meeting with MBD and EMD) as well as the usual technical sessions are planned. Dr. A. B. Kinzel, president, Union Carbide & Carbon Research Laboratories, Inc., will deliver the Howe Memorial Lecture on Tuesday at 11 a.m.

Extractive Metallurgy Div.—The EMD program begins on Monday morning and extends through Thursday morning. It includes sessions on copper, zinc, physical chemistry of extractive metallurgy; a joint meeting with the MBD and ISD on manganese conservation; round table discussion on addition agents in electrometallurgy; uncommon metals; and a round table discussion on the training of extractive metallurgists.

Luncheons—Monday, the Executive Committee, IMD, will meet after the all-Institute luncheon. Tuesday, the Executive Committee, ISD, will meet at luncheon. Wednesday, the Executive Committee, EMD, will meet at luncheon. Thursday, the Powder Metallurgy Committee will meet at luncheon.

Banquet—The 1952 Banquet Committee announced that the Banquet will take place in the Grand Ballroom of the Waldorf Astoria Hotel on the evening of Wednesday, Feb. 20, 1952, at 7:30 pm.

The hotel is prepared to furnish private rooms for groups desiring to hold cocktail parties prior to dinner. Arrangements should be made with the hotel.

Following the precedent established at the 1951 Banquet in St. Louis, the Committee has decided to adhere firmly to the practice of assigning seats in the order of receipt of paid reservations. Tables will accommodate ten persons and those desiring to be seated with friends should purchase tickets in a block and indicate to whom the ticket will be issued.

In addition to the preferential seating which will be given to the paid reservations in order of receipt, wives of head table guests will be given choice locations if such a desire is indicated.

Reservation cards will be mailed to all AIME members early in January.

Research in Progress

Research personnel are reminded of the Institute of Metals Division *Research in Progress* session planned for Wednesday afternoon, Feb. 20, 1952 during the Annual Meeting in New York. Abstracts of proposed papers not exceeding 200 words in length are to be submitted to Institute headquarters prior to Dec. 15, 1951, for inclusion in the February issue of the JOURNAL OF METALS. Abstracts not received in time for publication in the February issue may, nevertheless, be presented if received prior to Jan. 15, 1952, according to J. H. Scaff of the IMD Program Committee.

The Program Committee urges those interested to avail themselves of the opportunity of participating in this program in order that new research information be presented for discussion.

AIME Dues Bills In Mail

Pursuant to Article II, Section 2, of the bylaws of the AIME, notice is hereby given that dues for the year 1952 are payable Jan. 1, 1952, as follows: Members and Associate Members, $20; Junior Members for the first six years of Junior Membership, $12 and thereafter, $17; Student Associates (including an annual subscription to a monthly journal), $4.50.

Mailing of dues bills began in October and will be completed before the end of the year. Prompt payment will assure uninterrupted receipt of the publications desired in 1952. If, for any reason, a bill is not received within a reasonable time after the last mailing date, Dec. 31, 1951, headquarters should be notified.

How About You?

If either your address or position change, you owe it to yourself and friends to let AIME headquarters know as soon as possible, a month before the change is made if you can give your future address accurately. Please follow these suggestions: (1) Give your name and the address to which publications and correspondence should be sent. Mark this: "Publications address." (2) Give your name, title, or company position, and your address the way you want it to appear in the next Directory. Mark this: "Directory listing." (3) A short personal item for publication will be appreciated. (4) Mention the Branch of the Institute to which you belong—Mining, Metals, or Petroleum.

Local Section Cites Student Papers

The Philadelphia Section of AIME held its regular monthly dinner meeting on Thursday evening, Nov. 1, 1951. Chairman A. L. Jamieson presented awards to the winners of the local student prize paper contest. Winners were: Paul Dick, first prize, George Wolf, second prize, undergraduate level; G. J. Mills, Ph.D. level; and Nathan Davidson, Masters level.

Paul Dick presented his winning paper "The Role of Copper on Sulphur Pickup from Furnace Gases in the Open Hearth Furnace." The meeting closed with a question and discussion period. This student paper activity received enthusiastic support from the members and will be scheduled as an annual event.

Publications, Policies And Prices Established for Coming Year

Pursuant to Article X of the bylaws of the AIME, the following information is hereby given as to the "conditions, prices, and terms under which the various classes of members, and Student Associates, severally, shall be privileged to obtain publications of the Institute during the ensuing year."

Publications authorized for 1952 publication include the following: MINING ENGINEERING, published monthly, containing material, including technical papers, of interest to those engaged in exploration, mining geology and geophysics, and metal, nonmetallic, and coal mining and beneficiation, and fuel technology. The JOURNAL OF METALS, published monthly, containing material, including technical papers, of interest to those engaged in nonferrous smelting and refining, iron and steel, and physical metallurgy. The JOURNAL OF PETROLEUM TECHNOLOGY, published monthly in Dallas, containing material, including technical papers, of interest to those engaged in petroleum and natural gas drilling and production.

Annual subscriptions to any one of the above journals will be provided all members in good standing without further charge. (A member ceases to be in good standing if current dues are not paid by April 1.) If more than one of the monthly journals is requested, $4 extra will be charged for an annual subscription, or 75¢ for single copies of regular issues and $1.50 for special issues. The nonmember subscription price for each journal is $8 in the Americas; foreign, $9. Student Associates will be entitled to the same privileges for all publications as members.

Three volumes of "*Transactions*" are authorized for 1952 publication, as follows: No. 190, Mining Branch; No. 191, Metals Branch; and No. 192, Petroleum Branch. These volumes will be available to members at $3.50 each for a first copy if paid for in advance with dues; otherwise at the nonmember rate of $7 less 30 pct. Nonmembers $7 in the United States; foreign $7.50.

Special volumes now planned for publication in 1952 include the following: 1—*Open Hearth Proceedings*, price to AIME members $7; nonmembers, $10. 2—*Blast Furnace, Coke Oven, and Raw Materials Proceedings*, AIME members $7; nonmembers $10. 3—*Electric Furnace Steel Proceedings*, AIME members $7; nonmembers $10. 4—*Symposium on Tube Producing Practice*, $3. 5—*Statistics of Oil and Gas Development and Production*, covering data for year 1950, free to members (except Student Associates); nonmembers $6. 6—*Statistics of Oil and Gas Development and Production*, covering data for year 1951, members $5, nonmembers $10.

If dues are paid subsequent to January 31, back issues of Institute publications will be supplied only if adequate stocks are on hand. A member may not receive a volume of "*Transactions*", or a special volume, in lieu of a monthly journal, free of charge on membership. Members in arrears for dues are not entitled to special members' prices for publications.

Rocky Mountain members may have their choice of an annual subscription to one of the monthly journals on request.

Institute Allows Military Credit

Pursuant to Article I, Section 5 of the bylaws as amended, giving the Board power to waive the age limitation for Junior Membership in the case of veterans from military service, the Executive and Finance Committees AIME voted to allow all veterans from military service who apply for Junior Membership a credit of one year on the entrance age limit of 30 years for each year of military service. Also, it was voted to allow a similar credit on the 33 year age limit for changing status to Associate Member or Member.

AIME To Join Engineering Group

At the meeting on October 10 of the Executive and Finance Committees, AIME, the Secretary reported that the AIME had been formally invited to become a member of the Conference of Representatives from the Engineering Societies of Western Europe and the United States. The next meeting of this Conference will be held in Paris in 1953. The Committees voted to accept this invitation to membership.

IMD Fall Meeting Held In Detroit

Registration for the annual IMD fall meeting as part of the Metal Congress set an all time record when some 594 registered for the October 15 to 17 Detroit meeting. This was 30 pct higher than any of the recent years. High spot in the technical program was the seminar on DISLOCATIONS IN METALS, arranged by Morris Cohen. Frederick Seitz, W. T. Read, and Egon Orowan presented papers during the afternoon and evening sessions. Attendance at each of the papers was uniformly outstanding, varying between 350 and 400.

In addition to the other eight technical sessions, the following committees held meetings: Powder Metallurgy, Membership, Publications, Programs, and Executive.

As indicated in the picture below, an unusually large group attended the annual fall dinner to hear Clarence K. Streit, 700 Ninth St., N. W., Washington, D. C., speak on "FEDERAL UNION." Intense interest was indicated in his subject.

The Detroit Section, F. P. Bens, Chairman, acted as host at the cocktail party immediately preceding the dinner and outdid themselves in adding to the enjoyment of the evening and in making the necessary arrangements for the technical sessions throughout the meeting.

Father and Son "Legion of Honor" Members of Institute

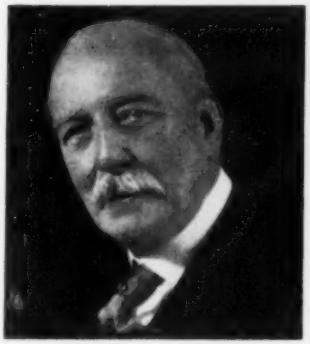

ANDREW S. McCREATH

LESLEY McCREATH

Andrew S. McCreath and **Lesley McCreath**, father and son, Harrisburg, Pa., together have been members of AIME for 100 years. Andrew S. McCreath joined in 1879 and was manager of the Institute in 1882. He died in 1930. Lesley McCreath joined AIME in 1902 — which adds up to the astounding total of 100 years.

The elder Mr. McCreath was born in Ayr, Scotland, in 1849, and came to United States in 1869. He was graduated from Andersonian University, Glasgow, and was doing postgraduate work at the University of Gottingen, when he was employed by the old Pennsylvania Steel Co., Steelton, Pa., as a chemist. He was one of the first men ever employed exclusively as a chemist by any steel company in United States. Subsequently he became chief chemist of the Pennsylvania Second Geological Survey, and when the survey was completed he established himself as an independent analytical and consulting chemist in Harrisburg.

Lesley McCreath, the son, was graduated from the Sheffield Scientific School of Yale University in 1901. He worked as chief chemist of Magnolia Sugar & Railroad Co., Lawrence, La. He subsequently worked in the coal fields of southeastern Kentucky correlating the various coal beds to show their continuity from Pennsylvania through West Virginia and Kentucky. In 1904, he joined his father's firm, Andrew S. McCreath and Son, as a partner.

Andrew S. McCreath became a Legion of Honor member of AIME in 1929, and at the annual meeting of the Institute in February, 1952, Lesley McCreath will become a member of the Legion of Honor.

Legion of Honor

Class of 1902

Addicks, Lawrence, Bel Air, Md.; Barker, H. A., Santa Fe, N. M.; Boyd, W. S., San Francisco, Calif.; Bradford, Seymour K., No address; Brown, Davenport, Boston, Mass.; Cornell, Russell T., Scarsdale, N. Y.; Crawford, H. E., Long Beach, Calif.; Emery, Augustus Bachelder, Bryanston, Transvaal, So. Africa; Eustis, Augustus H., Boston, Mass.; Eustis, Fredric A., Boston, Mass.; Fleming, Edward P., Los Angeles, Calif.; Fuchs, Fernando C., Lima, Peru; Jameson, A. H., Branford, Conn.; Landfield, J. B., San Francisco, Calif.; Leggat, Alexander, Butte, Mont.; Lidgerwood, John H., Beacon, N. Y.; McCreath, Lesley, Harrisburg, Pa.; Miller, D. I., Coshocton, Ohio; Morris, Henry C., Washington, D. C.; Oliver, Edwin Letts, San Francisco, Calif.; Pringle, Robert W., Salisbury, S. Rhodesia, Africa; Queneau, A. L. J., New York City; Roberts, Milnor, Seattle, Wash.; Russell, William, Reigate, Surrey, England; Sales, Reno H., Butte, Mont.; Smith, Hoval Arnold, Phoenix, Ariz.; Smith, Howard D., New York City; Sproat, A. D., Guanajuato, Gto., Mexico; Utley, H. H., Baxter Springs, Kans.; Walker, Etheredge, San Francisco, Calif.; Whitney, W. R., Schenectady, N. Y.; Wickes, L. Webster, Los Angeles, Calif.

Joseph Winlock Chosen to Deliver Howe Memorial Lecture for 1953

At the meeting of the Executive and Finance Committees, AIME, on Oct. 10, 1951, President Peirce announced that Joseph Winlock, chief metallurgist of The Budd Company, had been chosen as Howe Memorial Lecturer for 1953.

Following is an excerpt from Mr. Winlock's letter of acceptance:

"I consider this to be the greatest honor I have ever had and I accept with pleasure. I only hope that I will be able to live up to the standards of the other Howe Memorial Lecturers.

"Especially do I feel the honor keenly because I had the pleasure of doing research work with Dr. Howe in the private laboratory which he established in his home in Bedford Hills."

PROFESSIONAL SERVICES

Limited to AIME members, or to companies that have at least one AIME member on their staffs. Rates $40 per year per inch.

MAX STERN
Consulting Engineer
Expert for Scrap Recovery and Shipwrecking — Modernization of Plants and Yards for Ferrous and Nonferrous Metal Scrap
150 Broadway New York 7, N. Y.

ENGINEERS
CONSULTANTS
METALLURGISTS
Small Jobs Welcomed
SAM TOUR & CO., INC.
Laboratories and offices
44 Trinity Place, New York 6, N. Y.
Testing—Certifying
American Standards Testing Bureau, Inc.

R. S. DEAN LABORATORIES, INC.
Consulting, Research Development Chemistry, Electrochemistry, & Metallurgy Laboratory Research on a Contract Basis
5810—47TH AVENUE AP-2821
RIVERDALE, MD.

LEWIS B. LINDEMUTH
Consulting Engineer
140 CEDAR STREET, NEW YORK 6, N. Y.
STEEL PRODUCTION
DESIGN · OPERATION · CONSTRUCTION · METALLURGY

Fall Programs of Open Hearth Sections Underway

The Southern Ohio Section of the National Open Hearth Steel Committee held its annual meeting at the Deshler Wallick Hotel in Columbus, Ohio, on Oct. 26, 1951. V. W. Jones, Section Chairman, was in charge of the meeting. R. K. Thornberry, open hearth superintendent of Newport Steel Corp. and W. O. Richmond, assistant open hearth superintendent of Armco Steel Corp. were Co-Chairmen for the morning session. Clarence E. Sims, assistant director of Battelle Memorial Institute, and Joseph P. Fitzsimmons, metallurgist for Newport Steel Corp. were Co-Chairmen for the afternoon session.

Robert S. B. Holmes, director of training and safety for the National Tube Co. presented a paper on *"Safety in the Open Hearth."* The paper was developed around the theme that no matter how skillful a worker may be the safety factor must enter into the planning before and not after the operation.

Richard W. Lewry, open hearth superintendent for the Detroit Steel Corp., discussed *"Flush Practice,"* describing in detail the practice used at the Portsmouth plant. This practice involves a front flush where water and slag enter the thimble simultaneously. To date no explosions have occurred, even when the thimble has been full of water at the start of a flush.

Harlan W. Jarvis, purchasing agent for Armco Steel Corp. discussed *"Economics of Scrap Preparation."* It was explained that the scrap problem historically was nothing new. The problem will become more acute until additional blast furnace capacity is available. The present problem is one of individual facilities for scrap preparation to get the maximum weight per pan for charging into the furnace.

L. R. Astie, assistant general foreman of labor, brick and riggers dept., Jones & Laughlin Steel Corp., presented a paper on *"Improving Furnace Availability by Scheduling of Rebuilds and Labor Saving Devices."* Meetings are held prior to rebuilds where estimates are made by each group involved as to the time required for their particular part. This includes riggers, masonry, labor, pipefitters, etc. Materials required are listed. A practice engineer follows the work and issues a performance report after the job is completed. It was pointed out that furnace availability was materially increased by the use of modern equipment such as brick pallets, fork trucks, slag removal with front end buckets, conveyors for checker brick, and removal of slag pocket brick by contractors truck. A special rake attached to the charging machine is used to remove brick from the furnace hearth. Some modifications in various sections of the furnace were made to take full advantage of modern equipment.

W. F. Johnston, supervisor of training for Armco Steel Corp., presented *"Barnyard Economics."* The complex problem of business economics was presented in a simplified manner. The outline was designed to take the mystery out of economics and was illustrated with common everyday examples that would be understood readily.

H. V. Flagg, combustion engineer for Armco Steel Corp., in substituting for a paper on manganese conservation, led a discussion on the importance of steam in the atomization of fuel. A good discussion from the floor resulted, in which considerable variation of opinion was evident as to the benefits to be derived from different atomizing agents.

Stanleigh Elam, Sr. metallurgist for Armco Steel Corp., presented a paper on *"Effect of Hot Metal Temperature on the Proportioning of Heats and Production Rate."* It was found that with higher hot metal temperatures, the proportion could be cut with an increase in production. The study has resulted in a change in proportioning practice.

Frank G. Norris, metallurgical engineer for Wheeling Steel Corp., presented a paper on *"Statistics as a Tool in Production and Quality Control in the Open Hearth."* The operation of an open hearth is complex and a summary of the variables affecting quality and production need to be available to the operator as soon as possible for corrective action. This type of quality control has furnished the operator with more accurate information and quickly enough that corrective measures can be taken promptly. They are using modern statistical equipment such as card punching and sorting machine, and are able to furnish the operators with prompt accurate information.

Arthur P. Woods, research engineer for Armco Steel Corp., presented a paper on *"Some Factors Affecting Mold Life."* It was brought out that many of the variables which have an influence on mold life are subject to the limitations of individual shops. Some of the variables under the control of the operator are mold temperature, steel pouring temperature and stripping time.

Louis J. Alber, author, world traveler, foreign correspondent and business executive, was the dinner speaker. His subject was *"What the Near East and Iran Mean to Us."* He gave a vivid word picture on this area, with many of his facts based on his tour of the past summer. The importance of this area was stressed around four major points: The center of the Moslem Religion, and the center of Africa, Asia and Europe, transportation and communication, and oil production. Saudi-Arabia, India, Iran, Egypt, and Turkey were among the nations discussed, with their ideologies being brought out along with their weaknesses and strong points.

Eastern Section

Eastern Section held its annual meeting in Philadelphia at the Warwick Hotel on Oct. 12, 1951. Total registration of the meeting was 242 compared with 205 for last year. There appears to be an increased interest within this group, and with the new Fairless Works, there is reason to believe the registrations in the future should be second only to the national convention. At the directors meeting, Rex M. Baker, Bethlehem Steel Co., Sparrows Point, Md., was elected Chairman, and Paul Sultzbach, Stanley Works, New Britain, Conn., Vice-Chairman for 1952 and 1953.

The morning program was opened by R. M. Baker, Bethlehem Steel Co., Sparrows Point, and Co-Chairmen for the morning session were R. R. Fayles, Lukens Steel Co., and J. H. Kelley, Sparrows Point. J. H. Kelley presented *"Coke Gas Firing in Open Hearth,"* an abstract of the development and use of high pressure coke gas at Sparrows Point. *"Communication System in Open Hearth"* by Charles Kay, American Steel & Wire Co., described the use and benefits of their communication system between floors, engines, and stockyards. *"New Charging Machines"* by J. C. MacNeill, Bethlehem Steel Co., concerned new type charging machines using a hydraulic lift and peel head. A paper on *"Jet Tappers"* by D. R. Mathews, Alan Wood Steel Co. gave results obtained using jet tappers. Harry Davis and J. C. MacNeill of Bethlehem reported similar results. C. H. Alexander, Lukens Steel Co., described improvements that meant more production at Lukens, such as larger charging pans and a newly constructed suspended fantail roof. *"Heavy Duty Torch for Scrap Burning"* was presented by Boldgan, Roebling Steel Co. "Doc" Potter, Lukens Steel Co. gave the lead paper on *"Factors Contributing to Loss*

of Production," which was followed by general discussion.

Co-Chairmen for the afternoon session were C. B. Jenni, General Castings Co., and P. R. Sultzbach, Stanley Works. Carter Kendall, Bethlehem Steel Co. spoke on *"Safety in the Open Hearth."* A paper covering development of a new type holder for using Pt-Pt Rd thermocouples in the open hearth was presented by R. J. Harkel, Sparrows Point, and Parker, Fairless Works, discussed the use of the thermocouple. Les Walker, Fairless Works, and B. H. Redden, Sparrows Point, gave the lead off comments on *"Mold Coatings and Methods of Application"*, and a general discussion followed.

Eastern section is planning a plant visit in the spring of 1952, probably to the Sparrows Point Plant. The fall meeting will be held at the Warwick Hotel in Philadelphia on Oct. 10, 1952.

Southwestern Section

Southwestern Section held its fall meeting on Oct. 10 and 11, 1951, in Colorado, with Colorado Fuel & Iron as host. Following a plant visit and luncheon at CF&I, delegates were taken to the Broadmoor, Colorado Springs for the remainder of the meeting. Men attending the meeting were guests of the Lavino Co. for cocktails and dinner at the Garden of the Gods Club. The technical session began the morning of Oct. 11, under Chairman W. H. Carpenter, Colorado Fuel & Iron Corp. Papers presented were: *"Progress Report on Basic Brick Construction,"* by Don Baughman, Sheffield Steel Corp.; *"Manpower, Training and Human Relations in the Open Hearth,"* by Rudy Smith, Colorado Fuel & Iron Corp.; *"Hot Top Practice"* by Walter Serge, Jones & Laughlin Steel Corp.; *"Economics of Scrap Preparation"* by Martin Schuster, Granite City Steel Co.; *"Furnace Availability"* by Gordon Yocum, Wheeling Steel Corp.; *"Conservation of Ferromanganese, Ferrosilicon, Etc."* by Gordon McMillan, General Steel Castings; and *"Quality Control Through the Use of Bath Temperature Measurements"* by Frank Hahn, Scullin Steel Co. Discussion followed each of the papers.

There were a record number of registrants for the meeting, and guests arrived from California, Georgia, Alabama, and Mexico. It was decided by the program committee that the spring 1952 meeting be held in St. Louis, Mo. Al Sommers, Keystone Steel & Wire Corp. invited the session to hold its fall 1952 meeting at Peoria, Ill., and the invitation was accepted. W. A. Peters, Laclede Steel Co., Dan Murphy, Scullin Steel Co., and Russell Solomon, Granite City Steel Co. were appointed by Chairman C. L. King, Sheffield Steel Corp. to act on the nominating committee for 1952 officers.

Chicago Section

Chicago Section held a dinner meeting at Phil Schmidt & Sons, Whiting, Ind., Oct. 22, 1951. The subject of discussion at the meeting was *"Elimination of Bottlenecks in Production,"* with Oscar Pearson of U. S. Steel's Gary Works serving as technical chairman. Scrap handling and charging, furnace operation, and pit side operation were topics covered.

The future meetings planned include: An all day meeting, Mar. 12, 1952, at the Del Prado Hotel, Chicago, followed by a cocktail hour and dinner; An evening meeting Apr. 21, 1952, at Phil Schmidt & Sons, Whiting, Ind., on *"Training of Furnace and Operating Personnel,"* with M. F. Yarotsky, div. supt. of steel production at U. S. Steel's South Works acting as technical chairman; and an annual golf outing in June, 1952. Chairmen for the golf outing include R. Dwyer, asst. genl. supt., U. S. Steel's Gary Works; T. Hess, asst. openhearth supt., Youngstown Sheet & Tube Co., Chicago; and M. Nickel, asst. openhearth supt., of Wisconsin Steel Co. The plans for this year's activities of the Chicago Section were announced by J. R. Brady, chairman of the Chicago Section of the National Open Hearth Committee.

A Limited Edition of

Beautifully bound and printed, this durable new edition of *De Re Metallica* contains all 672 pages of the 1912 edition, all 289 of the 16th Century woodcuts, three appendices by Mr. Hoover, footnotes, three indexes, and a historical and biographical introduction.

Agricola's original preface, a facsimile of the 1556 title page, and four facsimile pages from the original Latin text are included in this heavy cloth bound edition.

This is your Reservation Coupon - - Mail it Today for a free examination copy of this outstanding volume.

DOVER PUBLICATIONS, INC.
1780 Broadway, New York 19, N. Y.

Reserve for me _____ copy (ies) of DE RE METALLICA. I understand that I need pay only $10.00 plus a few cents postage, *after* I have had a chance to examine the book at my leisure. Should the book not live up to my expectations, I shall return it within ten days without cost or explanation.

NAME _____

ADDRESS _____

☐ *Check here if you prefer to enclose payment with your order. In this case, transportation is free. Money-back guarantee.*

Headquarters Business Methods Studied and Changes Recommended

Recommendations for ways to improve the functioning of the New York headquarters office of AIME were made in a report presented to the Board of Directors at the Los Angeles Meeting on Oct. 25. At the May 9, 1951 meeting of the Executive and Finance Committees, Gail Moulton had been asked to collaborate with Secretary Robie in obtaining an independent expert to review procedures at AIME headquarters. At the June 13 meeting of the Board, it was reported that Herbert H. Vasoll, of the firm of Davies & Davies, certified public accountants, would make the study.

Highlights of the recommendations included (1) Immediate purchase of a modern Addressograph machine to replace present equipment, at an estimated cost of $2500. Such purchase was authorized by the Board. (2) Installation of a "Keysort" punch card system for membership records, at an initial cost of some $600. (3) Purchase of a Pitney Bowes postage meter at a cost of about $600. This was also approved by the Board for early action. (4) Engagement, from without the present organization, of a Controller and Business Manager, who would have supervision over all functions of the Business Office. (5) Reorganization of the office into four primary departments, each supervised by one individual who in turn shall be responsible to the Secretary of the Institute.

These shall be: (a) Institute Activities Dept. Convention planning, meeting arrangements, travel accommodations, membership control and promotion, special projects for the Secretary, public relations, and personnel. (b) Metals Branch Dept. (All activities pertaining to the Metals Branch of the Institute). (c) Publications Dept. (Editorial, Transactions, advertising, production, circulation promotion, publication of proceedings volumes, and any other Institute publications). (d) Business Office. (Accounts, Addressograph, orders, purchasing, filing, and mailing.)

The present Office Manager would be named Administrative Secretary of the Activities Dept. The Metals Branch Dept. would continue more or less as at present except that its functions dealing with the publication of volumes would be placed under the supervision of the Publications Dept. The Publications Dept. would be relieved of all student relations work and through installation of a Keysort system would be enabled to obtain more complete data regarding readers of the journals, and more readily than at present. Revision of the work of the Business Office, with a new head would permit several improvements in operation. In the Accounting Div., improvements are suggested in billing procedure and in cooperation with other departments which should eventually result in a reduction of staff. The Mail Room procedure would be revised to improve efficiency and to avoid delays, in several suggested ways. The Addressograph Div., would be divested of miscellaneous clerical duties and would become strictly a mechanical service unit, with new equipment, avoiding present mechanical breakdowns. All orders would be processed through one order clerk and all billing done by the Accounting Div.

Some revision of forms was suggested, and installation of a Multi-Lith machine in place of the present Mimeograph equipment. For publication of the Directory, installation of a Remington Rand Flexoprint system was felt worthy of investigation.

As to personnel, "in general we believe that the size of the headquarters staff is commensurate with the volume of work handled. However, due to unequal distribution of work, the services of certain individuals are not being utilized to the fullest extent and others with a greater sense of responsibility are doing more than their share. We also noticed some evidence, however slight, of friction between departments. This is not due to lack of cooperation, which is given when requested, but rather to lack of coordination."

"The salary scale of staff employees, excluding department heads, is in most cases in line with prevailing market levels. There are, however, several employees holding responsible jobs whose salaries are lower than they should be."

At a meeting of the Executive and Finance Committees November 14, authorization was voted for the employment of a Business Manager as proposed. Other recommendations are being studied.

Nominating Committee For 1953 Officers Named

As provided in Article IX, Section 2, of the AIME Bylaws, the names and addresses of the Nominating Committee for Institute officers for 1953 are given below. In each case, the name in parenthesis is that of the alternate, who will serve only in the absence of the principal at the meeting of the Committee.

Members designated by the Council of Section Delegates: Francis Cameron, St. Joseph Lead Co., 250 Park Ave., New York (Philip D. Wilson, Lehman Bros., 1 William St., New York); Henry A. Dierks, Glen Alden Coal Co., 631 Charles Ave., Kingston, Pa. (D. C. Helms, Lehigh Navigation & Coal Co., Lansford, Pa.); P. G. Spilsbury, Anaconda Copper Mining Co., Shoreham Hotel, Washington, D. C. (Thomas H. Miller, Bureau of Mines, Washington 25, D. C.); William A. Mueller, Ohio State University, Columbus (Harley Lee, Basic Refractories, Inc., 845 Hanna Bldg., Cleveland); Thomas M. Broderick, Calumet & Hecla Consolidated Copper Co., Calumet, Mich. (Raymond D. Satterly, Inland Steel Co., Box 360, Ishpeming, Mich.); Armor B. Martin, Montana Power Co., 40 E. Broadway, Butte (Tom Graham, Anaconda Copper Mining Co., Great Falls, Mont.); Drury A. Pifer, University of Washington, 505 Boston St., Seattle 9. (Albert H. Mellish, American Smelting & Refining Co., Tacoma, Wash.); George D. Dub, 1206 Pacific Mutual Bldg., Los Angeles 14, Calif. (alternate not selected); Edward M. Tittman, American Smelting & Refining Co., Box 1111, El Paso (Guy E. Ingersoll, Texas Western College, El Paso); S. S. Clarke, Tri-State Mines, Eagle-Picher Mining & Smelting Co., Cardin, Okla. (John W. Chandler, Eagle-Picher Mining & Smelting Co., First National Bank Bldg., Miami, Okla.).

Members designated by the Branch Councils: Edwin R. Price, Coal Properties, Inland Steel Co., Wheelwright, Ky. (J. Murray Riddell, dept. of mining engineering, Michigan College of Mining & Technology, Box 144, Houghton, Mich.); C. H. Behre, Jr., Geology Dept., Columbia Univ., New York 27 (Grover Holt, Cleveland-Cliffs Iron Co., Hibbing, Minn.); John D. Sullivan, Battelle Memorial Institute, 505 King Ave., Columbus 1 (Maxwell Gensamer, dept. of metallurgy, Columbia University, New York); John E. Sherborne, Union Oil Co. of California, 1004 Summit Drive, Whittier, Calif. (Lloyd Elkins, Stanolind Oil & Gas Co., P.O. Box 591, Tulsa 2).

Members designated by President Peirce: John R. Suman, Chairman, Standard Oil Co. (N. J.), 30 Rockefeller Plaza, New York 20. (Henry T. Mudd, 1206 Pacific Mutual Bldg., Los Angeles, Calif.); Kent R. Van Horn, Aluminum Co. of America, 2210 Harvard Ave., Cleveland (George P. Halliwell, H. Kramer & Co., 1339-45 W. 21 St., Chicago 8); H. M. Griffith, The Steel Co. of Canada Ltd., Hamilton, Ont., Canada (C. D. King, U. S. Steel Corp. (Del.), 436 Seventh Ave., Pittsburgh).

The Committee will welcome suggestions for the official slate for 1953. The following offices are to be filled: President-Elect for 1953 (President for 1954), two Vice-Presidents, and six other Directors. The terms of the following Directors eligible for reelection expire in February 1953: D. H. McLaughlin, R. W. Thomas, H. Decker, F. B. Foley, E. C. Meagher, C. V. Millikan, G. F. Moulton, and Howard I. Young.

Personals

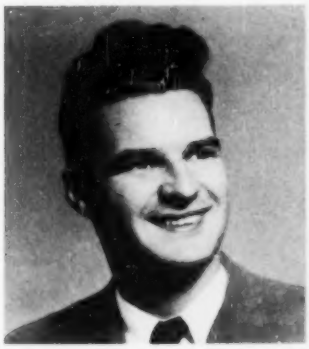

PAUL STEVAN METHE

RICHARD A. FLINN

HEDLEY S. FOWLER

Paul Stevan Methe has joined the Allegheny Ludlum Steel Corp., titanium research, Watervliet, N. Y.

Richard A. Flinn, assistant chief metallurgist, American Brake Shoe Co., research and development center, will accept an associate professorship of product engineering and metallurgical engineering at the University of Michigan. He will also be in charge of the University's experimental foundry.

Hedley S. Fowler has joined the Kaiser Magnesium Co. as mill superintendent at the Manteca, Calif. plant. He had been with the Columbia Steel Co., Pittsburg, Calif.

Richard P. Seelig and **George Stern** have been elected vice-presidents of the American Electro Metal Corp., Yonkers, N. Y. Mr. Seelig was formerly chief engineer at Powder Metallurgy Corp., div. of General Bronze and joined American Electro as chief engineer in 1946. Mr. Stern, who has been with the firm for 9 years, was research director before his promotion. He was previously with the Armour Research Foundation.

Andrew E. St. John was elected vice-president and treasurer of Alloys & Products, Inc., New York. He will also be in charge of the company's manufacturing operations. Mr. St. John was previously connected with Federated Metals and Barth Smelting Corp.

J. Morgan is now in Canada as chief metallurgist for Foundry Services (Canada) Ltd., Guelph, Ont.

Charles Henry Maak is standards metallurgist with the Sandia Corp., Sandia Base, Albuquerque, N. Mex.

Swan Bergstrom has been appointed director of the metalworking equipment div., National Production Authority. He is on leave as vice-president and director of the Cincinnati Milling Machine Co., Cincinnati.

W. F. Brazeau is now with W. R. Grace & Co., New York. He had been associated with the Intsel Metals Corp.

H. Theodore Sumsion, formerly with the Carborundum Co., Niagara Falls, N. Y. has joined the General Electric Co., Knolls Atomic Power Laboratory, Schenectady, N. Y.

Robert A. Lubker has been made associate chairman, metals research, Armour Research Foundation, Chicago.

Herman J. Schorle is now employed by the Bendix Aviation Corp., Teterboro, N. J.

Glenn W. Wensch has joined the Fansteel Metallurgical Corp., North Chicago, as research metallurgist. He had been with the Los Alamos Scientific Laboratory, Los Alamos, N. Mex.

K. Yoshizaki was appointed assistant works manager of the Toyo Kohan Co. Ltd. at Kudamatsu, Japan.

Paul F. Kohlhaas has been named assistant vice-president, design and appropriation control, U. S. Steel Co.

Adger S. Johnson has been appointed president of National Carbon Co., a division of Union Carbide & Carbon Corp.

A. L. Ascik is now plant and melting superintendent, Seidlhuber Steel Rolling Mill Corp., Seattle, Wash. He was formerly superintendent of melting, Universal Cyclops Steel Corp., Bridgeville, Pa.

GEORGE STERN

RICHARD P. SEELIG

ANDREW E. ST. JOHN

Harry Schwartzbart has joined the Armour Research Foundation, Illinois Institute of Technology, Chicago, as research metallurgist.

Thomas L. Hurst, Monsanto Chemical Co., Anniston, Ala., has been transferred to the Columbia, Tenn. office.

Alexander MacKenzie has been appointed president of Union Carbide International. **R. V. Farrell, H. P. Martin,** and **George C. Wells** have been appointed vice-presidents, and **N. H. Downs** has been named secretary-treasurer.

James W. Tracht and **G. R. Evans** have been appointed assistant chief engineers for the Pennsylvania Salt Mfg. Co., Philadelphia.

W. J. Welch has been appointed manager of National Lead Co.'s metal dept. Mr. Welch had been assistant to the manager of the metal dept. and was then made manager of the metal sales dept.

William R. Meikle has been named plant manager of the Middletown, Pa. plant of the National Radiator Co.

Boyd E. Cass was recently named manager of metallurgical sales for Foote Mineral Co., Philadelphia.

William H. Myers has been named general district superintendent, in charge of 6 plants, Harbison-Walker Refractories Co. and **J. H. Moore, Jr.** has been named general superintendent in charge of coke oven manufacture. **Charles W. Ayers** has been appointed superintendent of the firm's new Windham, Ohio silica plant and **William N. Bartleson** will be superintendent of the newly acquired plant at Warm Springs, Calif.

Linton D. Bylund, Reynolds Metals Co., formerly at the Adrian, Mich. USAF Mfg. Methods Pilot Plant, is now at Richmond, Va.

Albert M. Krainess has resigned from the Ford Motor Co. to join the engineering staff of the Burroughs Adding Machine Co., Detroit, as a metallurgical engineer.

NECROLOGY

Date Elected	Name	Date of Death
1936	Charles N. Becker	May 1951
1909	Henry T. Beckwith	Oct. 5, 1951
1921	Adolph Bregman	Oct. 4, 1951
1937	E. L. Clair	Unknown
1903	Will L. Clark	Sept. 4, 1951
1937	Robert S. Cockle	Sept. 21, 1951
1948	Andre Delruelle	July 23, 1951
1950	John Eck	Sept. 24, 1951
1922	Edward Griffith	Oct. 24, 1951
1944	J. H. Kerrick	October 1951
1947	Harry A. Knowlton	Aug. 31, 1951
1951	C. A. Norbury, Jr.	Unknown
1938	Hugh J. MacLean	Sept. 19, 1951
1937	Robert D. Maddox	Unknown
1903	Elwyn W. Stebbins	May 21, 1950
1911	Paul Sterling	Aug. 14, 1951
1922	John J. Tweedie	Unknown
1903	H. D. Williamson	Oct. 14, 1951

Proposed for Membership

Total AIME membership on Oct. 31, 1951, was 17,313; in addition 2,603 Student Associates were enrolled.

ADMISSIONS COMMITTEE

Thomas G. Moore, Chairman; Carroll A. Garner, Vice-Chairman; George B. Cortezz, F. W. Hanson, Albert J. Phillips, Lloyd C. Gibson, R. D. Mollison, John T. Sherman. Alternates: A. C. Brinker, H. W. Hitzrot, Plato Malozemoff, Ivan Given, T. D. Jones, and W. A. Clark, Jr.

Institute members are urged to review this list as soon as the issue is received and immediately to wire the Secretary's office, night message collect, if objection is offered to the admission of any applicant. Details of the objection should follow by mail. The Institute desires to extend its privileges to every person to whom it can be of service but does not desire to admit persons unless they are qualified. Objections must be received before the 30th of the month on Metals and Mining Branches.

In the following list C/S means change of status; R, reinstatement; M, Member; J, Junior Member; A, Associate Member; S, Student Associate.

California
Long Beach—Gilmore, John W. (J) (R, C/S—S-J)

Colorado
Telluride—Rumpf, Vincent G. (J) (C/S—S-J)
Victor—Phillips, Earl C. (M)

Connecticut
West Hartford—Conard, George P. (M) (C/S—S-M)

District of Columbia
Washington—Lloyd, Kenneth Barker (J) (C/S—S-J)

Illinois
Chicago—Billy, Joseph (J) (C/S—S-J), Borto, Edward J. (J) (C/S—S-J), Brown, Robert R. (M), Chojnowski, Eugene F. (J) (C/S—S-J), Lloyd, Lowell T. (J) (C/S—S-J), Owen, John H. (M), Ridgway, Robert H., Jr. (J) (C/S—S-J), Wilson, Richard J. (J)
Collinsville—Adler, Arthur G. (M) (C/S—J-M)
Flossmoor—Jones, Sam H. (A)
Moline—McCullough, Earl Martin (J)

Indiana
Hammond—Edmondson, Robert N. (J)
Highland—Mayberry, James F. (M)
West Lafayette—Cuthill, John R. (M) (R, C/S—S-M)

Maryland
Baltimore—Wolf, George J. (J) (C/S—S-J)

Massachusetts
Cambridge—Reynolds, James E. (J) (R, C/S—S-J)

Michigan
Ann Arbor—Phillips, Charles W. (M) (C/S—S-M)
Berkley—Mueller, August J. (M)
Birmingham—Doane, Douglas V. (M) (C/S—J-M)

Montana
East Helena—Johnson, Donald W. (J) (C/S—S-J)

Metals Branch AIME

New Mexico
Carlsbad—Lane, Robert H. (J)
Hurley—Dow, Wesley C. (M)

New York
Ballston Lake—Lacy, Charles E. (M) (C/S—J-M)
Brooklyn—(Miss) Griffin, Hildreth O. (M) (C/S—J-M)
Flushing—Perkins, Frank C. (J)
Levittown—Sama, Lawrence (J) (R, C/S—S-J)
Schenectady—Hirsch, Harold H. (M) (C/S—J-M), Newkirk, John B. (M) (C/S—S-M)
Staten Island—Mooz, William E. (J) (R, C/S—S-J)

Ohio
Canfield—Voss, Joseph A., Jr. (M) (R, C/S—S-M)
Chardon—Spare, Gordon T. (M) (C/S—S-M)
Cincinnati—Crenshaw, John R. (A)
Cleveland—Lockwood, Paul A. (J) (C/S—S-J)
Columbus—Lepkowski, William J. (J)
Conneaut—Boxk, Michael, II (M)
Youngstown—Hibbert, Edward N. (M)

Oregon
Portland—Czyzewski, Harry (M) (C/S—J-M)

Pennsylvania
Bethlehem—Gero, John B. (M) (C/S—J-M), Libsch, Joseph F. (M) (C/S—J-M), Luerssen, Frank W. (J)
Latrobe—Robbins, John S. (A)
Morrisville—Chisholm, James (M)
Philadelphia—De Luca, Robert R. (J) (C/S—S-J), Dick, Paul (J) (C/S—S-J)
Pittsburgh—Thomas, Donald E. (M) (C/S—J-M)
Whitaker—Danko, Joseph C. (J) (C/S—S-J)
Yardley—White, Richard H. ( )

Texas
Morris Co.—Brashear, Joseph M. (M)

Washington
Richland—Flint, George L. (M) (C/S—J-M)
Spokane—Russell, James B. (M) (C/S—J-M)

Wisconsin
West Bend—Anderson, John E. (J) (C/S—S-J)

Argentina
Provincia de Santa Fe Rep.—Diaz de Brito, Jose L. (M)

Canada
Montreal—Savard, Guy (M)
Toronto—Dewar, John Stuart (M) (C/S—J-M)

Chile
Chile—Fines, Leonard O. (M) (R, C/S—A-M)

Mexico
Mexico, D.F.—Agather, Victor N. (M), Holguin, Carlos C. (A), Soto, Felipe (M)
Piedras Negras—De Los Santos, Toma's M. (M)
San Luis De La Paz—Wilhelmi, Frederick A. (M)

Peru
La Oroya—Broenimann, Markus (J)

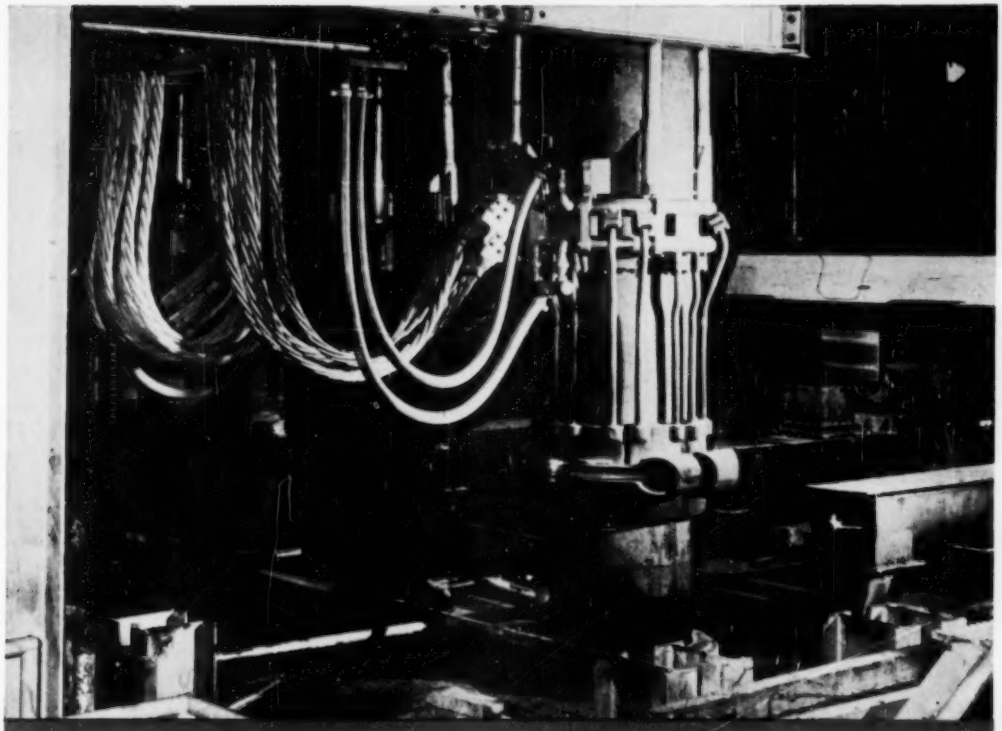

USE POORER GRADE RAW MATERIALS—GET A BETTER PRODUCT—

with OXIDE REDUCTION engineered by LECTROMELT

Processing phosphate rock in a Lectromelt-designed arc furnace offers you a big advantage over the sulfuric acid method. With a Lectromelt* you can use a *poorer* grade of rock and get a *better* product, because the phosphorus is volatilized.

Savings like this are typical of the advantages of Lectromelt furnaces for reduction of all these oxides: iron, cobalt, nickel, tin, lead, beryllium, antimony, magnesium, arsenic and zirconium.

You can also use Lectromelt furnaces for selective reduction of ores not sufficiently high in desired metallic content for direct reduction. A low manganese ore, for example, with a manganese-iron ratio of less than 6 to 1, can be selectively reduced to that ratio. The reduction potentials allow the iron to be reduced from the ore, leaving a high manganese slag suitable for the manufacture of standard ferro-manganese.

Whatever your melting problems, chances are Lectromelt engineers have done the research that supplies the answers. We'll be glad to talk them over with you. Pittsburgh Lectromelt Furnace Corporation, 326 32nd Street, Pittsburgh 30, Pennsylvania.

Write for your free copy!

Manufactured in . . . CANADA: Lectromelt Furnaces of Canada, Ltd., Toronto 2 . . . ENGLAND: Birlec, Ltd., Birmingham . . . AUSTRALIA: Birlec, Ltd., Sydney . . . FRANCE: Stein et Roubaix, Paris . . . BELGIUM: S. A. Belge Stein et Roubaix, Brossoux-Liege . . . SPAIN: General Electrica Espanola, Bilbao . . . ITALY: Forni Stein, Genoa.

*REG. T. M. U. S. PAT. OFF.

WHEN YOU MELT... MOORE RAPID *Lectromelt*

Giant with facile jaws

When the sturdy Brosius Auto Floor Forging Manipulator takes a billet or blank in its teeth, it improves upon every action possible with chain hoist and porter bar or cumbersome overhead equipment. More swiftly and easily it draws or charges . . . moves more quickly and independently across the forging floor . . . manipulates at hammer or press with more sensitive movements. Moreover, this remarkable modern mammoth brings to your forge shop added production, added safety, added economy — you should be using one. Write us.

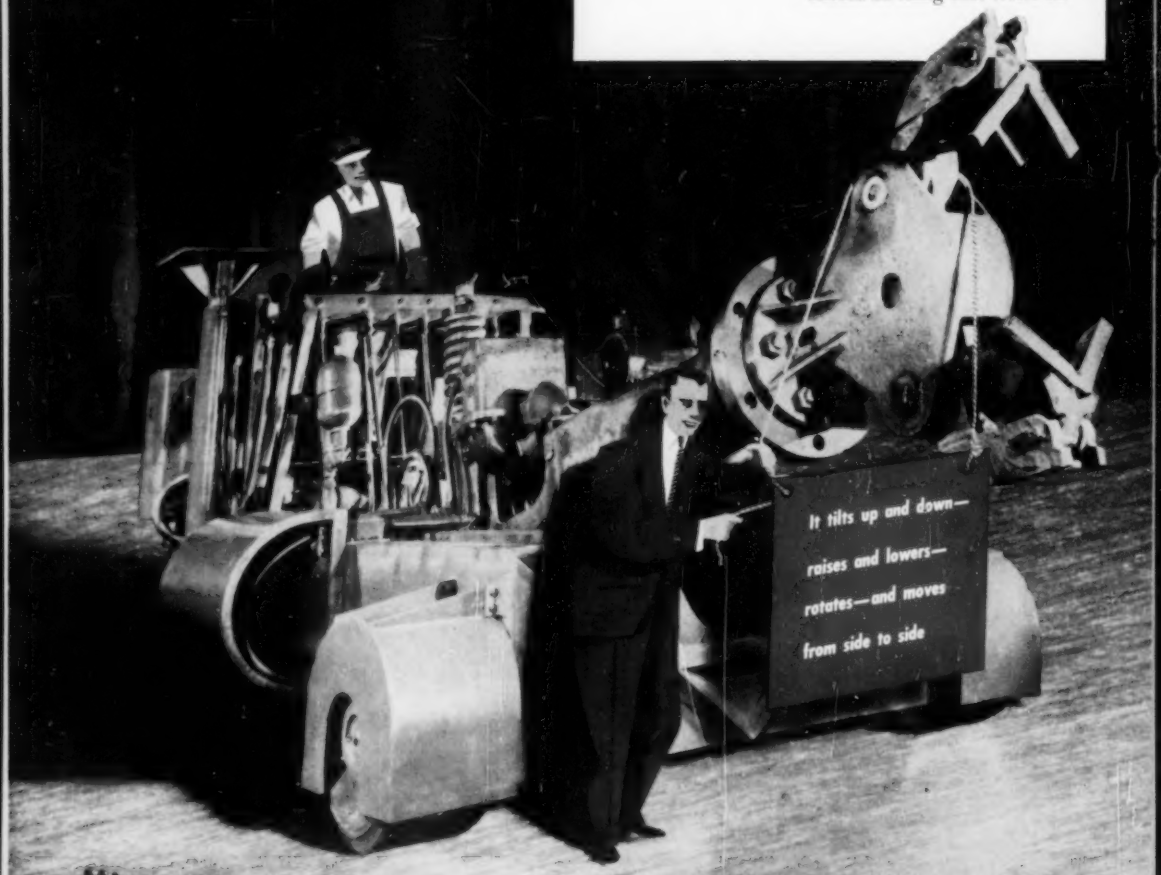

BROSIUS DIVISION

Salem-Brosius, Inc., Pittsburgh 15, Pa.

Affiliates: Salem Engineering Division,
Salem Engineering Co., Ltd., Milford nr. Derby, England; Salem Engineering (Canada) Ltd., Toronto, Canada